FINAL REPORT

Climate Changes Impacts on Fire Regimes, Plant Invasions, and Tick-Borne Diseases

SERDP Project RC-2636

SEPTEMBER 2021

Brian Allan
Page Fredericks
Allison Gardner
University of Illinois Urbana-Champaign

Michael Dietze
Tempest McCabe
Boston University

Whalen Dillion
Luke Flory
Drew Hiatt
University of Florida

Distribution Statement A
This document has been cleared for public release

SERDP
DOD ▪ EPA ▪ DOE

This report was prepared under contract to the Department of Defense Strategic Environmental Research and Development Program (SERDP). The publication of this report does not indicate endorsement by the Department of Defense, nor should the contents be construed as reflecting the official policy or position of the Department of Defense. Reference herein to any specific commercial product, process, or service by trade name, trademark, manufacturer, or otherwise, does not necessarily constitute or imply its endorsement, recommendation, or favoring by the Department of Defense.

REPORT DOCUMENTATION PAGE

Form Approved
OMB No. 0704-0188

Public reporting burden for this collection of information is estimated to average 1 hour per response, including the time for reviewing instructions, searching existing data sources, gathering and maintaining the data needed, and completing and reviewing this collection of information. Send comments regarding this burden estimate or any other aspect of this collection of information, including suggestions for reducing this burden to Department of Defense, Washington Headquarters Services, Directorate for Information Operations and Reports (0704-0188), 1215 Jefferson Davis Highway, Suite 1204, Arlington, VA 22202-4302. Respondents should be aware that notwithstanding any other provision of law, no person shall be subject to any penalty for failing to comply with a collection of information if it does not display a currently valid OMB control number. **PLEASE DO NOT RETURN YOUR FORM TO THE ABOVE ADDRESS.**

1. REPORT DATE *(29-09-2021)*

2. REPORT TYPE
SERDP FINAL REPORT

3. DATES COVERED *(21/09/2016 – 29-09-2021)*

4. TITLE AND SUBTITLE

Climate Changes Impacts on Fire Regimes, Plant Invasions, and Tick-Borne Diseases

5a. CONTRACT NUMBER
16-C-0053

5b. GRANT NUMBER
RC-2636

5c. PROGRAM ELEMENT NUMBER

6. AUTHOR(S)

Allan, Brian F.; Dietze, Michael; Dillon, Whalen; Flory, S. Luke; Fredericks, L. Page; Gardner, Allison; Hiatt, Drew; McCabe, Tempest.

5d. PROJECT NUMBER
RC-2636

5e. TASK NUMBER

5f. WORK UNIT NUMBER

7. PERFORMING ORGANIZATION NAME(S) AND ADDRESS(ES)
University of Illinois Urbana-Champaign, 505 S. Goodwin Ave., Urbana, IL 61801
University of Florida, 1676 McCarty Hall B, Gainesville, FL 32611
Boston University, 685 Commonwealth Ave., Boston, MA 02215
University of Maine, 5722 Deering Hall, Orono, ME 04469

8. PERFORMING ORGANIZATION REPORT NUMBER

RC-2636

9. SPONSORING / MONITORING AGENCY NAME(S) AND ADDRESS(ES)
Strategic Environmental Research and Development Program
4800 Mark Center Drive, Suite 16F16
Alexandria, VA 22350-3605

10. SPONSOR/MONITOR'S ACRONYM(S)
SERDP

11. SPONSOR/MONITOR'S REPORT NUMBER(S) RC-2636

12. DISTRIBUTION / AVAILABILITY STATEMENT

DISTRIBUTION STATEMENT A. Approved for public release: distribution unlimited.

13. SUPPLEMENTARY NOTES

14. ABSTRACT
Tick-borne diseases (TBDs) represent a major public health threat in North America, particularly for military personnel training on Department of Defense (DoD) installations. Ecological theory predicts that climate change will likely alter vector-borne disease transmission by a variety of direct and indirect pathways. This project explored several of the predicted consequences of climate change, including altered fire regimes and plant communities and their interactions with wildlife, for human risk of exposure to TBDs in the southeastern United States (U.S.). Project-specific objectives were to: 1) Evaluate the interactions between fire and plant invasions spanning a gradient in fire management, invasive plant distribution and abundance, and climatic conditions across the southeastern U.S. 2) Quantify the effects of fire and plant invasions, and their interactions, for variation in wildlife abundance, tick abundance, tick infection rates, and TBD risk to humans. 3) Calibrate a spatially explicit model of TBD risk in response to fire-invasion interactions and incorporate simulations of climate change scenarios. Benefits of this project to the Department of Defense include an improved understanding of current TBD risk on installations and of the potential consequences of climate change for TBD risk and human health.

15. SUBJECT TERMS
Climate change, prescribed fire, invasive plants, ticks, tick-borne diseases

16. SECURITY CLASSIFICATION OF: U

a. REPORT	b. ABSTRACT	c. THIS PAGE	17. LIMITATION OF ABSTRACT	18. NUMBER OF PAGES	19a. NAME OF RESPONSIBLE PERSON
UNCLASS	UNCLASS	UNCLASS	SAR	171	Brian Allan

19b. TELEPHONE NUMBER *(include area code)* 217-244-1341

TABLE OF CONTENTS

Page #

List of Tables iv

List of Figures vi

List of Acronyms xii

Acknowledgements xiii

ABSTRACT 14

EXECUTIVE SUMMARY 15
- Introduction 15
- Objectives 16
- Technical Approach 17
- Results and Discussion 19
- Implications for Future Research and Benefits 22

PART 1: FIELD SURVEYS ACROSS DOD INSTALLATIONS 23

TECHNICAL APPROACH 24
- Experimental design 25
- Field sampling design 27
- Plot design 27
- Tree and shrub data collection 28
- Ground cover and litter data collection 30
- iNaturalist project 31
- Tick sampling 32
- Estimating host density 33
- Climate Data 34
- Path Analysis 34

RESULTS AND DISCUSSION 38
- Installation and plot visits 38
- Path analysis 39
- Tick abundance sub-model 41
- Litter sub-models 42
- Canopy cover, time since fire, and fire return interval sub-models 43
- Host abundance sub-model 44
- Climate and Weather 45
- Trees and understory 47
- Host abundances 47
- Tick abundances 49
- Summary 52

PART 2A: TESTING THE EFFECTS OF COGONGRASS FUEL STRUCTURE ON FIRE TEMPERATURE AND RESIDENCE TIME: AN EXPERIMENTAL METHOD 53

TECHNICAL APPROACH 54
Experimental apparatus 57
Fuels and weather measurements 59
Experimental treatments 60
Fire intensity measurements 60
Statistical analyses 61
RESULTS AND DISCUSSION 61
Fire intensity 61
Discussion 63
Apparatus effectiveness 64
Cogongrass and fire 65
Potential bias 66

PART 2B: INVADED AND NATIVE PLANT COMMUNITIES ALTER TICK EXPOSURE RISK VIA DIFFERENT MECHANISTIC PATHWAYS 67

TECHNICAL APPROACH 68
Study system 69
Field Study: Tick survival and microclimate 69
Statistical analysis: Tick survival and microclimate 72
Field survey: Tick abundance and host use 73
Statistical analysis: Tick abundance and host use 74
RESULTS AND DISCUSSION 75
Filed study: Site conditions 75
Field study: Tick survival and microclimate conditions 76
Field survey: host use and tick abundance 81
Summary 82

PART 3: PATHOGEN ANALYSIS OF TICKS 84

TECHNICAL APPROACH 85
Introduction 85
Tick Collections 85
DNA Extraction 85
Primers 86
Fluidigm 2 Step Access Array Amplification 88
High Throughput Sequencing 90
Sequence Analysis 90
RESULTS AND DISCUSSION 91
Identification of Tick-borne Agents 91
Summary and Interpretation of Results 91

PART 4: ED2 MODELING 96

TECHNICAL APPROACH 97
Modeling Objectives 97
The Ecosystem Demography Model 97
The Predictive Ecosystem Analyzer: PEcAn 98
Objective 4A: Southern Pine Forest Under Different Climate Scenarios 98
Objectives 4B: Cogongrass Plant Functional Type Development 101
Objectives 4B/4C: Constraint of Cogongrass Root Respiration 102
Objectives 4B/4C: Constraint of Cogongrass Biomass and Allometries 105
Objectives 4B/4C: Constraint of Cogongrass Photosynthesis -- Data Collection....106
Objective 4A: Constraint of Cogongrass Photosynthesis -- Parameter Estimation 107
Objectives 4B/4C: Cogongrass Sensitivity to Drought 108
Objective 4D: Developing a Method for Scaling Contagious Disturbance in a Spatially Implicit Way 109
RESULTS AND DISCUSSION....110
Objective 4A: Southern Pine Forest Under Different Climate Scenarios 110
Objective 4B: Cogongrass Plant Functional Type Development....116
Objectives 4B/4C: Cogongrass Biomass and Allometries 120
Objectives 4B/4C: Cogongrass Sensitivity to Drought 120
Objective 4D: Developing a Method for Scaling Contagious Disturbance in a Spatially Implicit Way 123

PART 5: DECISION SUPPORT TOOL 134

TECHNICAL APPROACH 135
Structured Interviews with Installation Decisionmakers....135
R Shiny Web Application....135
RESULTS AND DISCUSSION....136
Structured Interviews with Installation Managers....136
Decision Support Tool....137

Literature Cited 140

APPENDIX A – SUPPLEMENTAL TABLES AND FIGURES 156

APPENDIX B – STRUCTUED INTERVIEW SCRIPT....166

APPENDIX C – PUBLICATIONS 168

List of Tables

Table Title — Page #

Table 1. Summary of plots sampled across all installations. 26

Table 2. Tree health categories and tree canopy positions.....30

Table 3. Path model variables and description.....37

Table 4. Coefficient estimates for each sub-model in the fitted path model (Figure 14). Coef = unstandardized coefficient estimate, SE = standard error of Coef, DF = degrees of freedom, P = estimated p-value of the coefficient, Std. Coef = standardized coefficient estimate. 40

Table 5. Estimated marginal (fixed-effects only) and conditional (fixed and random effects) R^2 for each sub-model in the path analysis. 41

Table 6: Direct, indirect, and total effects on tick abundance from the path model in Figure 14, assuming effects only when $P<0.05$ for the estimated path coefficient (bolded values in Figure 14). 41

Table 7. Totals from all dung surveys across installations. 45

Table 8. Laboratory and field methods used to experimentally manipulate fuel characteristics (fuel type and fuel bed) and the fire characteristics that can be measured using each method. See Figure 1 for a visual depiction of how different methods can be used to evaluate fuel type and fuel bed characteristics. 57

Table 9. Microclimate conditions across native and invaded plant communities....78

Table 10. Tick survival and hours below 80% RH 80

Table 11. Tick survival and daily maximum temperature at mortality....80

Table 12. Climate covariates for cox regression (hazard model)) 80

Table 13. Estimated effects from regression models for effects of habitat type, host activity, and their interaction on tick abundance from field observations....81

Table 14. Information on the amplicons used in this study. 87

Table 15. The number of ticks analyzed for tick-borne agent DNA, with information on tick species collected from each of nine military installations sampled. Not included here are 1 *A. maculatum* adult and 3 *I. scapularis* nymphs collected from non-DoD areas while sampling cogongrass-invaded habitats....89

Table 16. The number of ticks of each species that expressed specific tick-borne agent DNA. 94

Table 17: Data used to constrain Cogongrass Parameters 101

Table 18: Sample sizes of states, ecoregions, and disturbance mechanisms. 131

Table A1. Weather during experimental fires. Date of fire, fuel structure, amount of biomass, air temperature averaged over the duration of the fire, relative humidity averaged over the duration of the fire, and wind speed averaged over the duration of the fire ± standard error.....157

Table A2. Time above 100 ºC model coefficients. Includes significant interaction term of biomass and fuel structure. 160

Table A3. Maximum temperature model coefficients. 161

Table A4. Model coefficients for flame height, rate of spread, and proportion of mass consumed. 162

List of Figures

Figure Title Page #

Figure 1. Study area map showing the location of each installation sampled. 24

Figure 2. Typical native and invaded (cogongrass) communities. 25

Figure 3. Summary of overall experimental design for field data collection. 26

Figure 4. Burn unit map example.....27

Figure 5. Field plot design. 28

Figure 6. Example stem map for Eglin AFB plot B1.....29

Figure 7. Sampling 1 m and 25 cm quadrats.....31

Figure 8. iNaturalist SERDP project https://www.inaturalist.org/projects/serdp-species 32

Figure 9. Installing rain shield on tick trap. 33

Figure 10. Tick-hosts dung survey and identification. (a) Field technician Elena Meyer surveying for tick-host dung, (b) turkey dung, (c) deer dung, (d) rabbit dung. 34

Figure 11. Conceptual diagram of relationships among climate change, fire management, vegetation, host abundance, and tick-borne disease exposure risk. 35

Figure 12. Path model structure. Variable descriptions are in Table 3. 36

Figure 13. (a) Number of plots established at each of the DoD installations. (b) Number of plots established in each time since fire. The color shading indicates whether or not plots were in a cogongrass invasion - light blue is uninvaded and red is invaded. 38

Figure 14. Estimates from fitted path model using abundance of all hosts. Standardized path coefficients indicate relative strength of direct effects. In the dense portion of the graph, highlight color of coefficients corresponds to the response variable. AIC = 4833; Chi-squared = 20 (df = 23, P = 0.63); Fisher's C = 156 (df = 46, p = 0). Passes maximum likelihood test (Chi) but not d-sep (Fisher's) for acceptable fit because of very small P-values of "missing" paths. *Bold coefficient values = P<0.05. Values on dashed paths = P>0.1. Normal text on solid paths = 0.05<P<0.1. Red dash-dot-dot lines are "missing" paths identified during model fitting.* 39

Figure 15. Marginal effects plots for the significant predictors in the tick abundance sub-model in the path analysis. Predicted relationships are with all other variables held at their mean values. 42

Figure 16. Marginal effects plots for sub-models of logit litter cover (top row), litter depth (lower left), and understory biomass (lower right). 43

Figure 17. Marginal effects plots for canopy cover, time since fire, and fire return interval (left to right) sub-models of the path analysis. 44

Figure 18. Marginal effects plots for significant predictors in the host abundance sub-model of the path analysis.....45

Figure 19. Boxplots of annual averages (1980-2018) for Daymet climate variables at each installation.....46

Figure 20. Average maximum temperature (left) and average monthly precipitation (right) across the sampling region in the southeast U.S.....46

Figure 21. Number of trees recorded at each installation. The majority of trees belonged to the genus *Pinus* or *Quercus*. 47

Figure 22. Host species densities at each installation (dung clusters 400 m^{-2}). Note that the y-axis has different scales in each panel. Zeroes (no bars) are installations that weren't sampled during that year.....48

Figure 23. The four most commonly collected tick species. (a) *Amblyomma americanum* (lone star tick), (b) *Dermacentor variablis* (American dog tick), (c) *Amblyomma maculatum* (Gulf Coast tick), (d) *Rhipicephalus sanguineus* (brown dog tick). 50

Figure 24. Tick abundances grouped by (a) life stage and (b) species in each sample year. Am. am: *Amblyomma* americanum, Am. mac: *Amblyomma maculatum*, De. var: *Dermacentor variablis*, Rh. san: *Rhipicephalus sanguineus*. Blue indicates uninvaded and red indicates cogongrass-invaded.....51

Figure 25. Tick abundances at each installation for each sample year. Blue indicates uninvaded and red indicates cogongrass-invaded.....51

Figure 26. Conceptual diagram of laboratory and field methods used to experimentally manipulate fuel type and fuel bed characteristics. Dashed box (combustion table) indicates that vertical orientation is possible, however the predominant approach uses piled fuels. Dashed box (in situ) indicates areas where observational comparisons of fuel type and fuel bed characteristics can be made, but experimental manipulations are limited. Methods are ordered top to bottom by their applicability to natural systems (gray shading). There are few examples of experimental field methods that retain fuel structure, which is the primary purpose of the method described here. Adapted from tables and figures in Whelan (1995), DeBano *et al.* (1998), Gill and Zylstra (2005). See Table 1 for references and details on fire intensity measurements that can be made using each method.....56

Figure 27. Schematic of the fuel structure manipulation device (a) Schematic legend: 1. 3.18 cm (1-1/4") punched angle iron holding welded 4 gauge wire with approximately 10 cm x 10 cm openings; 2. 1.91 cm (¾") metal conduit; 3. flame retardant soaked cotton twine; 4. temperature data loggers (U12 HOBO J,K,S,T thermocouple loggers, Onset Computer Corporation, Bourne, MA, USA), inside of weatherproof cases (Pelican 1010 Micro Case, Torrance, CA, USA) with foam inserts (Pelican 1012 Pick N Pluck); and 5. type K thermocouples (Model TP875, Extech Instruments, Nashua, NH, USA) with braided steel wire leads and a 2 mm welded bead. The device during an experimental burn (b) and prior to burning an equal amount of standing (c) and piled (d) fuel.....59

Figure 28. Fitted regressions (solid lines) with 95% CI (shaded area) plotted over data from each experimental fire for the calculated estimates of heating duration (time temperatures exceeded 100 ºC) (a-c, note different scales of y-axes) and maximum temperature (ºC) (d-f) versus fuel load for piled and standing fuel structures at 50- , 25- , and 0-cm above ground level. The predicted line for maximum temperature at 50 cm is for air temperature at its mean of 26.55. Red is piled fuels; light blue is standing fuels. 62

Figure 29. Predicted relationships (solid lines) plotted over observed data points from each fire for flame heights (cm) (a), rate of spread (m s^{-1}) (b), and percent of mass consumed (c) for piled or standing fuel structure across fuel load treatments. Red lines are for piled fuels, light blue lines are standing fuels. The predicted lines for flame height and rate of spread are with air temperature held at its average of 26.55. 63

Figure 30. Conceptual diagram of two pathways that contribute to tick-borne disease risk. Native and invaded plant communities may have different effects on both host (e.g., deer, rodent) abundances and tick survival, which together determine tick abundance and, in turn, influence tick-borne disease risk. 68

Figure 31. Ticks in mesh bags inside wire mesh exclosures along with PVC housing for temperature and relative humidity loggers in (a) invaded and (b) native plant communities. Representation of (c) the field study site showing invaded to the left and native plant communities to the right, separated by managed boundary area to maintain distinct plant communities. 70

Figure 32. Adult and nymph ticks in mesh bag. 71

Figure 33. Site locations (purple circles) across Florida, background shading indicates documented invasions of cogongrass (n = 74,785) from 1990-2020 (eddmaps.org). 74

Figure 34. Changes in plant community structure within *I. cylindrica* invaded plant communities. Mean (± SE) (a) vegetation height, (b) standing biomass kg per m^2, and (c) light availability at the soil surface (µmoles m^2 sec^{-1}), and (d) overstory canopy cover for invaded and native plots of the tick survival experiment, significance between invaded and native treatments was determined using analysis of variance, *** $p < 0.001$.....75

Figure 35. Tick survival per plot and microclimate conditions in native and invaded areas. Mean (± SE) survival of (a) nymph, and (b) adult *Amblyomma americanum* in native (blue) and invaded (red) plots over time. Box plots below panels (a) and (b) represent the time to 100% mortality per plot. Microclimate conditions: (c) average daily minimum relative humidity (%), dotted line indicates critical equilibrium humidity for *Amblyomma americanum* (80% RH), and (d) average daily maximum temperature (ºC). Points in (c) and (d) are daily averages across all data loggers (n= 12) in each treatment. Curved lines in panels (c and d) indicate least squares regression (solid) and 95% CI (dashed) for native and invaded areas.....77

Figure 36. Microclimate stressors related to duration of individual tick survival in native and invaded areas. Number of days survived for individual nymph and adult life stage ticks and microclimate conditions that were experienced in either native (blue) or invaded (red) plots. Panels (a-b) depict the relationship between days survived and

hours per day below 80% relative humidity, panels (c-d) show the relationship between days survived and the maximum temperature that was experienced prior to mortality. Best fit line (dashed) with 95% confidence interval (solid) from ordinary least squares regression is also represented. Box plots indicate median and 25th and 75th percentile, with 10th and 90th percentile whiskers for days survived (y-axes) and microclimate conditions experienced by individual ticks in each treatment (x-axes). 79

Figure 37. The effect of host use (deer activity) on tick abundance (nymph and adult ticks) collected from tick traps in native (blue) and invaded (red) plant communities. Best fit lines (solid) from linear mixed effect models with 95% confidence interval (dashed lines). Invaded (n = 32, native n = 19). 81

Figure 38. Relative prevalence of tick-borne agents detected from 931 tick samples analyzed. Most ticks contain more than one tick-borne agent, including nonpathogenic endosymbionts, human pathogens, wildlife pathogens, and microbes of unknown pathogenicity.....93

Figure 40: Representation of individual-level fluxes within ED2 from Moorcroft et al 2001. Left is the partitioning of carbon and water among tissues (B_a is active tissue, B_s is structural tissue). *y* is the patch and *t* is time, g is growth rate, **x** is the plant functional type, **z** is the size, and **r** is the resources available to the plant. The lambda represents the fire scheme implemented in the original ED version, which we are not using for reasons discussed below. 98

Figure 41: Projected meteorological drivers for projections into 2100. With the exception of CO_2, all meteorological drivers are identical up until 2026. In the mean precipitation flux and temperature panels, "Elevated Temp" scenarios and "RCP4.5" scenarios are identical, and closely overlaid. In the CO_2 panel, "RCP4.5" and "Elevated CO2" are identical. Drivers that are not plotted include: specific humidity, northward and eastward wind, shortwave flux, longwave flux, and air pressure. Meteorology used to drive ED2 is at 3-hour resolution, plotted here with yearly means. 100

Figure 42: 2018 Field Season Open-path Root Respiration measurement technique using LI-COR 6400 104

Figure 43: 2019 Field Season Closed-path Root Respiration measurement technique using LI-Cor 6400-09 soil chamber. Box A shows soil respiration chamber. Box B shows example fine roots being weighed. Box C shows the average CO_2 measurements through time. Box C corresponds to fine root measurement #15. 105

Figure 44: Estimate of stomatal slope from light curves. Each leaf had photosynthesis measured across progressive light changes. Different colored dots are distinct leaves. Dotted lines show 95% confidence interval.....108

Figure 45: Red is regression of the form Drought Soil Moisture = Ambient soil moisture* 0.5375376. The green line is a 1:1 reference line. 109

Figure 46. Meteorological scenarios effect on Gross Primary Production in Duke Forest, North Carolina. Fluxes smoothed with ggplot loess function for ease of interpretation (Wickham 2011). 112

Figure 47. Temperature Sensitivity by Meteorological Scenario at Duke Forest.....113

Figure 48. Water Use Efficiency by Meteorological Scenario at Duke Forest.....114

Figure 49. Daily Leaf Area Index by Metrological Scenario. The lower "trend" is the leaf area index of the coniferous species in the winter, and the upper "trend" is the combination of coniferous species and deciduous species. Note that coniferous species and deciduous species are not plotted separately, but the lower "trend" is visible because coniferous species contribute all of the Leaf Area Index during winter months……...115

Figure 50. Annual Biomass by Metrological Scenario through time. Line textures distinguish the two different plant functional types, Late Temperate Deciduous (ie: *Quercus*) and Southern Pines (ie: *Pinus taeda*, *Pinus elliottii*, and *Pinus palustris*). Lines were smoothed using the ggplot loess function (Wickham 2011). 116

Figure 51. Variance Decomposition of Net Primary Production in a Cogongrass Stand.....117

Figure 52. Variance Decomposition of Gross Primary Production for Cogongrass Stand.....118

Figure 53. Variance Decomposition of Transpiration in a Cogongrass Stand.....118

Figure 54. Variance Decomposition of Leaf Area Index in a Cogongrass Stand.....119

Figure 55. Variance Decomposition of Respiration in Cogongrass Stand 119

Figure 56: Density plots of root allocation from BARS ambient and drought treatments. Calculated from ratio of rhizome and fine roots divided by aboveground biomass. A two-sample Kolmogorov-Smirnov test found a significant difference at a 0.05 alpha (p-value = 0.045, D = 0.59). 120

Figure 57: Comparison of trait sensitivity and uncertainty under ambient and drought conditions. 122

Figure 58. Comparison of Gap dynamics Contagious disturbance simulation. (Left column) Gap dynamic simulation. (Right column) Contagious disturbance simulation. (Top left) spatial map of stand age, with color on a log scale from youngest (red) to oldest (yellow), (Top right) spatial map of stand age for contagious disturbance, with color on a log scale from young (red) to old (yellow) and with new disturbances (age = 0) in white. (Middle left) simulated stand age distribution (black) when disturbance probability is 1% compared to geometric expectation (green), (Middle right) simulated stand age distribution (black) when disturbance probability is 1% and spread probability is 25% compared to geometric expectation (green), (Bottom) spatial adjacency matrix by age class aggregated into 10 year bins ([0 − 9] = 0, [10 − 19] = 1, etc.) with all patches 100 year or older in bin 10. Matrices are colored from white (highest adjacency) through orange to green (lowest adjacency). 127

Figure 59. Validation of the analytical model's ability to predict disturbance area as a function of spread probability (disturbance initiation probability of 1%). Simulations run on a 4-sided grid so, for example, a 0.25 spread probability corresponds to four independent chances, each 25%, to spread. The analytical approximation appears to underestimate disturbance at high spread probabilities. 128

Figure 60. Adjacency for small disturbances. Edges are labeled as (E)xterior and (I)nterior. For size 1, there is 0 probability of self-adjacency (disturbed patches adjacent to other disturbed patches). For size 2 and 3 it is 1/4 and 1/3 respectively, while for size 4 the adjacency is either 1/2 (square configuration) or 3/8 (all other configurations).....128

Figure 61. Comparison between adjacency matrices for a stochastic spatial simulation analytical approximation (top), and analytical approximation where a correction was applied to A00. All adjacency matrices are after 1,000 years (steady state). To the right are difference matrices between the simulation matrix and the two analytical matrices. Age class aggregated into 10 year bins ([0 − 9] = 0, [10 − 19] = 1, etc.) with all patches 100 year or older in bin 10. The 10th column of the error matrices was removed because of a summing to 1 constraint. 129

Figure 62. Size density plots showing the contrasts between ecoregion/state and disturbance type. Colored boxes next to disturbance size density curves show what ecoregion contains the respective disturbance. Sample sizes associated with density plots can be found in Table 18. 130

Figure 63. Mean trends of Ecoregion within State. Gray hexes correspond to binned-counts of number of disturbance events. Black lines correspond to core and linear bounding cases. 132

Figure 64. Mean trends of disturbance type. Gray hexes correspond to binned-counts of number of disturbance events. Black lines correspond to linear bounding cases. 133

Figure 65. Two sample screenshots from decision support tool prototype. Data shown come from tick sampling and pathogen analyses from earlier sections. Prototype is hosted at https://serdp2636.shinyapps.io/serdp2636/ 139

Figure A1. Experimental setup for simultaneous ignition of devices that have the same fuel loads but different fuel structures. 163

Figure A2. Temperatures recorded each second during each experimental fire (shaded areas) with the average temperature profile across the fires at each fuel load and probe height (solid lines) for piled (red) and standing (blue) fuels at (0, 25, and 50 cm heights). The inset figure to the right in each panel shows the mean (+SE) of the maximum fire temperatures. The bottom inset figure in each panel shows the average time across the set of fires that temperature exceeded 100 °C. 164

List of Acronyms

ALFRESCO: Alaska Frame Based Ecosystem Code
BARS: Bivens Arm Research Site
BGC: BioGeoCehmical
BLAST: Basic Local Alignment Search Tool
CMIP5: Coupled Model Intercomparison Project Phase 5
CO_2: Carbon dioxide
CWD: Coarse woody debris
DBH: Diameter at Breast Height
DNA: Deoxyribonucleic acid
DoD: Department of Defense
dsb: Disulfide Oxioreducatse gene
DVM: Dynamic Vegetation Model
ED or ED2: Ecosystem Demography or Ecosystem Demography version 2
EnKF: Ensemble Kalman Filter
FACE: Free-Air Carbon dioxide Enrichment
FIA P3: Forest Inventory & Analysis Phase 3
HPCBio: High Performance Computing in Biology
IPCC: Intergovernmental Panel on Climate Change
MCFIRE: Fire module of dynamic vegetation model MC1
MCMC: Markov Chain Monte Carlo
NCBI: National Center for Biotechnology Information
NFDRS: National Fire Danger Rating System
NGS: Next Generation Sequencing
NPP: Net Primary Productivity
NSF: National Science Foundation
NWR: National Wildlife Refuge
OLS: Ordinary Least Squares
ompB: Outer Membrane Protein B gene
PCR: Polymerase chain reaction
PEcAn: Predictive Ecosystem Analyzer
PFT: Plant Functional Type
PPFD: Photosynthetic Photon Flux Density
PVC: Polyvinyl chloride
RCP: Representative Concentration Pathways
RH: Relative Humidity
RLB: Reverse line blot
rRNA: Ribosomal Ribonucleic Acid
SEM: Structural Equation Model/Structural Equation Modeling
TBAs: Tick-Borne Agents
TBDs: Tick-borne Diseases
UF: University of Florida
VM: Virtual Machine
VMC: Volumetric Water Content

Acknowledgements

The research reported here is funded by the Strategic Environmental Research and Development Program (SERDP Project RC-2636). We are deeply grateful for the invaluable contributions of numerous personnel to this research, listed below. In addition, we wish to thank Mark Band, Chris Fields, Alvaro Hernandez and Gloria Rendon for their assistance in designing a Fluidigm Access Array system for the detection of the numerous tick-borne agents reported here. We also are grateful for the assistance from Penny Broga, Jessi Katterhenry, Betsy Lindsey, Kelly Wilder, and Ryan Chance with budget management and travel logistics. Finally, this work could not have been completed without the generous support of land management personnel and leadership at each installation.

Project Personnel:

Co-PIs: Michael Dietze, Luke Flory, Allison Gardner

Project Manager and Postdoctoral Associate: Whalen Dillion

Associate Project Manager: Drew Hiatt

PhD Candidate: Tempest McCabe

Pathogen analysis: L. Page Fredericks

Research technician: Steven Cabrera

Field technicians: Taylor Clark, Christina Harden, Tyler Hedlund, Elena Meyer, Alison Ochs, Manuel "Manny" Perez, Elizabeth White

Abstract

Objective: Tick-borne diseases (TBDs) represent a major public health threat in North America, particularly for military personnel training on Department of Defense (DoD) installations. Ecological theory predicts that climate change will likely alter vector-borne disease transmission by a variety of direct and indirect pathways. We explored several of the predicted consequences of climate change, including altered fire regimes and plant communities, and their interactions with wildlife, for human risk of exposure to TBDs in the southeastern U.S. Our specific objectives were to: 1) Evaluate the interactions between fire and plant invasions spanning a gradient in fire management, invasive plant distribution and abundance, and climatic conditions across the southeastern U.S.; 2) Quantify the effects of fire and plant invasions, and their interactions, for variation in wildlife abundance, tick abundance, tick-borne pathogen infection rates, and TBD risk to humans; and 3) Calibrate a spatially explicit model of TBD risk in response to fire-invasion interactions and incorporate simulations of climate change scenarios to examine the responses of fire, plant invasions, wildlife, TBD risk, and their interactions.

Technical Approach: We sampled nine DoD installations to empirically examine the interactions between fires and plant invasions spanning a climate gradient across the southeastern U.S. Across these sites we utilized gradients in fire management and plant invasions to perform multiple surveys of vegetation, wildlife, tick abundance, and tick-borne pathogen prevalence. We also conducted mechanistic experiments to quantify plant-fire-tick interactions. Using these empirically derived estimates from the field and laboratory, we employed a structural equation modeling (SEM) framework to test the direct and indirect effects of fire regimes, plant invasions, host abundance, tick abundance, and pathogen prevalence, on TBD exposure risk. Additionally, we developed an ecosystem-based model capable of capturing the physiology of a focal invasive plant species, and used these relationships to develop a web-based Decision Support Tool that will allow site managers to integrate decisions concerning application of prescribed fire, control of invasive plant species, and mitigation of tick-borne disease risk.

Benefits: Recent research has addressed only individual components for the effects of climate, fire, and plant invasions on TBD exposure pathways; no effort has evaluated the many potential interactions and feedbacks that may mediate the effects of any one component on the transmission of TBDs. This research will provide new understanding of the multitude of factors that determine TBD risk. The results of our study will be directly applicable to predicting TBD risk under non-stationary conditions, which can then be used to inform management decisions for mitigating disease risk currently and in the future. We created a web-based interface for forecasting TBD risk under alternative management scenarios accessible to land managers at DoD installations and other federally managed sites. Movements of military personnel could be adjusted to account for areas of high risk, and the strategic deployment of other management approaches will be enhanced. The combination of outputs and deliverables from these efforts will not only benefit personnel operating on military installations in the southeastern U.S. but potentially will offer widespread benefits to public health throughout the region.

Executive Summary

Introduction

Longleaf pine (*Pinus palustris*) was at one point the most ecologically significant tree species in the southern United States. A typical longleaf pine forest can be described as open-canopy, fire-dependent forests with an herbaceous ground layer littered with grasses and diverse showy forbs. Longleaf pine forests are some of the most diverse natural areas in North America, with up to 40 vascular plant species in $1m^2$ (Walker and Peet 1984). Before major logging and industrial efforts, longleaf pine forests dominated the southeast covering approximately 92 million acres (Frost 2007). The longleaf pine's native range stretched along the Gulf and Atlantic coasts from Eastern Texas through to Virginia, and as far south as Central Florida (Boyer 1990). By 2005, an estimated 2.6 million acres of longleaf pine forest remained in its native range (Frost 2007). After decades of conversion to agricultural lands and industrial urban developments, the longleaf pine ecosystem is one of the most endangered in the U.S. (Noss et al. 1995).

Prescribed fire has been established as an important ecological process for the restoration and maintenance of longleaf pine systems. Frequent fire, every 1-10 years (Chapman 1932), are vital to reducing fuel loads and promoting understory diversity (Kirkman et al. 2001). Regularly burned and maintained longleaf forests provide essential habitat for many threated and endangered wildlife species, including the gopher tortoise (*Gopherus polyphemus*), Eastern indigo snake (*Drymarchon couperi*), and red-cockaded woodpecker (*Picoides borealis*) (Wade et al. 1989). Without regular fire in this ecosystem, longleaf forests can suffer from invasion of hardwoods and shrubs, resulting in rapid loss of herbaceous diversity (Christensen 1981). However, tree mortality can be an issue when reintroducing fire to long-unburned pine forests. Drier duff layers (less than 55% VMC) during fire exhibit the most consumption of duff and can contribute to up to 20% overstory longleaf pine mortality in historically fire excluded areas (Varner et al. 2007). When restoring fire to long-unburned forests, Varner et al. (2007) argue to implement burn prescriptions at regular intervals and to include effects of duff consumption to minimize tree mortality.

Disturbance events such as fire, hurricanes, and harvesting also have been shown to increase risk of invasion by exotic plants. Cogongrass (*Imperata cylindrica*) is a cosmopolitan grass species that is a weedy pest in at least 73 countries and is especially problematic in the southeastern U.S. where it spreads and dominates in disturbed sites (Holm et al. 1977, MacDonald 2004). It is a successful invader in longleaf pine forests due to its extensive rhizome system, adaptation to poor soils, drought tolerance, and fire adaptability (Holm et al. 1977). Cogongrass rhizomes have been reported to account for 60% of a plant's total biomass and contribute to its quick regeneration after burning or cutting (Sajise 1973). In areas where cogongrass is already present, locations that have been burned or have had greater biomass removal experience an increase in the number and size of cogongrass patches (Holzmueller and Jose 2012). Once established, cogongrass can outcompete native vegetation creating a large monotypic understory with low species diversity and richness (Brewer 2008). Positive feedbacks between cogongrass and fire have been suggested due to greater fine fuel loads (Platt and Gottschalk 2001) and fire severity that is detrimental to southeastern pine forests (Lippincott 2000, Matlack 2002). Cogongrass may also alter typical fire cycles of southern forests. Fires in sites where cogongrass is dominant show higher maximum temperatures at greater heights, and

increased mortality of longleaf pines, which are typically fire-tolerant (Lippincott 2000). Research in Florida sandhill found cogongrass to burn at a maximum temperature of 458 °C with a mean of 260.9 ± 13.7 °C, and native areas burned at a maximum of 318 °C with a mean of 218.3 ± 14.5 °C (Lippincott 2000). The spread of cogongrass is responsible for the loss of thousands of hectares of native habitat in southeastern U.S. forested lands (MacDonald 2004).

Objectives

Tick-borne diseases (TBDs) represent a major public health threat in North America, particularly for military personnel training on Department of Defense (DoD) installations. Ecological theory predicts that climate change will alter vector-borne disease transmission both by direct and indirect pathways. A likely consequence of climate change is an increase in the frequency and intensity of wildfires and a decrease in the effectiveness of fire management (Oswald et al. 2007). The forests of the southeastern U.S. are predicted to experience a profound increase in wildfire frequency and severity (Scholze et al. 2006). This region of the U.S. also suffers high human incidence of several TBDs, particularly those transmitted by the lone star tick (*Amblyomma americanum*), an emerging disease vector that is affected significantly by plant invasions (Allan et al. 2010a) and by fire dynamics via direct effects on ticks (Davidson et al. 1994b) and indirect effects on tick hosts (Allan 2009).

We are investigating several of the predicted consequences of climate change, including altered fire regimes and plant communities, and their interactions with wildlife, for human risk of exposure to TBDs in the southeastern U.S. We utilize an integrated research effort to understand the consequences of climate change for TBD risk and human health, and to make specific, actionable recommendations to predict and ameliorate future changes in pathogen exposure pathways. Specific objectives of this research include to:

1) Perform field surveys across DoD installations spanning a climate gradient in the southeastern U.S. to quantify relationships among climate, prescribed fire, and cogongrass invasion, and their interactions, for effects on plant community composition and biomass, wildlife abundance, and tick abundance in longleaf pine habitats.
2) Conduct field experiments to determine the A) effect of fuel structure on fire temperature and residence time of invasive cogongrass, including relationships between fuel load, flame height, and fire intensity, and B) influence of cogongrass on off-host survival for *A. americanum* ticks.
3) Develop a next generation sequencing (NGS) protocol for the identification of a multitude of tick-borne agents (TBAs) associated with ticks in the southeastern U.S. and analyze the prevalence of pathogens that imperil human and wildlife health.
4) Calibrate a vegetation model (Ecosystem Demography 2, ED2) for DoD installations under future climate, fire, grass invasion, and management scenarios. Use relationship between tick abundance and vegetation to couple future vegetation with future TBD risk. Model TBD risk in response to fire-invasion interactions and incorporate simulations of climate change scenarios to examine the responses of fire, plant invasions, wildlife, TBD risk, and their interactions, in southern pine ecosystems.

Technical Approach

To assess the effects of climate, fire management, plant invasions, and their interactions on tick-borne disease risk, we took advantage of existing gradients in climate, fire management, and invasion history across numerous DoD installations spanning the southeastern U.S. Installations typically have multiple larger management units or training areas that are made up of smaller burn units. We obtained fire management history data for each of the DoD installations sampled in this study, and selected a representative subset for sampling biological parameters related to the study objectives. The goal of our experimental design was to assess the potential effects of fire history (e.g., years since most recent burn) and cogongrass infestation on host availability, plant community composition, and tick abundance across installations throughout the study region. The study region is defined as five states in the southeastern U.S. (i.e., Mississippi, Alabama, Georgia, South Carolina, and Florida). Within the study region, we collected data at nine military installations (i.e., Avon Park Air Force Range, Florida; Fort Benning, Georgia; Fort Gordon, Georgia; Camp Blanding, Florida; Eglin Air Force Base, Florida; Fort Jackson, South Carolina; Moody Air Force Base, Georgia; Camp Shelby, Mississippi; Tyndall Air Force Base, Florida). Each installation is divided into burn units, with different fire management histories. At least one sample plot was established within each burn unit selected. These plots were considered the smallest experimental unit of replication for all data analyses.

Following this experimental design, we established plots to achieve a stratified sampling that covered the range of fire history at each installation. We obtained fire history and known cogongrass invasions as GIS layers from each installation and identified potential plot locations based on time since last fire and history of cogongrass invasion. In burn units with a cogongrass invasion we established one plot in the invaded area and one plot in an uninvaded area, with at least 100 meters between the plots. In burn units without an invasion we established one plot in an area representative of the vegetation conditions in the burn unit. Each plot consisted of a main circular center plot (12.6 m radius, approximately 500 m^2), a circular subplot (5.64 m radius, approximately 100 m^2), four 1 m x 1 m quadrats, four 25 cm x 25 cm quadrats, four 50 m transects, and four locations for sampling tick abundance. In the main circular plot and subplot, we measured trees, saplings, and shrubs. Ground vegetation and litter were measured in 1 m and 25 cm quadrats located 10 m from plot center in each of the cardinal directions. The 50 m transects originated at the plot center going in each cardinal direction and were used to estimate tick-host abundance. Tick abundance sampling locations were placed 8-10 m from the plot center in the NW, NE, SE, and SW areas. We used structural equations modeling (SEM) to evaluate the hypothesized direct and indirect effects of climate, fire management, vegetation, and host abundance on tick-borne disease exposure risk.

Few studies have attempted to quantify changes in fire intensity in forests when invasive plants are present, greatly limiting predictions of forest invader impacts on fire behavior and effects. We developed a logistically tenable and relatively low-cost method for experimentally assessing the influence of fuel characteristics on fire behavior. The methodology we developed is general, enabling manipulation of fuel type and fuel bed characteristics. Specifically, our methodology utilized a free-standing metal device that maintains vertical orientation of fuels to more accurately mimic realistic fuel structure and generate inferences for ecological effects on forest systems. To test the methodology, we conducted experiments using cogongrass, a non-native invasive grass of Asian origin that is widespread in forests of the Southeast United States

To test the device and evaluate effects of fuel structure and fuel load on ecologically relevant measures of fire behavior, we conducted experimental fires where fuels were all piled or all standing for a range of fuel loads. We made and compared measurements of heating duration (time above 100 ºC in seconds, s), maximum temperature (ºC), flame height (cm), rate of spread (m s^{-1}), and proportion of fuel load consumed. Our primary objective was to evaluate the effect of fuel structure, specifically piled compared to standing fuels, on the above mentioned fire intensity metrics.

There is contradictory evidence on possible abiotic vs biotic mechanisms underlying invasive plant species effects on tick-borne disease. While there has been research on how different pathways may individually affect tick abundance, studies that simultaneously address multiple pathways are needed to improve disease risk predictions. Here, we sought to measure the contributions of plant invasion to tick survival, host activity, and their effects on tick abundance. Specifically, we evaluated how a plant invasion (cogongrass) affected microclimate conditions and survival of *A. americanum* compared to native species dominated areas, and how changes in relative host (i.e., white-tailed deer, *Odocoileus virginianus*) use influenced tick abundance. We conducted a field study where we measured temperature, relative humidity, and survival of experimental ticks in invaded and nearby native areas over 11 months. Separately, we evaluated relative host activity (via camera traps) and tick abundances in paired invaded and native areas in a field survey. To examine the effect of cogongrass invasions on tick survival, we established a survival assay in a planted longleaf pine (*Pinus palustris*) stand. We established 24 plots (1m x 1m), 12 in the invaded area and 12 native area, with at least 10m between plots. At the center of each plot, a 300-micron fine 10 x 20 cm nylon mesh bag containing 10 nymph and 10 adult (5 female and 5 male) *A. americanum* were placed in 50cm tall cylindrical wire mesh exclosures to deter interference from wildlife. Mesh bags were examined frequently for the first month (approx. every 7-10 days) and then approximately every 10-14 days afterward to determine nymph and adult survival.

Several of the most rapidly emerging vector-borne diseases in the U.S. are caused by zoonotic pathogens transmitted by the lone star tick (*Amblyomma americanum*). While several studies have assessed the distribution of some tick-borne agents (TBAs) in *A. americanum* across portions of the southeastern U.S. (e.g. Mixson et al. 2006), there has been no comprehensive analysis of field-collected tick specimens for all known TBAs due to the lack of an effective system for performing such an analysis. We developed a system using Fluidigm Access Array combined with Illumina sequencing to analyze all nymph and adult life stage ticks collected in this study for an unprecedented diversity of TBAs that imperil human, domestic animal and wildlife health. Ticks were collected from nine military bases in the southeastern United States during the summers of 2017 and 2018 using carbon dioxide-baited traps. We used primers developed for this study or published previously to target regions of four bacterial and one protozoan gene. Following DNA extraction and quantification, DNA samples were sent to the W. M. Keck Center for Comparative and Functional Genomics at the University of Illinois Urbana-Champaign where Fluidigm PCR and Illumina sequencing were performed. Library construction and sequencing were performed at the Roy J. Carver Biotechnology Center, University of Illinois Urbana-Champaign. A customized HiSeq analysis pipeline was created by the High Performance Computing in Biology (HPCBio) group at the University of Illinois Urbana-Champaign. After processing, “vsearch” was used to compare these sequences against a custom database. Reads were considered positive identifications to genus when a minimum

average percent identity of 97% to a database sequence was achieved, and were assigned to species when a minimum of 99% identity was achieved.

The fourth objective of this project was to connect modeled responses of forests, invasive cogongrass, fire regimes, land management under future climate scenarios to our understanding of the environmental controls on tick abundance and TBD risk (i.e., vegetation, climate, fire). Modeling future vegetation in the southeastern U.S. under different climate, disturbance, and invasion scenarios requires the development of new tools and techniques. We used the Ecosystem Demography 2 model (ED2), a spatially implicit cohort-based dynamic vegetation model (DVM), and the Predictive Ecosystem Analyzer (PEcAn), a common toolbox for working with and analyzing ecosystem models as well as accessible web-based tools for model execution. ED2 was run at a Duke forest in North Carolina, a southern pine forest site in the Southeast. Duke forest was chosen because it co-occurred with the site of a Free-air concentration enrichment experiment, which allowed more direct comparison of findings with other modeling and experimental studies. We wanted to explore how climate alone could affect the long-term successional trajectory of southern pine forests. We evaluated output for changes in successional trajectory, carbon sequestration, and water use efficiency. Next we incorporated cogongrass as a plant functional type (PFT) in ED2 by first incorporating our knowledge of a similar PFT developed for a grass of the same family with the same photosynthetic strategy (switchgrass; *Panicum virgatum*) into a new PFT that included cogongrass-specific knowledge. To determine which model parameters were most important to constrain against data, we first ran the cogongrass PFT at Avon Park AFR, FL under a range of parameter sets until we identified parameter ranges that produced appropriate levels of biomass that matched field observations. After that, we ran a full uncertainty and sensitivity analysis that formally quantified how uncertainty in different cogongrass traits contributes to uncertainty in state variables including evapotranspiration, net primary production, and biomass. This laid the groundwork for targeted constraint of cogongrass traits. Finally, we utilized the fire module in ED2 for scaling contagious disturbances in a spatially implicit way.

A final objective of our study was to synthesize our findings into a Decision Support Tool (DST) tailored to the needs of our partner installations. A number of DSTs exist already pertaining to the implementation of prescribed fire. However, these management decisions often are made in isolation from decisions concerning efforts to control plant invasions or mitigate tick-borne disease risk, for which there are no established DSTs at present to our knowledge. Therefore, we initiated development of a DST designed to integrate across multiple environmental management decisions in an effort to promote more holistic management practices better able to account for interacting environmental variables and multiple management objectives. To better understand installation needs for decision support surrounding tick-borne disease, invasive species, and fire, and how these fit into forest management goals more broadly, we completed 30-min structured interviews with a representative from five of the nine sampled installations. We built our DST as a R Shiny web application because 1) most of the underlying analyses performed for this project were conducted in R making for straight-forward harmonization of data, and 2) R Shiny is user-friendly and yet can perform complex data visualizations.

Results and Discussion

The overall objective of this research was to investigate the consequences of climate change, including altered fire regimes and plant communities, and their interactions with wildlife, for human risk of exposure to TBDs in the southeastern U.S. Through field surveys conducted in 2017 and 2018 spanning nine DoD installations, we evaluated the direct and indirect effects of climate, recent weather, fire management, vegetation, and host abundance, on ticks. We found that abiotic mechanisms are the major drivers of tick abundance, mediated by the indirect effects of fire on leaf litter accumulation and understory biomass. Litter cover and depth were positively related to tick abundance and time since fire, indicating that frequent fires lower tick abundance by removing litter. Interestingly, host abundance was unrelated to tick abundance, suggesting that abiotic effect of time since fire on litter cover and depth is a stronger determinant of tick abundance in longleaf pine forest than biotic pathway mediated by host abundance. Additionally, our results indicate that fire management (fire return interval) is primarily determined by characteristics of the installation (97% of variation explained by the random effect). Therefore, climate is not yet the most limiting factor for using prescribed fire as management tool at these installations but is predicted to be in the relatively near future.

One major experimental objective of this research was to accurately quantify the fire characteristics of invasive cogongrass. To meet this objective, we developed a freestanding, outdoor device that can be used to efficiently manipulate structure of fine fuels (<10 cm diameter) and measure fire characteristics relevant to assessing potential ecological effects of fire. The small-scale (1 m^2) experimental apparatus enabled repeated fires and measurements of fire characteristics across multiple fuel loads without the onerous task of establishing experimental plots prior to a prescribed fire. We demonstrated our methodology with cogongrass, a widespread and problematic invader in Southeast US pine forests that can limit the use of prescribed fire as a management tool in heavily invaded areas, and we report the most precise estimates to date of fire behavior from cogongrass-fueled fires. The maximum temperatures estimated during our experimental cogongrass fires frequently exceeded those reported by previous studies, as well as a number of others in longleaf pine ecosystems. Using thermocouples allowed us to measure, and report for the first time, heating duration (time above 100 ºC) for cogongrass-fueled fires. Notably, the heating duration from our experimental fires with standing fuels was similar to that of fires in native longleaf pine ecosystems. This similarity suggests that the effects of cogongrass on fire behavior in the Southeast USA, and its reported problematic nature, is driven by the higher fuel loads it generates compared to native vegetation.

Invasive plants are often linked to changes in tick-borne disease risk, but studies are needed that address both abiotic and biotic pathways. We examined mechanisms along the two main pathways that cogongrass invasions affect tick abundance (i.e. altered host activity and off-host tick survival). Using this approach, we showed that cogongrass increased longevity of ticks by buffering against hotter temperatures and lower relative humidity, and that time to 100% tick mortality was on average 57% longer for nymphs and 45% longer for adults in cogongrass-invaded compared to native plots. Our results suggest that tick abundance is maintained in cogongrass-invaded plant communities through the alteration of microclimate conditions that promote tick survival, while tick abundance is maintained in native areas by host activity. Contrary to previous studies, we did not find a correlation with increased host activity within invaded plant communities. Although similar abundances of host-seeking ticks were detected between invaded and native plant communities, the abundances appear to be maintained through different mechanistic pathways. Our results highlight that understanding just one of these pathways is not sufficient for predicting tick-borne disease risk within invaded areas. By

understanding how multiple abiotic and biotic mechanisms contribute to tick abundance, we can improve our predictions for how ongoing plant invasions impact tick-borne disease risk.

To assess the prevalence of a diversity of tick-borne pathogens and other microbes (collectively termed "tick-borne agents" or TBAs), we developed a next-generation sequencing (NGS) protocol using the Fluidigm Access Array system. We analyzed 931 ticks primarily collected as part of the field surveys across DoD installations in 2017 and 2018, and identified the presence of numerous pathogens, including causative agents in humans of anaplasmosis, ehrlichiosis, and spotted fever rickettsiosis. Using the NGS approach, we identified DNA from 32 unique TBAs in these field-collected ticks: 23 to species, seven to genus, and two which best matched to known sequences with 97% - 98.9% identity were designated as "-like" the closest species. Several important pathogens that may cause serious morbidity or mortality in humans were detected, including *A. phagocytophilum* (causative agent of anaplasmosis), *E. chaffeensis* and *E. ewingii* (causative agents of human ehrlichiosis), and the emerging *R. parkeri* (a causative agent of spotted fever rickettsiosis) associated with *A. maculatum*. We also detected a surprisingly high prevalence of "*E. muris subsp. eauclairensis subsp. nov.*" in *A. americanum*, which thus far has been reported only in *I. scapularis*, and likely is an important emerging agent of ehrlichiosis in humans. Collectively this generated a robust dataset across which to analyze the effects of time since fire and fire return interval, plant invasions, wildlife host densities, and climate, on the density of ticks, tick infection rates, and their product, the density of infected ticks. Together these dependent variables represent entomological estimates of disease risk, and the precise identification of a diversity of TBAs created an unprecedented knowledge of tick-borne disease risk for military installations in the southeastern U.S.

Through our development of ED2, we took advantage of the nine sampled southeastern DoD sites as an ecological system that have several interesting interacting dynamics. In the 2018 and 2019 field seasons, we collected six novel datasets, and incorporated 107 new measures into our representation of cogongrass in ED2, significantly reducing uncertainty in the representation of this plant species as a novel plant functional type. Our modeling demonstrates that cogongrass changes its carbon investment strategy based on climate, indicating a key mechanism by which future climate change may directly impact cogongrass invasions and indirectly impact tick-borne disease risk. Additionally, using the ED2 model we laid out a theoretical derivation for spatially implicit scaling of disturbances (e.g. prescribed and wildland fire), and explored the descriptive capacity of metrics that emerged. Implications of this technique apply widely to multiple problems in scaling through the improvement of ecosystem models, development of null models and characterization of disturbance regimes. Florida's disturbance regime reflects the fire management practices of the Southeast. We used a comparison between Oregon and Florida as a case study, and while both were frequently burned, Florida's fire regime was dominated by many small fires, and occasional large fires, whereas Oregon has a range of mid-sized fires. This lays the groundwork for coupling existing fire science to the ED2 model, and estimating the effects of fire. Next steps in this research include projections of interactions between cogongrass, fire, and tick populations.

Based on the considerable amount of data we collected on the interactions between climate, fire, plant invasions and tick populations on DoD installations, we sought to develop a Decision Support Tool (DST) for use by installation managers. To inform the development of this DST we conducted five interviews with managers at participating installations, and learned that day-to-day decision-making varied strongly between installations. However, installations have shared decision-making interests, and valued new insights from tick population and

pathogen data, cogongrass prevention and environmental effects data, as well as tree demographic change data. We have developed a prototype DST using R Shiny web application and at present it depicts three metrics of TBD exposure risk across the nine installations sampled in the course of this project. Development of the DST is ongoing.

Implications for Future Research and Benefits

This research yielded unprecedented insight into the complex pathways by which climate change, plant invasions and fire dynamics may interactively alter human risk of exposure to tick-borne diseases. Extensive field surveys spanning nine DoD installations in the southeastern U.S. revealed that abiotic factors, primarily the effect of frequent and recent prescribed fire on litter cover and depth, is the primary determinant of tick abundance in longleaf pine forests. From a management perspective, this evidence supports the application of prescribed fire as an efficacious strategy for reducing risk of exposure to tick-borne diseases on military installations. Using an experimental apparatus designed for this study, we confirmed that cogongrass creates high temperature fires, the duration of which are driven by the higher fuel loads it generates compared to native vegetation. These findings justify the considerable effort dedicated to control of cogongrass invasions on DoD installations. Additionally, we performed a field experiment in cogongrass-invaded and -uninvaded areas, and determined that cogongrass significantly enhances off-host tick survival. This suggests a possible benefit to human health from ongoing efforts to control or eradicate cogongrass invasions on DoD installations. For this research, we developed arguably the most sophisticated tool available for the detection of tick-borne pathogens in field-collected ticks, and detected a diversity of tick-borne agents not previously reported from DoD installations. Among these was "*E. muris subsp. eauclairensis subsp. nov.*", reported for the first time here in *A. americanum*. Our contributions to modeling of climate change impacts include the development and incorporation of cogongrass in ED2 as a plant functional type, which revealed the potential for future climate change to promote the invasion of this noxious invasive species in the U.S., further increasing the geographic range over which cogongrass can alter tick and fire dynamics. Finally, we are developing a DST for use by installation managers to integrate decision-making for the interacting challenges from performing fire management, controlling invasive plants, and mitigating tick-borne disease risk.

PART 1: FIELD SURVEYS ACROSS DOD INSTALLATIONS

TECHNICAL APPROACH

To assess the effects of climate, fire management, plant invasions, and their interactions on tick-borne disease risk, we took advantage of existing gradients in climate, fire management, and invasion history across numerous DoD installations spanning the southeastern U.S. Installations typically have multiple larger management units or training areas that are made up of smaller burn units. At some installations the burn units are the same as the training/management areas. There are training and ecological management needs that are considered in the management plan of each area, such as land navigation training for troops and maintaining habitat for species on the federal threatened and endangered species list (e.g. red cockaded woodpecker). The fire management applied to the burn blocks within the larger areas varies based on the vegetation and the training uses and management goals. The variety of objectives results in a range of fire histories across the study region. We obtained fire management history data for each of the DoD installations sampled in this study (Figure 1), and selected a representative subset for sampling biological parameters related to the study objectives (detailed below).

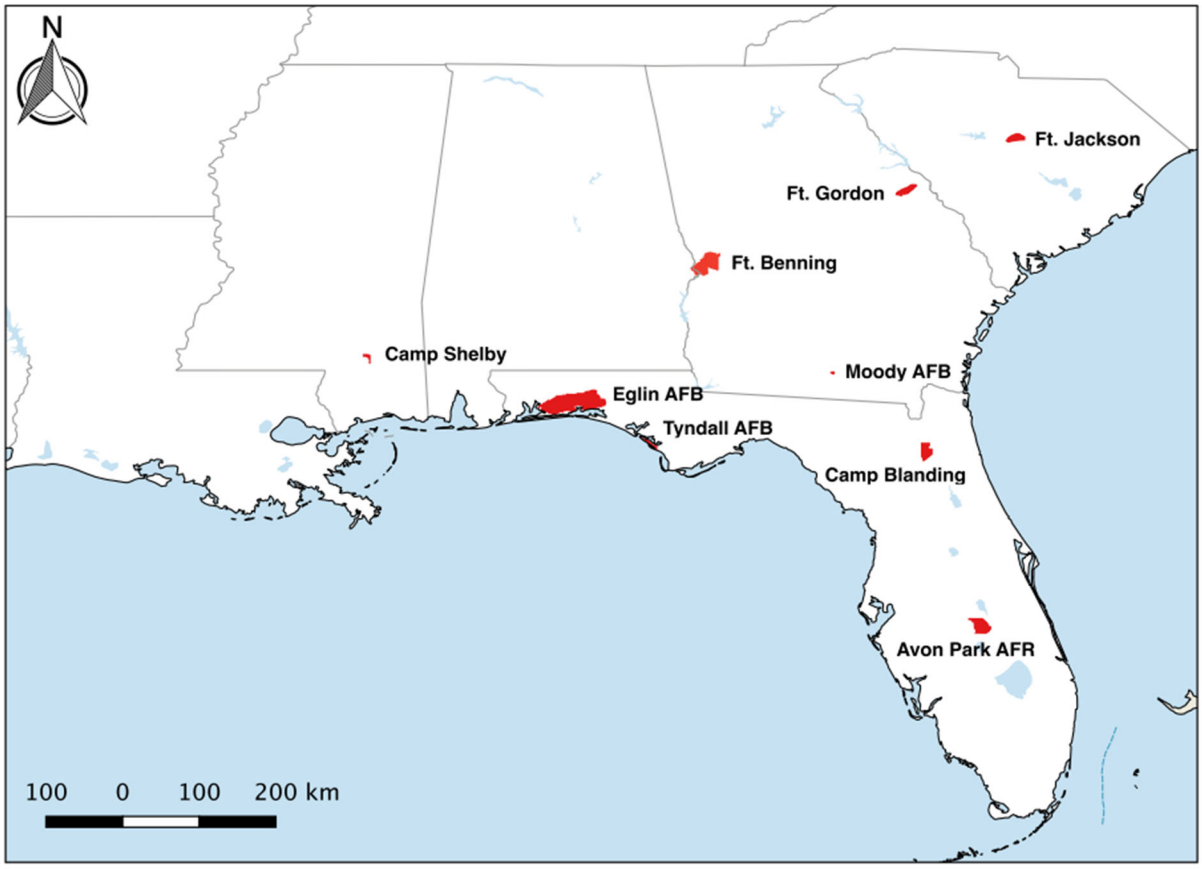

Figure 1. Study area map showing the location of each installation sampled.

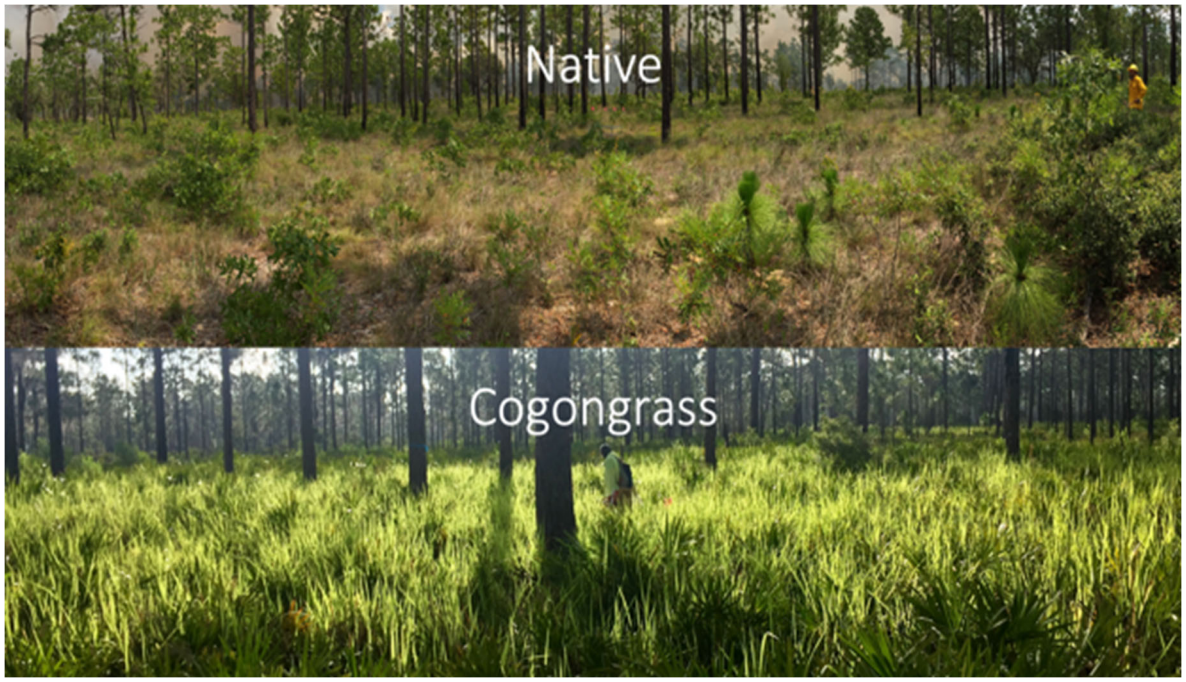

Figure 2. Typical native and invaded (cogongrass) communities.

Experimental design

The goal of our experimental design was to assess the potential effects of fire history (e.g., years since most recent burn) and cogongrass infestation (Figure 2) on host availability, plant community composition, and tick abundance across installations throughout the study region. The experimental design is summarized in Figure 3. The study region is defined as five states in the southeastern U.S. (i.e., Mississippi, Alabama, Georgia, South Carolina, and Florida). Within the study region, we collected data at nine military installations (i.e., Avon Park AFR, Fort Benning, Camp Blanding, Eglin AFB, Fort Gordon, Fort Jackson, Moody AFB, Camp Shelby, and Tyndall AFB). Each installation is divided into burn units, with different fire management histories. At least one sample plot was established within each burn unit selected. If part of a burn unit was infested with cogongrass, two plots were established (i.e., one in an invaded area and one in an uninvaded area). These plots were considered the smallest experimental unit of replication for all data analyses. The plots across all installations sampled are summarized in Table 1.

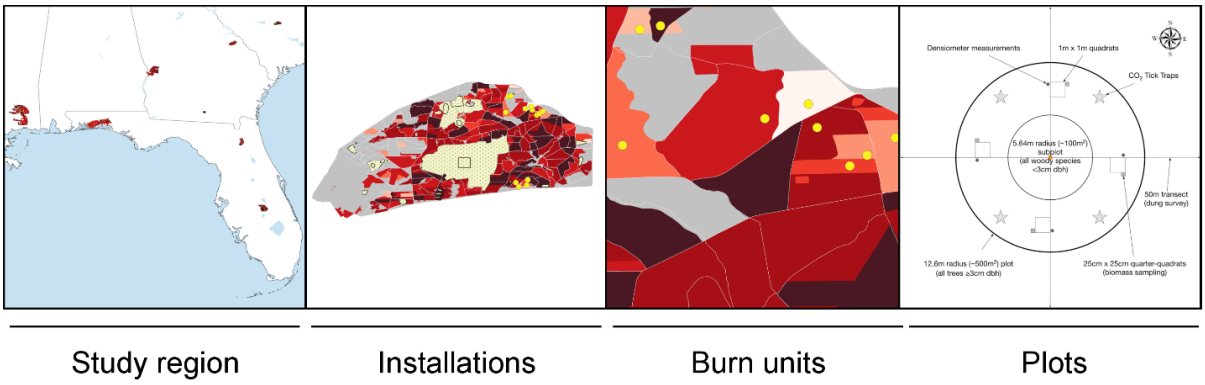

Figure 3. Summary of overall experimental design for field data collection.

Table 1. Summary of plots sampled across all installations.

Installation	Number of Plots			Years Since Fire	Years Sampled
	Uninvaded	Invaded	Total		
Avon Park AFR	8	4	12	0 – 6	2017, 2018
Fort Benning	10	0	10	0 – 4	2018
Camp Blanding	13	0	13	0 – 10	2017, 2018
Eglin AFB	11	0	11	0 – 11	2017, 2018
Fort Gordon	8	0	8	0 – 9	2018
Fort Jackson	13	0	13	0 – 11	2018
Moody AFB	3	0	3	0 – 11	2017
Camp Shelby	9	4	13	1 – 7	2017, 2018
Tyndall AFB	8	1	9	0 – 6	2017, 2018
Totals	**83**	**9**	**92**		

Due to intensive invasive plant management efforts by installation managers, many installations lacked cogongrass infestations; only Avon Park AFR, Camp Shelby, and Tyndall AFB had substantial cogongrass infestations. Thus, to maximize statistical power we preferentially selected burn units containing cogongrass infestations in which to collect data. Another major consideration in the overall experimental design was whether to prioritize collecting data at the same plots over multiple years versus collecting data at a larger number of plots for a single time point. In general, we prioritized the latter, because (1) this design increases the power of our statistical tests, which use plot as the experimental unit, and (2) the short duration of the study (i.e., three planned field seasons) precluded a repeated-measures analysis of the response variables over time. However, in the event that a plot that had been sampled in 2017 was burned, we revisited the same plot in 2018 to conduct a before-and-after comparison of the immediate impacts of the burn on the response variables. In 2018, we also revisited a subsample of the plots visited in 2017 to estimate inter-annual variation in the response variables, particularly tick density and host availability, throughout the study period.

Field sampling design

Following the experimental design, we established plots to achieve a stratified sampling that covered the range of fire history at each installation. We obtained fire history and known cogongrass invasions as GIS layers from each installation and identified potential plot locations based on time since last fire and history of cogongrass invasion. Potential locations were sent to contacts at the installation to solicit further guidance on selecting the final set of candidate locations and arranging access (e.g., Figure 4). In burn units with a cogongrass invasion we established one plot in the invaded area and one plot in an uninvaded area, with at least 100 meters between the plots. In burn units without an invasion we established one plot in an area representative of the vegetation conditions in the burn unit.

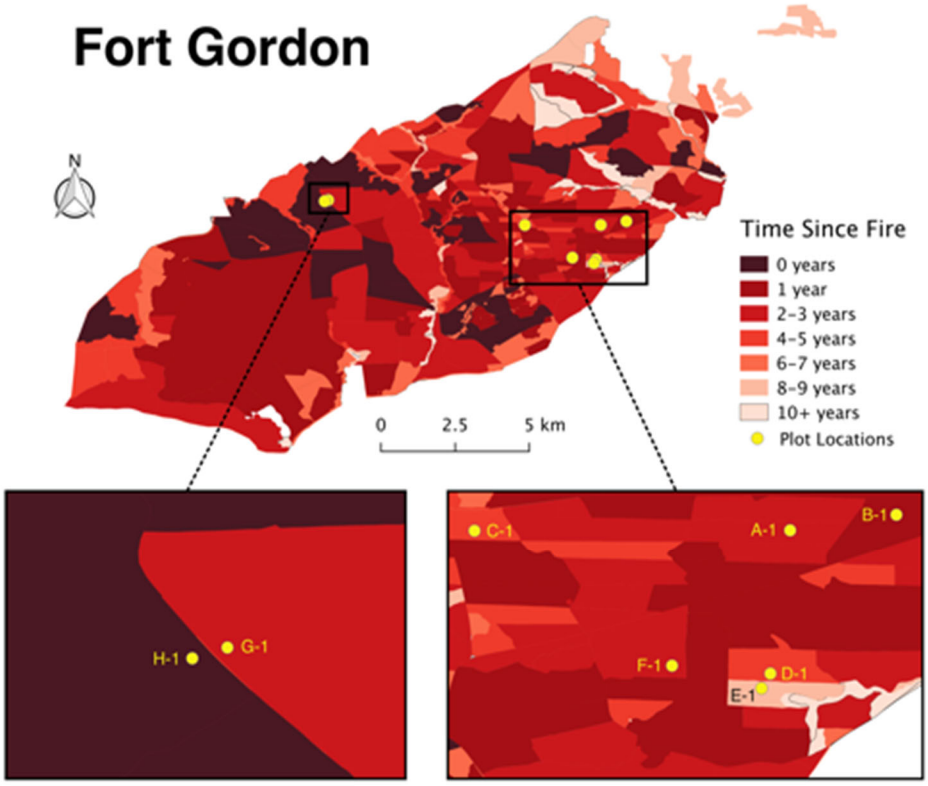

Figure 4. Burn unit map example.

Plot design

Each plot consisted of a main circular center plot (12.6 m radius, approximately 500 m^2), a circular subplot (5.64 m radius, approximately 100 m^2), four 1 m x 1 m quadrats, four 25 cm x 25 cm quadrats, four 50 m transects, and four locations for sampling tick abundance (Figure 5). In the main circular plot and subplot, we measured trees, saplings, and shrubs. Ground vegetation and litter were measured in 1 m and 25 cm quadrats located 10 m from plot center in each of the cardinal directions. The 50 m transects originated at the plot center going in each cardinal

direction and were used to estimate tick-host abundance. Tick abundance sampling locations were placed 8-10 m from the plot center in the NW, NE, SE, and SW areas. The center of each plot was marked with a flag and GPS coordinates were recorded using a Garmin Oregon 650t GPS unit (Olathe, KS).

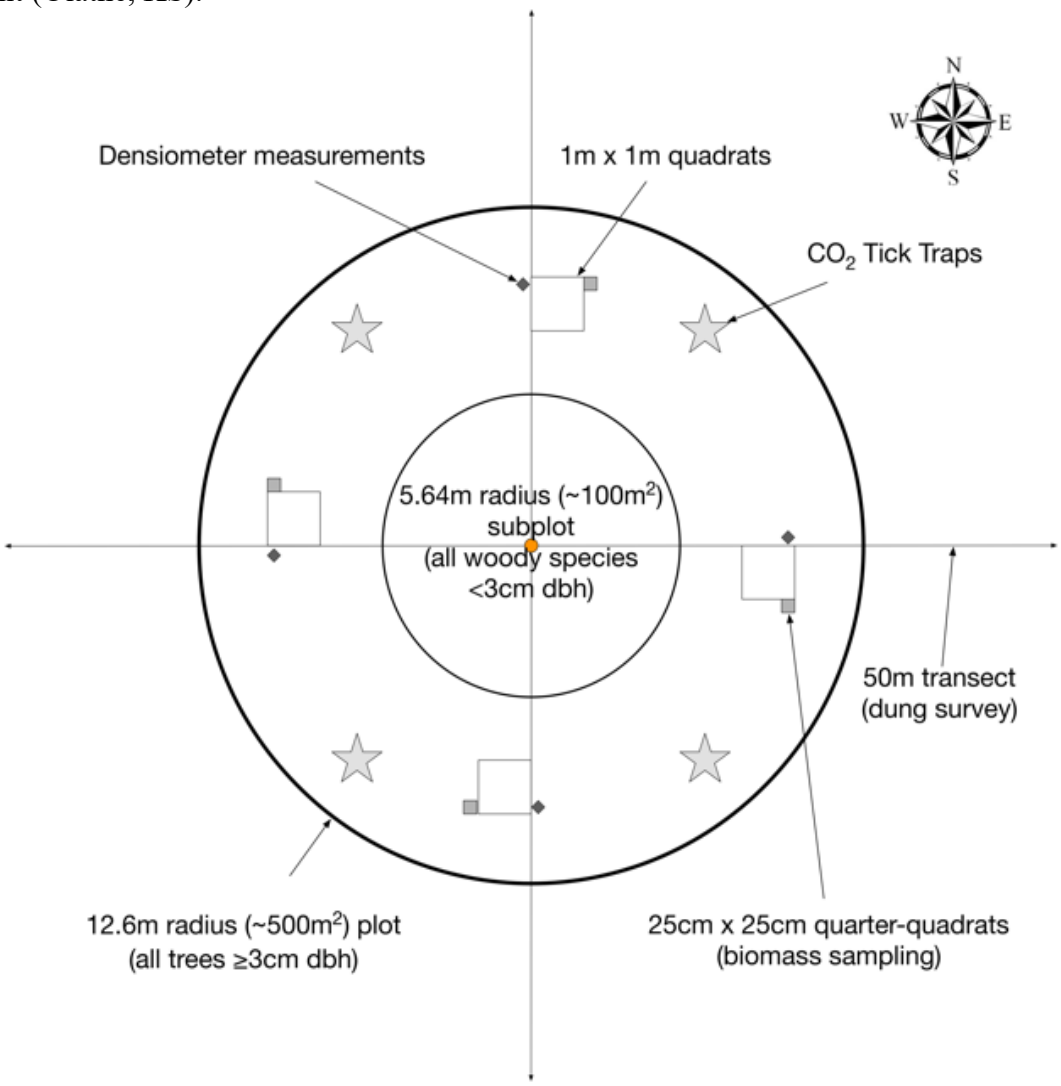

Figure 5. Field plot design.

Tree and shrub data collection

Within the 12.6 m radius plot we recorded the DBH of all trees ≥ 3 cm DBH to the nearest 0.1 cm, and the distance (nearest 0.1 m) and azimuth (compass degrees) from the plot center to the center of each tree. Using these measurements we created plot maps with the relative location of each tree (Figure 6). Each tree was assigned a health category (Table 2) and relative canopy position (Table 3). We recorded the heights of at least 10 trees in the plot (or all trees if fewer than 10) that were representative of each identified canopy position. In the 5.64 m radius subplot we recorded the abundance of woody species (shrubs and tree seedlings/saplings) that were < 3 cm DBH and ≥ 100 cm tall. We also estimated overstory canopy cover for the plot

by taking measurements using a spherical convex densiometer (Forestry Suppliers, Jackson, MS) while standing at each 1 m quadrat and facing plot center.

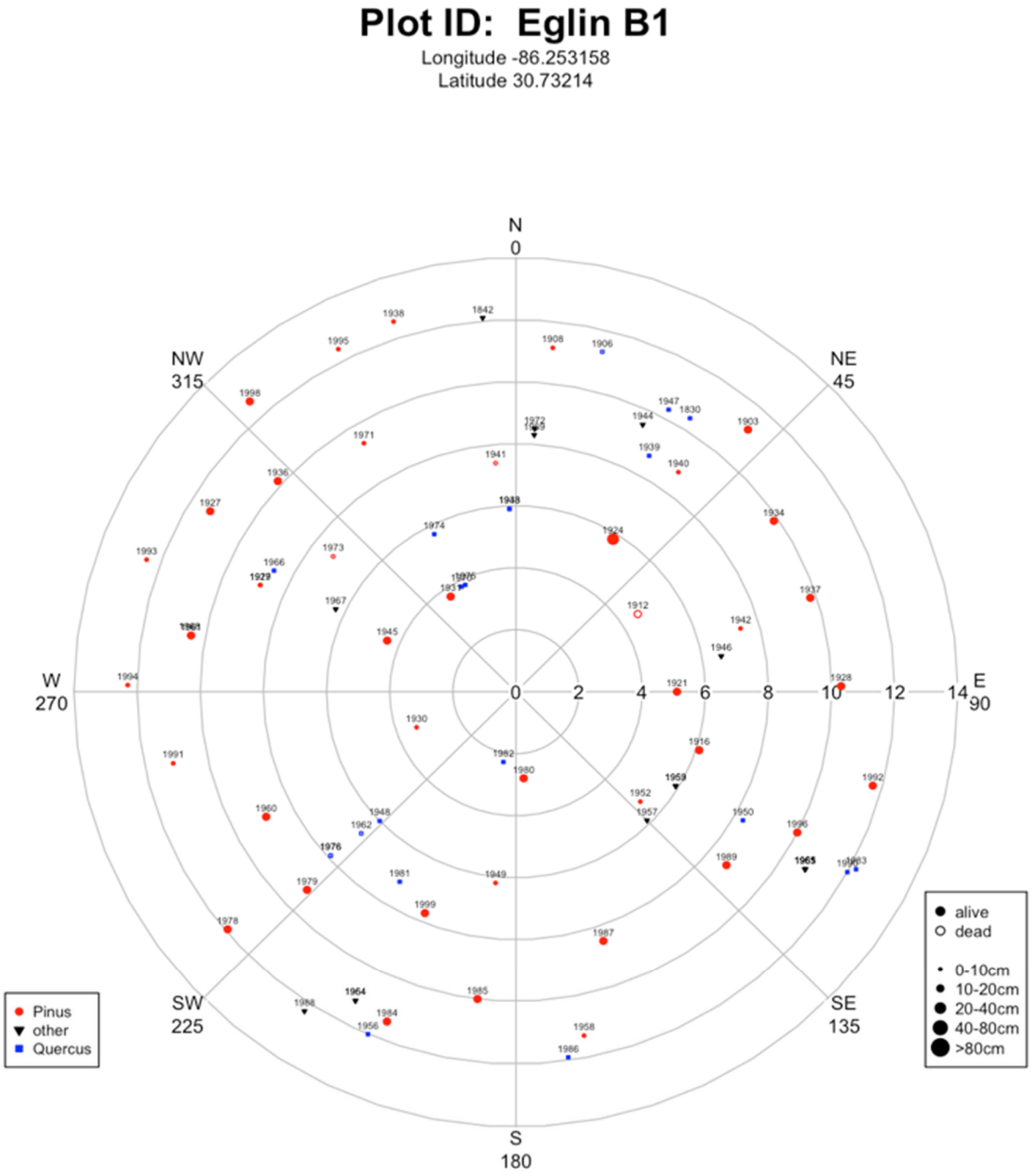

Figure 6. Example stem map for Eglin AFB plot B1.

Table 2A. Tree health categories.

Health code	Definition
0	dead, nothing living
1	healthy
2	relatively healthy
3	unhealthy, barely alive stem
4	all stems are dead, but has living sprouts not making DBH
5	missing tree, the tree can't be found during resampling

Table 2B. Tree canopy positions.

Canopy code	Definition
U	Understory, growing beneath the forest canopy, no direct sunlight
I	Intermediate, extend toward the over-story canopy but receive little or no direct sunlight from above and none from the sides
C	Co-dominant, receive direct sunlight from above but limited sunlight from the sides
D	Dominant, extend high into the canopy, sticking out above most other trees, and receive direct sunlight from above and partly on its sides
E	Emergent, crown extends well above all surrounding trees (typically mature redwoods or possibly Douglas fir)
S	Stump, tree no longer has any stems (dead or alive) that make the DBH cutoff, if it does it's a snag or dead standing stem. If stump present, but also has any stems ≥3cm dbh it is NOT a "stump." Assign canopy class of tallest stem even if it does not make DBH

Ground cover and litter data collection

We identified plant species and measured vegetation and litter conditions in each of the four 1 m quadrats. We recorded the percent cover of each plant species, total plant cover, litter cover, and bare ground, and counted the number of stems of each species rooted within the quadrat. Percent cover was visually estimated and estimates were calibrated among observers to ensure consistency. We measured the three tallest heights of woody species and the three tallest heights of non-woody species rooted within each quadrat. Heights were measured from the mineral soil surface. We also made three measurements of litter depth in each quadrat from the top of the litter level to the mineral soil surface. The 25 cm quadrats were placed adjacent to each 1 m quadrat in an area representative of the conditions in the larger quadrat, and we collected

vegetation and litter in order to estimate biomass (Figure 7). We collected all above-ground fine vegetation and litter within the 25 cm quadrat into separate bags. Samples were weighed at the end of the day to estimate fresh weights, then were returned to the Bivens Arm Research Site at the University of Florida, placed in a 60ºC drying oven for at least 72 hours, and then weighed to obtain dry weights. The difference between fresh weight and dry weight was used to estimate moisture content.

Figure 7. Sampling 1 m and 25 cm quadrats.

iNaturalist project

In order to improve confidence and consistency in plant identifications, we created an iNaturalist project (Figure 8) to enable easy reference in the field for identifying species that were not flowering and would have required a taxonomic key. iNaturalist is a digital platform available via iOS, Android, and a website, where scientists and naturalists can upload observations of plants, animals, and fungi, and offer or seek help in species identifications. Species identifications in iNaturalist may be tagged as "Research Grade" when the specimen was observed in the wild, includes a relatively accurate location and date, and the identification is supported by at least two members of the community. During our field surveys, we identified over 270 species and currently ~50% of these observations have become certified as "Research Grade." In the cases of rare and protected species, such as pitcher plants, we either excluded coordinates or included coordinates that were imprecise (resolution reduced to approximately 1500 m) using functions built into the iNaturalist application. The "Research Grade" observations are accessible by other databases such as the Global Biodiversity Information

Facility, which is used for analyzing species distributions, so a collateral benefit of this effort will be the availability of important data to other members of the scientific community.

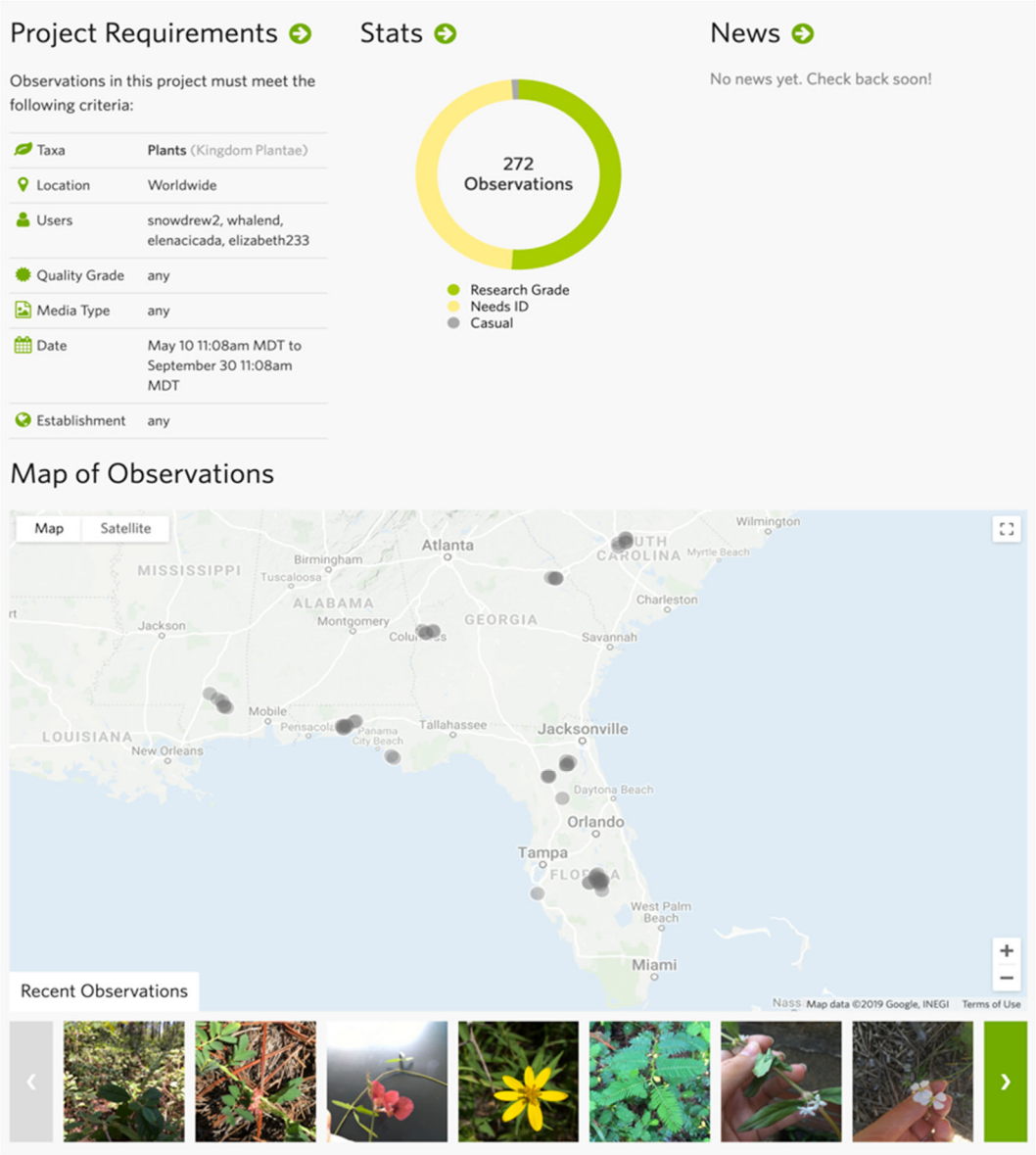

Figure 8. iNaturalist SERDP project https://www.inaturalist.org/projects/serdp-species

Tick sampling

We primarily collected ticks using CO_2 traps placed in each plot for 24 hours. Tick traps were constructed by mounting 5-quart hard-sided coolers (Igloo, Katy, TX) onto the center of 0.635 cm (0.25 inch) thick plywood pieces cut to 35 cm x 28 cm. There was approximately 7.6 cm between the edge of the plywood and all sides of the cooler. Two 0.48 cm (3/16 inch) holes were drilled through each side of the cooler just above the bottom of the interior. Strips of double-sided carpet tape (DF 545, ShurTape, Hickory, NC) measuring 4.77 cm (1.88 in) wide

were attached to the plywood surface surrounding the cooler. Each trap was baited with 1.5 kg of dry ice, which sublimated out through the holes drilled in the coolers. A rain cover made from corrugated plastic roofing cut to cover the entire footprint of the trap was attached to the top of each cooler by drilling a 0.48 cm hole through the center of the cooler lid and securing the roofing using a bolt and a wing-nut (Figure 9).

Figure 9. Installing rain shield on tick trap.

To collect ticks attracted by the traps but not stuck to the tape, we dragged a 1 m x 1 m white canvas cloth across the area directly below each trap three times. Ticks were also collected off of personnel and were assigned a plot, burn unit, or installation depending on the confidence in where the encounter occurred. Ticks collected on traps were counted and removed from the tape using tweezers, placed in 2 mL vials (Corning 430659) with 70% ethanol, and transported to the Flory Lab at the University of Florida where they were identified, sorted, and counted by species, life stage, and sex. Sorted ticks were then shipped to the Allan Lab at the University of Illinois where they underwent a second round of identification and sorting, and subjected to pathogen analysis.

Estimating host density

We conducted host-dung surveys along each 50 m transect to estimate abundance of tick hosts near the plot area. Observed dung clusters of host species (e.g. white-tailed deer, *Odocoileus virginianus*) were tallied within 1 m on either side of the transect line, totaling 400 m^2 of surveyed area within and nearby the plot. Species were identified by dung characteristics (Figure 10).

Figure 10. Tick-hosts dung survey and identification. (a) Field technician Elena Meyer surveying for tick-host dung, (b) turkey dung, (c) deer dung, (d) rabbit dung.

Climate Data

The DoD installations selected spanned a climate gradient across the southeastern U.S. to provide a range of climate conditions for modeling relationships between climate factors and tick-borne disease risk under current and future climate. To characterize this climate gradient, we retrieved daily climate data (1980-present) for each installation from the Daymet dataset (Thornton et al. 2016; https://daymet.ornl.gov/), which provides daily values for maximum and minimum temperature, precipitation, solar radiation, vapor pressure, and day length, at a 1 km x 1 km resolution. Values were extracted using the R package 'daymetr' (Hufkens et al. 2018) and then summarized in various ways (e.g., annual vs. seasonal averages, days above or below threshold values) to illustrate the climatic variation and gradient of the study region and evaluate the potential influence of climate and weather on tick abundance, host abundance, vegetation, and prescribed fire management.

Path Analysis

We used structural equations modeling (SEM) to evaluate the hypothesized direct and indirect effects of climate, fire management, vegetation, and host abundance on tick-borne disease exposure risk (Figure 11). Structural equations modeling is powerful in conceptualizing and then testing the direct and indirect effects of multiple process influencing ecological systems (Grace et al. 2010). Specifically, we applied path analysis (Wright 1921, Shipley 2004) to evaluate a specific set of factors representing the concepts outlined in Figure 11 (minus the Human Health component). Based on published knowledge of dynamics among climate change, fire, vegetation, wildlife, and tick abundances we developed the path model structure in Figure 12. Each box in this figure that has at least one arrow pointing to it is a response variable in a model and each box where an arrow is rooted is a predictor variable. We evaluated this path model using the R package piecewiseSEM (Lefcheck 2015), which allows models with different distributional forms to be evaluated together in the same SEM. Host and tick abundance responses were modeled using the Poisson distribution, while a Gaussian distribution was used for all other response variables. The percent litter cover was logit transformed and the time since fire was natural log-transformed to improve normality and homoscedasticity of residuals. The

global fit of the path model was checked using Fisher's C, which is based on topology of the SEM (Shipley 2000, 2013), and Chi-squared statistic based on maximum likelihood estimation (Shipley and Douma 2020) as implemented in the piecewiseSEM package, where P-values >0.05 indicate that the proposed structural model is consistent with the data. The maximum likelihood estimation comparison is made between model structures without paths between one or more variables and the fully saturated model where there are no missing paths. Finally, relative direct and indirect effects are interpreted using standardized coefficients reported on each path. Direct effects are arrows pointing directly to a response variable, while indirect effects are those that are at least once removed from another response variable. The indirect effect of a variable is calculated by multiplying the significant (we used $P<0.05$) coefficients along the path(s) to the response of interest. The total effect is the sum of the direct and indirect effects.

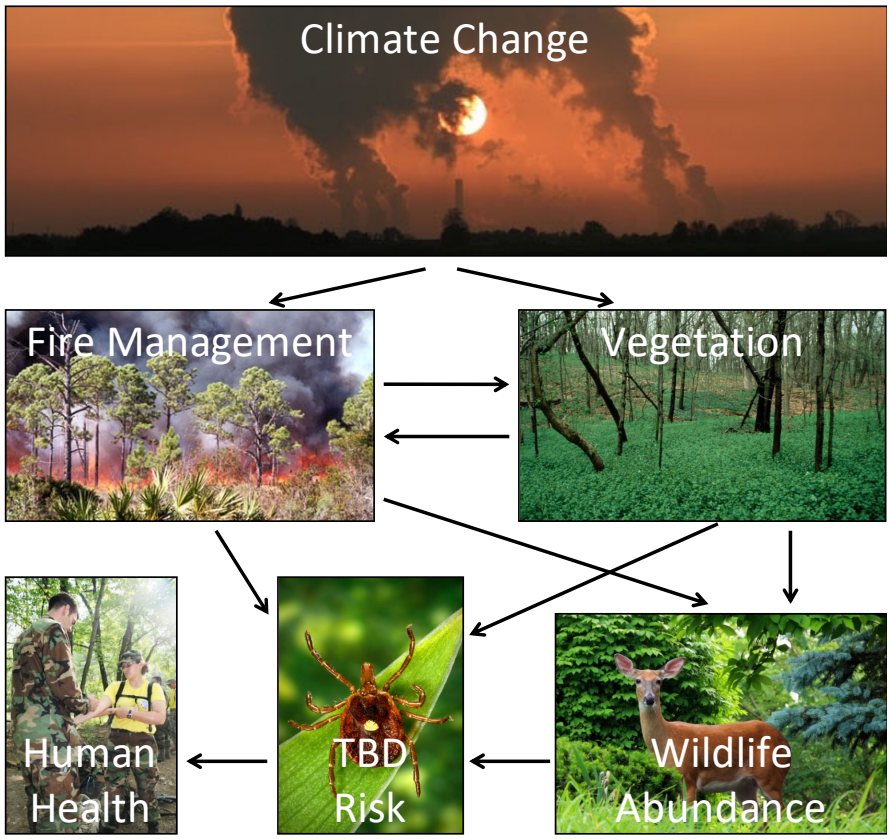

Figure 11. Conceptual diagram of relationships among climate change, fire management, vegetation, host abundance, and tick-borne disease exposure risk.

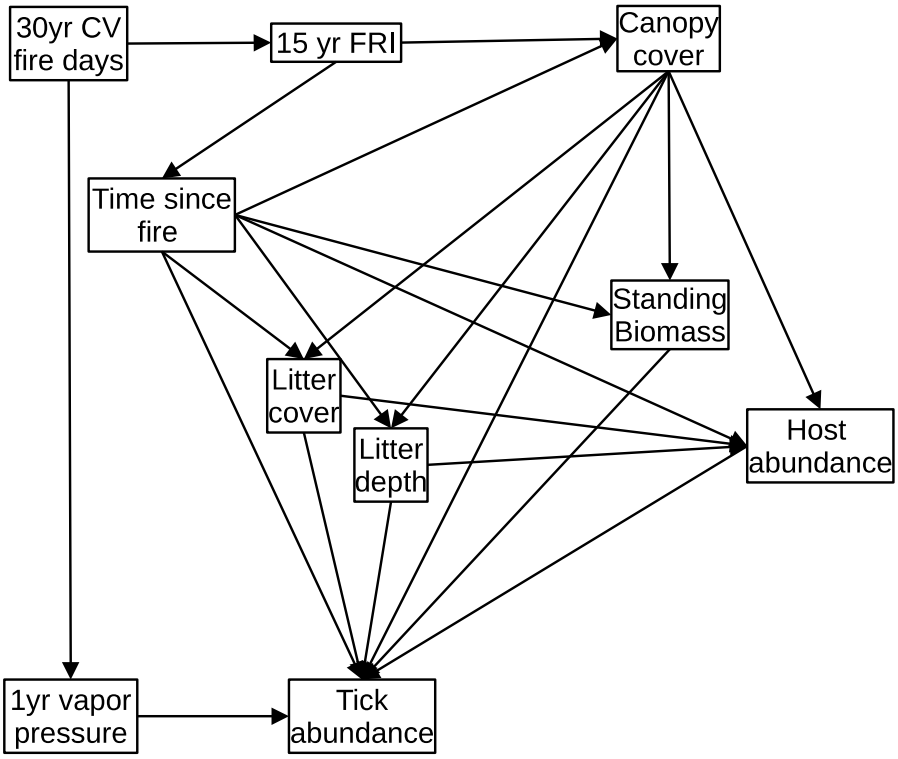

Figure 12. Path model structure. Variable descriptions are in Table 3.

Estimates of tick abundance were calculated for each plot visit as the number of ticks collected per trap. Tick abundance is directly related to TBD exposure risk because more ticks typically results in a higher prevalence of infected ticks and greater probability of being bitten. Host abundance was estimated simply as the count of dung clusters because for each plot visit sampling was equal, i.e. always 400 m^2 surveyed. With hosts being necessary for ticks to complete their life cycle, greater host abundance is expected to have the direct effect of greater tick abundance.

Litter cover, litter depth, and standing understory biomass are each expected to have a direct effect on tick abundance. Deeper litter and greater cover provide critical refuge for ticks when local microclimate conditions are unfavorable (i.e. dry and/or hot), thus having a positive effect on tick abundance. Similarly, standing understory biomass can further mediate microclimate to create more favorable local conditions when the weather is widely unfavorable (See Part 2). We also indicate testing the direct effect of each litter variable on host abundance, but this was due to the data collection process where we expected greater litter cover and depth to result in lower host abundance because detection is more difficult in these conditions.

Overstory canopy cover affects host abundance, standing biomass, both litter variables, and tick abundance directly. Effects on tick abundance are presumed through processes regulating microclimate across the plot area similar to standing biomass. The effect on host abundance is expected due to the structural and broader area microclimate conditions created and regulated by canopy cover. Greater canopy cover is expected to result in less standing biomass because of shading. Finally, greater canopy cover is expected to generate greater litter cover and depth because more leaves fall to the ground.

Recent weather conditions (during the previous year) are expected to directly affect tick abundances because overall poor or favorable conditions can affect success of each tick life stage. The resolution of the Daymet data covered more than one plot, so this is interpreted as the broad weather conditions over the area rather than local conditions in the plot.

We used two fire-related measures in the path model: time since last fire and the 15-year fire return interval. Time since last fire was intended to capture direct effects of fire (or lack thereof) on ticks, hosts, and vegetation, with expected increases in each of these with more time passing since the plot was last burned. The 15-year fire return interval represents the fire regime for the plot. Finally, to evaluate how climate may affect fire management we calculated coefficient of variation for the number of "fire days", defined as days with <6 mm of recorded precipitation.

Table 3. Path model variables and description.

Variable	**Description**
Tick abundance	Number of ticks per trap at each plot – tick abundance scaled by trapping effort
Host abundance	Total host dung clusters observed on transects (400 m^2 surveyed)
Litter cover	Percent litter cover in each plot averaged from four samples (logit transformed for models)
Litter depth	Average litter depth (cm) in each plot from four samples
Standing biomass	Average standing understory biomass (g) in each plot from four samples
Canopy cover	Percent overstory canopy cover in each plot averaged from four measurements
Recent weather 1yr vapor pressure	Averaged daily vapor pressure values at each plot calculated from Daymet data for the 365 days leading up to sampling date
Time since fire	Number of days since the plot was last burned
Fire regime – 15 yr FRI	15-year fire return interval for each plot (average number of years between fires). calculated in GIS using data provided by installations
Climate – 30yr CV fire days	30-year average of annual coefficient of variation of fire days defined as having <6 mm of recorded precipitation. Calculated from Daymet data.

RESULTS AND DISCUSSION

Installation and plot visits

We established 94 plots at 9 DoD installations across the southeast U.S. Of the 94 plots, only 10 had untreated cogongrass invasions (Figure 13a) and most of these invasions were relatively small. Fire history varied across the plots, ranging from 0 to 11 years since the last fire (Figure 13b). The small number of cogongrass-invaded plots was due to a high level of awareness and recognition of cogongrass as a problematic species, and diligent management practices that quickly eradicate identified invasions. With relatively few invaded plots we evaluated relationships by pooling all plots (invaded and uninvaded) together.

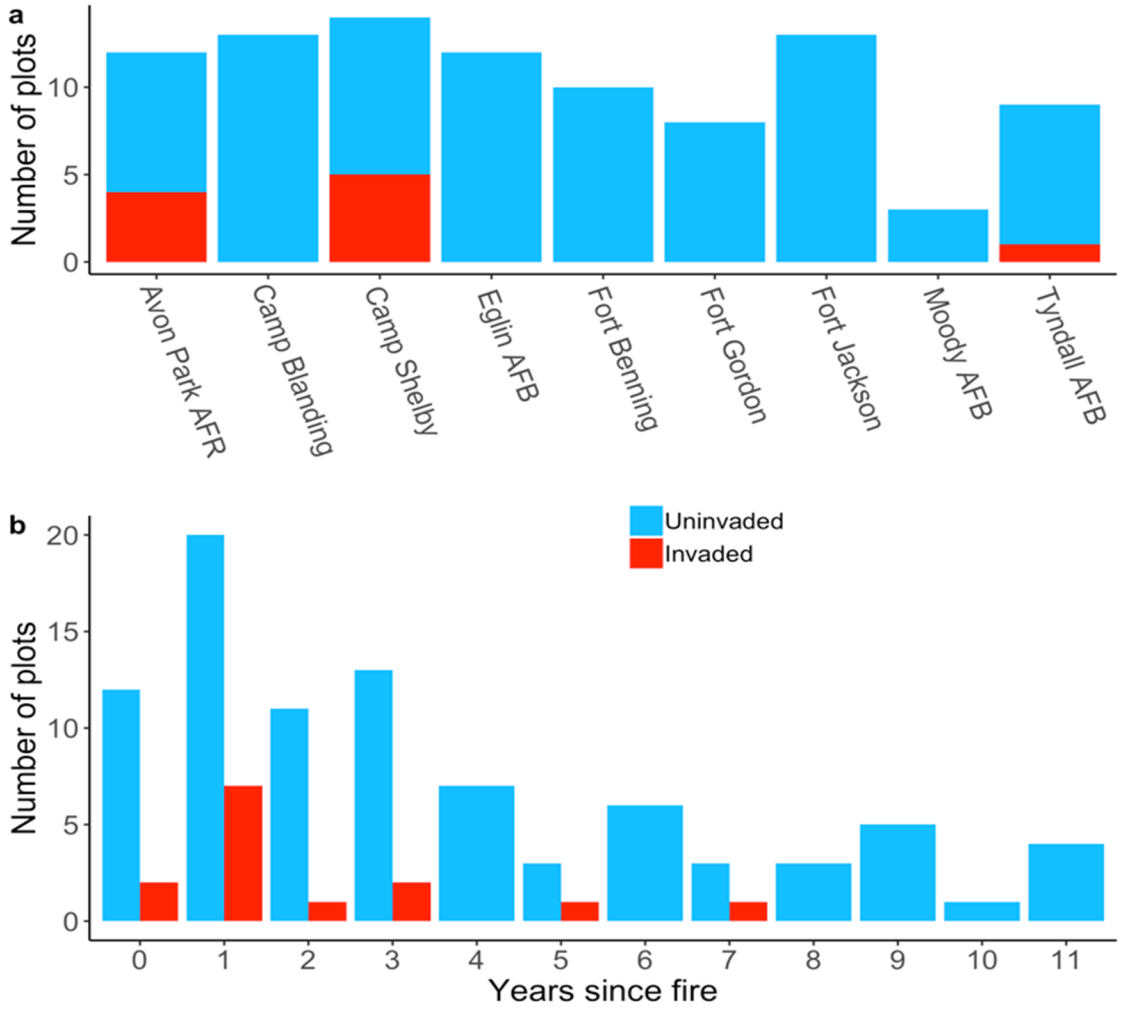

Figure 13. (a) Number of plots established at each of the DoD installations. (b) Number of plots established in each time since fire. The color shading indicates whether or not plots were in a cogongrass invasion - light blue is uninvaded and red is invaded.

Path analysis

The proposed path model structure was consistent with the data based on the maximum likelihood estimates ($\chi^2 = 35$, P = 0.63) though significant missing paths were identified (Fisher's C = 156, P = 0). There were three "missing" paths identified (illustrated as red dot-dot-dash lines in Figure 14): one each going from the average vapor pressure over the previous year to canopy cover and host abundance, and one going from the 30-year average of the coefficient of variation for fire days to host abundance. We did not identify any relevant biological mechanisms to explain these relationships, so deemed them spurious correlations perhaps in part due to the coarse resolution of the Daymet data relative to the plot sampling. Accounting for these correlations lowers Fisher's C to 39 with P = 0.507, indicating a topology consistent with the data. Given that the maximum likelihood value indicated the original graph topology was consistent with the data, we proceeded to interpret this path model. The full set of estimated coefficients, standardized and unstandardized are presented in Table 4.

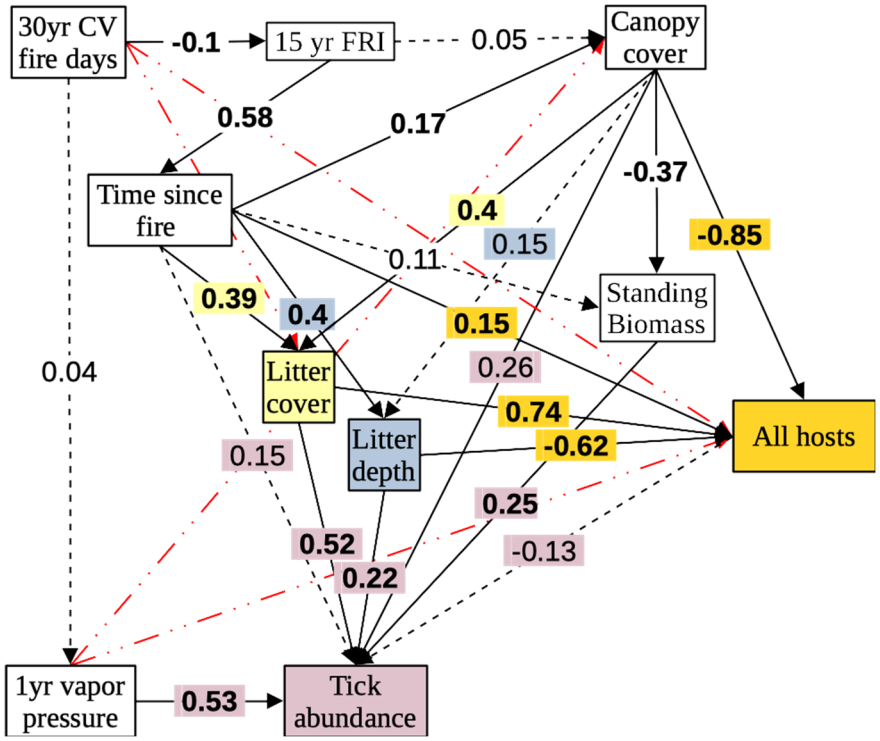

Figure 14. Estimates from fitted path model using abundance of all hosts. Standardized path coefficients indicate relative strength of direct effects. In the dense portion of the graph, highlight color of coefficients corresponds to the response variable. AIC = 4833; Chi-squared = 20 (df = 23, P = 0.63); Fisher's C = 156 (df = 46, p = 0). Passes maximum likelihood test (Chi) but not d-sep (Fisher's) for acceptable fit because of very small P-values of "missing" paths. *Bold coefficient values = P<0.05. Values on dashed paths = P>0.1. Normal text on solid paths = 0.05<P<0.1. Red dash-dot-dot lines are "missing" paths identified during model fitting.*

Table 4. Coefficient estimates for each sub-model in the fitted path model (Figure 14). Coef = unstandardized coefficient estimate, SE = standard error of Coef, DF = degrees of freedom, P = estimated p-value of the coefficient, Std. Coef = standardized coefficient estimate.

Response	Predictor	Coef	SE	DF	P	Std. Coef
Ticks per trap	Days since fire	0.18	0.13	101	0.162	0.15
Ticks per trap	Litter Cover	0.46	0.14	101	**0.001**	**0.52**
Ticks per trap	Litter Depth	0.15	0.07	101	**0.048**	**0.22**
Ticks per trap	Canopy cover	0.014	0.01	101	0.095	0.26
Ticks per trap	Standing biomass	0.28	0.14	101	**0.047**	**0.25**
Ticks per trap	Host abundance	-0.002	0.002	101	0.373	-0.13
Ticks per trap	Vapor pressure	0.004	0.002	101	**0.011**	**0.53**
Host abundance	Days since fire	0.31	0.11	101	0.006	0.15
Host abundance	Canopy cover	-0.07	0.01	101	0	-0.85
Host abundance	Litter Cover	1.08	0.16	101	0	0.74
Host abundance	Litter Depth	-0.68	0.07	101	0	-0.62
Litter Cover	Days since fire	0.53	0.09	86.8	0	0.39
Litter Cover	Canopy cover	0.02	0.004	93	0	0.4
Litter Depth	Days since fire	0.71	0.17	93	0	0.4
Litter Depth	Canopy cover	0.01	0.007	91.6	0.126	0.15
Canopy cover	Days since fire	3.85	1.31	11	0.017	0.17
Canopy cover	FRI	0.33	0.73	95	0.663	0.05
Standing biomass	Days since fire	0.12	0.067	21	0.116	0.11
Standing biomass	Canopy cover	-0.02	0.004	92	0	-0.37
Days since fire	FRI	0.2	0.023	57	0	0.58
FRI	CV fire days	-1.1	0.462	8.8	0.046	-0.1
Vapor pressure	CV fire days	19.8	12	91.4	0.104	0.04

Table 5. Estimated marginal (fixed-effects only) and conditional (fixed and random effects) R^2 for each sub-model in the path analysis.

Response	Family	Link	R^2 method	Marginal R^2	Conditional R^2
Ticks per trap	poisson	log	trigamma	0.34	0.65
Host abundance	poisson	log	trigamma	0.33	1
Litter cover	gaussian	identity	none	0.42	0.59
Litter depth	gaussian	identity	none	0.21	0.26
Canopy cover	gaussian	identity	none	0.04	0.94
Standing biomass	gaussian	identity	none	0.12	0.9
Days since fire	gaussian	identity	none	0.33	0.33
FRI	gaussian	identity	none	0.01	0.98
Vapor pressure	gaussian	identity	none	0	0.97

Tick abundance sub-model

The model of tick abundance captured 65% of the variation, with the fixed-effects portion accounting for 34% (Table 5). Two especially interesting results came from this model: 1. host abundance was not a strong factor in explaining tick abundance, and 2. time since fire had only an indirect effect on tick abundance (ticks per trap). The lack of an effect of host abundance suggests that abiotic factors are stronger determinants of tick abundance in this ecosystem. The major abiotic driver, fire, has only an indirect effect, primarily through effects on litter cover and litter depth (Figure 14). The indirect effect of time since fire was relatively stronger than the direct effects of litter depth and standing biomass, and overall had the third strongest effect following the direct effects of litter cover and vapor pressure (Table 6). The predicted marginal effects of predictors with $P<0.05$ on ticks per trap were all positive, i.e., predicted tick abundance was greater with increasing litter cover, litter depth, standing understory biomass, and vapor pressure (Figure 15). These relationships illustrate the dominant abiotic effects on tick abundance and support litter and understory vegetation mediating the influence of weather.

Table 6: Direct, indirect, and total effects on tick abundance from the path model in Figure 14, assuming effects only when $P<0.05$ for the estimated path coefficient (bolded values in Figure 14).

Variable	Direct	Indirect	Total
CV fire days	0.00	0.018	0.018
FRI	0.00	0.181	0.181
Time since fire	0.00	0.313	0.313
Canopy cover	0.00	0.104	0.104
Litter cover	0.51	0.000	0.510
Litter depth	0.24	0.000	0.240

Variable	Direct	Indirect	Total
Standing biomass	0.27	0.000	0.270
Vapor pressure	0.51	0.000	0.510

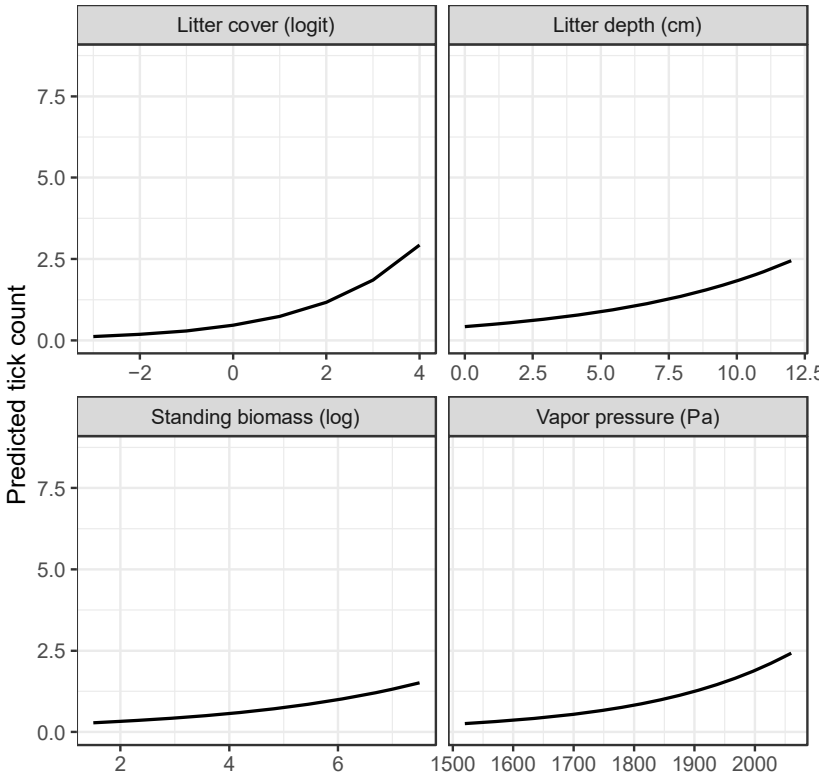

Figure 15. Marginal effects plots for the significant predictors in the tick abundance sub-model in the path analysis. Predicted relationships are with all other variables held at their mean values.

Litter sub-models

Litter cover and depth were both influenced by overstory canopy cover and time since fire. As expected, both increased with time since fire but surprisingly litter depth was lower with greater canopy cover (Figure 16). This may be due to understory vegetation substantially contributing to litter accumulation relative to overstory trees. The models explained up to 59% of the variation in litter cover and 26% of the variation in litter depth (Table 5).

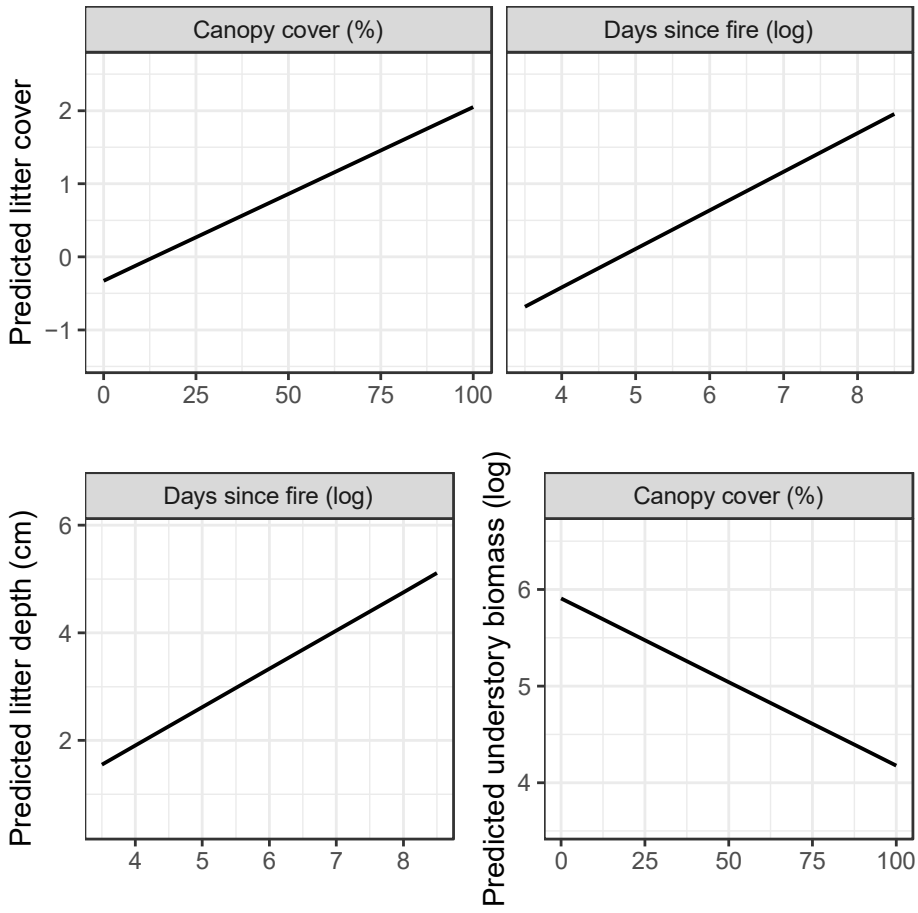

Figure 16. Marginal effects plots for sub-models of logit litter cover (top row), litter depth (lower left), and understory biomass (lower right).

Canopy cover, time since fire, and fire return interval sub-models

Overstory canopy cover increased with time since fire but was not explained by the direct effect of fire return interval. The strong predicted collinear relationship between fire return interval and log-transformed time since fire may be part of the explanation (Figure 17). By collecting data in primarily pine-dominated forest stands we selected for areas that are managed to have a sparse mid-story, which may be driven by using fire as a preferred management method. However, the fixed effects portion of the canopy cover model explained only 4% of the variation while the random effect term captured an additional 90% (Table 5), suggesting that other factors at the installation and plot levels, such as land use and soils, are substantial contributors to observed canopy cover. Fire return interval explained 33% of the variation in time since fire while the influence of variation in fire days during the past 30 years very weakly explained fire return interval (marginal $R^2 = 0.01$). Our results indicate that fire management (fire return interval) is primarily determined by characteristics of the installation (97% of variation explained by the random effect), which would include factors that aren't climate or weather related, such as preferred management methods, personnel for prescribed fire, and budgetary differences. Essentially, climate is not yet the most limiting factor for using prescribed

fire as management tool at these installations but is predicted to be in the relatively near future (Kupfer et al. 2020)

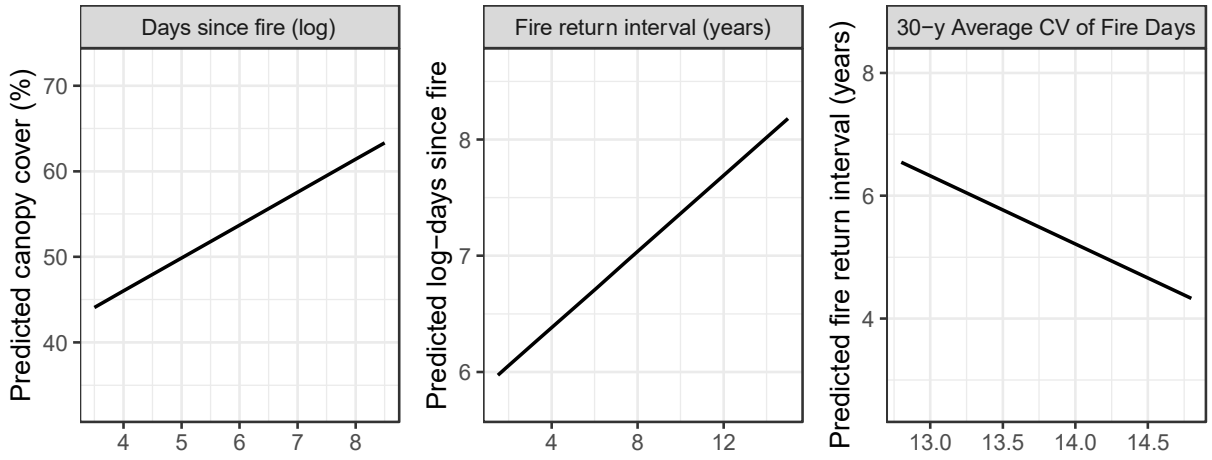

Figure 17. Marginal effects plots for canopy cover, time since fire, and fire return interval (left to right) sub-models of the path analysis.

Host abundance sub-model

While we did not see a direct effect of host abundance on tick abundance, the host abundance sub-model revealed some surprising relationships. Canopy cover, litter cover, and litter depth all had relatively strong effects, while time since fire had a relatively weak effect (Figures 14 and 18). We had hypothesized that both litter variables would negatively influence host abundance because detection would be more difficult but they had opposing relationships – host abundance estimates were greater with more litter cover while lower with greater litter depth. So, the relationship with litter depth is consistent with the effect on our detection process but there may be a threshold of litter cover that is associated with host abundance for biological reasons, resulting in the positive effect. The same explanation may be applicable to the negative relationship between overstory canopy cover and host abundance – some level of cover is desirable for hosts (a biological effect) but very dense cover may have lower host abundance for biological and detection process reasons simultaneously. Finally, the host abundance data are very skewed, with eastern cottontail rabbits the vast majority of observations (Table 7).

Table 7. Totals from all dung surveys across installations.

Cottontail	Cow	Deer	Turkey	Other	*Total*
2112	100	398	23	19	*2652*

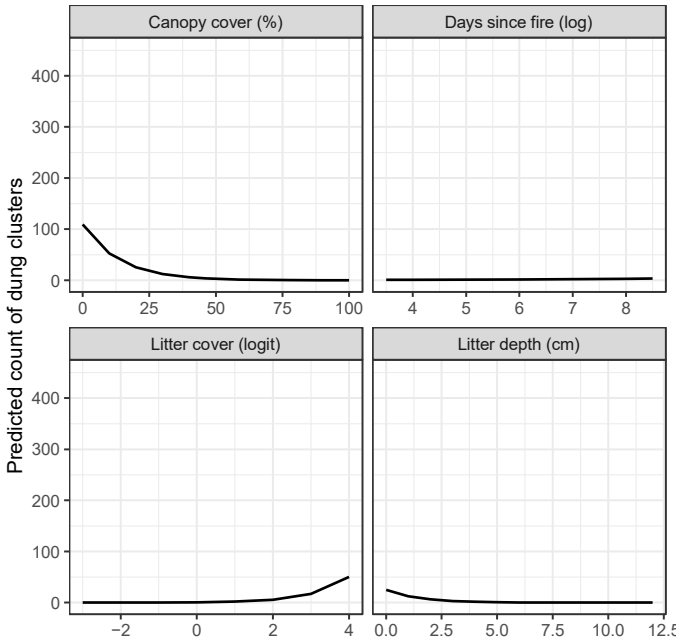

Figure 18. Marginal effects plots for significant predictors in the host abundance sub-model of the path analysis.

Climate and Weather

Averages of climate variables at the selected installations illustrate the climate gradient across which sampling occurred (Figures 19 and 20). There is some interannual variation within installations across factors, though this is very narrow for precipitation (Figure 19). The spatial resolution of Daymet data results in small or no difference in values between plots at the same installation, so these data do not capture the "local" microclimate conditions that are influenced by vegetation cover and more directly affect tick survival (see Part 2). Temperature followed an expected latitudinal gradient with the highest average maximum temperatures at Avon Park AFR, the southernmost installation, and lower average maximum temperatures at the northernmost installations in Georgia at Fort Gordon and in South Carolina at Fort Jackson (Figure 19). We examined a suite of 30-year aggregations of these variables in an attempt to evaluate the effect of climate on prescribed fire management. We selected the coefficient of variation for the number of available prescribed fire days (precipitation <6mm) as the best explanatory variable.

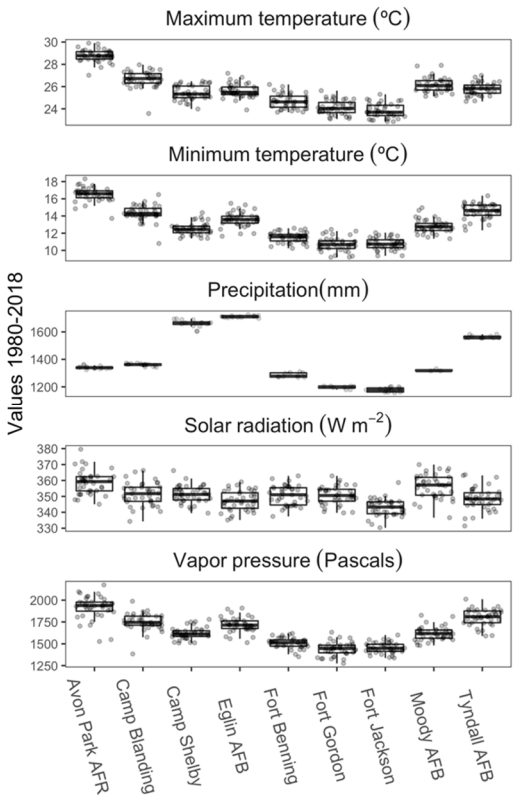

Figure 19. Boxplots of annual averages (1980-2018) for Daymet climate variables at each installation.

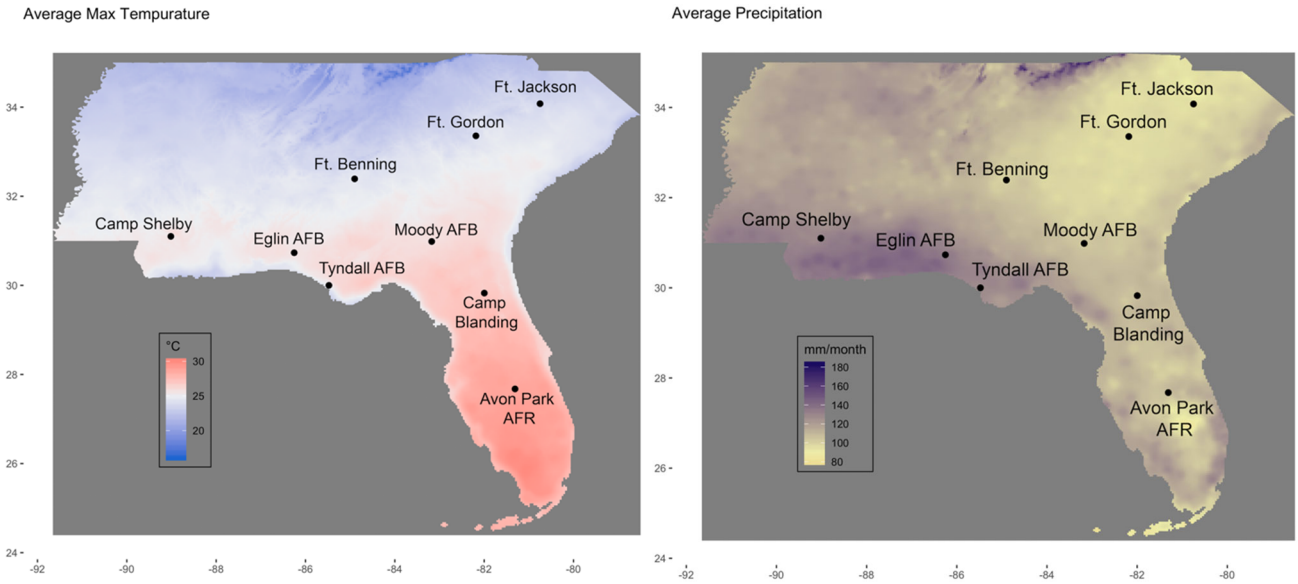

Figure 20. Average maximum temperature (left) and average monthly precipitation (right) across the sampling region in the southeast U.S.

Trees and understory

We recorded 38 different tree species. The vast majority of the 3633 trees recorded were either *Pinus* (pine) or *Quercus* (oak) genus, with pines making up more than 50% of all trees recorded (Figure 21). Plots with low overstory tree and shrub density are likely to be less hospitable for ticks because incoming solar radiation reaches the ground resulting in higher temperatures and more rapid evapotranspiration. Fewer trees and shrubs also results in less buildup of litter that can provide refuge for ticks from high temperatures and low humidity. The biomass of standing understory vegetation ranged widely from 0.006 to over 1.6 kg m^{-2}.

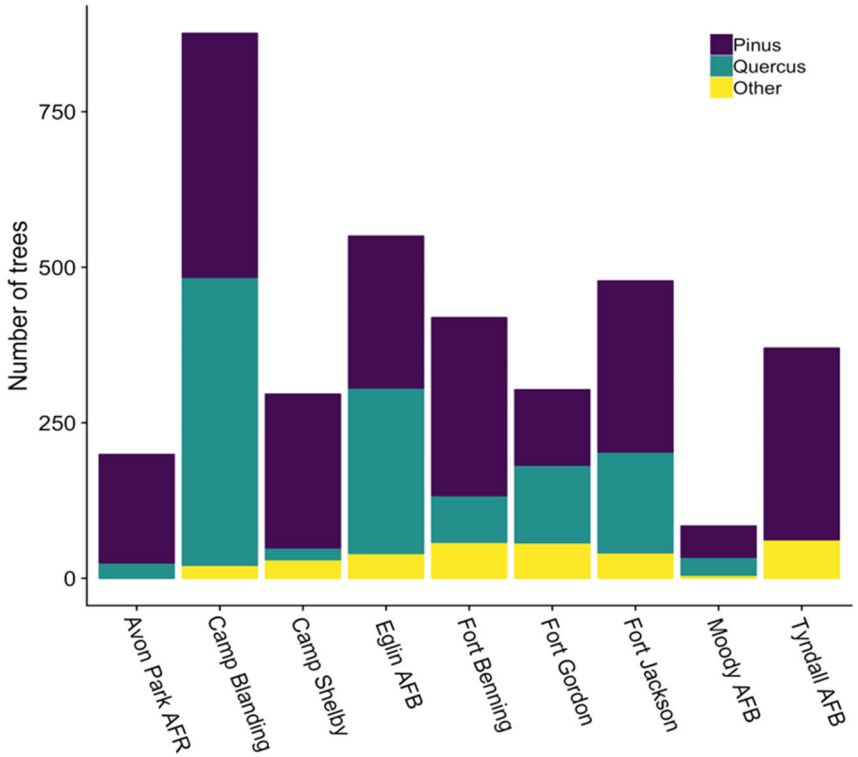

Figure 21. Number of trees recorded at each installation. The majority of trees belonged to the genus *Pinus* or *Quercus*.

Host abundances

We positively identified eight tick host species during dung surveys across all installations. White-tailed deer (*Odocoileus virginianus*) and eastern cottontail rabbit (*Sylvilagus floridanus*) were typically the most abundant host species at each installation (Figure 16, Table 5). At Avon Park AFR, cow dung made up a substantial amount of dung encountered due to domestic cattle grazing leases, illustrating the multi-use character of this installation. Wild turkey (*Meleagris gallopavo*) made a notable contribution to host density at Camp Blanding and Eglin AFB during 2018 surveys. All of these host species may influence tick abundances and the risk of exposure to tick-borne pathogens as hosts for different life stages of ticks and/or reservoirs for infectious agents. White-tailed deer and eastern cottontail rabbits are important hosts for nymph and adult life-stage *A. americanum* and both host species may serve as reservoirs for zoonotic diseases that threaten human health (Allan et al. 2010b). Though encountered at low relative

abundance in our surveys, feral hogs (*Sus scrofa*) also are hosts for multiple tick species and reservoirs for tick-borne pathogens (Allan et al. 2001). Dung from domestic cattle were the only domesticated host species encountered in our surveys and are interesting hosts for their potential negative effect on tick abundances. Cattle may be treated with topical acaricides to prevent ticks from feeding and, if present in sufficient densities, can reduce environmental tick abundances (Keesing et al. 2018).

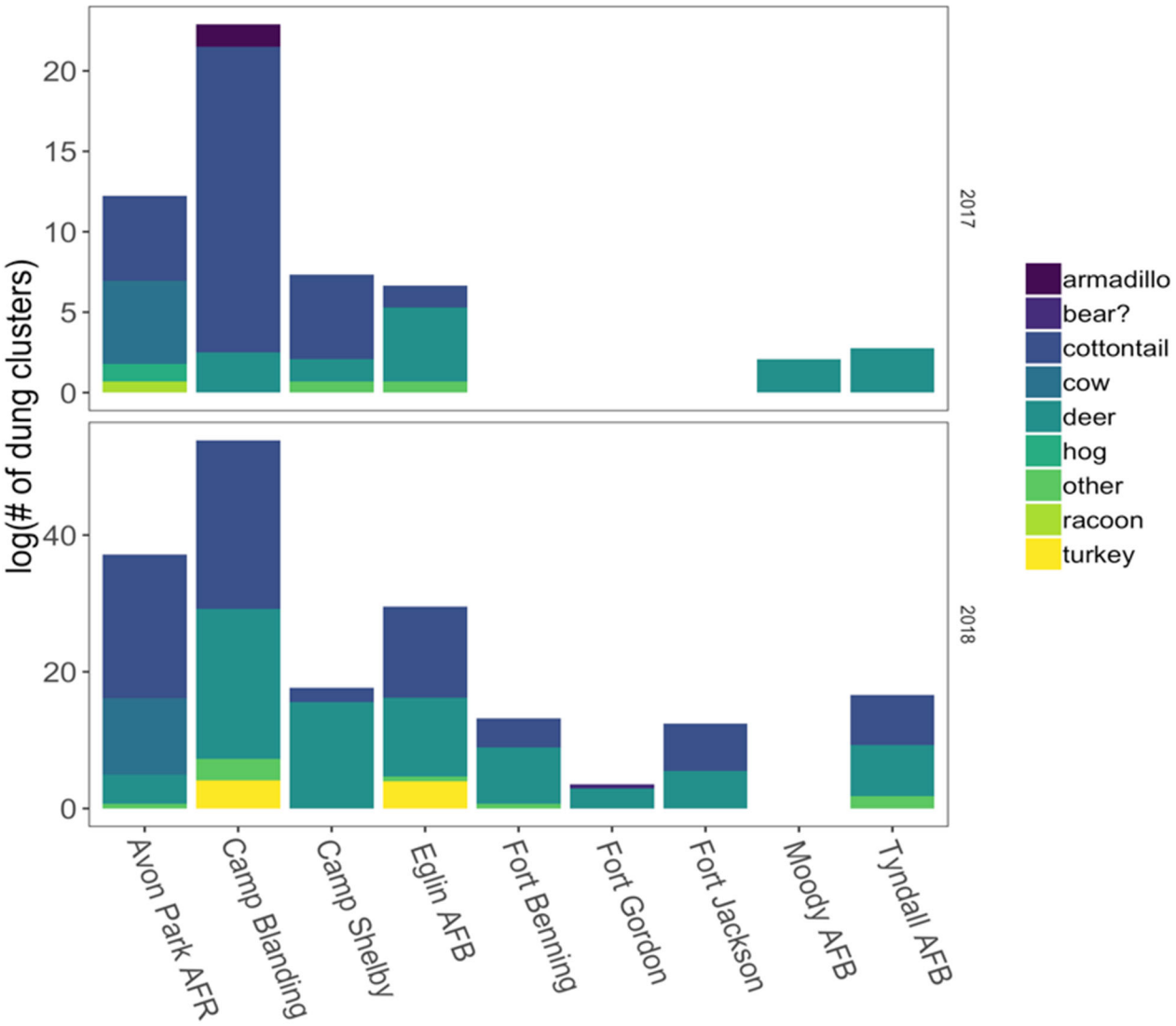

Figure 22. Host species densities at each installation (dung clusters 400 m^{-2}). Note that the y-axis has different scales in each panel. Zeroes (no bars) are installations that weren't sampled during that year.

Tick abundances

We collected four different tick species across all installations (Figure 23). The majority of ticks collected were in the nymph life stage during both sample seasons (Figure 24a) and belonged to the target species, *Amblyomma americanum* (Figure 24b). The small number of invaded areas had few ticks (Figure 24). The majority of ticks collected in 2017 were from Camp Blanding, FL and Eglin AFB, FL, while in 2018 most ticks collected were from Camp Blanding, FL, Fort Gordon, GA, and Tyndall AFB, FL (Figure 25). Among the lowest tick abundance observed for both sample years was at Avon Park AFR, which may be partly attributable to habitat management resulting in poor microclimates for ticks at this installation, as well as the high temperatures. An additional factor that may contribute to the low tick abundance at Avon Park AFR is the presence of cattle that are treated with acaricides (Figure 22; Kateri Tonyan personal communication June 18, 2018).

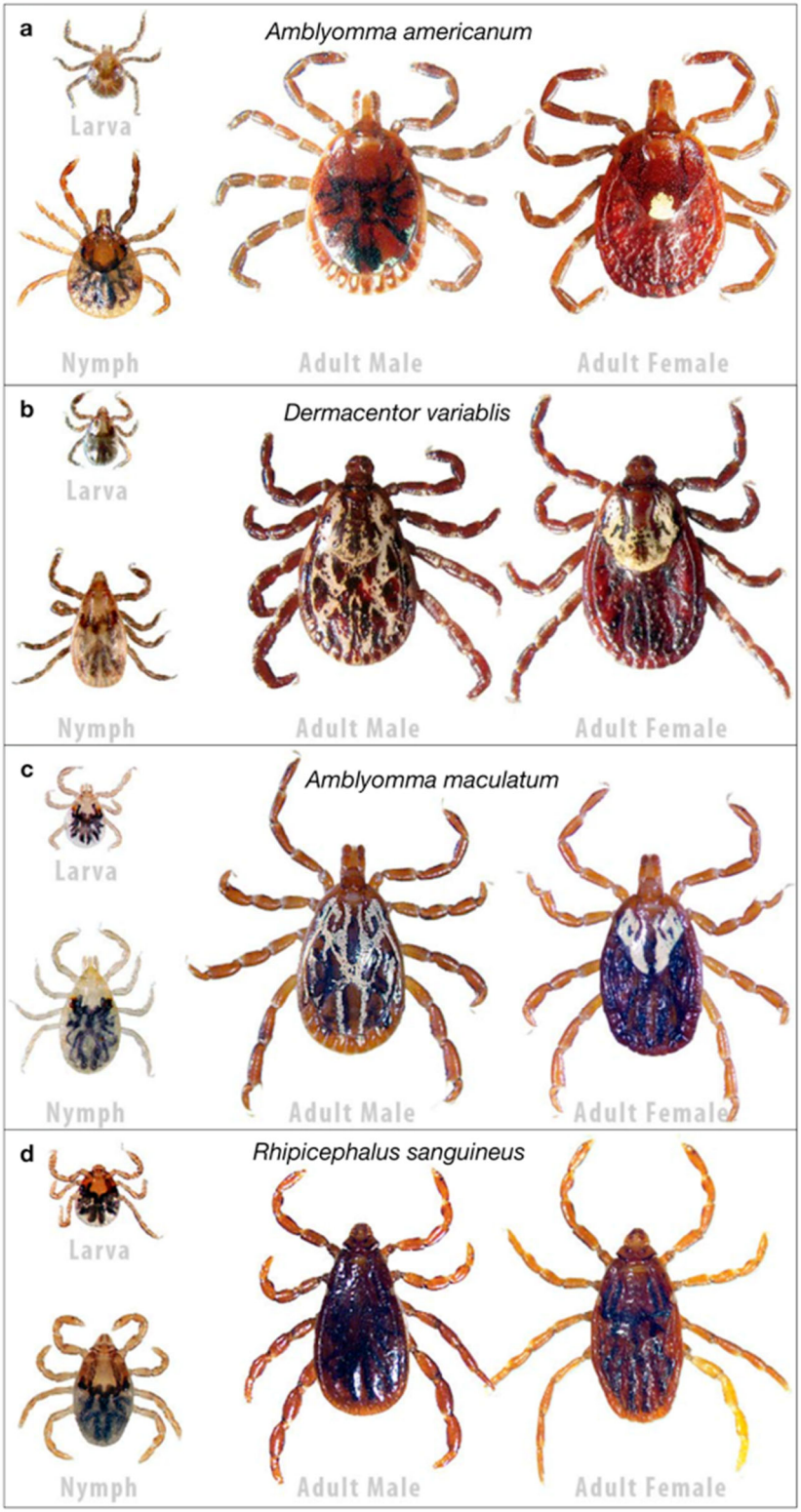

Figure 23. The four most commonly collected tick species. (a) *Amblyomma americanum* (lone star tick), (b) *Dermacentor variablis* (American dog tick), (c) *Amblyomma maculatum* (Gulf Coast tick), (d) *Rhipicephalus sanguineus* (brown dog tick).

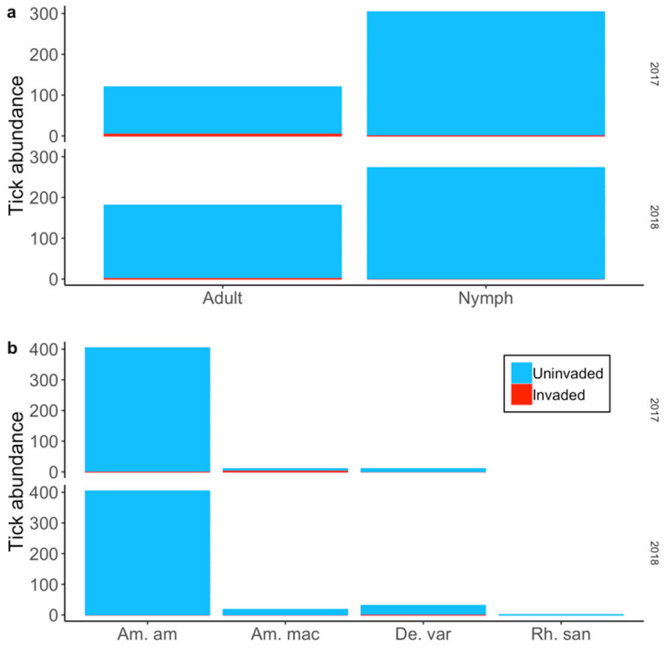

Figure 24. Tick abundances grouped by (a) life stage and (b) species in each sample year. Am. am: *Amblyomma* americanum, Am. mac: *Amblyomma maculatum*, De. var: *Dermacentor variablis*, Rh. san: *Rhipicephalus sanguineus*. Blue indicates uninvaded and red indicates cogongrass-invaded.

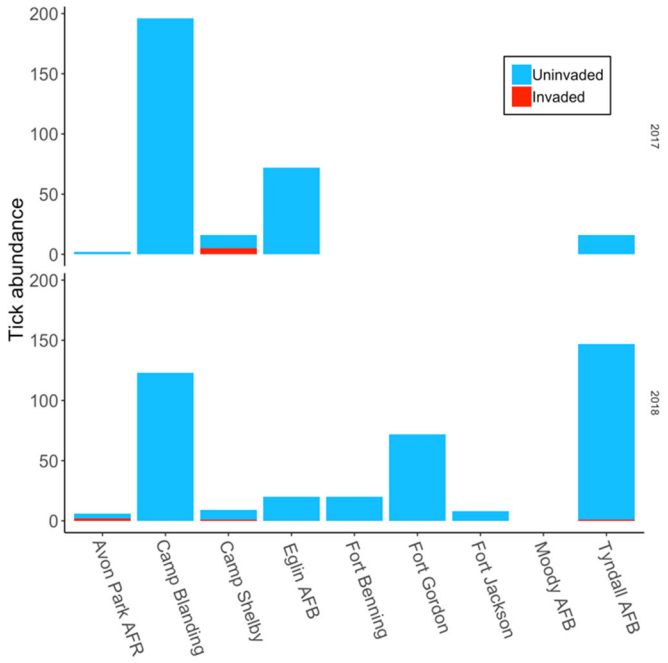

Figure 25. Tick abundances at each installation for each sample year. Blue indicates uninvaded and red indicates cogongrass-invaded.

Summary

In our study, prescribed fire management had only an indirect effect on tick abundance, mediated by litter cover and depth. Longer time since fire resulted in greater litter cover and depth, in turn resulting in greater tick abundance. We hypothesize that the underlying mechanism driving tick abundance in these pine-dominated stands are abiotic conditions, whereby litter and understory vegetation provides microclimatic refuge for ticks during stressful weather conditions, which was supported by experiments presented in Part 2. The relationships between litter cover and depth and tick abundance and time since last fire also suggest there are both direct and indirect effects of prescribed fire management. We found weak to no effects of long-term aggregated climate variables (15- to 30-years) on relationships between fire management, vegetation characteristics, and tick abundances. Applying prescribed fire depends on a complex combination of factors including current weather conditions that determine whether a fire falls within the prescription and can be conducted that day. Among these factors are relative humidity, smoke dispersion (wind speeds and atmospheric mixing), precipitation, and air temperature – currently climate is not a limiting factor. For example, we learned from communications with land managers that Fort Benning, one of the larger and more actively used installations in our study, maintains nearly every management unit on an 18- to 36-month fire return cycle and is equally capable of conducting prescribed fires during the dormant or growing season. In comparison, Moody AFB, the smallest installation, has a small natural resources management staff and are limited to conducting dormant season burns.

PART 2A: TESTING THE EFFECTS OF COGONGRASS FUEL STRUCTURE ON FIRE TEMPERATURE AND RESIDENCE TIME: AN EXPERIMENTAL METHOD

TECHNICAL APPROACH

Fire is a natural disturbance in many forests that maintains understory species diversity, enhances tree regeneration, and mediates tree species composition (Brockway and Lewis, 1997; Dell et al., 2017; Tiribelli et al., 2018). Frequent (2- to 4- year return interval) fires in Southeast US pine forests result in lower fuel loads and low-intensity ground fires that aid in maintenance of ecosystem structure and function (Landers et al., 1995). When these habitats become invaded by non-native plant species, prescribed fire may produce unintended consequences, including high intensity fires and unnaturally high tree mortality (Flory et al., 2015). As a result, few studies have attempted to quantify changes in fire intensity in forests when invasive plants are present, greatly limiting predictions of forest invader impacts on fire behavior and effects (Brooks et al., 2004).

Fire behavior and effects depend on *fuel type* characteristics (moisture, chemistry, and particle size and shape) and *fuel bed* characteristics (continuity, compactness, composition, fuel load, and vertical orientation) (DeBano et al., 1998; Marino et al., 2012; Rossa and Fernandes, 2017; Weise et al., 2016; Whelan, 1995). Fuel characteristics influence all aspects of fire behavior (e.g., heating duration, maximum temperature, flame heights, and rates of spread), which can ultimately determine the structure of ecosystems by altering the abundance and distribution of plants, animals, and soil nutrients (Bowman et al., 2017; Keeley, 2009; Weise et al., 2016; Whelan, 1995). In addition, fires are a common management tool for maintaining the integrity and diversity of fire-adapted ecosystems (Brockway and Lewis, 1997; Driscoll et al., 2010; Shappell and Koontz, 2015). As a result, quantifying how fuel characteristics influence fire behavior and subsequently inferring effects on ecological processes are key to understanding these systems and achieving management goals.

Assessing the influence of fuel characteristics on fire behavior is often accomplished by using small-scale fires from either laboratory or field-based experiments to inform larger area phenomena (Fernandes and Cruz, 2012; Schwilk, 2015) (Fig. 26; Table 8). Laboratory experiments vary in scale of implementation and applicability to natural systems. For example, bench top approaches are designed to measure plant flammability, ignitability, and combustibility, while manipulating fuel type characteristics of different species (e.g., Etlinger and Beall 2004; Engstrom et al. 2004; Simpson et al. 2016). Larger scale laboratory methods have examined fire behavior responses to manipulated fuel beds and environmental conditions, including varying bulk density, fuel moisture, fuel type (species), proportion of live and dead fuels, and wind velocities (Marino et al., 2012; Rossa and Fernandes, 2017; Weise et al., 2016) (Fig 26; Table 8). A particularly distinctive approach mimicked natural vertical fuel structure by placing cut shrubs in a clay aggregate substrate but the method was difficult to implement and has not been widely used (Rossa and Fernandes, 2017).

Field-based approaches measure effects of fuel characteristics on fire effects *in situ* often during and following prescribed fires (e.g., Thaxton and Platt 2006; Loudermilk *et al.* 2012; Flory *et al.* 2015), or by burning smaller individual plots (Bowman et al., 2017; Emery et al., 2013) (Fig 26; Table 8). Both approaches allow for fuel manipulations by adding or removing fuels to alter fuel type, fuel load, or both (e.g., Thaxton and Platt 2006; Bowman et al. 2017). Fuel addition treatments utilizing a combustion table are predominantly piled for efficiency, similar to many lab-based experiments (Marino et al., 2012; Weise et al., 2016), but this approach disregards fuel bed characteristics, such as vertical structure, that can critically affect fire behavior (Ganteaume et al., 2014). Rosa and Fernandez (2017) mimicked natural vertical

structure while using a combustion table approach by placing cut shrubs in a clay aggregate substrate, but acknowledged the difficulty of this process has discouraged researchers from doing so. Even the most realistic experiments that utilize prescribed fires have additional logistical challenges because they depend on appropriate weather conditions and availability of personnel and equipment. Measurement of fire behavior and ambient conditions may also be limited in field settings where experimental control is difficult. Finally, there may be situations that preclude applying fire and recording measurements because the risk of an undesirable outcome is too high, such as when a forest is dominated by an invasive species with very high fuel loads. Field-based approaches may more accurately represent natural fire behavior and ecological effects compared to laboratory approaches but replication and fuel manipulations are typically limited. Laboratory approaches don't often, nor are they intended to, scale up to provide inference on ecological effects. Ideally, a method to manipulate fuels and measure fire behavior and effects would simultaneously enable relatively high experimental replicability for various fuel manipulations while also producing results from which reasonable ecological inferences can be made (Fernandes and Cruz, 2012).

Here, we describe a logistically tenable and relatively low-cost method for experimentally assessing the influence of fuel characteristics on fire behavior. The methodology is general, enabling manipulation of fuel type and fuel bed characteristics. Specifically, our methodology utilizes a free-standing metal device that maintains vertical orientation of fuels to more accurately mimic realistic fuel structure and generate inferences for ecological effects on forest systems. To test the methodology, we conducted experiments using cogongrass (*Imperata cylindrica* (L.) Beauv.), a non-native invasive grass of Asian origin that is widespread in forests of the Southeast United States (Bryson and Carter, 1993; Estrada and Flory, 2015; MacDonald, 2004; Yager et al., 2010). Cogongrass is recognized as one of the top five costliest terrestrial plant invaders in Florida (Hiatt et al., 2019) and a problematic invader in part because of its potential to alter fire regimes and impair longleaf pine regeneration (Daneshgar et al., 2008; Lippincott, 2000; Platt and Gottschalk, 2001). However, there are few studies quantifying how this invader affects fire behavior that provide inference on ecological effects (e.g., heating duration, flame heights) across a range of fuel conditions. The lack of quantified relationships between cogongrass, and many fuels of many other invaders, and fire measurements is due in part to the higher risk of undesirable outcomes (i.e., intense fires causing severe tree mortality) if fire were applied to an invaded forest. The apparatus we developed offers a low-risk method for inferring the potential impacts of extreme fuel loads and structural combinations, which may be especially useful for assessing species invading fire-prone and fire-dependent landscapes.

To test the device and evaluate effects of fuel structure and fuel load on ecologically relevant measures of fire behavior, we conducted experimental fires where fuels were all piled or all standing for a range of fuel loads. We made and compared measurements of heating duration (time above 100 ºC in seconds, s), maximum temperature (ºC), flame height (cm), rate of spread (m s^{-1}), and proportion of fuel load consumed. Our primary objective was to evaluate the effect of fuel structure, specifically piled compared to standing fuels, on the above mentioned fire intensity metrics.

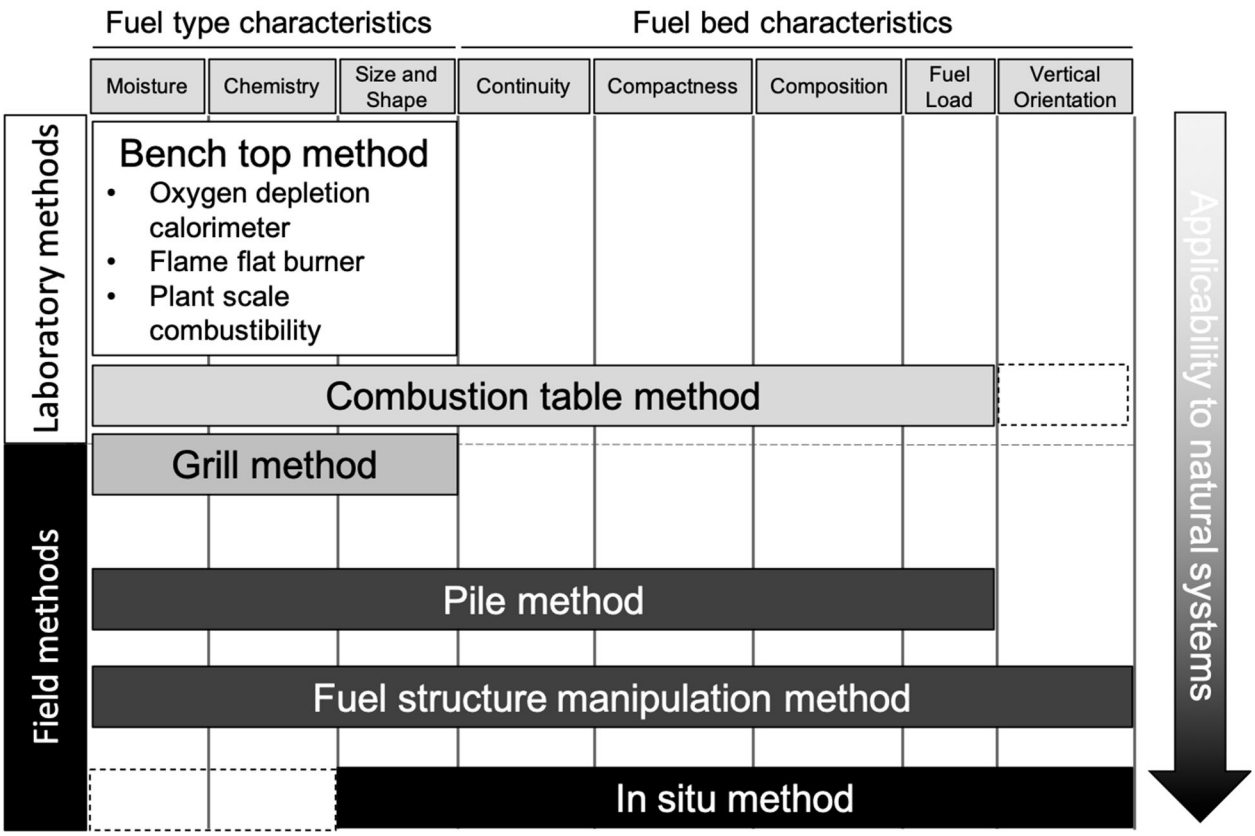

Figure 26. Conceptual diagram of laboratory and field methods used to experimentally manipulate fuel type and fuel bed characteristics. Dashed box (combustion table) indicates that vertical orientation is possible, however the predominant approach uses piled fuels. Dashed box (in situ) indicates areas where observational comparisons of fuel type and fuel bed characteristics can be made, but experimental manipulations are limited. Methods are ordered top to bottom by their applicability to natural systems (gray shading). There are few examples of experimental field methods that retain fuel structure, which is the primary purpose of the method described here. Adapted from tables and figures in Whelan (1995), DeBano *et al.* (1998), Gill and Zylstra (2005). See Table 1 for references and details on fire intensity measurements that can be made using each method.

Table 8. Laboratory and field methods used to experimentally manipulate fuel characteristics (fuel type and fuel bed) and the fire characteristics that can be measured using each method. See Figure 1 for a visual depiction of how different methods can be used to evaluate fuel type and fuel bed characteristics.

Approach	Fuel type manipulations	Fuel bed manipulations	Measurements	Vertical orientation	References
Bench top	moisture, chemistry, size and shape	n/a	maximum temperature, temperature duration, fuel consumed	yes	Etlinger and Beall 2004; Engstrom et al. 2004; Simpson et al. 2016
Combustion table	moisture, chemistry, size and shape	continuity, compactness, composition, fuel load	fuel consumed, rate of spread, flame height	yes	Weise et al. 2005; Marino et al. 2012; Rossa and Fernandes 2017
Grill	moisture, chemistry, size and shape	n/a	maximum temperature, temperature duration, fuel consumed	no	Jaureguiberry et al. 2011
Pile	moisture, chemistry, size and shape,	continuity, compactness, composition, fuel load	maximum temperature, temperature duration, fuel consumed, rate of spread, flame height	no	Thaxton and Platt 2006; Bowman et al. 2017
Fuel structure manipulation	moisture, chemistry, size and shape,	continuity, compactness, composition, fuel load	maximum temperature, temperature duration, fuel consumed, rate of spread, flame height	yes	This study
In-situ	size and shape	continuity, compactness, composition, fuel load	maximum temperature, temperature duration, fuel consumed, flame height	yes	Lippincott 2000; Wenk et al. 2011; Loudermilk et al. 2012; Flory et al. 2015

Experimental apparatus

To test the importance of fuel load structure (vertical orientation) we constructed a free-standing metal device to measure fire intensity with fuels of the same fuel load (kg/m^2) either piled or standing in the device. The standing metal device (Fig. 27) was constructed using

punched 90-degree angle-iron held together with bolts and wing nuts, and horizontally-oriented "goat panel" with 10-cm square openings to support fine fuels vertically. To measure relative temperatures during fires, we equipped the device with nine type K model TP875 braided steel insulated wire thermocouples (Extech Instruments, Nashua, NH, USA) that were 100-cm long with a 2-mm bead tip. The thermocouples were connected to U12 HOBO thermocouple loggers (Onset Computer Corporation, Bourne, MA, USA) capable of recording temperatures between 0 and 1250 ºC at one second intervals on the K channel. Loggers were housed in Pelican cases (1010 Micro Case, Torrance, CA, USA) with foam inserts (1012 Pick N Pluck). A small hole was drilled in the lid of each case to pass through the thermocouple wire. To measure relative temperatures throughout the duration of the fire, three thermocouples were placed across the center line of the device, one at the center and one 25 cm to either side of center, at each of three heights (ground level, 25 cm, and 50 cm). The tips of the thermocouples were extended 3-5 cm away from the steel framing to minimize residual heat exposure and were secured with binder clips. Flame height was measured at two locations using passive flame height sensors (Ryan, 1981) consisting of 2-lb. (0.91 kg) load limit twisted cotton string (Wellington, Inc., Madison, GA, USA) soaked in flame retardant (Phos-Chek LC-95, ICL Performance Products LC, Ontario, CA, USA) for 48 hours and dried at 60 ºC for at least 24 hours. The strings were tied to a horizontal piece of steel conduit to hang vertically with approximately 25 cm between the strings and the edges of the frame (Fig. 27). Applying fire retardant to the string results in the fire charring but not consuming the string so flame height can be measured based on the char height of the string. Flame height sensors could measure heights up to 275 cm and string could be quickly replaced between experimental fires. Passive flame height sensors provide a reasonably accurate measurement of flame heights for inferring ecological effects that is relatively free from human bias (Finney and Martin, 1992; Kolaks et al., 2004; Simard et al., 1989).

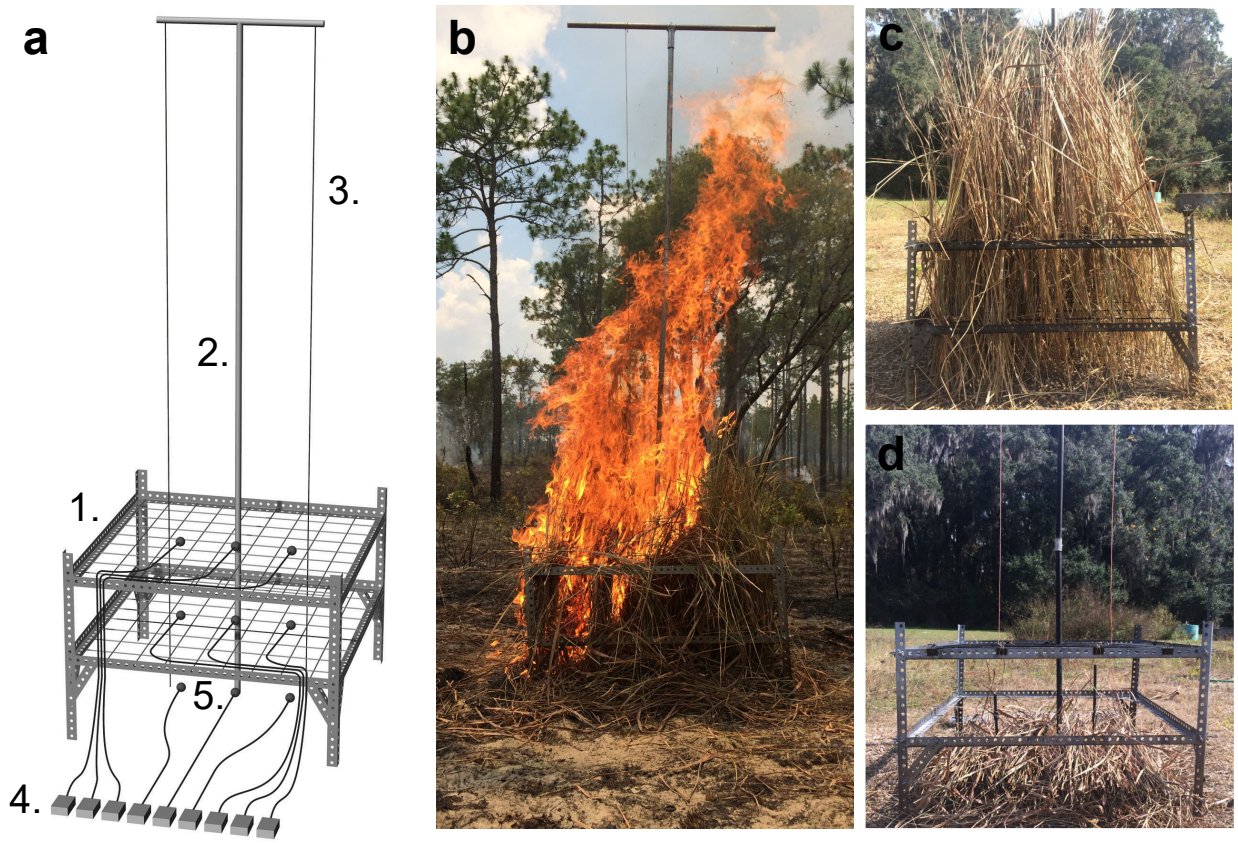

Figure 27. Schematic of the fuel structure manipulation device (a) Schematic legend: 1. 3.18 cm (1-1/4") punched angle iron holding welded 4 gauge wire with approximately 10 cm x 10 cm openings; 2. 1.91 cm (¾") metal conduit; 3. flame retardant soaked cotton twine; 4. temperature data loggers (U12 HOBO J,K,S,T thermocouple loggers, Onset Computer Corporation, Bourne, MA, USA), inside of weatherproof cases (Pelican 1010 Micro Case, Torrance, CA, USA) with foam inserts (Pelican 1012 Pick N Pluck); and 5. type K thermocouples (Model TP875, Extech Instruments, Nashua, NH, USA) with braided steel wire leads and a 2 mm welded bead. The device during an experimental burn (b) and prior to burning an equal amount of standing (c) and piled (d) fuel.

Fuels and weather measurements

We collected green cogongrass from a natural invasion at the Bivens Arm Research Site (BARS) in Gainesville, FL, USA (29.629° N, -82.353° W) and let it air-dry in a shallow pile for 72 h to achieve a relatively consistent fuel moisture. We determined fuel moisture by collecting and weighing a small subsample of the fuel load (approximately 20 g), drying the sample for 72 h at 60 °C to constant mass and reweighing. Across all experimental fires, fuel moisture content ranged from 4.6 % to 19.6%, which is at the lower end of fuel moisture estimates from field collections of standing cogongrass that ranged from 8.5% to 72% (mean = 40.5%, SD = 19.6%, n = 24). Average moisture content was not significantly different ($t = -0.8$, $p = 0.42$) between piled and standing fuels, at 11.2% (SE 0.7%) and 11.8% (SE 0.9%) respectively. Fuel moisture values for each fire are reported in Table A1. The fuel pile was raked each day to promote even drying,

while carefully maintaining stem orientation in the same direction to make weighing and loading fuels vertically into the device more efficient.

Experimental burns were conducted at the BARS on December 1st, 4th, and 5th 2017, under dry conditions. December through March are typically favorable fire weather for dormant season prescribed fires in northern Florida. During all fires a weather station (Kestrel 5500 Fire Weather Pro, Nielsen-Kellerman, Boothwyn, PA) was mounted on a tripod at 1.5 m above ground level and approximately 5 m from each experimental fire. Relative humidity, wind speed, and air temperature were recorded every 2 seconds during each fire and summarized. Ambient weather conditions had minimal influence on experimental fires and are reported in Table A1.

Experimental treatments

We selected five fuel loads (250, 500, 1000, 1500, and 2000 g) representative of congongrass in naturally occurring invasions (Clark et al. 2017, unpublished data) and conducted 32 experimental fires in a "replicated regression" design (Cottingham et al., 2015) with either piled (n = 16) or standing (n = 16) fuel structure arranged in the 1 m^2 footprint of the device. Each fuel load-structure combination was replicated three times except 1000 g had four replicates because we had enough fuel for an additional pair of fires. Piled fuels were loosely and evenly spread on the ground and plant material was trimmed so that the entire fuel load lay within the footprint of the device. Standing fuels were evenly spaced and inserted vertically through both raised gridded platforms (Fig. 27b, c). To minimize potential effects of weather conditions when evaluating fuel structure effects, we used two devices, one with piled and one with standing fuels, each with the same fuel load, burned simultaneously (Fig. A1). All fires were ignited as head fires using a drip torch (Sure-Seal, Forestry Suppliers, Jackson, MS), with a 50:50 gasoline to diesel mixture. If the fire failed to carry on the first ignition attempt, three additional attempts were made before determining that the fire failed to burn. Failure to burn occurred for standing structure small fuel loads (i.e. 250 g) due to a lack of fuel continuity that prevented the fire from carrying. Measurements of ambient temperatures when fires failed to carry, as well as zeroes for rate of spread and flame height, were retained in analyses.

Fire intensity measurements

For the experimental fires, heating duration was estimated as the average of the total number of seconds during which the temperature was above 100 ºC from the three thermocouples at each height. We selected 100 ºC as a conservative threshold temperature for inferring potential ecological effects to limit possible bias arising from heat retention in the metal frame. Temperatures rapidly fell below 100 ºC after the flame front passed and smoldering ceased.

The maximum temperature for each fire was estimated by first averaging the five highest temperatures for each probe and then averaging the values from the three probes at each height. This calculation produced a conservative estimate of maximum temperature and smoothed over brief temperature spikes. We did not correct for thermal inertia of the thermocouples because the main goal was inferring ecological effects rather than very precise estimates of temperatures. The rate of spread was estimated by recording the time (seconds) it took for the base of the fire to travel between two visual markers on the edge of the device spaced 50 cm apart. The visual markers were each placed 25 cm inside each edge so that the rate of spread was based on combustion of plant material and not influenced by fuel from the drip torch. Fires did not carry

through the 250 g standing fuel loads so these were zero values in the model. Flame height for each fire was the averaged scorch height measured from ground level of both passive flame height sensors (Fig. 27). Flame lengths could have been underestimated if flames had significant horizontal angle but because flames were near vertical during our experimental fires, flame height would be similar to flame length. After each fire, remaining intact biomass (not ash) was collected by hand-sifting the ash on the ground and weighed to estimate the proportion of biomass consumed.

Statistical analyses

We used ordinary least squares linear regressions (OLS) to model the response variables of heating duration >100 ºC and maximum temperature at each height, as well as flame height, and rate of spread. We used beta regression (Ferrari and Cribari-Neto, 2004) to model the proportion of biomass consumed. Fuel load (mass) and fuel structure (piled vs. standing) were used as explanatory variables in each model, and fuel load was entered as a continuous variable. We tested the effects of fuel load and its interaction with fuel structure, as well as effects of fuel height, fuel moisture, and weather covariates (e.g., air temperature, wind speed, relative humidity). Fuel height, fuel moisture, wind speed, and relative humidity did not improve fits of any models and were not statistically significant ($p>0.1$); therefore, we excluded them from reported models. Because our main goal was to assess the effect of fuel structure (piled vs. standing) on fire behavior, we retained fuel structure and biomass in all models regardless of statistical significance. R was used for all analyses and OLS models were fit using the lm function in the stats package (R Core Team, 2018). The betareg package (Cribari-Neto and Zeileis, 2010) was used to fit the beta regression.

RESULTS AND DISCUSSION

Fire intensity

Heating duration during experimental fires ranged from 0 to 814 s (0-13.6 minutes), with the longest durations recorded at ground level for 2000 g m^{-2} of piled fuels (Figs. 28a-c, A2). Overall, heating duration was greater for piled fuel structure (mean = 157 s) than for standing fuel structure (mean = 48 s) and there was a significant interaction of fuel load fuel structure, with larger fuel loads weakly affecting heating duration of standing fuels compared to piled fuels (Fig. 28a-c, Table A2). Adjusted R^2 of models for heating duration were 0.67, 0.86, and 0.73 at 50, 25, and 0 cm, respectively.

The calculated maximum temperatures recorded during experimental fires of either piled-only or standing-only fuels ranged from the “near-ambient” temperature of 40 ºC for 250 g of standing fuel (fires that didn’t carry) to a high of 824 ºC for 1500 g of piled fuel at the 50 cm height. We assigned 40 ºC as “near-ambient” due to heat retention of the ground and experimental apparatus making the thermocouple reading higher than the actual ambient air temperature, which ranged from 22.3 ºC to 30.3 ºC during experimental fires (Table A1). Larger fuel loads generated higher maximum temperatures, with piled fuels generating greater maximum temperatures at lower fuel loads and closer to the ground (Fig. 28 d-f); however, the interaction between fuel load and structure was not significant and we therefore excluded it from the final model (Table A3). Fuel load and fuel structure had significant effects in models of maximum temperature at 0 and 25 cm, but only fuel load was significant at 50 cm (Table A3).

Adjusted R^2 of maximum temperature models were 0.80, 0.74, and 0.53 at 50, 25, and 0 cm heights, respectively.

Flame heights were greater with higher fuel loads and for standing than piled fuel structure for fuel loads ≥1000 g m^{-2} (Fig. 29a). The model of flame height had significant effects of fuel load, the interaction of fuel load and fuel structure, and air temperature (Table A4) with an adjusted R^2 of 0.81.Rate of spread significantly increased with larger loads of standing fuel, but decreased slightly with larger piled fuel loads (Fig. 29b). The model for rate of spread had significant effects of air temperature and the interaction of fuel load and fuel structure (Table A4), with an adjusted R^2 of 0.53. The model for proportion of biomass consumed had significant effects of fuel load, fuel structure, and the interaction of fuel load and fuel structure (Table A4), with a pseudo-R^2 of 0.73. All fires with piled fuels, or with standing fuel loads ≥1000 g m^{-2}, had over 95% of fuel mass consumed (Fig. 29c).

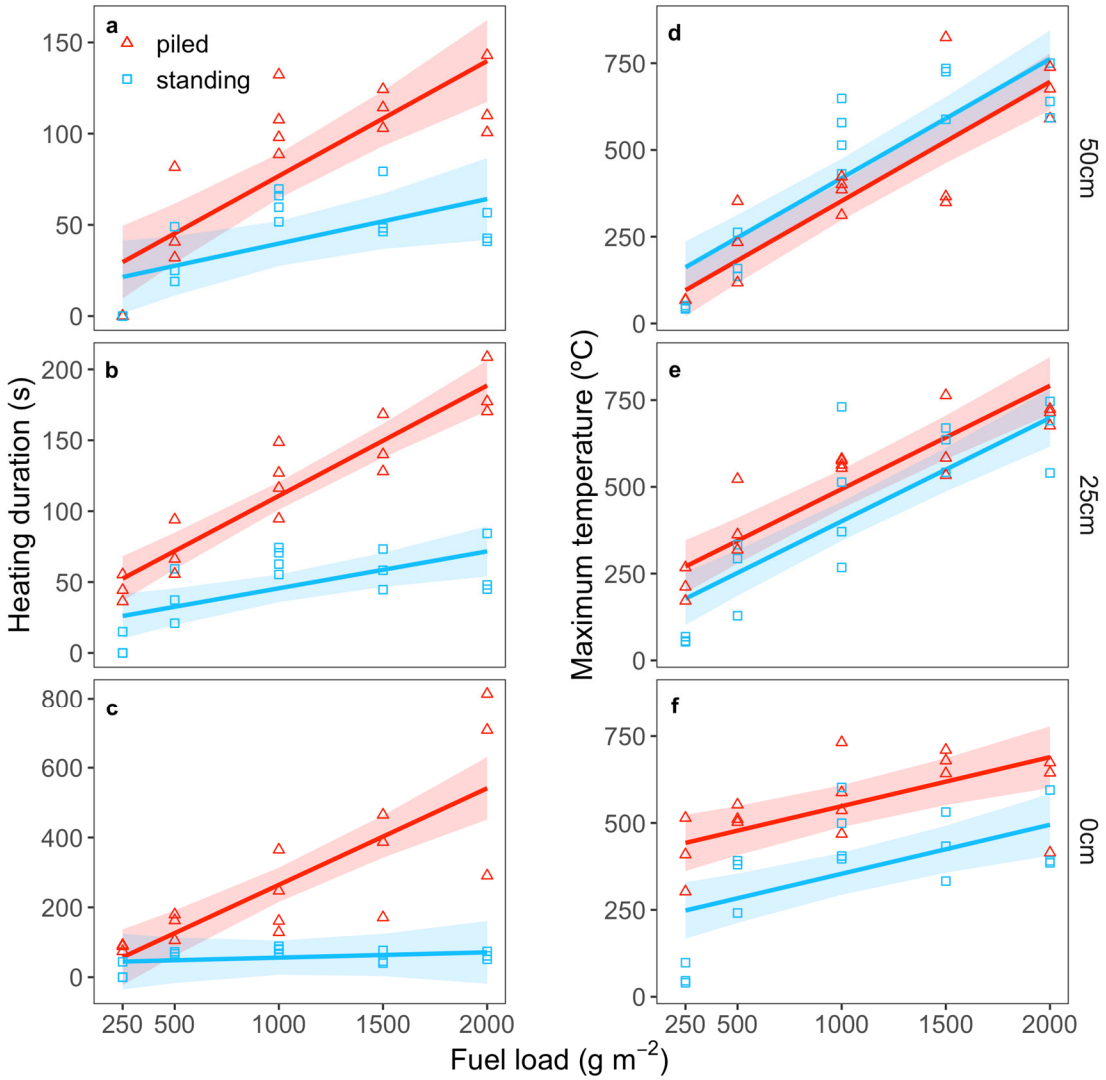

Figure 28. Fitted regressions (solid lines) with 95% CI (shaded area) plotted over data from each experimental fire for the calculated estimates of heating duration (time temperatures exceeded 100 ºC) (a-c, note different scales of y-axes) and maximum temperature

(ºC) (d-f) versus fuel load for piled and standing fuel structures at 50- , 25- , and 0-cm above ground level. The predicted line for maximum temperature at 50 cm is for air temperature at its mean of 26.55. Red is piled fuels; light blue is standing fuels.

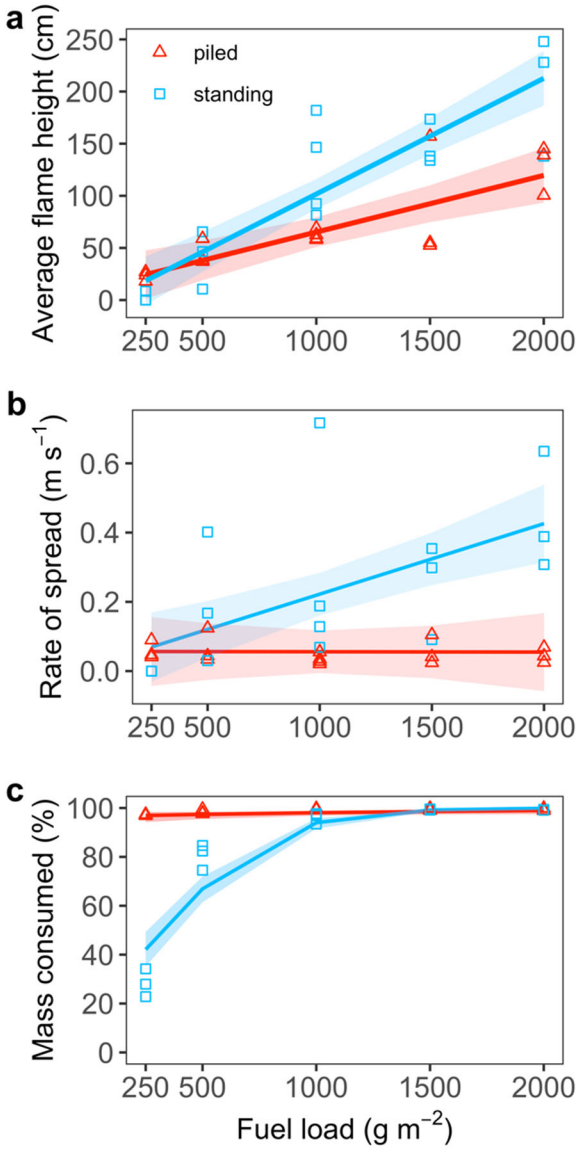

Figure 29. Predicted relationships (solid lines) plotted over observed data points from each fire for flame heights (cm) (a), rate of spread (m s^{-1}) (b), and percent of mass consumed (c) for piled or standing fuel structure across fuel load treatments. Red lines are for piled fuels, light blue lines are standing fuels. The predicted lines for flame height and rate of spread are with air temperature held at its average of 26.55.

Discussion

We developed a new device and method to achieve greater precision, accuracy, and realism of fire experiments seeking to understand how fine fuel structure influences fire behavior

and the potential ecological effects of fire. The device enabled relatively rapid testing of how different fuel bed structures affected fire characteristics without the logistical constraints posed by working within a prescribed fire setting. Furthermore, the methodology distinguished which differences between standing grass and litter fuels were due to the inherent nature of the fuels, and which were due to the fuel structure. More generally, our results illustrate that not accounting for fine fuel structure in manipulative experiments may lead to inaccurate extrapolations of the ecological effects of fire (Fernandes and Cruz, 2012; Ganteaume, 2018; Varner et al., 2015). We demonstrated our methodology with cogongrass, a widespread and problematic invader in Southeast US pine forests that can limit the use of prescribed fire as a management tool in heavily invaded areas, and we report the most precise estimates to date of fire behavior from cogongrass-fueled fires. We first discuss the effectiveness of the apparatus in manipulating fine fuel structure and whether we saw expected patterns in fire behavior. Then, we make comparisons of our results to other studies on cogongrass and fire. Finally, we end with discussing some potential biases stemming from the experimental methodology and apparatus.

Apparatus effectiveness

Maximum temperature, heating duration, and flame height all increased with fuel load for piled and standing fuel structures, while changing fuel load affected the rate of spread and mass consumed only of standing fuels. The longer heating duration and slower rate of spread for piled fuels was likely because these responses depend on characteristics of continuity and compactness (Ganteaume et al., 2014; Loudermilk et al., 2012). Regardless of fuel load, piled fuel had essentially the same continuity and was more densely packed compared to the standing fuel structure, thereby reducing fuel bed aeration and rate of spread, and exposing the probes to higher temperatures for longer. In contrast, standing fuels were better aerated, with more exposed surface area to burn, and continuity increased with greater fuel loads, thereby resulting in faster spreading fires and shorter heating durations. These effects of fuel structure on fire characteristics, which can be used to assess potential and actual ecological effects (e.g., Bigelow and Whelan 2019), illustrate that mimicking natural fine fuel structure may be paramount in bridging the gap between real-world fire measurements, field experiments, and laboratory flammability assessments (Fernandes and Cruz, 2012).

Since 60 ºC is widely accepted as the temperature at which plant tissue damage occurs, even a relatively short period of time above 100 ºC may result in severe damage and mortality (Dickinson and Johnson, 2004; Jones et al., 2006). Fuel structure significantly affected heating duration, so whether fine fuels are piled or standing in fire experiments can influence the interpretation of potential ecological effects. The increasing heating duration we observed with greater fine fuel loads, particularly 25-50 cm above ground-level, could have severe ecological effects. Greater exposure to high temperatures above ground may increase sapling (or shrub) mortality (Bowman et al., 2017; Swezy and Agee, 1991) via xylem failure in the stem or canopy (Michaletz et al., 2012). Our results suggest that piled fuels may cause a greater ecological impact via heating duration compared to standing fuels, while standing fuels may cause more top-kill due to greater flame heights. Because the overall ecological impact of fires varies according to fuel conditions, more realistic fine fuel conditions in fire experiments will provide more accurate extrapolations of risk for tree and plant mortality under real-world fire conditions.

Cogongrass and fire

Our experimental design included either piled or standing fuel structures but standing structure most closely mimics real-world cogongrass fuel beds, so we refer to standing fuels in our experiment for comparisons unless otherwise noted. To date, most reports on how cogongrass affects fire behavior in the USA have been qualitative. We are aware of only two studies that have compared temperatures from cogongrass fires to native vegetation fires in the longleaf pine savanna ecosystem. Lippincott (2000) recorded maximum temperatures of 458 ºC for a cogongrass fuel bed versus 290 ºC for native vegetation at heights of 50 and 150 cm in a longleaf pine ecosystem using temperature-indicating paints. Similar peak temperatures were reported using thermocouples positioned 25 cm above the soil surface in a native-dominated longleaf pine ecosystem where three understory fuel complexes were differentiated (mean ±SE): 294 ±34.9 ºC for longleaf pine litter; 376 ±20.3 ºC for turkey oak dominated fuel; and 321 ±20.2 ºC for wiregrass (Wenk et al., 2011). The maximum temperatures estimated during our experimental cogongrass fires frequently exceeded those reported by both of these studies, as well as a number of others in longleaf pine ecosystems (Bigelow and Whelan, 2019; Cronan et al., 2015; Ellair and Platt, 2013; Hiers et al., 2009; Kennard et al., 2005; Thaxton and Platt, 2006). For example, the average maximum temperature at 50 cm for 1000 g m^{-2} standing fuel fires in our experiment was 543 ºC, 197 ºC greater than the maximum of 346 ºC reported in Lippincott (2000) at the same height and similar fuel load. The substantial discrepancy in temperatures is at least partly due to the different measurement methods but also external factors such as wind speed and fuel moisture that can dramatically influence fire behavior in any given area during prescribed fires (Whelan, 1995).

Using thermocouples allowed us to measure, and report for the first time, heating duration (time above 100 ºC) for cogongrass-fueled fires. Notably, the heating duration from our experimental fires with standing fuels was similar to that of fires in native longleaf pine ecosystems (Bigelow and Whelan, 2019; Cronan et al., 2015; Ellair and Platt, 2013; Hiers et al., 2009; Kennard et al., 2005; Thaxton and Platt, 2006). This similarity suggests that the effects of cogongrass on fire behavior in the Southeast USA, and its reported problematic nature, is driven by the higher fuel loads it generates compared to native vegetation. In this study, we used air-dried fuel to maintain relatively consistent fuel moisture among treatments. Future experiments could be conducted using this apparatus and variations in fuel moisture to explore if cogongrass potentially creates a barrier to fire spread when fuel moisture is high (e.g., when litter levels are low). The taller flame heights produced by standing cogongrass fuel loads ≥1000 g further illustrate the potential ecological impacts of this invader. Flames reached over 1 m height during nine of the fires, indicating that cogongrass-fueled fires have the potential to top-kill seedlings and saplings in invaded forests.

Our experimental fires with standing fuels produced rates of spread ranging from 0.02 to 0.72 m s^{-1}, which covers values measured in the field and produced from fire models. Cogongrass-fueled fires in a natural setting had an estimated rate of spread of 0.14 m s^{-1} (Lippincott, 2000); and a modeled rate of spread under drought conditions for native species in pine flatwoods of Florida was 0.3 m s^{-1} (Brose and Wade, 2002). While the small area of our device and few measurements of cogongrass fires in the field mean that these rates of spread estimates could change dramatically (e.g. influence of wind speed), the potentially rapid rate of spread of cogongrass-fueled fires may present a greater danger to personnel during prescribed fires, an otherwise preferred management method in longleaf pine ecosystems. Similarly,

experimental approaches that do not utilize this apparatus, and use piled fuels, will drastically underestimate rate of spread.

Potential bias

Experimental measurements are subject to bias from their design and the tools and apparatuses used. In this experiment, there were several aspects that could bias the measurements. The bead thickness of the probes may underestimate actual temperatures (Bova and Dickinson, 2008), although this issue should be less critical for making ecological inference about relative heat output than if the goal was to very precisely measure combustion. In addition to temperature probe characteristics, the metal frame may affect measurements of heating duration by retaining heat. Given the goal of inferring potential ecological impacts, our selection of a 100 ºC threshold temperature for heating duration provided a conservative estimate because temperatures rapidly fell below 100 ºC after the flame front passed and smoldering ceased. Although our experimental method may introduce some biases to the measurements taken, they are likely to be small in terms of evaluating ecological effects relative to weather conditions and fuel structure and moisture. Therefore, the method can be useful for evaluating actual or potential ecological effects of fire, especially when it is problematic to burn particular fuels over a large area.

PART 2B: INVADED AND NATIVE PLANT COMMUNITIES ALTER TICK EXPOSURE RISK VIA DIFFERENT MECHANISTIC PATHWAYS

TECHNICAL APPROACH

Among the major threats to human health are emerging infectious diseases transmitted from animals to humans via arthropod vectors such as ticks (Morens et al. 2004, Jones et al. 2008). Tick-borne disease transmission results from complex species interactions that are often embedded in forest communities (Ostfeld et al. 2018, Morand and Lajaunie 2021). Non-native plant invasions can alter these species interactions, with potential to facilitate or inhibit infectious disease spread to humans (Allan et al. 2010, Mack and Smith 2011, Stewart et al. 2021). There is contradictory evidence on possible abiotic vs biotic mechanisms underlying invasive plant species effects on tick-borne disease (Civitello et al. 2008, Allan et al. 2010, Williams and Ward 2010, Mack and Smith 2011, Racelis et al. 2012). While there has been research on how different pathways may individually affect tick abundance, studies that simultaneously address multiple pathways are needed to improve disease risk predictions.

Invasive plants may affect disease risk by altering abiotic conditions that affect off-host tick survival or by modifying biotic conditions that affect host use (Fig. 30) (Civitello et al. 2008, Allan et al. 2010, Williams and Ward 2010, Racelis et al. 2012, Adalsteinsson et al. 2016). For example, invaders may increase tick abundances by providing favorable microclimate conditions that reduce tick desiccation (Williams and Ward 2010, Racelis et al. 2012). However, the limited mechanistic studies of tick survival in invaded and native areas show either no difference (Allan et al. 2010) or reduced tick survival (Civitello et al. 2008) in invaded areas compared to native plant communities. Additionally, invaders have been shown to enhance habitat use by tick hosts, leading to greater abundance of ticks (Elias et al. 2006) and pathogen-infected ticks (Allan et al. 2010) compared to native areas. Collectively, evidence on mechanisms that determine tick abundances in invaded areas is inconsistent.

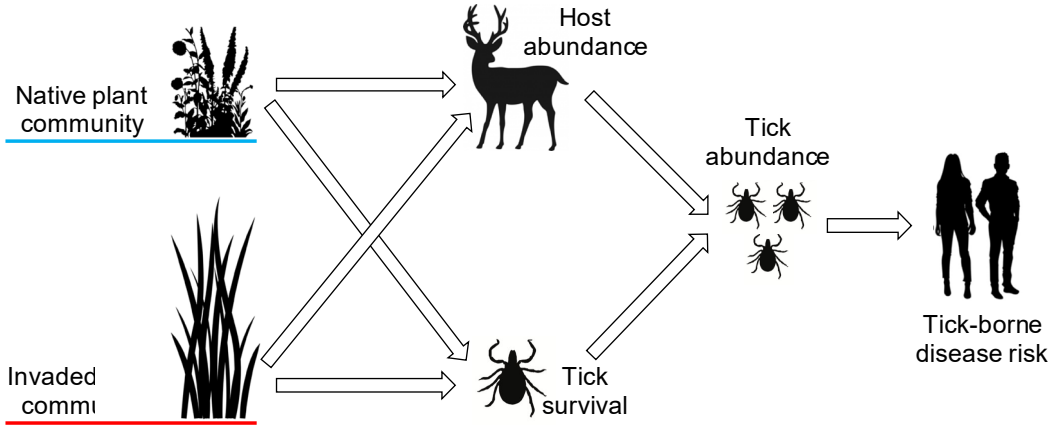

Figure 30. Conceptual diagram of two pathways that contribute to tick-borne disease risk. Native and invaded plant communities may have different effects on both host (e.g., deer, rodent) abundances and tick survival, which together determine tick abundance and, in turn, influence tick-borne disease risk.

Here, we sought to measure the contributions of plant invasion to tick survival, host activity, and their effects on tick abundance. Specifically, we evaluated how a plant invasion (cogongrass; *Imperata cylindrica*) affected microclimate conditions and survival of the lone star tick (*Amblyomma americanum*) compared to native species dominated areas, and how changes in

relative host (i.e., white-tailed deer, *Odocoileus virginianus*) use influenced tick abundance (Fig. 1). We conducted a field study where we measured temperature, relative humidity, and survival of experimental ticks in invaded and nearby native areas over 11 months. Separately, we evaluated relative host activity (via camera traps) and tick abundances in paired invaded and native areas in a field survey. We hypothesized that invaded areas buffered environmental conditions by providing lower maximum temperatures and higher relative humidity, on average, which would promote tick survival relative to native areas. We also hypothesized that relative host use would be greater in invaded communities because the dense cover of the invasion could provide protection from predators or suitable bedding habitat, thereby increasing tick abundance.

Study system

One of the most problematic invasive plant species in the Southeast US is *Imperata cylindrica,* (L.) Beauv. (cogongrass; hereafter *I. cylindrica*), and economically it is one of the top five costliest terrestrial invasive plants in Florida (Hiatt et al. 2019). *Imperata cylindrica* can invade a wide variety of habitats in part by its greater trait plasticity (Hiatt and Flory 2020), and drought tolerance (Fahey et al. 2018) compared to co-occurring native species. *I. cylindrica* has also been shown to alter microclimate conditions, increasing soil moisture and relative humidity, and elicits cooler temperatures at ground level compared to native plant communities (Alba et al. 2017, Cabrera et al. 2021). Currently it is unknown how this dominant invasive plant species may be altering tick-borne disease risk to humans in the Southeast USA.

Lone star ticks (*Amblyomma americanum*) are hard ticks in the family Ixodidae (Keirans and Litwak 1989) that can transmit pathogens including the causative agents of human ehrlichiosis, Rocky Mountain spotted fever, and southern tick associated rash illness (Childs and Paddock 2003). Time between blood meals (off-host) comprises over 90% of a three-host Ixodid tick's life cycle, and a primary cause of tick mortality is desiccation (i.e., loss of water through the cuticle) (Needham and Teel 1991). To maintain water balance, ticks must be in microclimate conditions that are at or above their critical equilibrium humidity (CEH), which is 80-82% RH for adult *A. americanum* (Hair et al. 1975, Knülle and Rudolph 1982). While desiccation is primarily driven by low relative humidity (at or below CEH), temperatures in excess of 35 ºC can also contribute to desiccation and mortality (Sauer and Hair 1971). Local abundance of *A. americanum* can also be regulated by host activity. For example, white-tailed deer (*Odocoileus virginianus*) serve as a host for all three life stages of *A. americanum* (Bloemer et al. 1986). An invasive plant species, *Lonicera maackii*, increases habitat use by white-tailed deer, leading to more infected *A. americanum* nymph ticks compared to native plant dominated communities (Allan et al. 2010).

Field Study: Tick survival and microclimate

To examine the effect of *I. cylindrica* invasions on tick survival, we established a survival assay in a planted longleaf pine (*Pinus palustris*) stand near La Crosse, FL with distinct *I. cylindrica*-invaded and native areas (Figure 31c). The invasion was a monotypic stand of *I. cylindrica* spanning approximately 6300 m^2, surrounded on all other sides by uninvaded, native understory. The plant community of the native area was typical of a longleaf pine stand, with *Aristida stricta* (wiregrass), *Rubus flagellaris* (common dewberry), *Carya sp.* (hickory), and *Andropogon sp*. grasses.

Figure 31. Ticks in mesh bags inside wire mesh exclosures along with PVC housing for temperature and relative humidity loggers in (a) invaded and (b) native plant communities. Representation of (c) the field study site showing invaded to the left and native plant communities to the right, separated by managed boundary area to maintain distinct plant communities.

We established 24 plots (1m x 1m), 12 in the invaded area and 12 native area, with at least 10m between plots. At the center of each plot, a 300-micron fine 10 x 20 cm nylon mesh bag (Skimz, Singapore) (Fig 32), containing 10 nymph and 10 adult (5 female and 5 male) *A. americanum* obtained from the National Tick Research and Educational Resource (Department of Entomology and Plant Pathology, Oklahoma State University, Stillwater, OK) were placed in 50cm tall cylindrical wire mesh exclosures to deter interference from wildlife (Fig 31). Each mesh bag containing ticks was oriented vertically and remained in contact with the litter layer to facilitate some natural diurnal tick questing behavior (Schulze and Jordan 2003) throughout the experiment (see Figure 31a / 31b).

Figure 32. Adult and nymph ticks in mesh bag.

Start date of the survival assay (June 21, 2018) was selected to coincide with typical off host periods for *A. americanum* nymphs and adults in this area (Davidson et al. 1994, Gleim et al. 2014). During these long non-parasitic phases ticks will seek refuge in areas that promote a constant water balance (Knülle and Rudolph 1982, Davidson et al. 1994). Mesh bags were examined frequently for the first month (approx. every 7-10 days) and then approximately every 10-14 days afterward to determine nymph and adult survival. At each visit, bags were removed from the cages but not opened, and survival of each individual tick was determined by assessing the response of the tick to CO_2 stimulation. Any signs of movement qualified the tick as living. If there was no response by the tick, it was marked as dead and monitored in subsequent visits to assure the previous mortality designation was correct. Visits continued to the site until May 23, 2019, by when all ticks succumbed to mortality.

Within each 1m x 1m plot we collected understory herbaceous plant height and standing biomass, light availability at the soil surface, and overstory canopy cover. Plant height was measured as the tallest point of living leaf tissue from soil surface. Standing biomass was collected and dried at 60 ºC to a constant mass and weighed (± 0.01g). Light availability, photosynthetically active radiation (PAR), was measured at ground level for each plot using an ACCUPAR LP-80 PAR/LAI ceptometer (Decagon Device Inc., Pullman, WA, USA). Overstory

canopy cover was measured using a concave spherical densiometer from the average of four readings facing each cardinal direction. We also recorded ground-level microclimate conditions (temperature and relative humidity) at five-minute intervals immediately adjacent to each exclosure containing the mesh bags using HOBO U23 Pro v2 loggers (Onset Computer Corporation, Bourne, MA). Each logger was housed in a capped 18-inch length of 3.8 cm diameter PVC pipe to protect it from rainfall and direct sunlight. Holes were drilled on four sides six inches apart along the length of the pipe to allow airflow and better reflect ambient temperature and relative humidity (see Figure 32a/32b). Temperature and relative humidity data loggers operated for the duration of the study.

Statistical analysis: Tick survival and microclimate

We conducted our statistical analysis in four phases. First, we conducted two analyses to understand how *I. cylindrica* invasions change plant community characteristics that influence microclimate conditions. We used analysis of variance (ANOVA) to test the hypothesis that *I. cylindrica* invasions alter plant community characteristics (i.e., vegetation height, standing biomass, and light availability at soil surface). We also fit non-linear ordinary least squares regressions to test the hypothesis that *I. cylindrica* invasions alter microclimate conditions (average daily minimum relative humidity and average daily maximum temperature) throughout the duration of the survival assay. These analyses were done using R version 3.6.1 (R Development Core Team 2019).

Second, we used linear regression models to identify how both microclimate conditions (hours per day under 80% RH and daily maximum temperature) contributed to *A. americanum* longevity or mortality within each treatment. We fit ordinary least square linear regression models to individual tick survival (days) and hours per day under 80% RH (total hrs. below 80% RH/ days survived) as well as maximum temperature experienced prior to mortality for both nymph and adult life stage ticks. Maximum temperature at mortality was estimated as the maximum temperature recorded at the respective plot between survival checks (i.e. the maximum temperature between the time when the tick was last alive and when it was observed as dead). We also included plot as a random effect to account for repeated measures. Models were fit using R 3.6.1 (R Development Core Team 2019).

Third, to test the hypothesis that *I. cylindrica* invasions increase survival of *A. americanum*, we used separate stratified Kaplan-Meier analyses to compare survival and hazard functions across treatments (i.e., invaded versus native), within tick life stages (i.e., nymph versus adult), and between sexes (i.e., female vs male adult ticks). The survival function estimates the probability that a tick has not died by a given time interval, while the hazard function estimates the probability that a tick will die during a given time interval. Tick survival status was the binary response variable, coded as “0” if an individual tick was alive or “1” if the tick was dead at a given time interval. Plot was included as a random effect to reflect unaccounted habitat variation within the study area. The analysis was conducted using PROC LIFETEST in SAS 9.4 (SAS Institute Inc., Cary, NC).

Fourth, to identify microclimate conditions that may mechanistically drive *A. americanum* mortality over time, we fit a Cox regression model to tick survival status using the exact calculation of the partial likelihood to handle ties. Predictor variables included the fixed effects of life stage, mean temperature, maximum temperature, mean vapor pressure deficit, and time (minutes) below 80% RH, between 80-82% RH, and greater than 82% RH within the interval since ticks last had been examined for survival status. Again, plot was included as a

random effect. We fit multiple candidate models including combinations of these variables; the model that minimized the Akaike information criterion (AIC) was considered the most parsimonious. The analysis was conducted using PROC PHREG in SAS 9.4 (SAS Institute Inc., Cary, NC).

Field survey: Tick abundance and host use

To examine the impact of *I. cylindrica* invasions on host activity and tick abundance, we conducted field surveys within invaded and native plant communities across north central Florida (Fig 33). Across these eight sites, we established 21 plots within *I. cylindrica* invaded areas and 12 comparable native plots. Invaded plots were located at least 20 m away from native plots and *I. cylindrica* invasions varied across sites but covered a minimum of 500 m^2. Plots were located so that overstory tree species and canopy cover was similar between invaded and native plots, making the main difference the presence or absence of the invader. Since we encountered many large invasions with limited comparable native plant communities, at some sites we were able to conduct multiple surveys within a plot at different dates so that the total amount of sampled plots for tick sampling was (n=32) for invaded plots and (n=19) for native plots. When plots were resampled tick sampling was conducted in areas of the plot that did not overlap with the previous sampling efforts. To estimate relative host use, we placed two motion-activated cameras (Primos 12MP Proof Cam 02 HD, Primos Hunting, Flora, MS) in each plot to monitor wildlife activity. Cameras were positioned on opposite sides of the plot at a distance between 10 m and 15 m from the plot center and approximately 1.5m aboveground. Cameras were positioned so that their fields of view did not overlap, maximizing the field of view for the plot. Cameras were active from 11 April to 1 June 2019, which coincides with peak questing activity for nymph and adult *A. americanum* in this area (Davidson et al. 1994, Gleim et al. 2014). Photos were used to estimate relative activity by deer (i.e. a metric of host use).

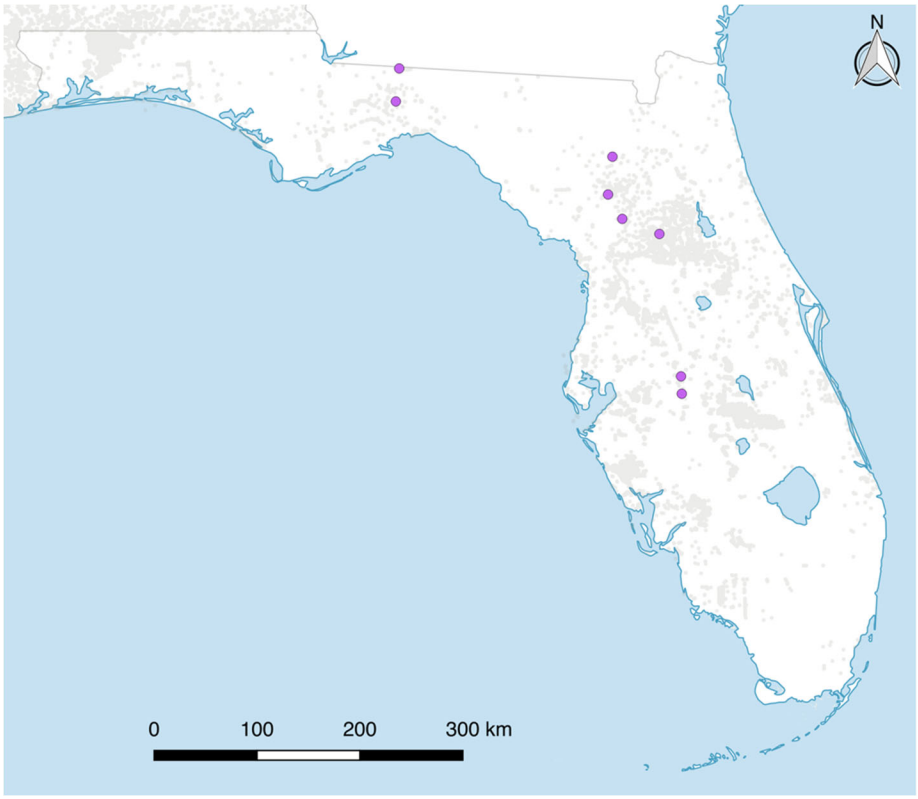

Figure 33. Site locations (purple circles) across Florida, background shading indicates documented invasions of cogongrass (n = 74,785) from 1990-2020 (eddmaps.org).

We estimated tick abundance for each plot using carbon dioxide-baited traps (hereafter CO_2 trap). The CO_2 trap is one of the most effective means of sampling *Amblyomma americanum* nymph and adult life stage ticks (Schulze et al. 1997) and is less biased by different vegetation structures than drag sampling (Kensinger and Allan 2011). The CO_2 trap consists of a mini cooler (Igloo) mounted on a sheet of plywood with vent holes drilled along the sides near the base to disperse gaseous CO_2 from sublimating dry ice. Double-sided carpet tape (3M) covered the perimeter of the plywood to capture ticks attracted by the CO_2. Each trap was filled with approximately 2 kg of dry ice and left for 24 hours before collection. We placed four CO_2 traps per plot, one in each cardinal direction 10 m from the plot center. Ticks ensnared on the tape were counted and preserved in 70% ethanol for identification and to determine life stage.

Statistical analysis: Tick abundance and host use

Relative host activity was estimated and standardized by dividing the number of camera trap photos by the number of photos with deer by the number of days the camera was deployed and operating. This allowed for comparison of data from cameras with different lengths of operable deployment. This effort allowed us to detect relative differences in activity by hosts in the invaded and native areas. We fit a linear mixed effects model to examine the effect of host activity on tick abundance in native and invaded plant communities. Models included tick abundance (nymph + adult ticks) and included effects of treatment (native vs invaded), host

activity, and their interaction. We also included site as a random effect in the model to account for repeated measures. Host activity was log-transformed to meet the assumptions of normality. Models were fit using R 3.6.1 (R Development Core Team 2019).

RESULTS AND DISCUSSION

Filed study: Site conditions

Plant height was taller in invaded plant communities compared to native (p<0.001) (Fig. 34a). The amount of standing biomass (kg/m^2) was greater within invaded plant communities (p<0.001) (Fig. 34b). The height and density of the invaded conditions contributed to a significant reduction in light availability at the soil surface (p<0.001) (Fig. 34c). However, there was no difference in overstory canopy cover (p = 0.706) indicating that differences between the plots is due to the presence or absence of *I. cylindrica* (Fig. 34d).

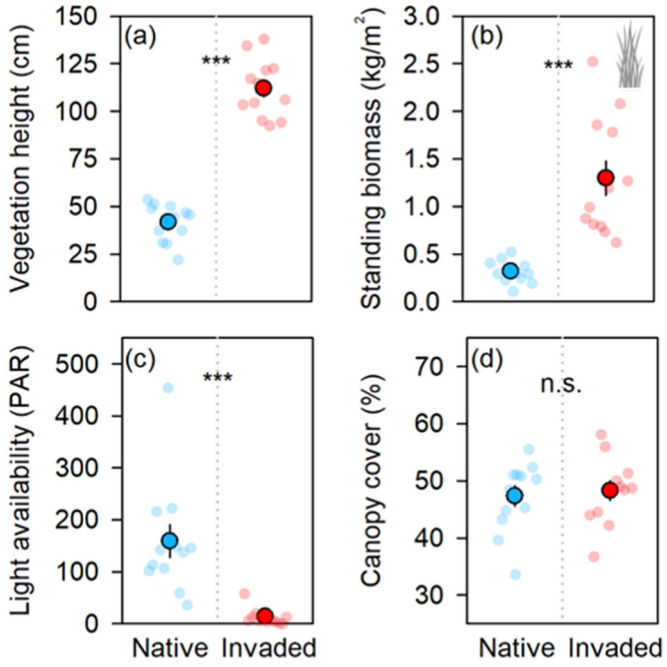

Figure 34. Changes in plant community structure within *I. cylindrica* invaded plant communities. Mean (± SE) (a) vegetation height, (b) standing biomass kg per m^2, and (c) light availability at the soil surface (µmoles m^2 sec^{-1}), and (d) overstory canopy cover for invaded and native plots of the tick survival experiment, significance between invaded and native treatments was determined using analysis of variance, *** p < 0.001.

Field study: Tick survival and microclimate conditions

Regardless of sex or life stage, ticks survived longer in invaded areas compared to native plant communities (Fig. 35 a, b). Across the 12 plots in each treatment, time to 100% mortality was on average 57% longer for nymphs and 45% longer for adults in the invasion compared to the native plots (Fig 36. a, b). Invaded areas consistently buffered harsh microclimate conditions, with greater relative humidity and lower daily maximum temperature (Fig. 35 c, d). Daily minimum relative humidity was on average 16% higher in invaded areas and daily maximum temperature was approximately 6 ºC cooler (Fig. 35 c, d; Table 9). The average daily minimum RH in the invaded area was at or above the CEH for adult *A. americanum* for approximately 200 days of the survival assay and was under the CEH in native areas for almost the entirety of the experiment (Fig 35c).

For both nymph and adult life stages, exposure time (hours per day) to RH below 80% contributed to a decrease in the number of days survived within native plant communities (Fig. 36a, b) (Table 10). Exposure time to RH below 80% was lower in invaded areas and had no effect on the number of days survived for nymph or adult ticks. Maximum temperature prior to mortality was associated with increases in mortality among nymph ticks regardless of invasion (Fig. 36c) (Table 11). For adult ticks, maximum temperature prior to mortality was only correlated with reduced survival time for ticks in the native area (Fig 36d) (Table 11).

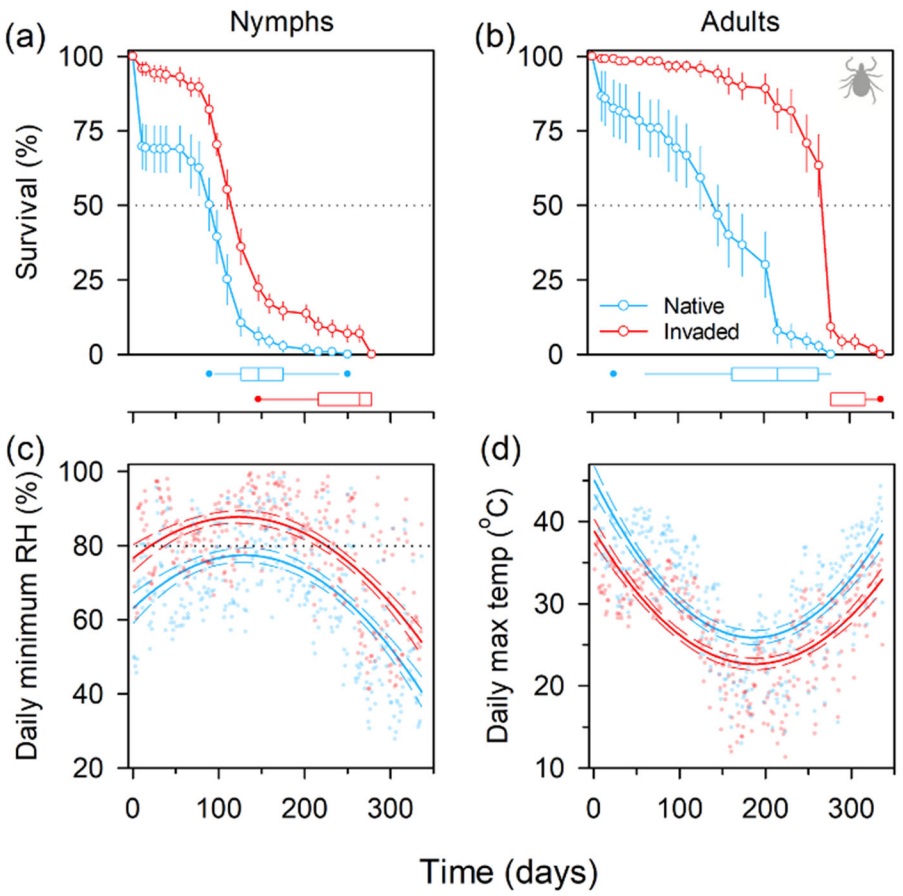

Figure 35. Tick survival per plot and microclimate conditions in native and invaded areas. Mean (± SE) survival of (a) nymph, and (b) adult *Amblyomma americanum* in native (blue) and invaded (red) plots over time. Box plots below panels (a) and (b) represent the time to 100% mortality per plot. Microclimate conditions: (c) average daily minimum relative humidity (%), dotted line indicates critical equilibrium humidity for *Amblyomma americanum* (80% RH), and (d) average daily maximum temperature (ºC). Points in (c) and (d) are daily averages across all data loggers (n= 12) in each treatment. Curved lines in panels (c and d) indicate least squares regression (solid) and 95% CI (dashed) for native and invaded areas.

Table 9. Microclimate conditions across native and invaded plant communities

	Term	Estimate	Std. Error	T value	P value
Daily Min_RH	Intercept	79.39	1.830	43.382	**<0.001**
	Treatment (native)	-16.62	2.588	-6.422	**<0.001**
	Days	0.0991	0.026	3.953	**<0.001**
	$Days^2$	-0.00055	0.000072	-7.668	**<0.001**
	Trt (native)*Days	0.1107	0.03546	3.121	**0.0018**
	Trt (native)*$Days^2$	0.00026	0.000101	-2.587	**0.009**
Daily Max_Temp	Intercept	38.95	0.8113	48.011	**<0.001**
	Treatment (native)	6.228	1.147	5.428	**<0.001**
	Days	-0.1740	0.01112	-15.648	**<0.001**
	$Days^2$	0.00046	0.000032	14.543	**<0.001**
	Trt (native)*Days	-0.0336	0.01572	-2.137	**0.0329**
	Trt (native)*$Days^2$	0.00009	0.000045	-2.066	**0.0392**

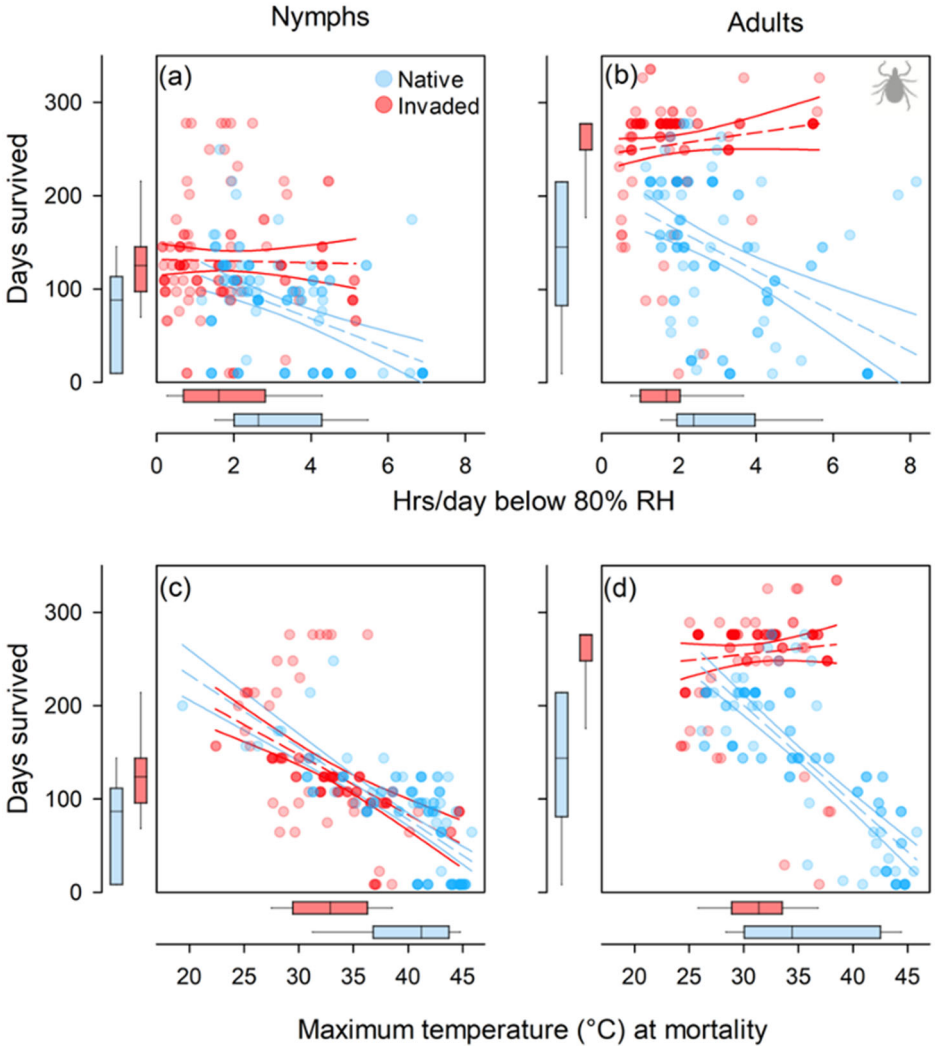

Figure 36. Microclimate stressors related to duration of individual tick survival in native and invaded areas. Number of days survived for individual nymph and adult life stage ticks and microclimate conditions that were experienced in either native (blue) or invaded (red) plots. Panels (a-b) depict the relationship between days survived and hours per day below 80% relative humidity, panels (c-d) show the relationship between days survived and the maximum temperature that was experienced prior to mortality. Best fit line (dashed) with 95% confidence interval (solid) from ordinary least squares regression is also represented. Box plots indicate median and 25th and 75th percentile, with 10th and 90th percentile whiskers for days survived (y-axes) and microclimate conditions experienced by individual ticks in each treatment (x-axes).

Table 10. Tick survival and hours below 80% RH

	Term	Estimate	Std. Error	t value	p value
Nymphs	Intercept	136.15	12.36	11.02	**<0.001**
	Treatment (native)	8.612	19.24	0.448	0.654
	Hours per day below 80%	-2.972	4.866	-0.611	0.541
	Trt (native)*Hours per day under 80%	-16.81	6.160	-2.729	**0.006**
Adults	Intercept	247.14	22.666	10.90	**<0.001**
	Treatment (native)	-54.01	31.129	-1.735	0.083
	Hours per day below 80%	4.535	9.099	0.498	0.618
	Trt (native)*Hours per day below 80%	-21.77	10.506	-2.072	**0.038**

Table 11. Tick survival and daily maximum temperature at mortality

	Effect	Estimate	Std. Error	t value	p value
Nymphs	Intercept	393.56	32.81	11.99	**<0.001**
	Treatment (native)	18.244	49.20	0.371	0.711
	Max temp	-8.022	0.976	-8.220	**<0.001**
	Trt (native)*Max temp	-0.324	1.334	-0.243	0.808
Adults	Intercept	195.67	43.64	4.484	**<0.001**
	Treatment (native)	240.06	54.16	4.433	**<0.001**
	Max temp	1.939	1.365	1.421	0.155
	Trt (native)*Max temp	-10.201	1.609	-6.338	**<0.001**

Table 12. Climate covariates for cox regression (hazard model))

	Effect	**Wald c^2**	**P value**
All Ticks	Treatment	10.17	**0.002**
	Life stage	64.48	**< 0.001**
	Trt*Life stage	27.10	**< 0.001**
	Max Temp	23.70	**< 0.001**
Adults Only	Treatment	37.61	**< 0.001**
	Sex	0.15	0.69
	Trt*Sex	1.91	0.17
	Max Temp	22.63	**< 0.001**

Field survey: host use and tick abundance

Outside of *I. cylindrica* invaded habitats, tick abundance was correlated with greater deer activity ($p = 0.025$) (Fig. 37) (Table 13). In the invaded habitats, there was no effect of deer activity on tick abundance ($p = 0.18$). In the absence of deer, invaded plant communities had greater tick abundances than native plant communities ($p = 0.038$) (Fig. 4) (Table 13).

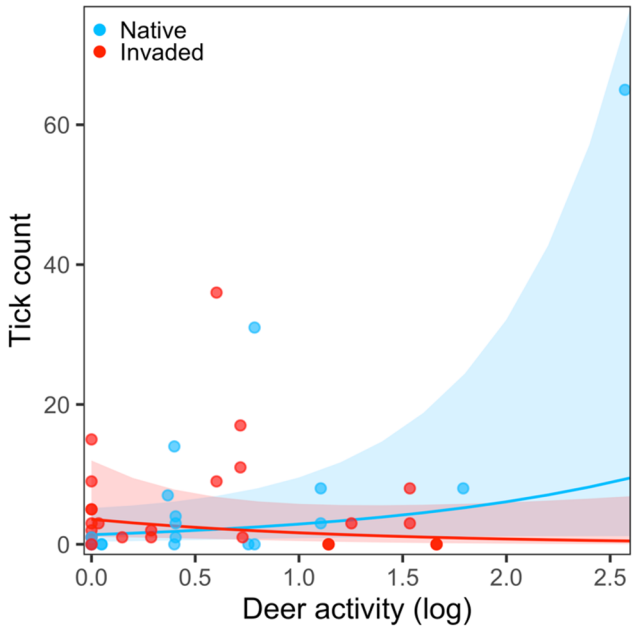

Figure 37. The effect of host use (deer activity) on tick abundance (nymph and adult ticks) collected from tick traps in native (blue) and invaded (red) plant communities. Best fit lines (solid) from linear mixed effect models with 95% confidence interval (dashed lines). Invaded (n = 32, native n = 19).

Table 13. Estimated effects from regression models for effects of habitat type, host activity, and their interaction on tick abundance from field observations

	Effect	Estimate	Std. Error	z value	P value
Tick abund.	Intercept	1.2739	0.6170	2.065	**0.0389**
	Treatment (native)	-0.9579	0.5982	-1.601	0.1093
	Deer activity (log)	-0.7765	0.5801	-1.339	0.1807
	Trt (native)*Deer activity (log)	1.5212	0.6807	2.235	**0.0254**

Summary

Invasive plants have been linked to changes in tick-borne disease risk, but studies are needed that address the relative contribution of abiotic and biotic pathways underlying disease risk (Wei et al. 2020). Here, we show that a widespread grass invader in the southeastern US significantly increased tick survival, likely by buffering high temperatures and lower relative humidity. Contrary to our original hypothesis, we did not see an increase in host activity within invaded areas. Our results highlight that understanding just one of these effects is not sufficient in predicting tick-borne disease risk within invaded areas.

Vegetation removal studies have demonstrated the importance in managing invasive plants to reduce tick abundances as well as the number of infected ticks within invaded areas (Allan et al. 2010, Williams and Ward 2010, Mandli et al. 2021). Studies that incorporate tick survival within invaded and native areas have concluded either no difference (Allan et al. 2010) or reduced tick survival (Civitello et al. 2008) in invaded areas compared to native plant communities. Our results suggest that tick abundances in *I. cylindrica* invaded plant communities are maintained through alteration of microclimate conditions that promote tick survival. Here we provide a mechanistic link between abiotic stressors (RH and temperature) and the length of tick survival. In the uninvaded area, consistently low RH at or below the CEH was a "press" stressor, which made ticks more sensitive to rapid increases in temperature because they were dehydrated. The effect of RH at or below the CEH was cumulative and this stress predisposed ticks to mortality during hotter periods or brief spikes in maximum temperature. While our results were conducted in field conditions, we were still able to validate the microclimate thresholds described in early laboratory work between RH and temperature on tick desiccation and mortality (Sauer and Hair 1971, Hair et al. 1975).

Contrary to previous studies, we did not find a relationship between tick abundance and host activity in invaded plant communities (Williams et al. 2009, Allan et al. 2010). However, these studies evaluated non-native invasive shrubs, which may promote deer activity by providing forage or greater cover. While other species are known to use *I. cylindrica* invaded areas for refuge (Cabrera et al. 2021), our results highlight that white-tailed deer utilize *I. cylindrica* invasions, but are likely not to preferentially choose invaded areas over suitable native habitat. Although similar tick abundances were detected in invaded and native plant communities, abundances appear to be maintained through different mechanistic pathways. While greater tick survival in invaded areas appears to play a strong role in maintaining tick abundances, tick abundance in native areas was maintained through greater host activity. This idea is reinforced in plots where we detected no deer activity within invaded areas and yet collected more ticks than native areas with similar host use.

The distribution of *Ixodes scapularis* has expanded southward as the number of confirmed county records has increased in the southeastern US from 1996-2005 (Eisen et al. 2016). The black legged tick is the primary vector for Lyme disease in the United States (Steere et al. 2004). The black legged tick also has a similar CEH to that of *A. americanum* and could have a similar benefit in survival from *I. cylindrica* invasions and the buffering of low RH and maximum temperature (Berger et al. 2014). Currently the primary tick species that overlaps with the distribution of *I. cylindrica* is *A. americanum*, however, this is predicted to change under future conditions. Climate change is also predicted to facilitate the spread of *I. cylindrica* and cause a range expansion from southeastern Gulf States to as far north as Virginia along the eastern seaboard (Bradley et al. 2010). As *I. cylindrica* spreads northward it is likely that it will interact with other tick species such as the black legged tick (*Ixodes scapularis*).

We were able to do a rigorous test of tick-borne disease risk across a wide latitudinal gradient, but only for one invasive plant species, and one tick species. Thus, we encourage future work to explore these relationships more broadly across other invasive plant species as well as other tick species. Understanding the relative contribution of both host use and microclimate conditions within invaded areas will aide in our ability to project future tick-borne disease risk.

PART 3: PATHOGEN ANALYSIS OF TICKS

TECHNICAL APPROACH

Introduction

Several of the most rapidly emerging vector-borne diseases in the U.S. are caused by zoonotic pathogens transmitted by the lone star tick (*Amblyomma americanum*), including *Ehrlichia chaffeensis* and *E. ewingii*, both agents of ehrlichiosis, *Rickettsia rickettsii*, the agent of Rocky Mountain spotted fever (Stromdahl et al. 2011), and *Francisella tularensis*, the agent of tularemia (Childs & Paddock 2003). *Amblyomma americanum* is distributed broadly across the southeastern U.S. and along the eastern seaboard; in the southeastern U.S. it is the primary vector of TBDs to humans (Demma et al. 2005). Also occurring in the southeastern U.S. is the gulf coast tick (*Amblyomma maculatum*), an important vector of *R. parkeri*, the American dog tick (*Dermacentor variabilis*), an important vector of *R. rickettsii*, and the brown dog tick (*Rhipicephalus sanguineus*), a species capable of transmitting a variety of pathogens particularly affecting canids (Demma et al. 2005). The black-legged tick (*Ixodes scapularis*), vector of *Borrelia burgdorferi*, the causative agent of Lyme disease, also occurs in this region. However, this species is considerably less important in the southeastern U.S. as a disease vector, and is not efficiently sampled via carbon dioxide-baited traps. While several studies have assessed the distribution of some tick-borne agents (TBAs) in the species mentioned above across portions of the southeastern U.S. (e.g. Mixson et al. 2006), there has been no comprehensive analysis of field-collected tick specimens for all known TBAs due to the lack of an effective system for performing such an analysis. Here, we describe the development of a system using Fluidigm Access Array combined with Illumina sequencing to analyze all nymph and adult life stage ticks collected in this study for an unprecedented diversity of TBAs that imperil human, domestic animal and wildlife health.

Tick Collections

Ticks were collected from nine military bases in the southeastern United States (Avon Park Air Force Range, Florida; Fort Benning, Georgia; Fort Gordon, Georgia; Camp Blanding, Florida; Eglin Air Force Base, Florida; Fort Jackson, South Carolina; Moody Air Force Base, Georgia; Camp Shelby, Mississippi; Tyndall Air Force Base, Florida) during the summers of 2017 and 2018 using carbon dioxide-baited traps (Kensinger & Allan, 2011). A total of 937 ticks were collected from the nine military bases in 2017-2018, and four additional ticks of interest were included from sampling performed in 2019: 849 *Amblyomma americanum* (606 nymphs, 243 adults), 51 adult *Dermacentor variabilis*, 34 *Amblyomma maculatum* (1 nymph, 33 adults), 3 adult *Ixodes scapularis*, 1 adult *Rhipicephalus sanguineus* and 3 unknown ticks that were lost. All ticks were counted and preserved in 2 ml vials containing 70% ethanol. All ticks were identified to species using a Zeiss Stemi DV4 dissecting microscope. DNA extractions were performed on 938 of the 941 ticks collected (3 were lost) and 7 *A. americanum* nymphs were not analyzed by Fluidigm due to insufficient DNA, yielding detailed pathogen information for 931 ticks.

DNA Extraction

All ticks were rinsed in 70% ethanol, air dried, and individually homogenized in 30 µl digestion buffer (10 mM Tris HCl, ph 8; 5 mM EDTA; 100 mM NaCl; 0.2% SDS; 2 mg/ml

protease K). Each tube contained a 5 mm steel bead (Qiagen). Ticks were homogenized twice at 25 Hz for 3 min each using a TissueLyzer II (Qiagen, Germantown, MD). A brief centrifugation was done between the two rounds of homogenization. DNA was extracted using a standard phenol-chloroform protocol in a total volume of 600 µl followed by an ethanol precipitation, excluding the addition of sodium acetate to reduce the final salt concentration. We included the addition of glycogen to enhance DNA precipitation. After ethanol precipitation, samples were re-suspended in 30 µl elution buffer and stored at -20 degrees Celsius. All DNA samples were quantified on a Qubit 2.0 (Life Technologies) using the Qubit dsDNA HS Assay Kit. All but seven samples contained enough DNA (at least 2 ng/µl) and were submitted for Fluidigm and next generation sequencing (NGS).

Primers

Target regions of four bacterial and one protozoan gene were amplified using a subset of the primers from Keesing et al. (2018) (Table 14). We used five 16S rRNA primer sets: three universal eubacteria sets targeting different regions of the gene, one specific to the Rickettsiaceae, and one specifically targeting *Coxiella* spp. We also targeted the disulfide oxidoreductase (dsb) gene for *Anaplasma* and *Ehrlichia* for greater species specificity. As the 16S rRNA gene is highly conserved in the genus *Rickettsia* we used specific primers targeting the outer membrane protein B (*ompB*) (also known as *sca5*) for North American *Rickettsia* of interest and the 23S – 5S rRNA intergenic spacer region (23S-5S IGS), modified from Jado et al. (2006). All protozoan species of interest belong to the genera *Babesia* or *Theileria*. The Jado et al. (2006) primers BT18SF and BT18SR provide sufficient species-specific resolution within these two genera with little cross-reactivity. All primers designed for this study were created using the Primer3 option in Geneious (version 8, Auckland, New Zealand) and synthesized by IDT Corporation (Coralville, IA).

Table 14. Information on the amplicons used in this study.

Primer (F)	Sequence 5'-3'	Primer (R)	Sequence 5'-3'	Gene Target	Product size	Target Species
[1]16S8FE3	AGAGTTTGATCCTGGCYCAG	[2]B-GA1B2	GGAGTTTGCCGGGACTTYTTCT	16S rRNA	441 - 474	bacterial spp.
AMdsb1F	GCTAAGCCCCTAGTAGCGTC	AMdsb1R	GAAATGCGGAAGAAGGTGGC	*dsb1*	431	*A. marginalis*
APdsb1F	AGGGTTGATAAAATGCACGGC	APdsb1R	TAAGTCGCTGGGTCTCTGGA	*dsb1*	392	*A. phagocytophilum*
APdsb2F	AGGTCCCTAAGCATCACTCCT	APdsb2R	TCTGCCTGTTGAGTCTGGTG	*dsb1*	370	*A. phagocytophilum*
[3]BT18SF	GACACAGGGAGGTAGTGACAAG	[3]BT18SR	CTAAGAATTTCACCTCTGACAGT	18S rRNA	399 - 449	*Babesia/Theileria spp.*
[2]CB16S8FE3	AGAGTTTGATTCTGGCTCAG	CB475seqR	CGTCAACGCCCAAGGATATT	16S rRNA	474 - 476	*Coxiella spp.*
ECdsb1F	ACTAGTAGCAAGCTTTCCGT	ECdsb1R	AACAGCTTTCAGTGATGCTTCT	*dsb1*	391	*E. chaffeensis*
ECdsb2F	AACTAGAGGGCAAGCACAAG	ECdsb2R	ATAGTGTCGGAATTCTTGGC	*dsb1*	429	*E. chaffeensis*
EEdsb1F	GAAGCATCATTGAAAGCAGTACG	EEdsb1R	CCAACTATCATAGCAGGAGTTCC	*dsb1*	269	*E. ewingii*
ENdsb1F	GTTCTTTGATTACTCATGCGGCT	ENdsb1R	ATATCAGCTGCACCACCGAT	*dsb1*	408	*E. canis*
EWdsb1F	CTAGTAGCGAGCTTCCCATT	EWdsb1R	GATGCCTCGCCGAGTATAGG	*dsb1*	377	*E. muris subsp. eauclairensis,subsp. nov.*
EWdsb2F	ACAGGATGGCAAAGTACGTGT	EWdsb2R	ATATATCAGCTGCTCCACCGA	*dsb1*	350	*E. muris subsp. eauclairensis,subsp. nov.*
FBbslF	CGAGTTCGCGGGAGAGTA	FBbsl2b_R	TCCTAGGCATTCACCATAGACT	5S-23S IGS	249 - 253	*Borrelia burgdorferi sensu lato*
[4]FRK23-5_F1	GATAGGTCRGGTGTGGAAG	[4]FRICK23-5R1	GGAYGGGATCGTGTGTTTCA	23S-5S IGS	384	*Rickettsia spp.*
[4]FRK23-5_F1	GATAGGTCRGGTGTGGAAG	[4]FRICK23-5R4	CTCATGCTATAACCACCAAGC	23S-5S IGS	359 - 375	*Rickettsia spp.*
RambOB1F	AGGTATTGGCKCTTCAMAGT	RambOB1R	AATAGCAGTAGTACCRCCGC	*ompB*	442 - 448	*Rickettsia amblyommatis*
RambOB2F	AATCMCGSTAACACTGCAGG	RambOB2R	AYTCGCATCAACAACGCCTG	*ompB*	525 - 534	*Rickettsia amblyommatis*
RbelOB1F	CCTAATGGTGTTGCTGCTGG	RbelOB1R	CCTTGCCCACTTGCTAAACC	*ompB*	419	*Rickettsia bellii*
RbelOB2F	AGTGCAGATAACCCACTTGCA	RbelOB2R	CTGTACCACCCGCAGCATTA	*ompB*	352	*Rickettsia bellii*
RcasOB1F	TCCCCATGTTGAAGTACCGC	RcasOB1R	TCAAGCAGGTGGTGTAGTCG	*ompB*	401	*Rickettsia canadensis*
RcasOB2F	CGACTACACCACCTGCTTGA	RcasOB2R	GTAACGGTCTGGTCGGTGAC	*ompB*	364	*Rickettsia canadensis*
RmasOB1F	TGAAGCATYAGGTRTCGGAG	RafOB1R	CCCGTACCGTCTGTTCCATT	*ompB*	422 - 431	*Rickettsia massilliae*
RparOB2F	ACCGGCGATATAGGGAAYGC	RparOB2R	TGACCRGCAGCATTTGTAGT	*ompB*	449 - 455	*Rickettsia parkeri*
RrhiOB2F	TAATCCTGGTGCTGCGACTG	RrhiOB2R	CCGTCAAAATCTGTTCCGGC	*ompB*	522	*Rickettsia rhipicephali*
[5]V1-V3_F28	GAGTTTGATCNTGGCTCAG	[5]V1-V3_R519	GTNTTACNGCGGCKGCTG	16S rRNA	462 - 527	bacterial spp.
[5]V4_515F_new	GTGYCAGCMGCCGCGGTAA	[5]V4_806R_new	GGACTACNVGGGTWTCTAAT	16S rRNA	291 - 293	bacterial spp.

[1]Berggoetz et al., 2014; [2]modified from Berggoetz et al., 2014; [3]Schwartz et al., 1992; [4]modified from Jado et al., 2006; [5]W. M. Keck Center for Comparative and Functional Genomics at the University of Illinois at Urbana-Champaign.

Fluidigm 2 Step Access Array Amplification

Following DNA extraction and quantification, DNA samples (Table 15) were sent to the W. M. Keck Center for Comparative and Functional Genomics at the University of Illinois at Urbana-Champaign where Fluidigm PCR and NGS were performed. Samples were diluted to 2 ng/μl as needed. A mastermix for amplification was prepared using the Roche High Fidelity Fast Start Kit and 20x Access Array loading reagent according to Fluidigm protocols. The mastermix was composed of: 0.5 μl 10X FastStart Reaction Buffer without MgCl2; 0.9 μl 25 mM MgCl2; 0.25 μl DMSO; 0.1 μl 10 mM PCR grade Nucleotide Mix; 0.05 μl 5 U/ul FastStart High Fidelity Enzyme Blend; 0.25 μl 20X Access Array Loading Reagent; 1.95 μl Water. This mastermix (4 μl) and 1 μl DNA sample were added to each of 48 wells of a PCR plate. Primer pairs were prepared (20X primer master mix: 2 μl each forward and reverse primer (50 μM each), 5 μl 20X Access Array Loading Reagent, water to 100 μl) and aliquoted into a separate plate. All primers were synthesized by IDT Corp. (Coralville, IA).

Samples (4 μl) and primers (4 μl) were loaded into their respective inlets of a previously primed Fluidigm LP48.48 IFC. The IFC was placed in a Fluidigm Juno for loading, PCR amplification and harvesting used the following PCR conditions: 50ºC 2 min; 70ºC 20 min; 95ºC 10 min; 10 cycles of 95ºC 15 sec, 55ºC 30 sec, 72ºC 1 min; 2 cycles of 95ºC 15 sec, 80ºC 30 sec, 60ºC 30 sec, 72ºC 1 min; 8 cycles of 95ºC 15 sec, 55ºC 30 sec, 72ºC 1 min; 2 cycles of 95ºC 15 sec, 80ºC 30 sec, 60ºC 30 sec, 72ºC 1 min; 8 cycles of 95ºC 15 sec, 55ºC 30 sec, 72ºC 1 min; 5 cycles of 95ºC 15 sec, 80ºC 30 sec, 60ºC 30 sec, 72ºC 1 min. The PCR product was diluted 1:100 and 1 μl was placed in a new 96-well PCR plate. PCR was performed for amplification with (4 μl) Illumina linker barcodes. To this was added master mix (15 μl) containing (per sample): 2.0 μl 10X FastStart Reaction Buffer without MgCl2; 3.6 μl 25 mM MgCl2; 1.0 μl DMSO; 0.4 μl 10 mM PCR grade Nucleotide Mix; 0.2 μl 5 U/μl FastStart High Fidelity Enzyme Blend; 7.8 μl water. The PCR cycling program consisted of 1 cycle of 95ºC 10 min; 14 cycles of 95ºC 15 sec, 60ºC 30 sec, 72ºC 1 min; 72ºC 3 min.

Products were quantified on a Qubit fluorimeter and stored at -20 degrees Celsius. All samples were run on a Fragment Analyzer (Advanced Analytics, Ames, IA) and amplicon regions and expected sizes confirmed. Samples were then pooled in equal amounts according to product concentration. The pooled products were then size selected on a 2% agarose E-gel (Life Technologies) and extracted from the isolated gel slice with Qiagen gel extraction kit (Qiagen). Cleaned size selected products were run on an Agilent Bioanalyzer to confirm appropriate profile and determination of average size.

Table 15. The number of ticks analyzed for tick-borne agent DNA, with information on tick species collected from each of nine military installations sampled. Not included here are 1 *A. maculatum* adult and 3 *I. scapularis* nymphs collected from non-DoD areas while sampling cogongrass-invaded habitats.

	Site	Avon Park	Fort Benning	Camp Blanding	Eglin AFB	Fort Gordon	Fort Jackson	Moody AFB	Camp Shelby	Tyndall AFB	TOTAL
Tick Species	**Life Stage**										
Amblyomma americanum	Nymph		20	248	88	66	5	7	34	131	599
	Adult		10	151	26	4	3			49	243
Amblyomma maculatum	Nymph									1	1
	Adult	1		2		1	1		14	13	32
Dermacentor variabilis	Nymph										
	Adult	6		7	13				3	22	51
Rhipicephalus sanguineus	Nymph										
	Adult									1	1
Total		7	30	408	127	71	9	7	51	217	927

High Throughput Sequencing

Library construction and sequencing were performed at the Roy J. Carver Biotechnology Center, University of Illinois at Urbana-Champaign. Approximately 1ng of DNA was used for amplification of the targeted regions in the Fluidigm Access Array (Fluidigm, CA) as previously described (Muturi et al., 2016). The pooled amplicons were sequenced on one lane with 2 x 250nt paired-reads on a HiSeq 2500 with a Rapid sequencing kit version 2 (Illumina, CA). Fastq files were generated and demultiplexed with the bcl2fastq v2.17.1.14 Conversion Software (Illumina®).

Sequence Analysis

A customized HiSeq analysis pipeline was created by the High Performance Computing in Biology (HPCBio) group at the University of Illinois at Urbana-Champaign. In brief, raw sequences were 1. assessed for quality with FastQC (Andrews, 2010); 2. trimmed with Trimmomatic (Bolger, et al., 2014); 3. stitched together when applicable with PEAR (Zhang et al, 2014); and 4. converted to FASTA format. Paired reads were not stitched together, and only the trimmed R1 (forward) read was used, when the expected size of the PCR products were either too large for forward and reverse sequences to overlap sufficiently (>450 nt) or were of variable length. Variable lengths occurred due to amplification in TBAs whose target regions varied in size by more than 10bp.

After processing, vsearch (Rognes et al., 2016) was used to compare these sequences against a custom database (Fredericks et al., in preparation). A maximum of 50 reads per query were reported when these conditions were met: a minimum percent identity of 93% and an alignment length of 50%. Due to the lack of species specific DNA sequence arrays for TBAs in available datasets, we created a custom DNA database using target sequences from expected or closely related TBAs obtained from published sequences in the National Center for Biotechnology Information's (NCBI) Basic Local Alignment Search Tool (BLAST) (https://blast.ncbi.nlm.nih.gov/Blast.cgi) (access date: November 2017).

Reads were considered positive identifications to genus when a minimum average percent identity of 97% to a database sequence was achieved, and were assigned to species when a minimum of 99% identity was achieved. With the exception of *Rickettsia akari*, *R. bellii* and *R. felis*, no Rickettsia was distinguishable to species using any of the 16S rRNA primer sets (V1-V3_F28/V1-V3_R519, V4_515F_new/V4_806F_new or 16S8FE3/B_GA1B2), and were reported only to genus when hits occurred with these targets only. Otherwise, species-level identification of *Rickettsia* species was accomplished using hits obtained from the amplification of the 23S-5S IGS and *ompB* targeted regions. The most useful criteria for determining the quality of the match were the 1. total number of hits; 2. average percent identity; 3. average alignment length; and 4. fifth percentile of the percent identity, which gave an estimate of the variance in the percent identity.

RESULTS AND DISCUSSION

Identification of Tick-borne Agents

Using a next-generation sequencing approach, we identified 32 unique TBAs in these field-collected ticks: 23 to species, seven to genus, and two which best matched to known sequences with 97% - 98.9% identity were designated as "-like" the closest species (Table 16). These encompassed eight different genera and known human pathogens included *Anaplasma phagocytophilum*, *Ehrlichia chaffeensis*, *Ehrlichia ewingii*, *Rickettsia parkeri* and *E. muris eauclariensis subsp. nov.* (Figure 38). These are causative agents of important tick-borne diseases in humans in the southeastern U.S., including anaplasmosis, ehrlichiosis, and spotted-fever rickettsiosis.

There were distinct differences between military installations in the abundance, species distribution (Table 15), and infection rates of collected ticks (Table 16). *Amblyomma americanum* was the most commonly collected tick species and was detected from all installations except for Avon Park Air Force Range. *Amblyomma maculatum* and *Dermacentor variabilis* were detected from six and five installations, respectively. One specimen of *Rhipicephalus sanguineus* was found at Tyndall Air Force Base only. Installations that yielded a high abundance and diversity of ticks also had the largest diversity of identified TBAs, and included Camp Blanding, Eglin Air Force Base, and Tyndall Air Force Base.

The majority (93.8%; 873/931) of the ticks carried a non-pathogenic *Coxiella* endosymbiont. The second most common TBA was *R. amblyommatis sp. nov.* at 40.8% (380/931) prevalence, followed by *E. muris subsp. eauclairensis subsp. nov.* at 11.7% (109/931). This is the first report of *E. muris eauclairensis subsp. nov.* DNA in a tick other than *Ixodes scapularis*; here we detected it in *A. americanum* with average percent identities from 99.1 – 99.7 and a maximum of 100%. Sequence hits to the V4 region of *E. muris subsp. eauclairensis subsp. nov.* 16S rRNA ranged from 10 – 28,279 with an average of 1939. This TBA was first discovered in Wisconsin in human patients exhibiting ehrlichiosis subsequent to a tick bite (Pritt et al., 2017) and has been reported to date only in Wisconsin and Minnesota (Pritt et al., 2017). *Ehrlichia chaffeensis* and *E. ewingii* were detected in 0.6% (5/842) and 0.4% (3/842) of *A. americanum*, two of the most important human pathogens transmitted by this tick species. *Rickettsia bellii* was found in 84 (9.0%) ticks: 9.6% (81/842) of *A. americanum*, 5.9% (2/34) of *A. maculatum*, and 2.0% (1/51) of *D. variabilis*, but only with small numbers (10 – 102; average = 20) of sequence hits. Another important human pathogen, *Rickettsia parkeri* was detected in 17.6% (6/34) of *A. maculatum*, consistent with high infection rate for this pathogen-tick combination reported elsewhere.

Summary and Interpretation of Results

Extractions and analysis of pathogen DNA from 931 ticks collected 2017-2019 is complete Collectively this generated a robust dataset across which we are able to analyze the effects of time since fire and fire return interval, plant invasions, wildlife host densities, and climate, on the density of ticks, tick infection rates, and their product, the density of infected ticks. Together these dependent variables represent entomological estimates of disease risk. Our results indicate a high diversity but low prevalence of human pathogens, suggesting that

entomological exposure risk is driven more strongly by tick abundance than tick infection rates. However, several important pathogens have been detected from these specimens that may cause serious morbidity or mortality in humans, including *E. chaffeensis* and *E. ewingii* (causative agents of human ehrlichiosis), *A. phagocytophilum* (causative agent of anaplasmosis), and the emerging *R. parkeri* (a causative agent of spotted fever rickettsiosis) associated with *A. maculatum*. We also detected a surprisingly high prevalence of "*E. muris subsp. eauclairensis subsp. nov.*" in *A. americanum*, which thus far has been reported only in *I. scapularis*, and likely is an important emerging agent of ehrlichiosis in humans. Finally, among potential human pathogens, as expected we detected a high prevalence of *R. amblyommatis* in *A. americanum*, although this TBA likely only causes disease in humans rarely despite presumably high exposure rates. We also detected a high prevalence of wildlife pathogens, such as *Theileria* spp., and as expected a very high prevalence of non-pathogenic endosymbionts such as the *Coxiella* endosymbiont of *A. americanum*. Through this study, the precise identification of a diversity of TBAs has created an unprecedented knowledge of tick-borne disease risk for military installations in the southeastern U.S.

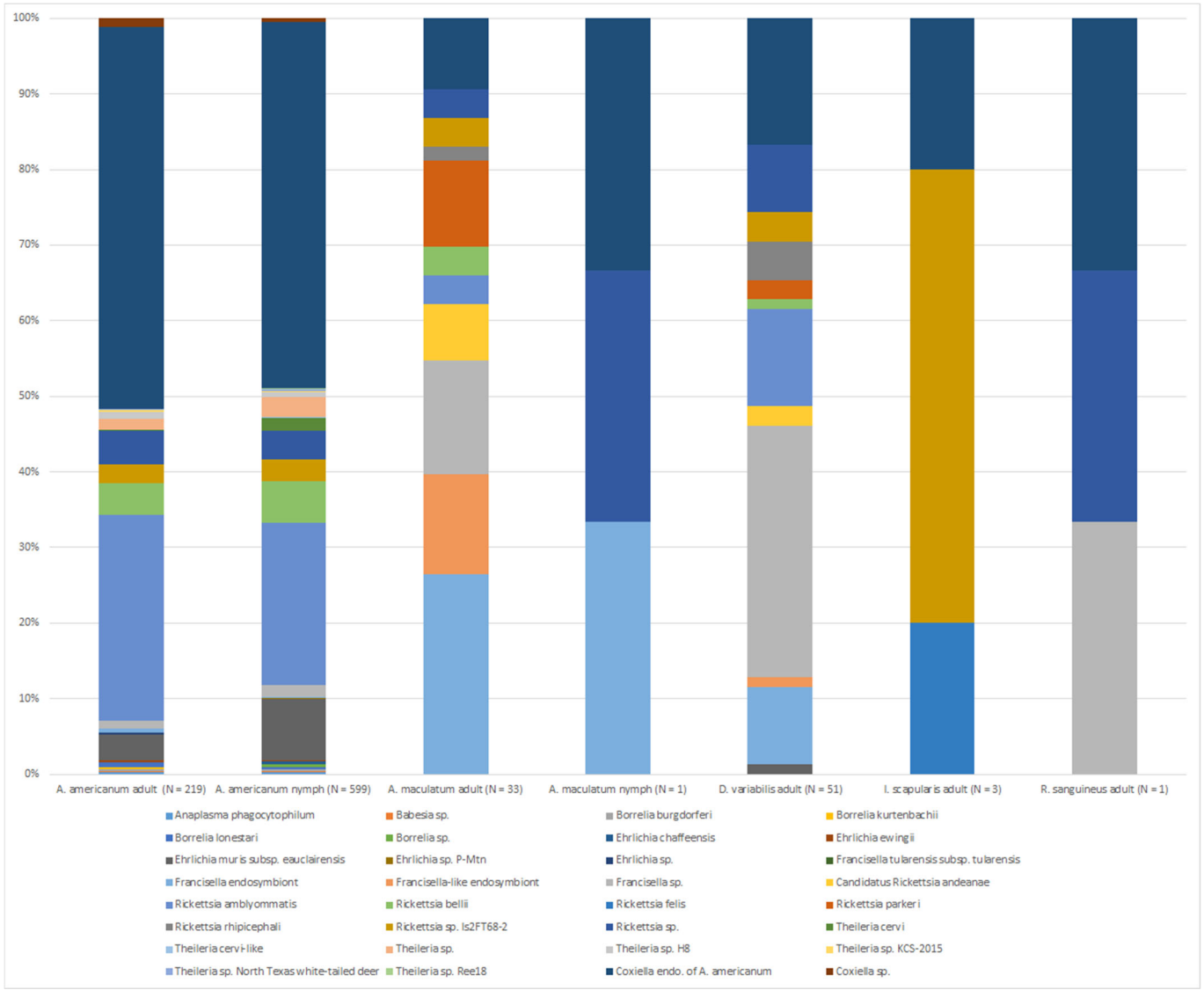

Figure 38. Relative prevalence of tick-borne agents detected from 931 tick samples analyzed. Most ticks contain more than one tick-borne agent, including nonpathogenic endosymbionts, human pathogens, wildlife pathogens, and microbes of unknown pathogenicity.

Table 16. The number of ticks of each species that expressed specific tick-borne agent DNA.

Tick-borne Agent	*Amblyomma americanum*		*Amblyomma maculatum*		*Dermacentor variabilis*	*Ixodes scapularis*	*Rhipicephalus sanguineus*
	adult	nymph	adult	nymph	adult	adult	adult
Anaplasma phagocytophilum	1	3	0	0	0	0	0
Babesia sp.	1	1	0	0	0	0	0
Borrelia burgdorferi	1	4	0	0	0	0	0
Borrelia kurtenbachii	1	0	0	0	0	0	0
Borrelia lonestari	3	3	0	0	0	0	0
Borrelia sp.	0	4	0	0	0	0	0
Ehrlichia chaffeensis	0	5	0	0	0	0	0
Ehrlichia ewingii	1	2	0	0	0	0	0
Ehrlichia muris subsp. eauclairensis	15	93	0	0	1	0	0
Ehrlichia sp. P-Mtn	0	2	0	0	0	0	0
Ehrlichia sp.	1	0	0	0	0	0	0
Francisella tularensis subsp. tularensis	0	0	0	0	0	0	0
Francisella endosymbiont	2	2	14	1	8	0	0
Francisella-like endosymbiont	0	0	7	0	1	0	0
Francisella sp.	5	17	8	0	26	0	1
Candidatus Rickettsia andeanae	0	0	4	0	2	0	0
Rickettsia amblyommatis	118	250	2	0	10	0	0
Rickettsia bellii	18	63	2	0	1	0	0
Rickettsia felis	0	0	0	0	0	1	0
Rickettsia parkeri	0	0	6	0	2	0	0
Rickettsia rhipicephali	0	1	1	0	4	0	0
Rickettsia sp. Is2FT68-2	11	33	2	0	3	3	0
Rickettsia sp.	19	43	2	1	7	0	1
Theileria cervi	1	21	0	0	0	0	0
Theileria cervi-like	0	1	0	0	0	0	0
Theileria sp.	6	31	0	0	0	0	0

Theileria sp. H8	4	7	0	0	0	0	0
Theileria sp. KCS-2015	1	2	0	0	0	0	0
Theileria sp. North Texas white-tailed deer	1	3	0	0	0	0	0
Theileria sp. Ree18	0	1	0	0	0	0	0
Coxiella endo. of A. americanum	219	561	5	1	13	1	1
Coxiella sp.	5	6	0	0	0	0	0
Number of ticks tested	243	599	33	1	51	3	1

PART 4: ED2 MODELING

TECHNICAL APPROACH

Modeling Objectives

The fourth objective of this project is to connect modeled responses of forests, invasive cogongrass, fire regimes, land management under future climate scenarios to our understanding of the environmental controls on tick abundance and TBD risk (vegetation, climate, fire). Modeling future vegetation in the southeastern U.S. under different climate, disturbance, and invasion scenarios requires the development of new tools and techniques. To organize how each component contributes to this overarching goal, we subdivide this task into four sub-objectives:

4A) Analyze ED2 projections for southeastern pine forests under different climate scenarios
4B) Develop and validate cogongrass Plant Functional Type (PFT)
4C) Use ED2 to explore different invasion & climate scenarios
4D) Use ED2 outputs to estimate the effect of fires

The Ecosystem Demography Model

The Ecosystem Demography 2 model (ED2) is a spatially implicit cohort-based dynamic vegetation model (DVM). It has a closed energy, water, and carbon budget, and can be coupled to atmospheric models or products (Figure 40; objective 4A, C). ED2 keeps track of individual-plant-level ecophysiological processes (photosynthesis, respiration, allocation, turnover) and demographic rates (growth, mortality, reproduction, disturbance) and aggregates this information into cohorts. ED2 aggregates cohorts into different patches, allowing the model to capture landscape-scale heterogeneity in both abiotic factors, like differences in slope or soil type, and in stand age and successional status. ED2's spatially implicit cohort and patch representations capture ecological processes across scales: individual competition for light and water through whole-forest demography through across-stand patch-mosaic dynamics (Moorcroft et al. 2001, Medvigy 2006, Medvigy et al. 2009; objectives 4A-C). Multi-scale processes emerge in part because spatially implicit representations are more computationally tractable (Cowdery 2018). ED2 is well suited for this project because it is able to capture ecological dynamics that span scales, has a history of validation in the southeastern US, and is incorporated into global modeling frameworks (Walker and Hanson 2014, Miller, Dietze, DeLucia, et al. 2016, Fisher et al. 2018).

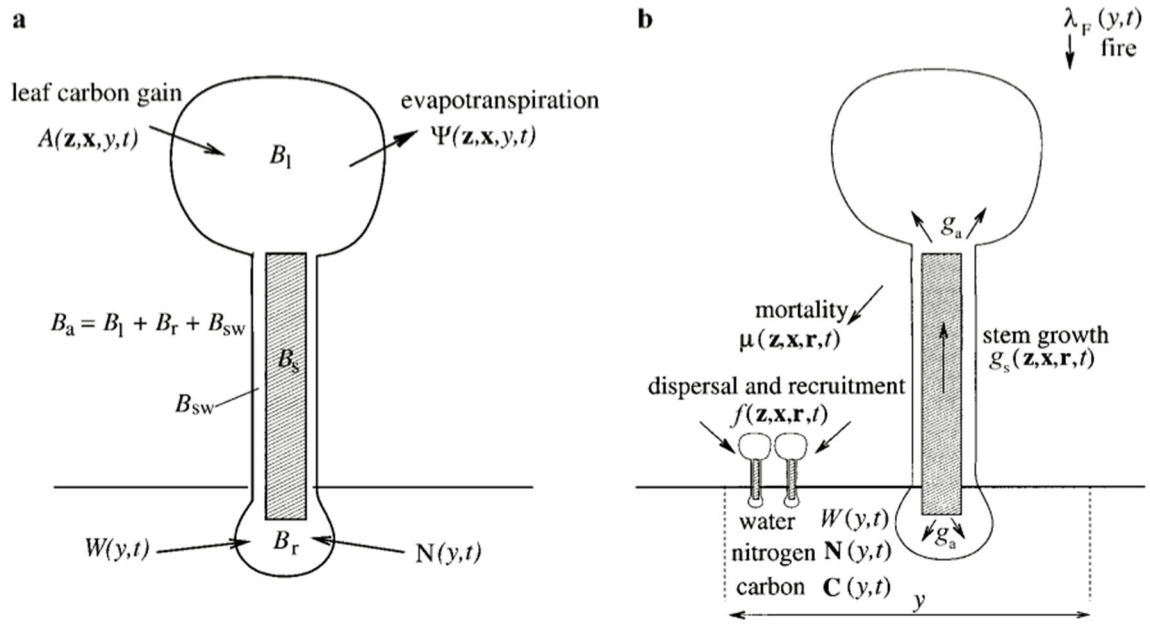

Figure 40: Representation of individual-level fluxes within ED2 from Moorcroft et al 2001. Left is the partitioning of carbon and water among tissues (B_a is active tissue, B_s is structural tissue). *y* is the patch and *t* is time, g is growth rate, **x** is the plant functional type, **z** is the size, and **r** is the resources available to the plant. The lambda represents the fire scheme implemented in the original ED version, which we are not using for reasons discussed below.

The Predictive Ecosystem Analyzer: PEcAn

PEcAn provides a common toolbox for working with and analyzing ecosystem models as well as accessible web-based tools for model execution (LeBauer et al. 2013). PEcAn has a workflow for parameterizing new vegetation types by compiling field and literature data that provide constraints for individual model parameters. These data are synthesized within PEcAn in an automated Hierarchical Bayes meta-analysis that estimates each model parameter as a probability distribution (LeBauer et al. 2013). We are running the ED2 model through the PEcAn toolbox for several reasons: 1) the PEcAn web interface and associated database creates an accessible archive of results and a reproducible workflow, 2) several climate-scenario downscaling tools already exist within PEcAn and allow for easier coupling to climate scenarios (objective 4A, C), and 3) the Hierarchical Bayesian meta-analysis allows us to develop a cogongrass Plant Functional Type (PFT) by combining the field data from this project with existing literature (objective 4B) .

Objective 4A: Southern Pine Forest Under Different Climate Scenarios

ED2 was run at a Duke forest in North Carolina, a southern pine forest site in the Southeast. Duke forest was chosen because it co-occurred with the site of a Free-air concentration enrichment experiment, which allowed more direct comparison of findings with

other modeling and experimental studies (De Kauwe et al. 2013, Walker and Hanson 2014, Miller, Dietze, DeLucia, et al. 2016). We wanted to explore how climate alone could affect the long-term successional trajectory of southern pine forests. To separate the effects of elevated CO_2 from elevated temperatures ED2 was run from 2006-2099 under four separate scenarios (Figure 41): 1) RCP4.5 CO_2 concentrations and climate, 2) RCP4.5 climate only, with constant CO_2 concentrations, 3) RCP4.5 Elevated CO_2 only, with climate randomly selected from 2006-2026, 4) Present Day, made from randomly selected measures of CO_2 and radiation from 2006-2026. We evaluated output for changes in successional trajectory, carbon sequestration, and water use efficiency.

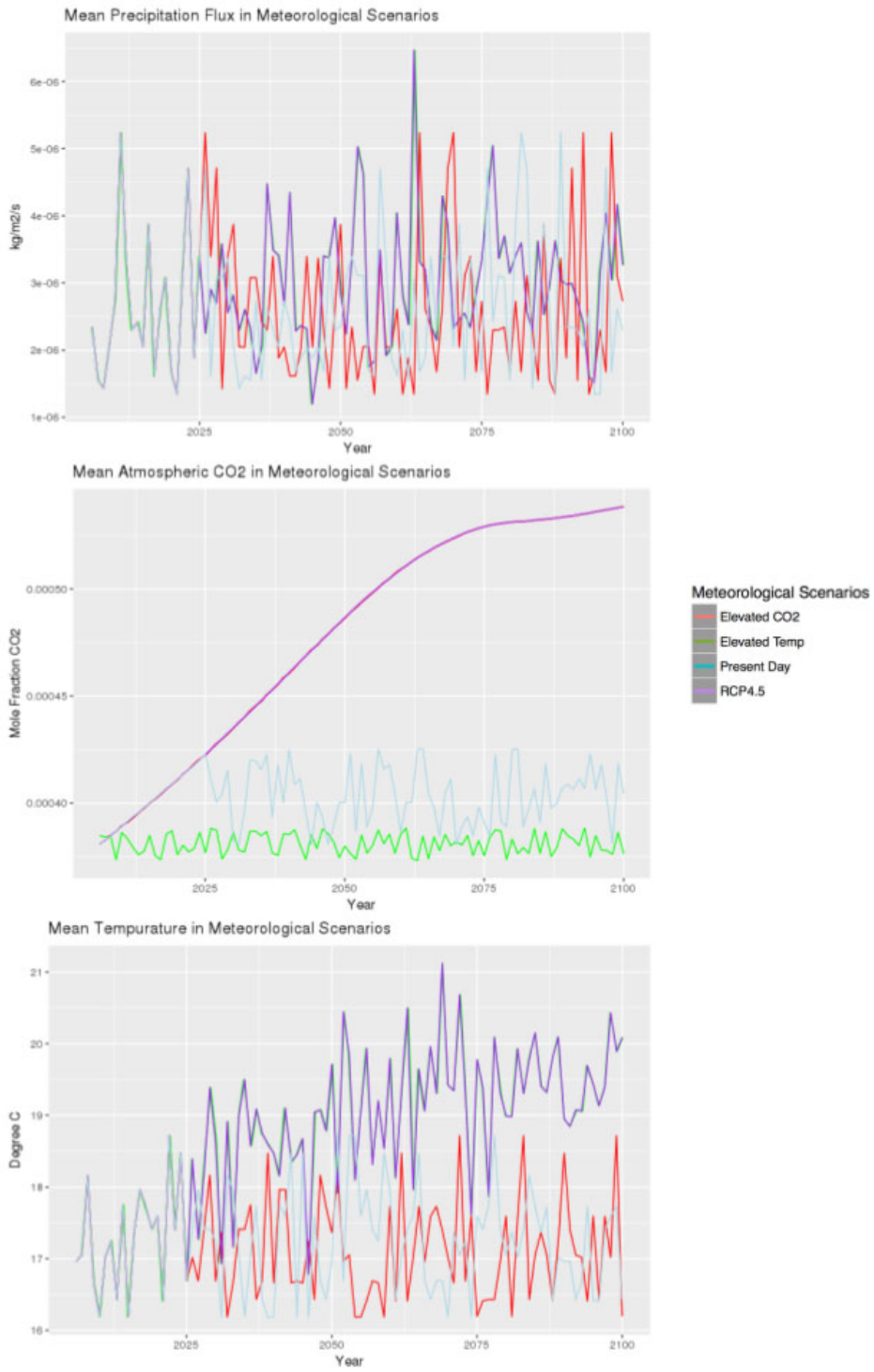

Figure 41: Projected meteorological drivers for projections into 2100. With the exception of CO_2, all meteorological drivers are identical up until 2026. In the mean precipitation flux and temperature panels, “Elevated Temp” scenarios and “RCP4.5” scenarios are

identical, and closely overlaid. In the CO_2 panel, "RCP4.5" and "Elevated CO2" are identical. Drivers that are not plotted include: specific humidity, northward and eastward wind, shortwave flux, longwave flux, and air pressure. Meteorology used to drive ED2 is at 3-hour resolution, plotted here with yearly means.

Objectives 4B: Cogongrass Plant Functional Type Development

We began our development of the cogongrass PFT by first incorporating our knowledge of a similar PFT developed for a grass of the same family with the same photosynthetic strategy (switchgrass; *Panicum virgatum*) into a new PFT that included cogongrass-specific knowledge (LeBauer et al. 2013). To determine which model parameters were most important to constrain against data, we first ran the cogongrass PFT at Avon Park AFR, FL under a range of parameter sets until we identified parameter ranges that produced appropriate levels of biomass that matched field observations. After that, we ran a full uncertainty and sensitivity analysis that formally quantified how uncertainty in different cogongrass traits contributes to uncertainty in state variables including evapotranspiration, net primary production, and biomass (Figures 51-55 and Objective 4B: Cogongrass Plant Functional Type Development). This laid the groundwork for targeted constraint of cogongrass traits. We were able to constrain root turnover and specific leaf area (SLA) by incorporating pre-existing datasets collected by collaborators in the Flory lab. However, we determined that we needed targeted field sampling to measure biomass allometries, photosynthesis parameters, and root respiration (Table 17). Some parameters could not be directly constrained because they do not represent individual physical traits in cogongrass (water conductance, reproduction allocation, growth respiration), and some would have required infeasibly long field seasons and manipulative experiments (density dependent mortality coefficient). See Objective 4B: Cogongrass Plant Functional Type Development for further discussion.

Table 17: Data used to constrain Cogongrass Parameters

Parameter	Definition	Units	Definition Citation	Source
Fine Root Allocation	ratio of fine root to leaf biomass	ratio		2019 Biomass measurements
Root Turnover Rate	Temperature dependent rate of fine root loss	year-1		Fahey et al., in prep
Stomatal Slope	The slope of relationship between stomatal conductance and photosynthesis	ratio	(Leuning 1995, Longo et al. 2019)	2019 Photosynthesis measurements
Vcmax	Maximum rate of carboxylation	umol CO_2 m-2 s-1	(Farquhar et al. 1980)	2019 Photosynthesis measurements
Quantum Efficiency	Percentage of light converted to carbon	Mol CO_2 fixed per mol irradiance	(Farquhar et al. 1980)	2019 Photosynthesis measurements
Specific Leaf Area (SLA)	Leaf area per unit dry biomass	m2 kg-1		(Hiatt and Flory 2020)

Root Respiration	Temperature dependent rate of CO_2 released by roots	umol CO_2 kg-1 s-1		2018 and 2019 Root Respiration measurements

Objectives 4B/4C: Constraint of Cogongrass Root Respiration

The cogongrass uncertainty analysis pointed to a range of different parameters in need of constraint (Figures 51-55 and Objective 4B: Cogongrass Plant Functional Type Development). Some parameters proved constrainable via existing cogongrass datasets or databases (Kattge et al. 2011, Alba et al. 2017). However, root respiration emerged as relevant to the overall carbon budget of the system (Figures 51, 54, 55). Root respiration is a difficult parameter to constrain because it is often measured in conjunction with soil respiration, and the partitioning between fine roots, rhizosphere, and soil aggregates is ill-defined and difficult to separate physically (Kelting et al. 1998, Kuzyakov 2006). In 2018, we set out to conduct a pilot measurement of root respiration in cogongrass by adapting previously developed methods (Makita et al. 2009, Abramoff and Finzi 2016).

During the 2018 field season we sampled root respiration in an old field at the University of Florida Bivens Arm Research Site (BARS) in Gainesville, Florida (29°37′42.4″N, 82°21′14.4″W). Root respiration measurements were collected on August 2 and 3, 2018. In our methodology, we used a LI-COR 6400 to measure CO_2 concentrations of root respiration by interrupting the flow through the incoming air stream with a mason jar filled with roots (Figure 42A). Inflow and outflow tubes into the mason jar were sealed with Scotch brand Sticky Tack (Figure 42C). The roots were dug up from a cogongrass invasion and placed into the jar. After the jar was sealed, and with the LI-COR leaf chamber closed, the LI-COR was matched to a reference level of CO_2, and the CO_2 concentration of the inflow tube, along with temperature and humidity, was measured for at least 5 minutes (Figure 42C). Concurrently, a temperature logger was buried at approximately root depth (Figure 42B). After CO_2 rates were measured, the roots were weighed for dry biomass. Dry biomass was acquired after drying in an oven set to 130 degrees C for at least 24 hours. At each sampling, fine roots and rhizomes were measured and weighed separately.

In the 2018 field season we collected 25 samples that include rhizomes and fine roots. Samples were taken spatially from a range of areas in BARS, but could have been the same clonal population. Some overlap in clonal population is likely because samples were at minimum approximately one meter apart. The naturally occurring invasion at BARS had been recently mowed, so measurements came disproportionally from unmowed edges of the invasion or unmowed sections near structural features. Some individuals in the central mowed section were also sampled.

As a trial of the methodology, our 2018 field work around root respiration was a success. We were able to answer questions about the feasibility of respiration measurements from attached fine roots (possible for rhizomes, not for fine roots), identify pit falls in methodology (root sun and heat exposure before respiration measurements can damage the fine roots). However, when we made corrections for changes in temperature and humidity that occurred during the measurement process, we realized that the signal to noise ratio of these measurements made estimates unreliable – particularly with regard to fine roots, that had consistently smaller biomass amounts. We designed our 2019 field season around reducing the noise around our measurements, and changed our methodology considerably.

Our 2019 root respiration methods were updated in three key ways: 1) we switched from an open-path measurment technique to a closed-path teqnique, 2) we measured larger quantities of root biomass, and 3) we moved the measurments into a lab setting where tempurature and humidity were controlable. All were attempts to boost the signal of respiration while minimizing noise. The closed-path technique used a sealed soil respiration chamber (Figure 43). Respiration measures were taken by running the soil respiration program on roots placed in a small jar that was then put into the sealed soil chamber 6400-09 (Figure 43A). As part of the automatic soil program, a target CO_2 is set based on ambient CO_2, and then the CO_2 level in the chamber is drawn down to below the target and allowed to increase past the target for a number of cycles and based on a change in CO_2 (Figure 43C). By recording how quickly CO_2 levels grow to the target amount, the program estimates the rate at which the contents of the chamber are respiring (Healy et al. 1996, "6400-09 Soil CO_2 Flux Chamber Instruction Manual" 2003). Because the estimates are based on a slope and multiple cycles, they are less sensitive to enviromental noise than the open-path method. To increase the biomass of the measured roots, and to move measurements to a lab setting, we dug out a natural cogongrass invasion with as much soil and root structure as possible. 15-25 stems were dug out and packed into a bin with damp paper-towels and soil. The bin was brought into a lab setting, where 1-3 grams of fine roots and rhizomes were weighed out and measured within the soil-respiration chamber (Figure 43B). To amplify the signal, samples from multiple plants were aggregated. In cases where our mass of fine-root biomass was still not enough to distiguish a signal, we measured rhizomes and fine roots both independently and together. For all samples we then dried the roots and rhizomes in a drying oven set to 60 degrees C for 48 hours, and normalized the respiration rate by dried biomass. After quality control, we had 11 estimates of rhizome respiration and 19 estimates of fine root respiration.

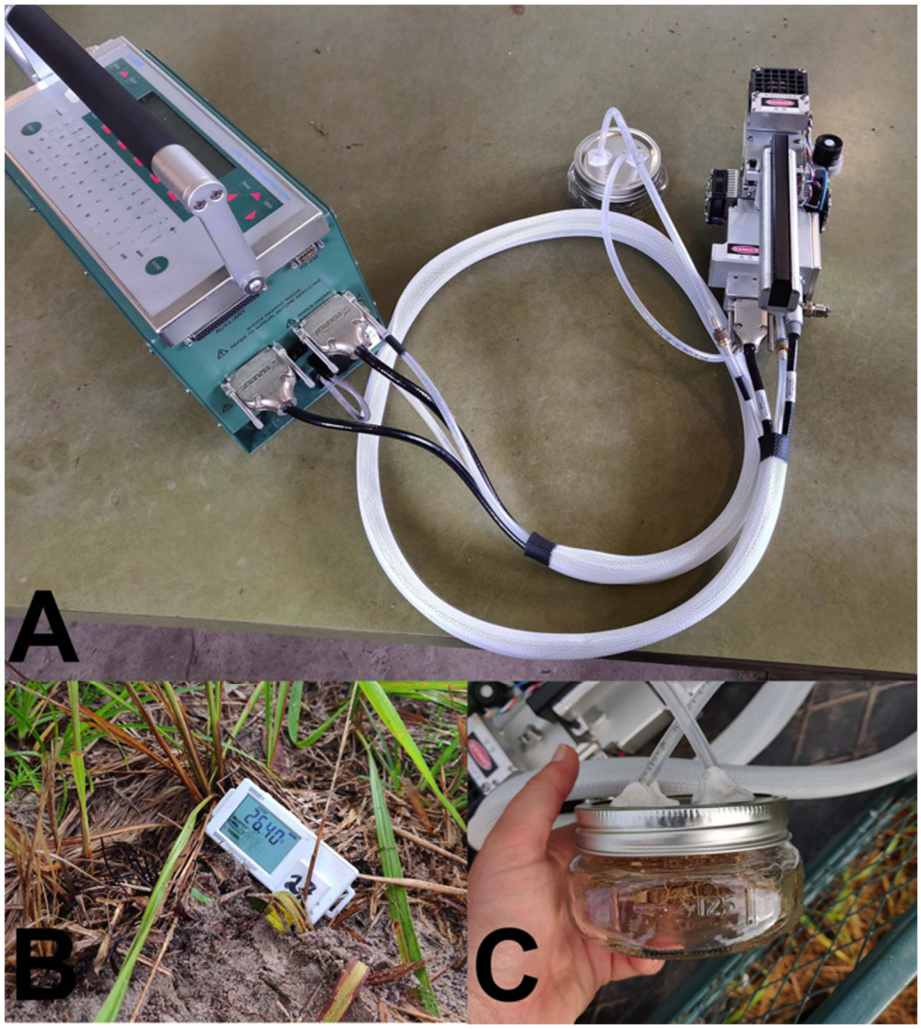

Figure 42: 2018 Field Season Open-path Root Respiration measurement technique using LI-COR 6400

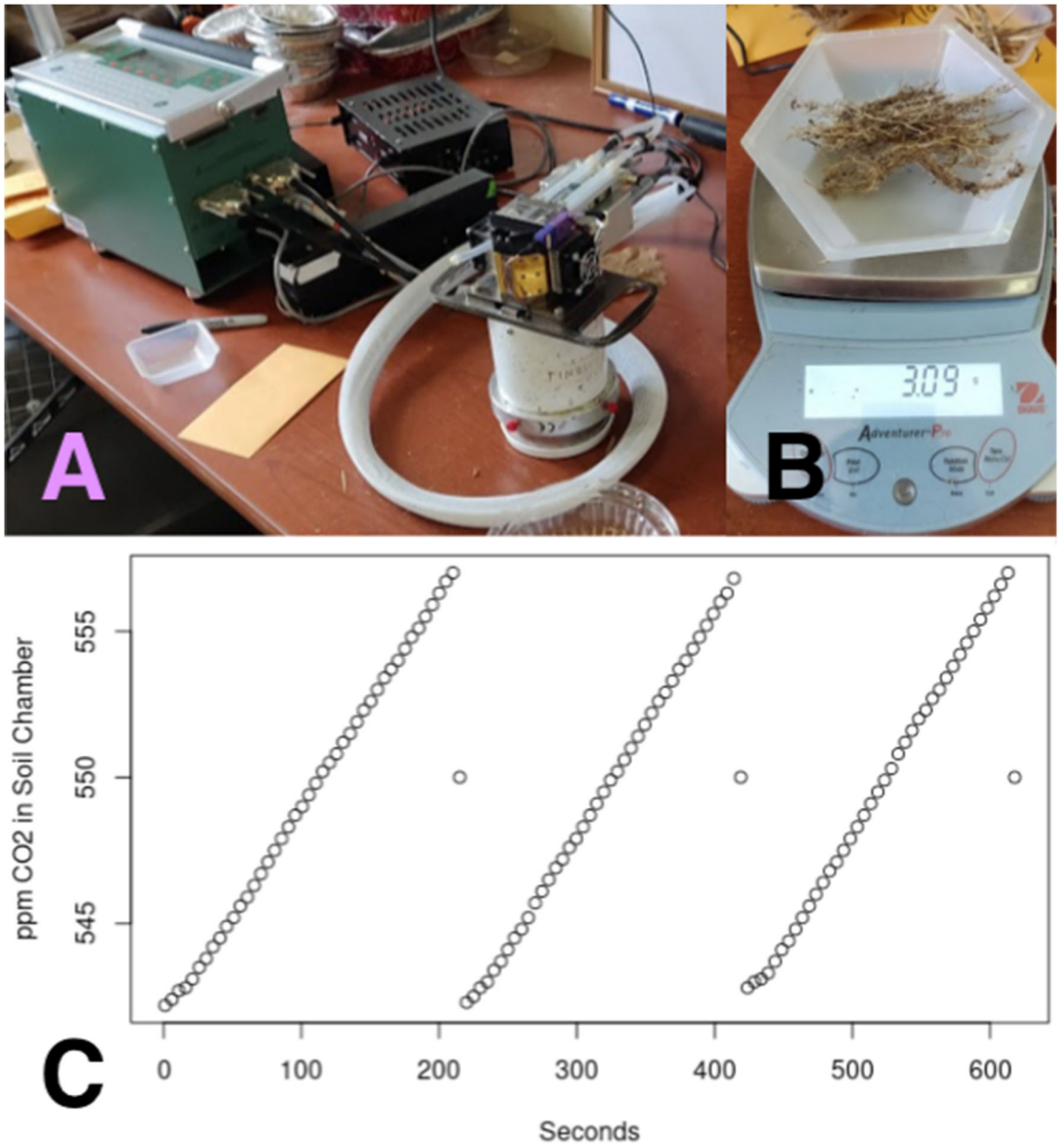

Figure 43: 2019 Field Season Closed-path Root Respiration measurement technique using LI-Cor 6400-09 soil chamber. Box A shows soil respiration chamber. Box B shows example fine roots being weighed. Box C shows the average CO_2 measurements through time. Box C corresponds to fine root measurement #15.

Objectives 4B/4C: Constraint of Cogongrass Biomass and Allometries

Fine root biomass allocation (expressed relative to leaf allocation) is another important parameter to constrain cogongrass uncertainty (Figures 51-55 and Objective 4B: Cogongrass Plant Functional Type Development). Synergistic with our measurements of root respiration, to be able to constrain fine root allocation ratio we made measurements of fine root and leaf biomass at BARS. In addition, because the BARS precipitation reduction experiment was

planted with a known rhizome density, any biomass measurements provide useful calibration data for how ED2 partitions cogongrass carbon. Finally, because the BARS experiment is a precipitation exclusion experiment, the difference in biomass between the plots could inform how cogongrass is (or isn't) affected by changes in water availability.

For each plot, a 30 cm^2 quadrat was placed in a subplot location cleared for harvesting. Quadrats were moved within a subplot grid cell to avoid seedlings and pre-existing measurements. All the live tillers were counted, and then harvested with garden shears. The harvested aboveground biomass was put into a drying oven set at 60 degrees C for 7 days. All non-cogongrass biomass was harvested and placed in a separate bag. Every unique species of non-cogongrass was counted. Then, a soil core was taken from the center of the plot. Soil cores were taken using a hammer-style soil corer, with a depth of 15.5 cm and a diameter of 5.5 cm. The cores were then stored in a freezer until processing.

The belowground biomass was processed by first thawing the soil core, then sieving through a 2mm opening sieve and a 420 micron opening sieve. When possible, the soil was sieved dry; however, most soil cores required water-draining. Rhizomes and fine roots were kept separate. Roots were rinsed of soil before drying. Roots clearly dead or non-cogongrass were excluded. Roots with unknown origin were included. Because fine roots can become quite small, the stopping point for root picking was to remove roots until the only roots found were unbranched roots 4mm in length or smaller. After that, roots were removed for an additional ten minutes. Each soil core took approximately two hours of devoted root-removal. After roots and rhizomes were removed from the soil they were put into a drying oven at 60 degrees C degrees for 48 hours and then weighed.

To test if cogongrass allocated carbon differently under drought conditions, we compared the ratio of belowground biomass to aboveground biomass collected in the precipitation exclosure plots to control plots using a two-sample Kolmogorov-Smirnov test. Overall, 19 new data points were added to the PEcAn database and used to constrain fine root biomass, with 20 new aboveground biomass measures to constrain model-runs (Table 17, Figure 56, Figure 57).

Objectives 4B/4C: Constraint of Cogongrass Photosynthesis -- Data Collection

Stomatal slope, vcmax, and quantum efficiency all emerged as a measurable parameter that control photosynthetic rates and how cogongrass trades water for carbon at the leaf level (Figures 51-55 and Objective 4B: Cogongrass Plant Functional Type Development). In order to measure these parameters, we used a LI-COR 6400 to measure light response curves where the level of light is started at maximum and slowly ramped down to zero, over 8-21 measurements while other environmental variables are held constant. Light curves used a standard leaf-chamber portable infrared gas analyzer with a 1098 light source. CO_2 was held at either 400 ppm or 450 ppm depending on ambient levels. The LI-COR was calibrated before all measurements by zeroing the flow rate, CO_2 and humidity levels.

Light curves were taken following the technique found in (Leakey et al. 2006, Wolz et al. 2017, Leakey et al. in prep). Our methods differ from Leakey's in three small ways. First, there existed no prior work suggesting that excised cogongrass leaves could reproduce maximum photosynthesis levels (Leakey et al. 2006, Ainsworth and Rogers 2007). Cogongrass is an invasive and highly productive grass, suggesting it might be a candidate for excised leaves reproducing maximum photosynthesis rates. In our 2019 field season we attempted five excised leaf light curves, and were able to produce two curves. We measured field curves separately to compare to the excised curves and found that excised leaves occasionally had comparable levels

of photosynthesis – but sometimes had low or no detectable photosynthesis. We attributed this to embolisms forming during the excising process. Leaf-harvesting proved difficult enough that we switched to in-vivo leaves early in our measurements. Second, Leakey was able to hold all other environmental variables constant. Because the majority of our curves were taken in vivo, temperature varied as the day progressed and several curves were subject to dramatic humidity swings. Finally, the area for cogongrass leaves was smaller than that of the chamber. The width of the leaf was measured, and multiplied by the length of one side of the leaf gasket chamber ($\sqrt{6}$cm^2).

In order to let the stomatal slope stabilize, we set a minimum wait period between two light steps to ten minutes, and a maximum wait period of a half hour. In addition, CO2, humidity and flow rate had to be stable for a full minute before measurements were taken. All light curves but one began at a starting value of 2000 photon flux density before measurement began at 1500 photon flux density. We set the final light curve to start at 2300 based on observations that typical days in Florida can achieve up to 2300 photon flux densities. The LI-COR was matched before each measurement.

Excised leaves were harvested pre-dawn and cut underwater. Leaves were harvested from the BARS long-term garden experiment (Alba et al. 2017) using edge leaves that had grown out from under the precipitation exclosures. Leaves suspected of embolism were discarded. In vivo leaves were measured in the field. Field curves were taken during a range of times, from dawn until roughly 2:00 pm.

To provide additional constraint, two humidity curves were taken. For the first curve, incoming radiation was fixed at 1500 photon flux density. The second was 700 photon flux density. We started at roughly 80% humidity, and kept it steady for about 15 mins. Every 15 minutes, we would manually reduce the humidity by about 20-25%. Humidity reached a minimum of about 10%.

Objective 4A: Constraint of Cogongrass Photosynthesis -- Parameter Estimation

Light and humidity curves were used to estimate values for stomatal slope, vcmax, and quantum efficiency. Stomatal slope represents how quickly plants adjust their stomata to environmental changes like light, humidity, and temperature (Table 17). Stomatal slope was estimated by fitting a linear model to a plot of stomatal conductance versus photosynthesis corrected for humidity and temperature, using the light curves from 6 different plants (Figure 44). Specifically, stomatal slope was estimated from:

$$stomatal\ conductance = conductance_{closed\ stomata} + \frac{stomtatal\ slope * photosynthesis}{respiration * (1 + \frac{vapor\ pressure\ deficit}{leaf\ level\ water\ deficit})}$$

where leaf-level water deficit was set to a C4 default, 0.016. Photosynthesis, respiration, vapor pressure deficit, and stomatal conductance were all measured. Vapor pressure deficit is a measure that combines temperature and humidity. This equation is from Luening 1995, and its implementation in ED2 is equation 89 of Longo et al. (2019). Vcmax and quantum efficiency are both parameters that describe how photosynthesis could be limited by the plant's photosynthetic machinery itself (Table 17). We estimated vcmax and quantum efficacy using a hierarchical Bayesian implementation of the Farquhar, von Caemmerer, and Berry (1980) photosynthesis model as described in Feng and Dietze (2013), and implemented in the PEcAn photosynthesis module (https://github.com/PecanProject/pecan/tree/develop/modules/photosynthesis).

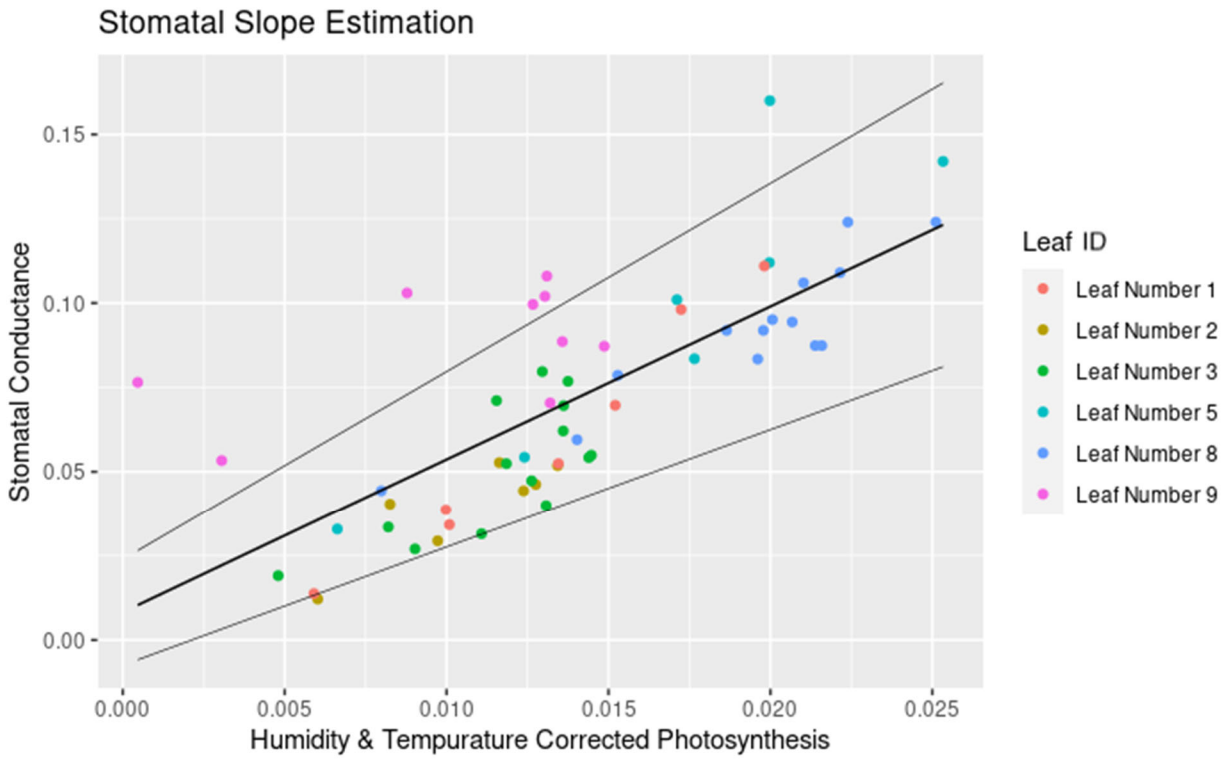

Figure 44: Estimate of stomatal slope from light curves. Each leaf had photosynthesis measured across progressive light changes. Different colored dots are distinct leaves. Dotted lines show 95% confidence interval.

Objectives 4B/4C: Cogongrass Sensitivity to Drought

After incorporating seven new datasets into our estimates of cogongrass traits, we needed an estimate of the remaining uncertainty that surrounded cogongrass. Cogongrass is most sensitive to water-conductance (Figures 51-55 and Objective 4B: Cogongrass Plant Functional Type Development). However, water conductance is not directly constrainable. We needed to test the extent our collected trait data may have indirectly constrained water conductance. In addition, we wanted to know how sensitive cogongrass would be to external conditions, like droughts. The BARS precipitation reduction experiment allowed us to test what traits remain uncertain under drought conditions. We ran two new sensitivity and uncertainty analyses. Both were set performed at BARS and included new data. One represented ambient climate condition at BARS, and the second represented the precipitation exclosure plots. We used the meteorology product ERA5 to drive both analyses. To simulate the levels of precipitation exclusion experienced by cogongrass under the drought condition, we fit a regression to measured soil moisture levels in ambient and drought treatments (Figure 45). The drought analyses was driven by ERA5 data that had precipitation reduced by the same coefficient (approximately half) as soil moisture.

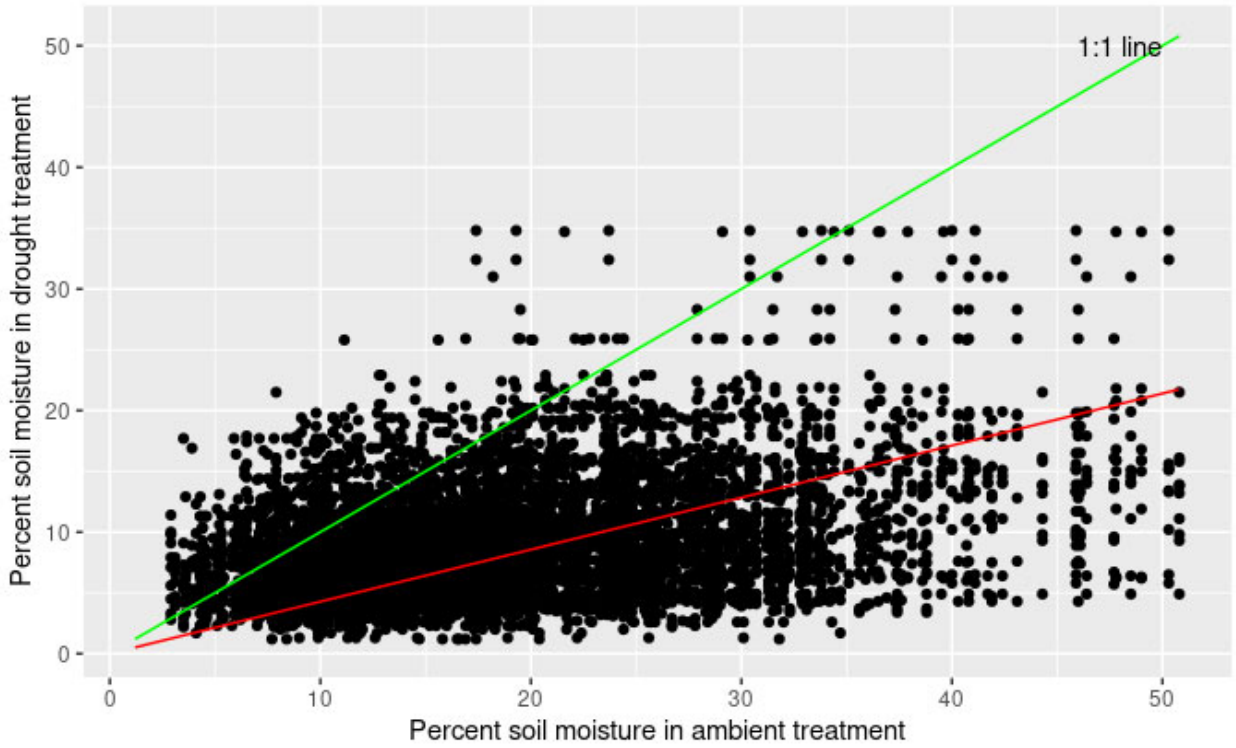

Figure 45: Red is regression of the form Drought Soil Moisture = Ambient soil moisture* 0.5375376. The green line is a 1:1 reference line.

Objective 4D: Developing a Method for Scaling Contagious Disturbance in a Spatially Implicit Way

The Southeastern pine forests are fire adapted and experience a range of fire severities, but primarily frequent low intensity fires that maintain biodiversity and control carbon fluxes (Kirkman et al. 2004, Mitchell et al. 2006, Starr et al. 2015). As outlined in Part 2a, cogongrass has a significant effect on fire intensity, but capturing fire regime and cogongrass interactions requires a representation of fire that distinguishes between the understory and overstory, and allows for a mechanistic understanding of fire severity. The fire module currently implemented in ED2 is simple and fully stand-replacing. Many candidate fire models and methodologies (e.g., FARSITE) come from a spatially explicit framework (Finney 2004). Combining ED2 outputs with the most common fire metrics requires translation between the spatially explicit framework of mechanistic fire understanding and the spatially implicit scaling of ED2 (objective 4D). To facilitate this translation, we developed, tested, and compared to data a method for scaling contagious disturbances in a spatially implicit way. A more complete accounting of the method is available in the paper "*Scaling Contagious Disturbance: A Spatially-Implicit Dynamic Model*" (McCabe and Dietze 2019). We summarize our methodology below.

We developed this method in roughly four parts: first, we looked at how one could approximate spatial disturbance using adjacency. Second, we looked at how one could update a dynamically changing landscape using an evolving adjacency matrix and evolving fractional areas. Third, we validated our approximation against a simulation after 1000 years of growth and disturbance. Finally, we explored how our derivation's description of disturbance regimes

compared to observations. Our model suggested that two metrics could describe disturbance regimes: the size distribution of disturbances, and the relationship between the size distributions and the ratio of interior edges to total edges of the disturbance shape.

We explored whether our theoretically emergent metrics could distinguish between different regional disturbance regimes and different disturbance mechanisms. We looked at the size distributions and interior-total ratios of all of the disturbances in Florida and Oregon that were in the 2014 LANDFIRE disturbance product. The LANDFIRE disturbance product is a raster of disturbances at 30-by-30 meter resolution for the entire contiguous United States. Oregon was chosen as a contrast to Florida because both states have active timber industries and are strongly influenced by fire, but disturbance regimes are very different. We used two different statistical tests for the two different disturbance metrics.

We compared the size distributions of disturbance type, US states, and ecoregions using a two-sided Kolmogorov–Smirnov test. For the interior to total ratio, we fit and statistically compared curves corresponding to null models and different hierarchy levels. The curves were fitted using a modified Michaelis-Menten curves of the form $y = \frac{ax^c}{b+x^c}$ using a maximum-likelihood approach assuming Gaussian error. Comparing the curves meant comparing different hierarchical levels. We fit two hierarchies, one starting at the US state level, and one at the disturbance-type level. In the US state hierarchy, an all-data null model was compared to a model where Oregon and Florida were fit separately. The US state-model was then compared to a model where each ecoregion was fit separately. In the second hierarchy, an all-data null model was compared to a model where each disturbance type was fit separately. The disturbance-model was then compared to a disturbance-by-US state model. Because all single-pixel, double-pixel, and triple-pixel configurations produce the same interior ratio (Figure 60), curves were fit only to disturbances over 3 pixels (0.27 ha) large. To meet requirements of likelihood ratio tests, the data were subset to include only the disturbance types that were common amongst all ecoregions. To contextualize modeled curves, we included hexagonal density plots, representing the spread and overall shape of all the data used to generate curves (ggplot2, 3.0.0; Wickham et al., 2018). To aid in interpretation, the upper and lower bounds for the interior ratio were also visualized based on calculations of the theoretical minimum (linear disturbance) and maximum (round disturbance) interior ratios for a given disturbance size. All analyses were performed in R version 3.5.0 (R Core Team, 2018) with adjacency calculations performed using the raster library (2.6-7; Hijmans, 2018)

RESULTS AND DISCUSSION

Objective 4A: Southern Pine Forest Under Different Climate Scenarios

Different meteorological scenarios had different effects on the successional trajectory of forest. The combined elevated CO_2 and elevated temperature scenario (equivalent to the RCP4.5 scenario) had the largest gross primary production (Figure 46). Higher growth with higher CO_2 concentrations is consistent with a "Carbon dioxide enrichment" hypothesis which states that because C3 photosynthesis becomes more energetically efficient when the atmospheric carbon dioxide levels are higher, C3 plants will be able to uptake more carbon (Ainsworth and Long 2004). The elevated carbon dioxide scenario also assimilated more carbon compared to the other scenarios, but with less dramatic gains. This could be because the combination of elevated CO_2

and temperature is metabolically favorable, or because elevated temperatures favor different species with higher carbon uptake potential. The present day scenario had the smallest gross primary productivity overall but similar gross primary production levels as elevated temperature around year 2099.

To separate potential causes of differences in scenarios, we plotted gross primary production by temperature (Figure 47). Scenarios with elevated temperatures had peak gross primary productivity at warmer temperatures, but elevated carbon dioxide scenarios had peaks at higher levels of gross primary production (better carbon assimilated to temperature ratio). The elevated temperature scenario had a lower carbon assimilated to temperature ratio than the present day scenario, but the combined temperature and elevated carbon dioxide scenario had a higher carbon to temperature ratio than just elevated carbon dioxide. This suggests either that there is an interaction between elevated temperatures and elevated carbon dioxide that is not detectable in either of these treatments alone, or a species composition shift.

One potential interaction is a change in water-use-efficiency, where the ratio of carbon gained per water lost during photosynthesis changes as a result of higher atmospheric carbon. Globally, forests could be experiencing an increase in water-use-efficiency due to rising CO_2 concentrations (Keenan et al. 2013). Figure 48 shows plots of gross primary production by transpiration. Elevated temperatures use more water, while elevated carbon dioxide levels increase the level of carbon assimilated per unit transpiration. There were differences in water-use-efficiency between scenarios, but those differences don't explain why the combined RCP4.5 scenario had higher gross primary production levels.

Figure 49 shows the daily leaf area index for Duke Forest. The contribution of deciduous species and coniferous species is visible, and with it you can begin to see changes in species composition. The lower "trend" is the leaf area index of the coniferous species in the winter, and the upper trend is the combination of coniferous species and deciduous species. Figure 50 shows the difference in biomass between the two PFTs formally separated. In Figure 50, it's clear that different scenarios have different compositional structures. Elevated temperatures increase the biomass of late temperate deciduous trees while decreasing the relative biomass of southern pine. Elevated carbon dioxide has almost the opposite effect, increasing southern pines and not increasing the biomass of deciduous. The combined scenario, RCP4.5, could have the highest gross primary production because both PFTs grow in biomass. Figure 50 suggests that changes in physiology (like water use efficiency and optimal photosynthetic temperature) need to be evaluated by each PFT separately.

These scenarios are explorations of different climate effects, and not projections of the likely successional trajectory of southeastern US forests. One of the hypotheses of the Free-air concentration enrichment experiment at Duke suggests that while the sites do experience an initial boost in gross primary production with elevated carbon dioxide levels, it would become limiting as time went on. The Duke Free-air concentration enrichment experiment was able to maintain elevated levels of growth for over 10 years without signs of dramatic nitrogen limitation, but may not have been nitrogen limited (Ellsworth et al. 2012). That hypothesis is consistent with an ED2 experiment by Miller et al., which found that the nitrogen cycle affected the successional trajectory (Miller, Dietze, DeLucia, et al. 2016). In addition, similar model-based explorations of meteorological scenarios by Thomas et al. found that nutrient availability and precipitation levels have a large effect on the carbon cycling of the system (Quinn Thomas et al. 2017). Finally, this area frequently experiences management and fire (Platt et al. 2015,

Abatzoglou et al. 2018). A full projection would require more exploration of other RCP scenarios, management, as well as a better accounting of the nitrogen cycle.

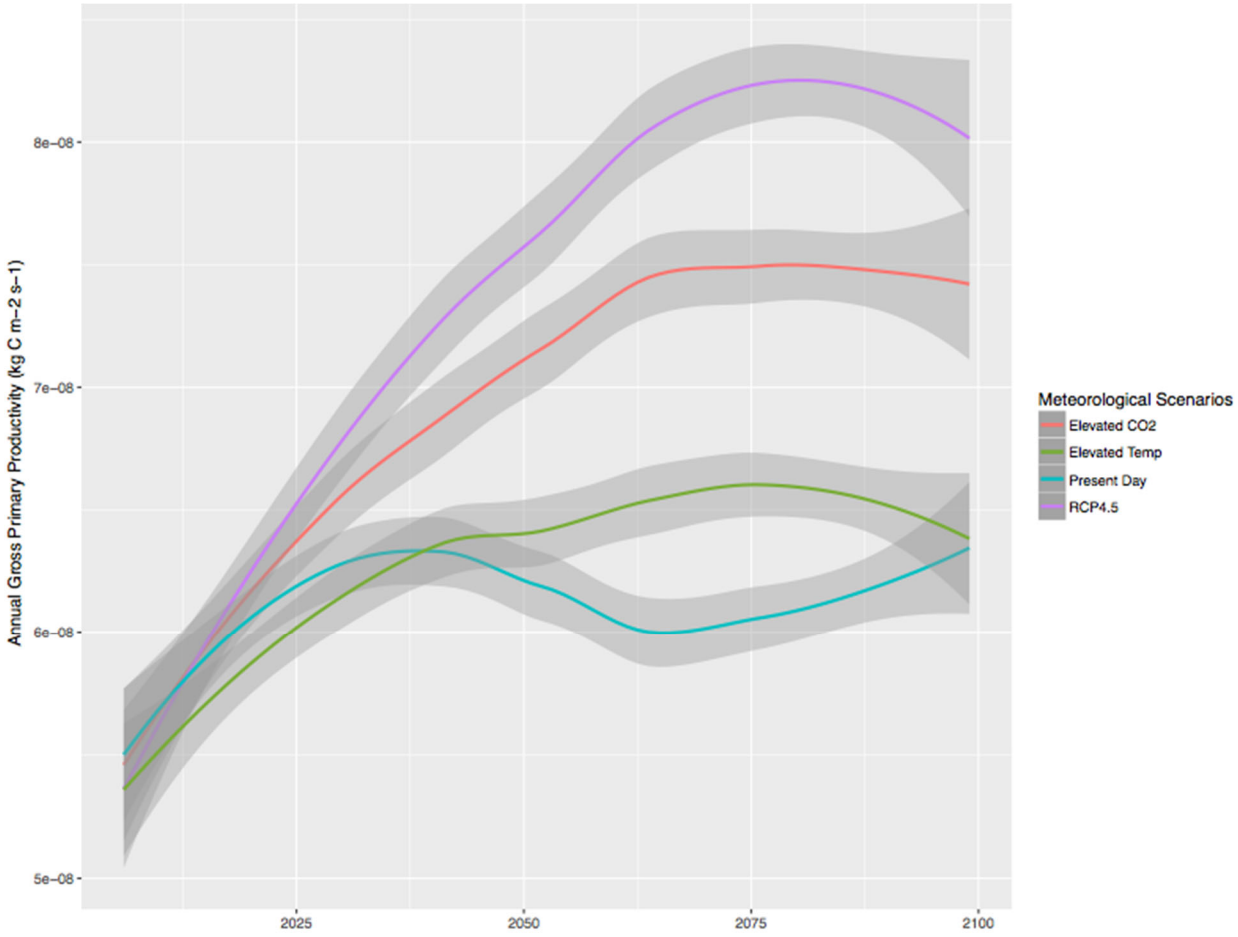

Figure 46. Meteorological scenarios effect on Gross Primary Production in Duke Forest, North Carolina. Fluxes smoothed with ggplot loess function for ease of interpretation (Wickham 2011).

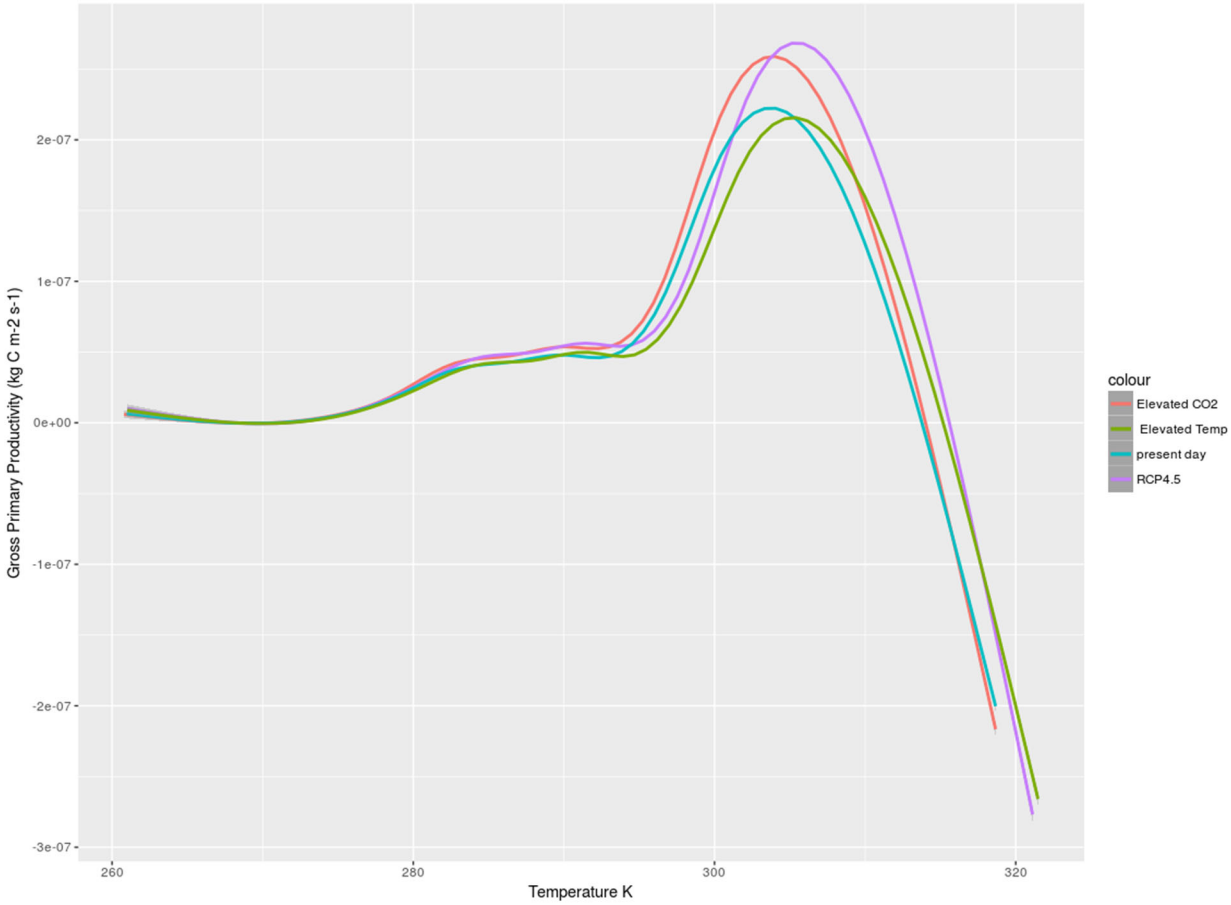

Figure 47. Temperature Sensitivity by Meteorological Scenario at Duke Forest.

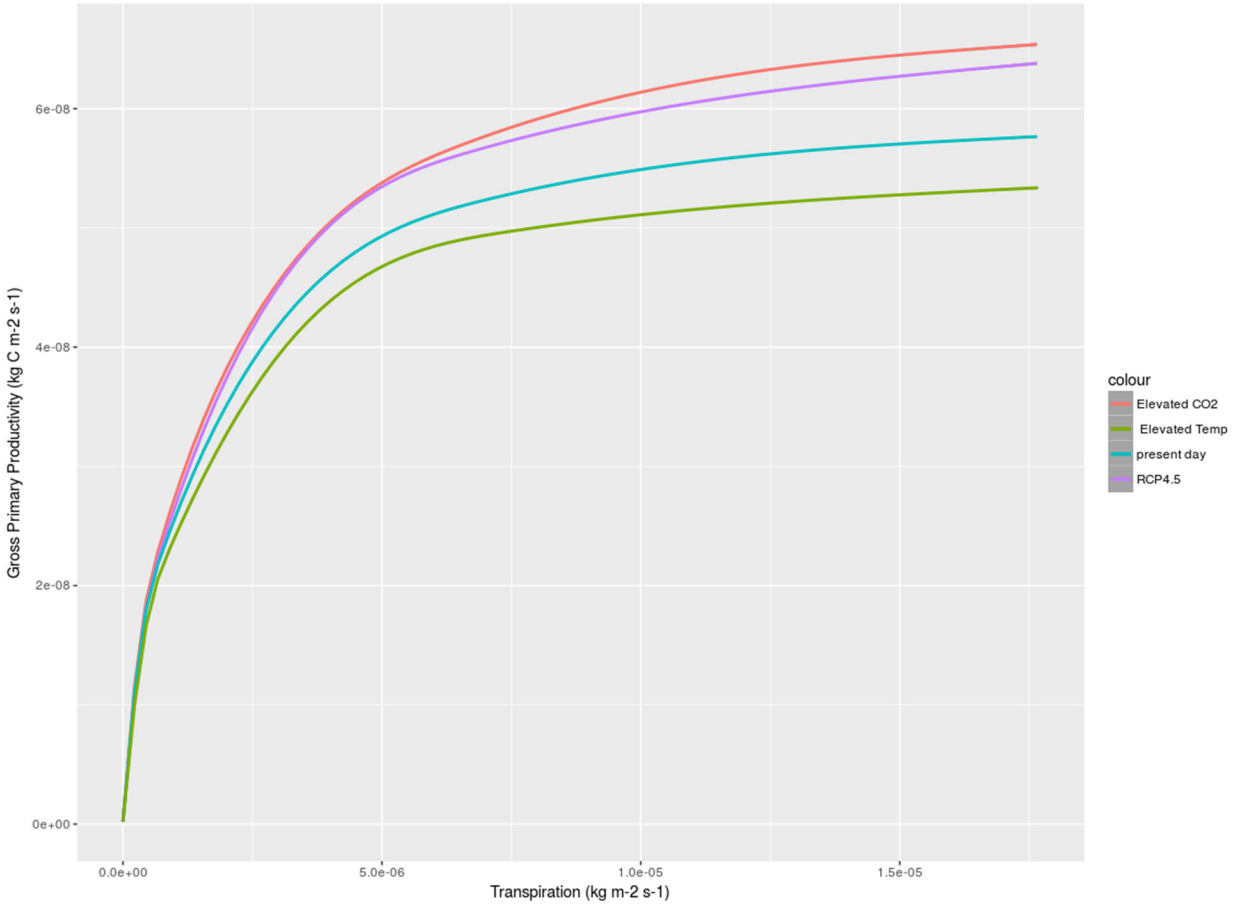

Figure 48. Water Use Efficiency by Meteorological Scenario at Duke Forest.

Figure 49. Daily Leaf Area Index by Metrological Scenario. The lower "trend" is the leaf area index of the coniferous species in the winter, and the upper "trend" is the combination of coniferous species and deciduous species. Note that coniferous species and deciduous species are not plotted separately, but the lower "trend" is visible because coniferous species contribute all of the Leaf Area Index during winter months.

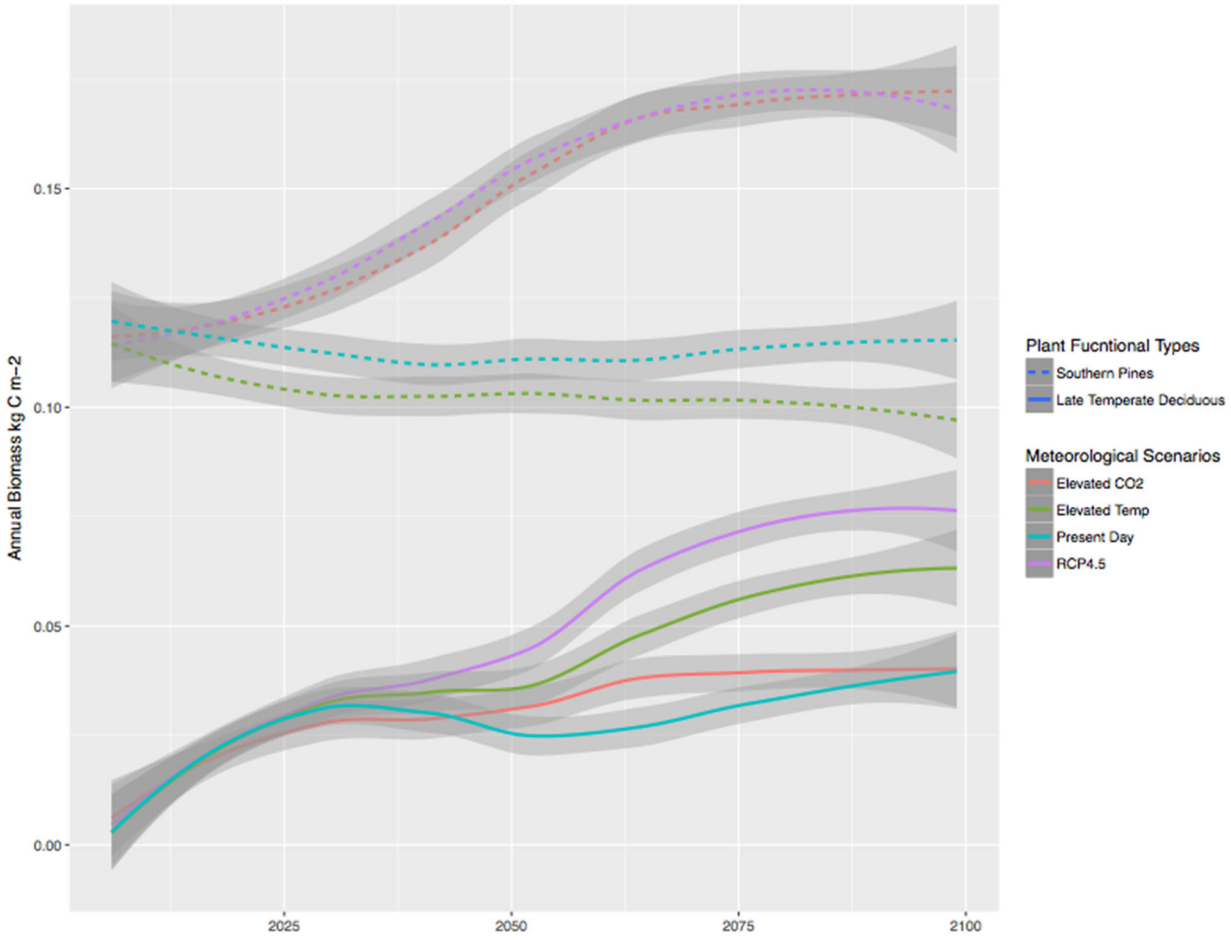

Figure 50. Annual Biomass by Metrological Scenario through time. Line textures distinguish the two different plant functional types, Late Temperate Deciduous (ie: *Quercus*) and Southern Pines (ie: *Pinus taeda*, *Pinus elliottii*, and *Pinus palustris*). Lines were smoothed using the ggplot loess function (Wickham 2011).

Objective 4B: Cogongrass Plant Functional Type Development

Our uncertainty analysis of the cogongrass plant functional type outlines areas where cogongrass can be constrained. Figures 51-55 all show how either the variance around parameters (rightmost column), or the model's elastic response to parameters (middle column) combine to contribute to the overall uncertainty in a model variable (the leftmost column). Different parameter uncertainties have different effects depending on the model variable in question. Looking at the uncertainty breakdown for different variables, water conductance consistently emerges as the largest source of uncertainty (Figures 51-55). Other visible sources of uncertainty include specific leaf area (Figures 51, 53-55), quantum efficiency (Figures 51-55), root respiration (Figures 51, 54, 55), stomatal slope (Figures 52-55), and fine root allocation (Figure 51).

Constraining water-conductance directly poses a challenge, because in the current version of ED2 water conductance is a hydraulics term that is not directly analogous to any measurable quantity. Because methods of direct constraint don't exist for water conductance, we elected to

indirectly constrain water conductance, and test how sensitive cogongrass outputs were to drought conditions. However, we did weigh switching to a model with measurable water conductance. ED HYDRO is a version of ED developed to allow for better representation of hydraulic diversity in PFTs (Xu et al. 2016). Using it would allow for direct measurement of hydraulic parameters, but could come at the cost of uncertainty around other parameters. In a recent presentation by Cowdery et al., authors looked at uncertainty breakdown at tropical sites for both ED2 and ED HYDRO. They found that while the ED HYDRO was able to reduce hydraulic uncertainty, it could increase the uncertainty around carbon dynamics – particularly belowground carbon dynamics (Cowdery et al. 2018). This suggests that pursuing a direct hydraulic calibration could require additional constraint on several carbon-sensitive parameters. In addition, not all of the new parameters introduced by ED HYDRO are analogous to cogongrass. For example, ED HYDRO requires parameters from a xylem vulnerability curve – a curve representing the risk of embolism in the stem/trunk of a plant as pressures increase. Techniques for measuring hydraulic vulnerability curves in herbaceous species have only been developed recently and in specific circumstances (Brodribb et al. 2016). Because of these reasons we elected to constrain water conductance indirectly by measuring other parameters. This process took place in the 2018 and 2019 field season, where we measured quantum efficiency, specific leaf area, root respiration, vcmax, root turnover, fine root allocation, and stomatal slope (Table 17).

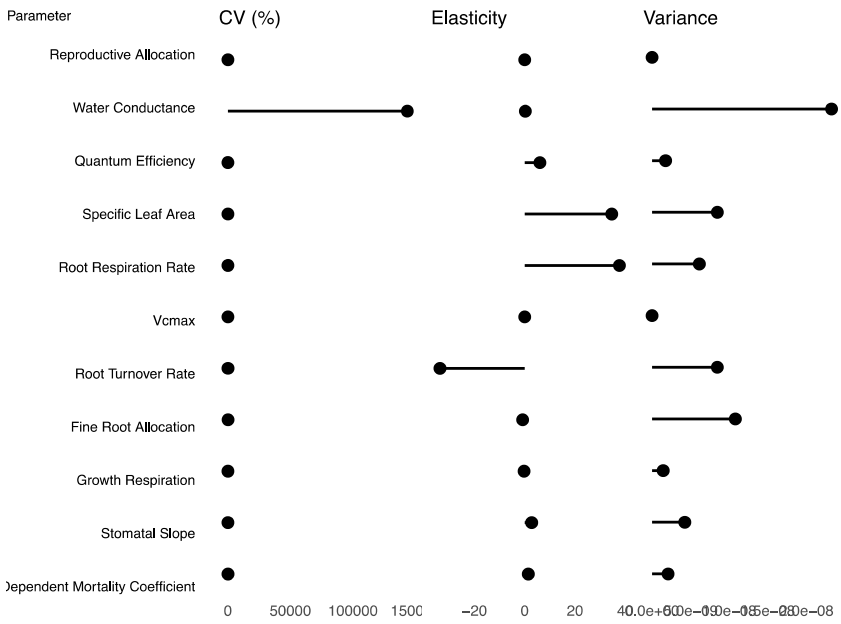

Figure 51. Variance Decomposition of Net Primary Production in a Cogongrass Stand

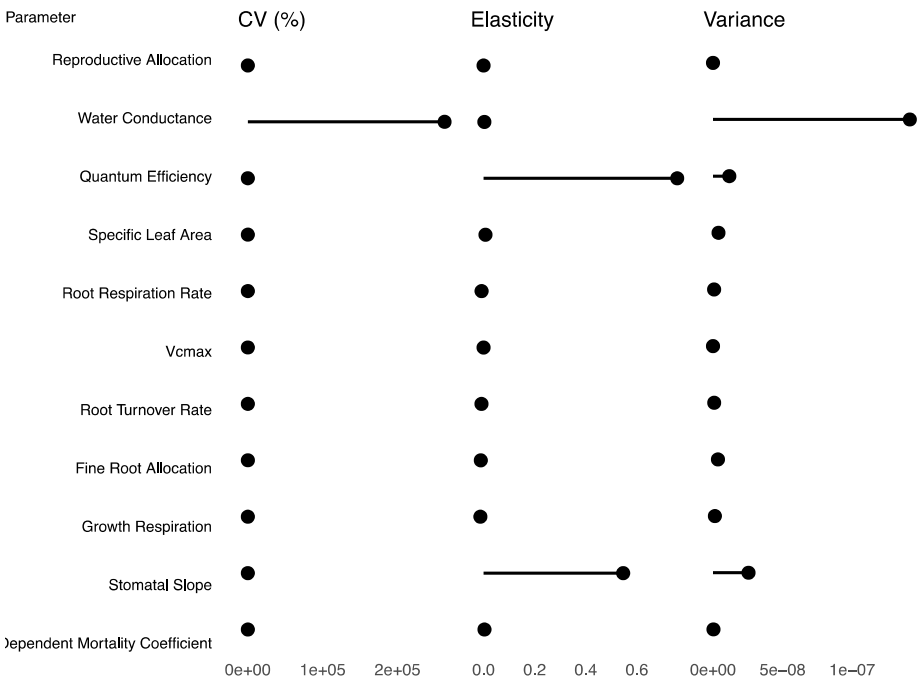

Figure 52. Variance Decomposition of Gross Primary Production for Cogongrass Stand

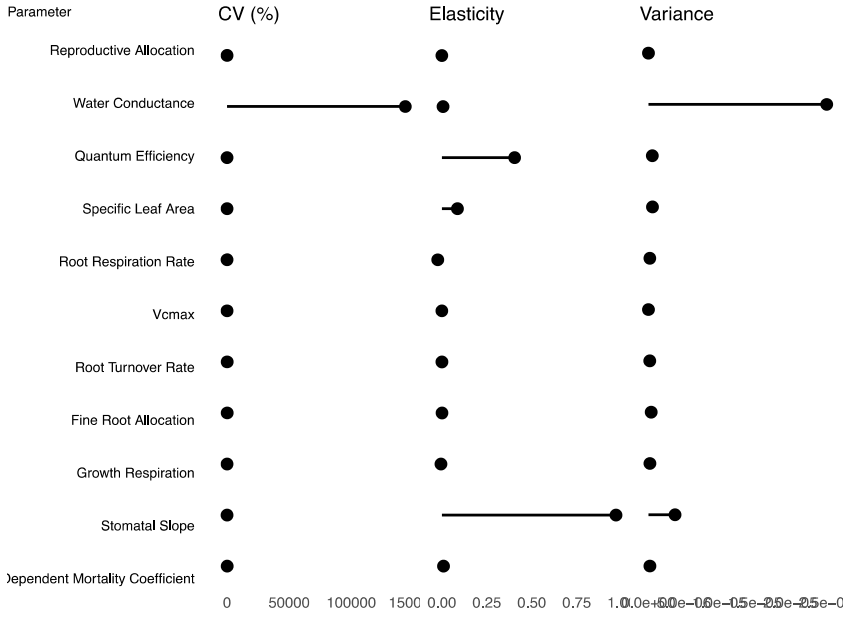

Figure 53. Variance Decomposition of Transpiration in a Cogongrass Stand

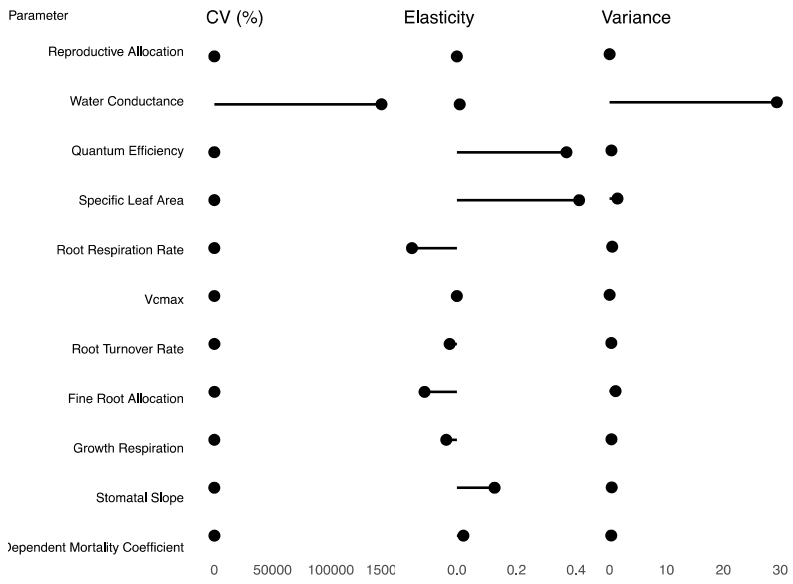

Figure 54. Variance Decomposition of Leaf Area Index in a Cogongrass Stand

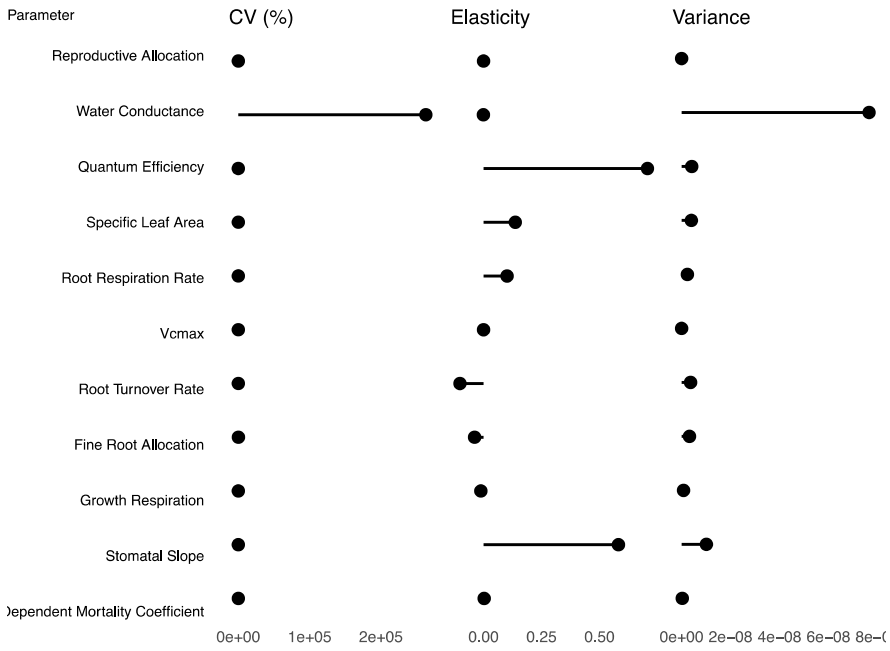

Figure 55. Variance Decomposition of Respiration in Cogongrass Stand

Objectives 4B/4C: Cogongrass Biomass and Allometries

We compared how cogongrass allocated biomass in drought conditions and ambient conditions. We found that both treatments have bi-modal distributions, with mostly very small fine root to leaf ratios (i.e. more leaves than roots), but occasionally ratios larger than one (Figure 56). The ambient treatment may have smaller root:leaf ratios overall, which comes from either larger aboveground biomass, or less belowground biomass. As expected, drought seems to have slightly larger ratios root:leaf. A two-sample Kolmogorov-Smirnov test found a significant difference between both distributions at a 0.05 alpha (p-value = 0.045, D = 0.59). This suggests that the drought treatment changes how cogongrass allocates biomass to favor roots. However, the bi-modality of the data and the low sample size make interpretation difficult. Cogongrass investing in roots could be an example of a way cogongrass adapts to drought long-term – or transports water within a clonal unit. Cogongrass will transport photosynthate through rhizomes within a clonal unit (Estrada et al. 2020).

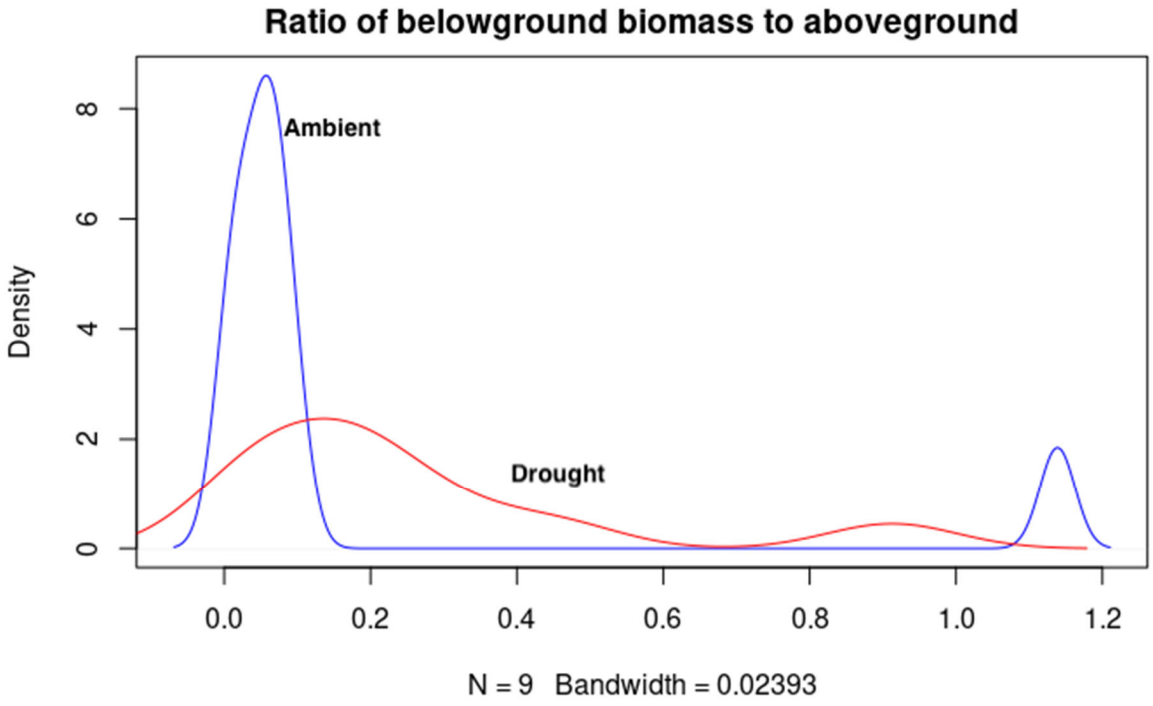

Figure 56: Density plots of root allocation from BARS ambient and drought treatments. Calculated from ratio of rhizome and fine roots divided by aboveground biomass. A two-sample Kolmogorov-Smirnov test found a significant difference at a 0.05 alpha (p-value = 0.045, D = 0.59).

Objectives 4B/4C: Cogongrass Sensitivity to Drought

After the 2018 and 2019 field seasons, we wanted to test how our new datasets may have changed the uncertainty around cogongrass traits. We also wanted to see if that uncertainty would increase under drought conditions. In Figure 57, two sensitivity and uncertainty analyses are presented, one for ambient conditions and one for drought conditions. Comparing the ambient condition for Figure 57 to our pre-constraint estimates (Figures 51-55), we tightly constrained stomatal slope, root respiration, root turnover, quantum efficiency and root allocation. The largest remaining sources of variation were growth respiration, specific leaf area, and water conductance. While water conductance is still a large source of uncertainty, the data we collected reduced uncertainty noticeably. Comparing the ambient portion of Figure 57 to the drought portion, it's clear that under drought conditions, the model becomes more sensitive to changes in parameters. Carbon-cycling parameters like growth respiration and photosynthesis parameters become more important – but notably water conductance remains the largest source of uncertainty.

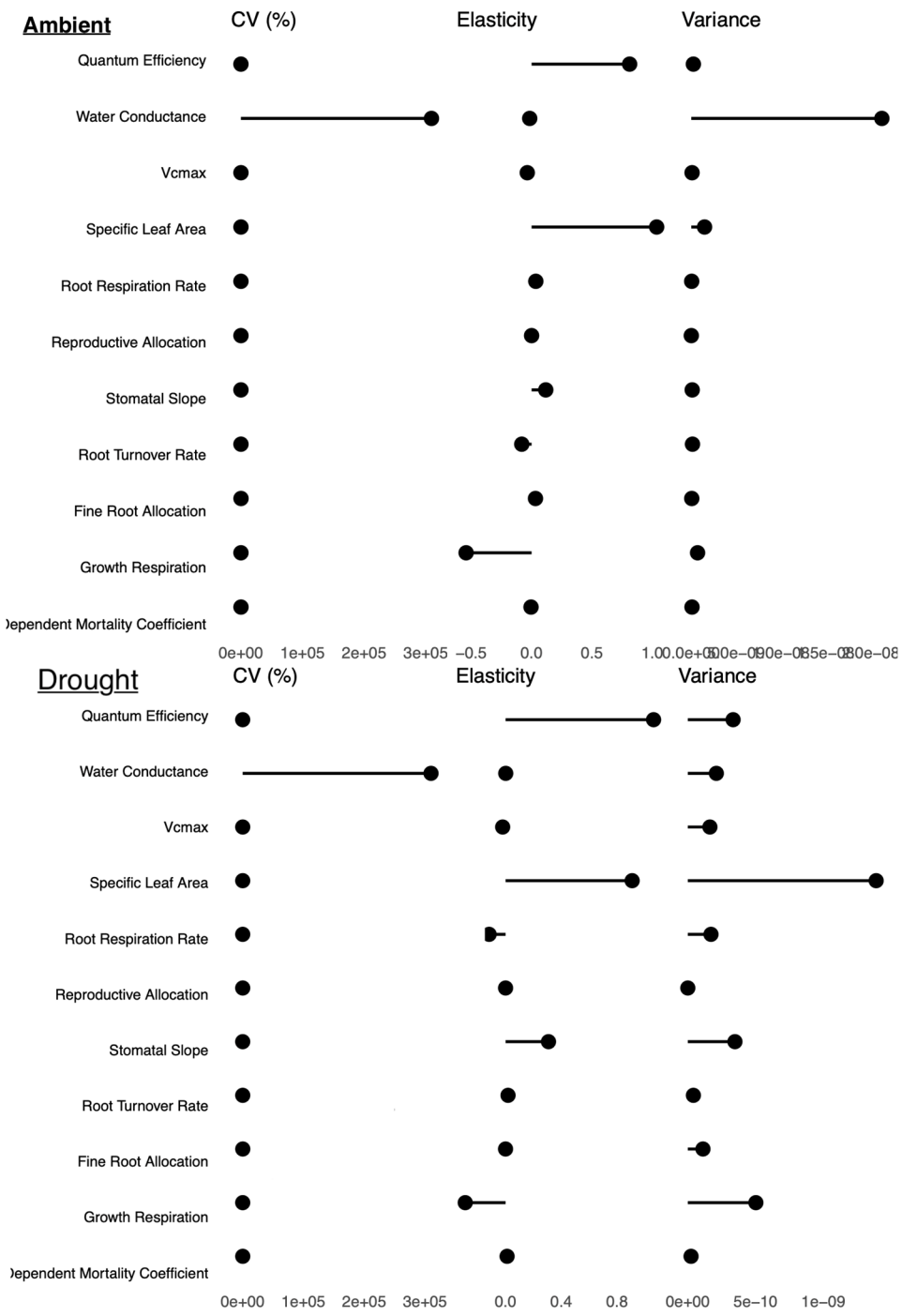

Figure 57: Comparison of trait sensitivity and uncertainty under ambient and drought conditions.

Objective 4D: Developing a Method for Scaling Contagious Disturbance in a Spatially Implicit Way

Simulating Disturbance Using Adjacency

To start approximating disturbance in a spatially implicit way, we began by thinking about how disturbances cause heterogeneity. We represent the shape a disturbance makes on a landscape as a function of initiation probability and spread probability; two probabilities that are influenced by both the landscape and the disturbance type. Because both of the probabilities are influenced by the landscape, we needed a spatially implicit representation of the landscape. An adjacency matrix is a matrix of all of the classes of interest (e.g. age of stand, species of trees, etc.), and shows what percentage of that class is adjacent to the other type of classes. Figure 58 is an example of this. The top row shows two simulated disturbed landscapes, with example adjacency matrices in the last row. In the middle, is the histogram of individual ages. The adjacency matrices capture spatial features without an explicit map. ED2 conceptually is already using adjacency matrices to represent landscape features and adjacency-based ecological phenomena (nutrient competition, shading). We represented disturbance area as a function of disturbance spread probabilities, initiation probabilities and the adjacency matrix. The initial disturbance area (for disturbances with size = 1 patch) is given by:

$$I_1 = p_0 \circ a$$

where a is a vector of the fractional areas of each age class and $\circ$ denotes element-wise Hadamard multiplication. p_0 is the initiation probability. For a spreading patch, the next step would be represented as:

$$I_2 = (p_2 \circ A) I_2$$

And so on spreading to h + 1 patches:

$$I_{h+1} = (p_s \circ A) I_h = S I_h = S^h I_1$$

Where $S = p_s A$. The overall disturbance rate accumulating the spread over different disturbance sizes is:

$$D = \sum_{h=1}^{\infty} I_h$$

Where D is a vector by class. Figure 59 shows the performance of this approximation compared to an explicit simulation.

Dynamically Updating Adjacency and Fractional Areas

We then needed to make our representation able to update the A matrix in response to the new area of disturbance. We can update the fractional areas of each of the age classes by assuming a vector of fractional areas for each age class:

$$a_t = [a_0 \quad a_1 \quad \dots \quad a_{n-1} \quad a_n]$$

Then the new fractional areas for age 0 (the area that was disturbed) is:

$$a_{0,t+1} = \sum_{k=0}^{n} a_{k,t} D_{k,t}$$

And all other age classes is:

$$a_{k,t+1} = a_{k-1,t}(1 - D_{k-1,t})$$

Which modifies the remaining area of age class $a_{k,t+1}$ by the area disturbed in $a_{k-1,t}$. After updating the fractional areas, we needed to update the adjacency itself. For newly disturbed patches, we noted that the shapes of different disturbances matter. For example, in Figure 60 for the 4-pixel case, there are 5 different configurations which can have different self-adjacencies (e.g. square to straight line). This means that the tendency of a disturbance to spread more linearly can affect its adjacency to itself and other classes. In contrast, a core-spreading disturbance would be more self-adjacent and less adjacent to other classes. We account for the tendency of a disturbance to spread in specific shapes by including the ratio of internal-edges to total edges (Figure 60). Because the range of possible ratios grows as a function of size of the disturbance (number f pixels), we represent the adjacency of newly disturbed pixels as:

$$A_{00} = \frac{\sum_{size} I\,nt(size)p(size)}{\sum_{size} I\,nt(size)p(size) + \sum_{size} E\,xt(size)p(size)}$$

Or as a function of the probability of a size disturbance, and of the ratios of interior-total edges. There is a special case where disturbances can be adjacent to one another by chance. We correct our A_{00} values to account for this random chance with the equation:

$$\boldsymbol{A_{00} = \frac{\sum_{size} I\,nt(size)p(size) + \sum_{size} a_0\,Ext(size)p(size)}{\sum_{size} I\,nt(size)p(size) + \sum_{size} E\,xt(size)p(size)}}$$

Figure 61 refers to this corrected A_{00} value in the bottom right matrix. In the section *Comparison of Metrics to Data* we explore how the size distributions and interior-total ratios compare to observations of disturbances. Our final adjacency to update is the adjacency of non-disturbed patches. We make the simplifying assumption that the adjacency of each age class changes in proportion to that age class D_k. For disturbances adjacent to non-disturbances, we normalize by the overall disturbance area to get:

$$A_{0k,t+1} = \frac{D_{k-1}}{\sum D}(1 - A_{00,t+1})$$

For the adjacency of non-disturbed patches adjacent to other non-disturbed patches we use the equation:

$$\boldsymbol{A_{j,k,t+1} = A_{j-1,k-1,t}(1 - D_{j-1}/a_{j-1})}$$

Which takes into account the fractional area of the non-disturbed classes. Finally, the adjacency of non-disturbed classes to newly disturbed classes is:

$$\boldsymbol{A_{j,0,t+1} = 1 - \sum_{k=1} A_{j,k,t+1}}$$

Comparing Analytical method to Simulation

To test the performance of the analytical adjacency approximation, we compared the adjacency matrix predicted by this model to that generated by a fully spatial stochastic simulation, analogous to the one shown in the right column of Figure 60 but with a disturbance

initiation probability of 1% and a spread probability of 10%. In both the analytical model and stochastic simulation we initiated the landscape from bare ground (age = 0) and ran the model for 1000 years to reach a steady-state (Figure 60). Both models had the same structural features: patches within an age class tended to be more self-adjacent, but that self-adjacency decays geometrically with age; there is also a geometric decay along rows, but with greater adjacency above the diagonal. Numerically, the predicted adjacencies were also very similar, though with the analytical model slightly overpredicting $A_{0,0}$. Because so many of the other rates in the adjacency matrix decay from $A_{0,0}$, there are slight biases elsewhere. However, the error propagation from $A_{0,0}$ is consistent with the underlying structure for updating the matrix being correct, because it means that structural elements are preserved as the landscape ages.

This impact of errors in $A_{0,0}$ on the overall adjacency calculation was tested with a third model (Figure 61 bottom left), where the analytical model was run using the $A_{0,0}$ derived from the numerical simulation. Overall this model improved the overall pattern in the adjacency matrix, especially along the main diagonal. The remaining error (Figure 61 bottom right) is largely concentrated in two places. First, there is greater adjacency with the oldest 'absorbing' age class than observed in the simulation (left hand column). Second, because of this the bottom left corner (adjacency of old age classes to young classes) is a bit lower than observed. Matrix rows have a sum-to-one constraint, so some of these errors are inevitable compensating errors. It is also worth noting that in adjusting $A_{0,0}$ directly we are not adjusting the underlying terms used to calculate $A_{0,0}$ (I, D, a), which are also used in update the rest of A, meaning this test is not strictly internally consistent. An open question is how much of the remaining error in the adjacency matrix updating is in the underlying analytical simulation of disturbance spread (I, D, a) versus approximations in the updating of A.

Comparison of Metrics to Data

Our Kolmogorov–Smirnov pairwise comparison of disturbance type size distributions found that the majority of disturbance types had significantly distinct distributions ($p << 0.001$) (Figure 62). The three exceptions were clearcut, wildland fire, and harvest, which had non-significant differences with roughly half of the disturbance classes. Finally, mastication had no significant difference between wildfire or chemical. The size distributions of disturbances in Florida and Oregon were significantly different, as well as the two ecoregions nested within Oregon ($p < 0.001$). The two ecoregions size distributions nested within Florida were not found to be significantly different. However, in other size distributions significant differences were found despite visual similarity in part due to large sample sizes (Table 18). The size distributions have a large range in sample sizes. US state-level size distributions were based on very large sample sizes (Oregon N = 27137, Florida N = 20329). Disturbance sample sizes range from harvest with N = 22 to unknown N = 34560. Unknown disturbances accounted for the majority of disturbance events in the overall dataset, and a large proportion of the area (20%). All four ecoregions had a similarly shaped size distribution, with peaks at single-pixel (0.09 ha) disturbances and at 7 ha disturbances. The 7 ha peak aligns with disturbance peaks in the disturbance categories unknown, thinning, wildland fire, mixed, harvest and wildfire (Figure 62).

Disturbance plots show more varied patterns; wildfire and prescribed fire distributions have long tails, reflecting the influence of rare but large disturbances. In contrast, thinning and mastication have distinct peaks and sharper drop-offs, suggesting more standardized anthropogenic disturbances and smaller sizes. Mixed disturbance has the longest tail, and no peak at small disturbances.

We found a significant effect of US state ($p < 0.001$) and ecoregion nested within state ($p < 0.01$). Oregon had a wider range of interior ratios, with a higher occurrence of linear disturbances than Florida (Figure 63). Within Oregon, small disturbances were more compact in Marine West Coast forests than in the Western Cordillera small disturbances, but this relationship crosses, such that Marine West Coast disturbances were less round at large disturbance sizes. The curves fit for the two ecoregions in Florida are nearly identical (Figure 63). Despite visual similarity, the two ecoregion curves were found to be significantly different even when compared to just a Florida curve model.

In our second hierarchy, there was a significant effect of disturbance type ($p < 0.0001$), but not US state nested within disturbance ($p > 0.1$). Herbicide is the most distinctively linear, followed by other mechanical, and then unknown. Fire disturbance types (prescribed and wildfire) were closer to the maximum interior ratio curve, suggesting that fires tended to be compact and burned pixels were predominantly adjacent to other burned pixels (Figure 64). Disturbance-level curves show that prescribed fires are less compact at smaller sizes and larger sizes than natural fires, but at the most frequent size are similarly shaped. Thinning resembles other compact disturbances, but begins to become more linear at large sizes relative to wildfire. Clearcut follows a similarly compact pattern to wildfire.

We developed a method for taking spreading disturbances and modeling them in a spatially implicit way. In the paper we derived a way to represent spreading disturbances, which performed well against a stochastic simulation (Figure 59). Our derivation suggested that size distributions and ratio of interior to total edges captured how a specific disturbance spread. We were able to use these two sources of information to distinguish between the disturbance regimes of Florida and Oregon (Figures 62, 63), and to distinguish between different disturbance metrics (Figures 62, 64). Florida is influenced by small and large disturbances, and fewer mid-sized disturbances than Oregon. Anthropogenic disturbances tend to spread with different ratios than natural disturbances. This work will allow us to combine ED2 outputs and our current understanding of cogongrass' effect on fires (objective 4D).

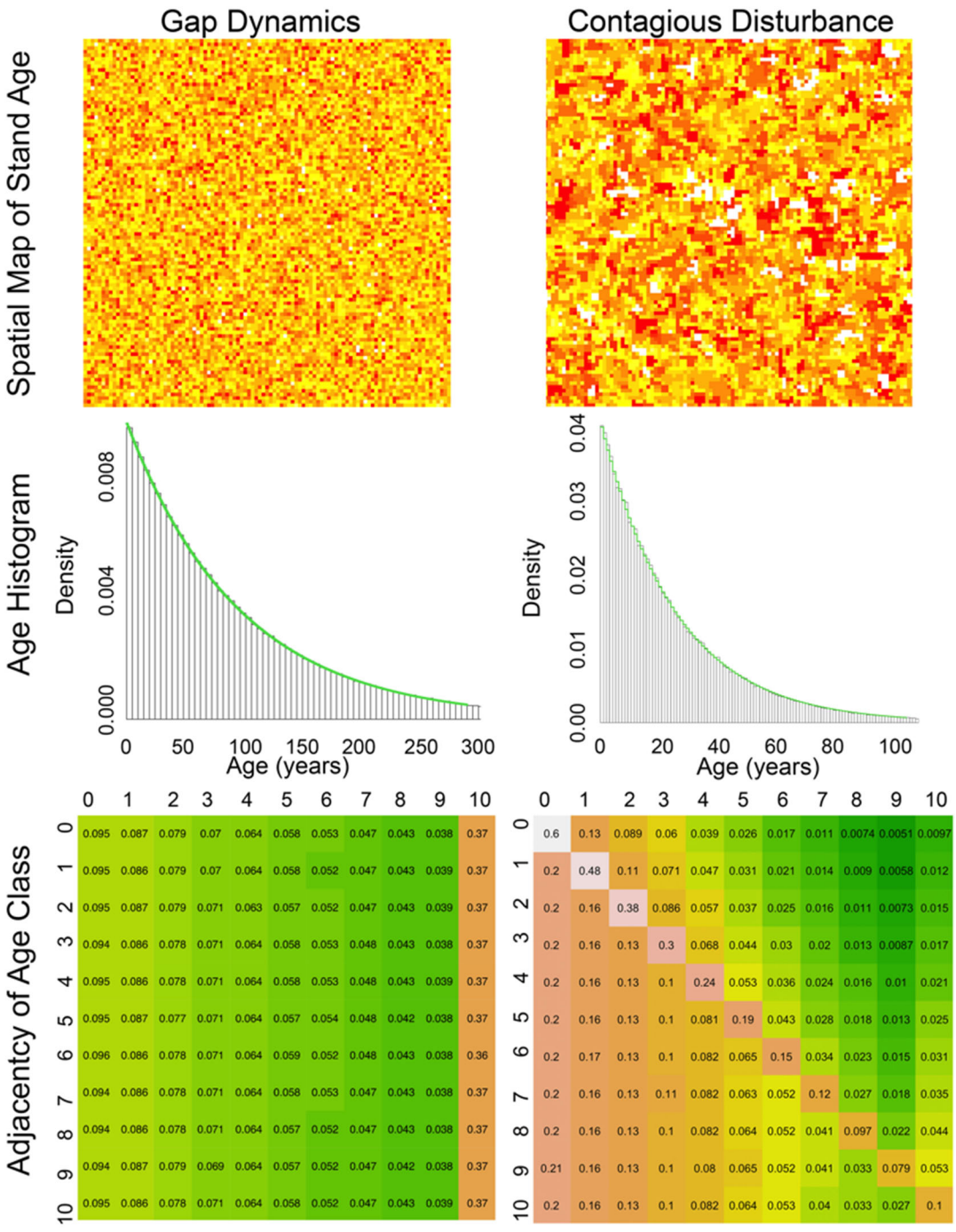

Figure 58. Comparison of Gap dynamics Contagious disturbance simulation. (Left column) Gap dynamic simulation. (Right column) Contagious disturbance simulation. (Top left) spatial map of stand age, with color on a log scale from youngest (red) to oldest (yellow), (Top right) spatial map of stand age for contagious disturbance, with color on a log scale from young (red) to old (yellow) and with new disturbances (age = 0) in white. (Middle left) simulated stand age distribution (black) when disturbance probability is 1% compared to geometric expectation (green), (Middle right) simulated stand age distribution (black) when disturbance probability is 1% and

spread probability is 25% compared to geometric expectation (green), (Bottom) spatial adjacency matrix by age class aggregated into 10 year bins ([0 − 9] = 0, [10 − 19] = 1, etc.) with all patches 100 year or older in bin 10. Matrices are colored from white (highest adjacency) through orange to green (lowest adjacency).

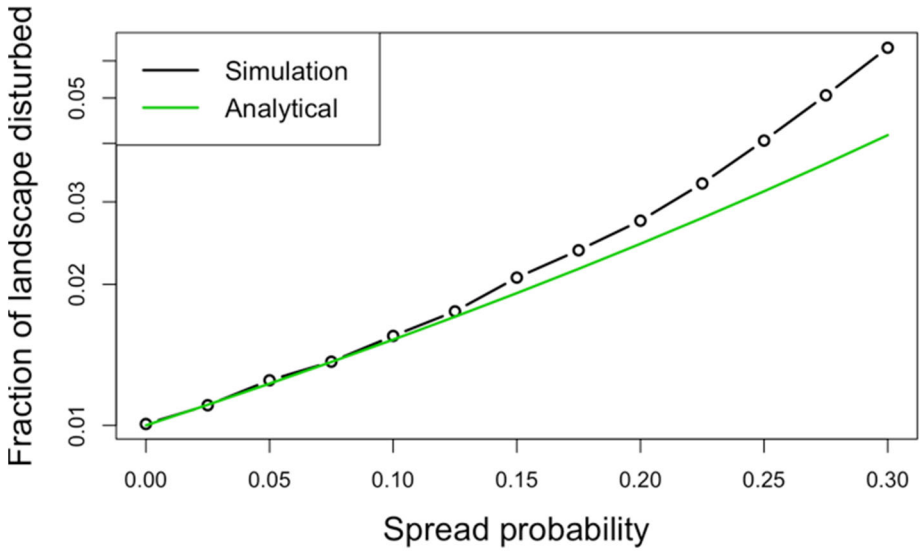

Figure 59. Validation of the analytical model's ability to predict disturbance area as a function of spread probability (disturbance initiation probability of 1%). Simulations run on a 4-sided grid so, for example, a 0.25 spread probability corresponds to four independent chances, each 25%, to spread. The analytical approximation appears to underestimate disturbance at high spread probabilities.

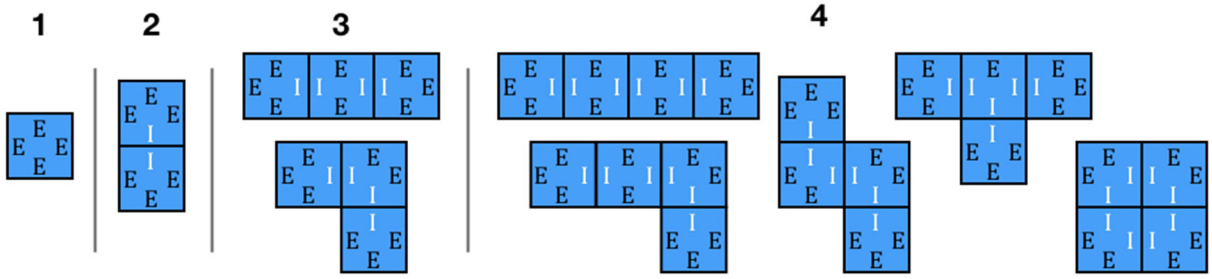

Figure 60. Adjacency for small disturbances. Edges are labeled as (E)xterior and (I)interior. For size 1, there is 0 probability of self-adjacency (disturbed patches adjacent to other disturbed patches). For size 2 and 3 it is 1/4 and 1/3 respectively, while for size 4 the adjacency is either 1/2 (square configuration) or 3/8 (all other configurations).

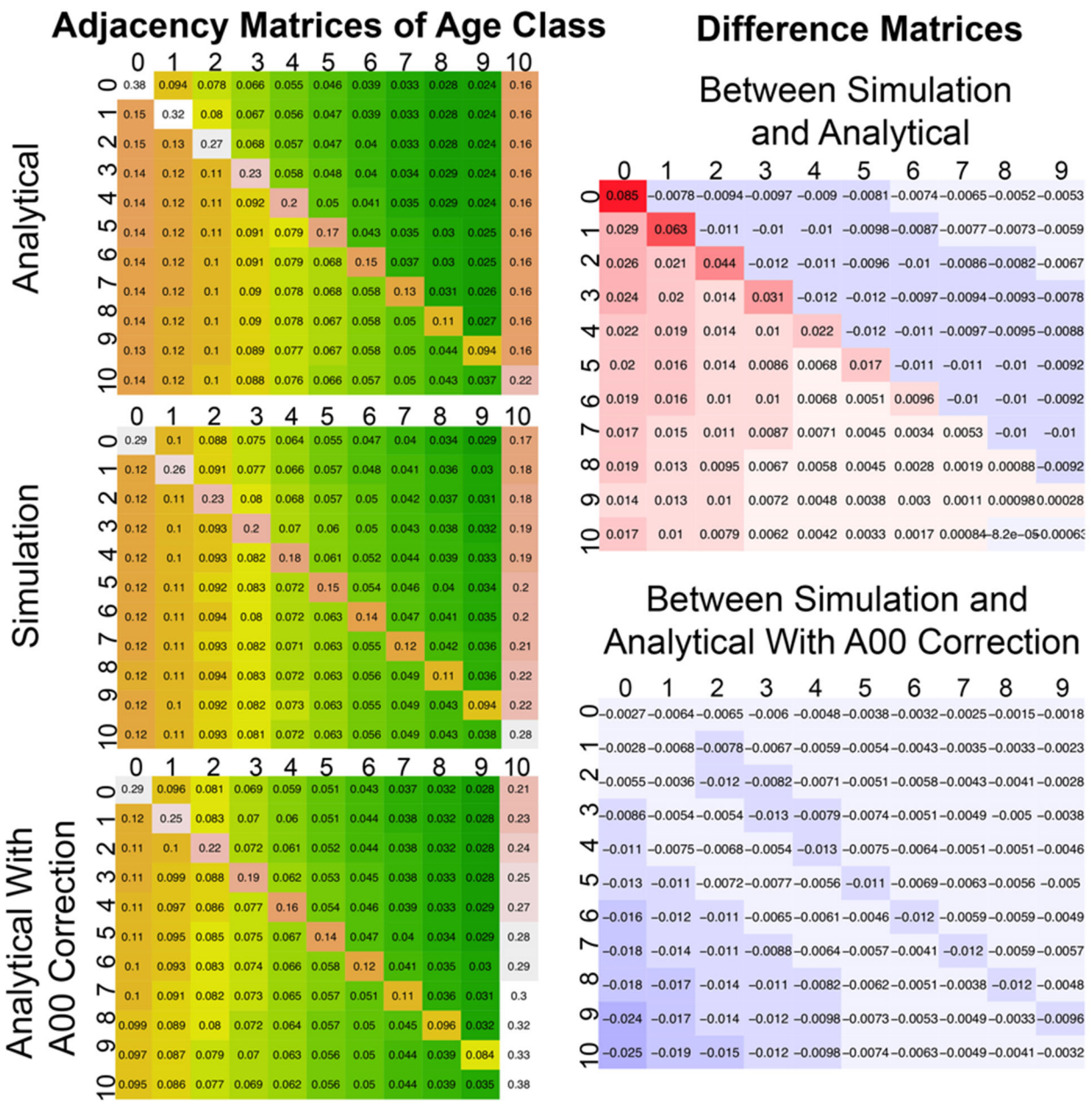

Figure 61. Comparison between adjacency matrices for a stochastic spatial simulation analytical approximation (top), and analytical approximation where a correction was applied to A00. All adjacency matrices are after 1,000 years (steady state). To the right are difference matrices between the simulation matrix and the two analytical matrices. Age class aggregated into 10 year bins ([0 − 9] = 0, [10 − 19] = 1, etc.) with all patches 100 year or older in bin 10. The 10th column of the error matrices was removed because of a summing to 1 constraint.

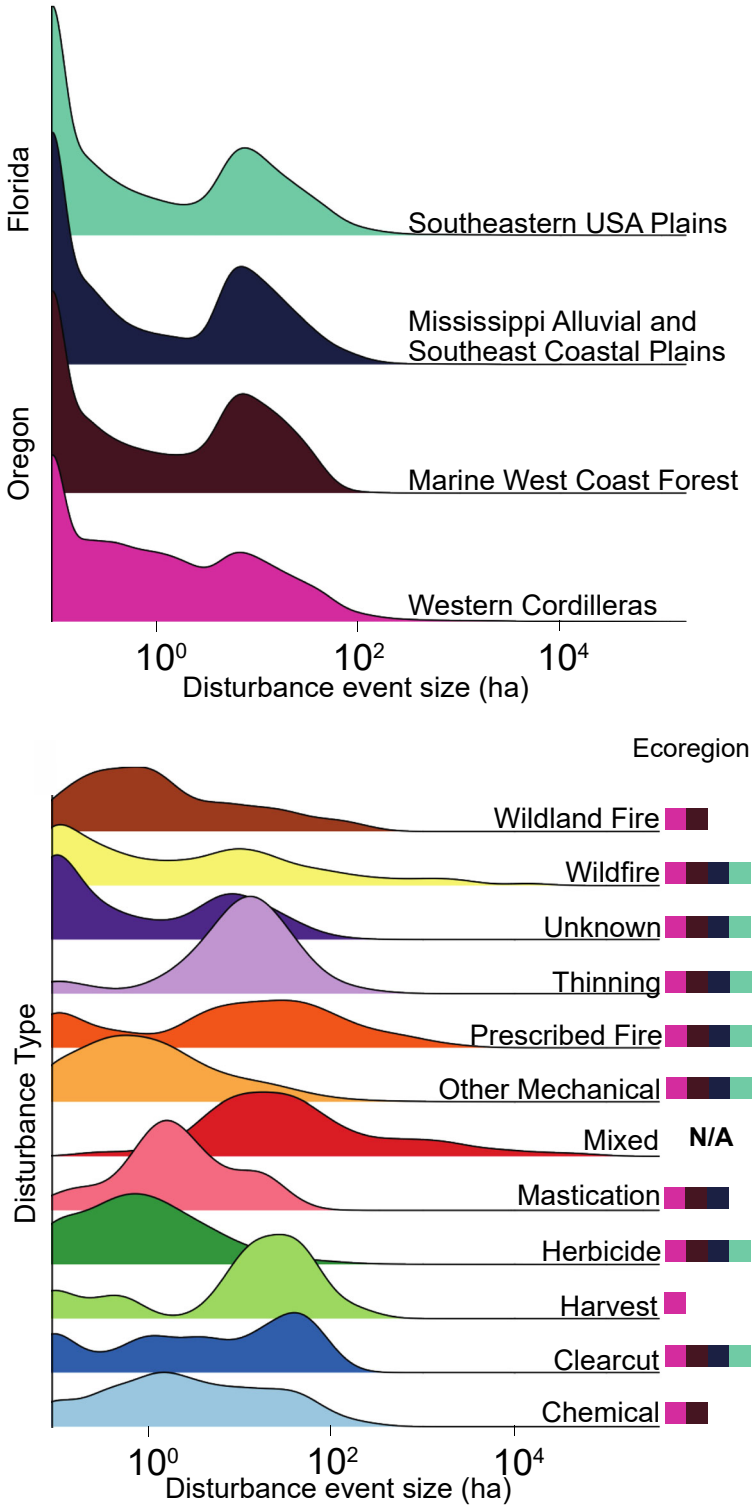

Figure 62. Size density plots showing the contrasts between ecoregion/state and disturbance type. Colored boxes next to disturbance size density curves show what ecoregion contains the respective disturbance. Sample sizes associated with density plots can be found in Table 18.

Table 18: Sample sizes of states, ecoregions, and disturbance mechanisms.

	Percent Event	Percent Area	Number of Events
Unknown	7.3e-01	2.0e-01	34560
Prescribed Fire	1.0e-02	3.6e-02	483
Clearcut	8.0e-04	5.9e-04	38
Thinning	1.3e-02	1.1e-02	623
Other Mechanical	7.5e-02	3.0e-02	3546
Herbicide	9.8e-02	9.3e-02	4655
Wildfire	6.6e-03	6.0e-02	315
Mastication	1.6e-03	3.2e-04	77
Wildland Fire	2.6e-03	1.3e-03	125
Chemical	5.2e-03	3.1e-03	246
Biological	8.4e-05	5.0e-05	4
Harvest	4.6e-04	5.5e-04	22
Disease	1.3e-04	2.0e-04	6
Mixed	1.2e-02	5.6e-01	582
Florida	4.3e-01	2.1e-01	20329
Southeastern USA Plains	1.8e-01	5.9e-02	8618
Southeast Coastal Plains	2.5e-01	1.5e-01	11711
Oregon	5.7e-01	7.9e-01	27137
Western Cordilleras	4.2e-01	7.6e-01	19852
Marine West Coast Forest	1.5e-01	3.6e-02	7285

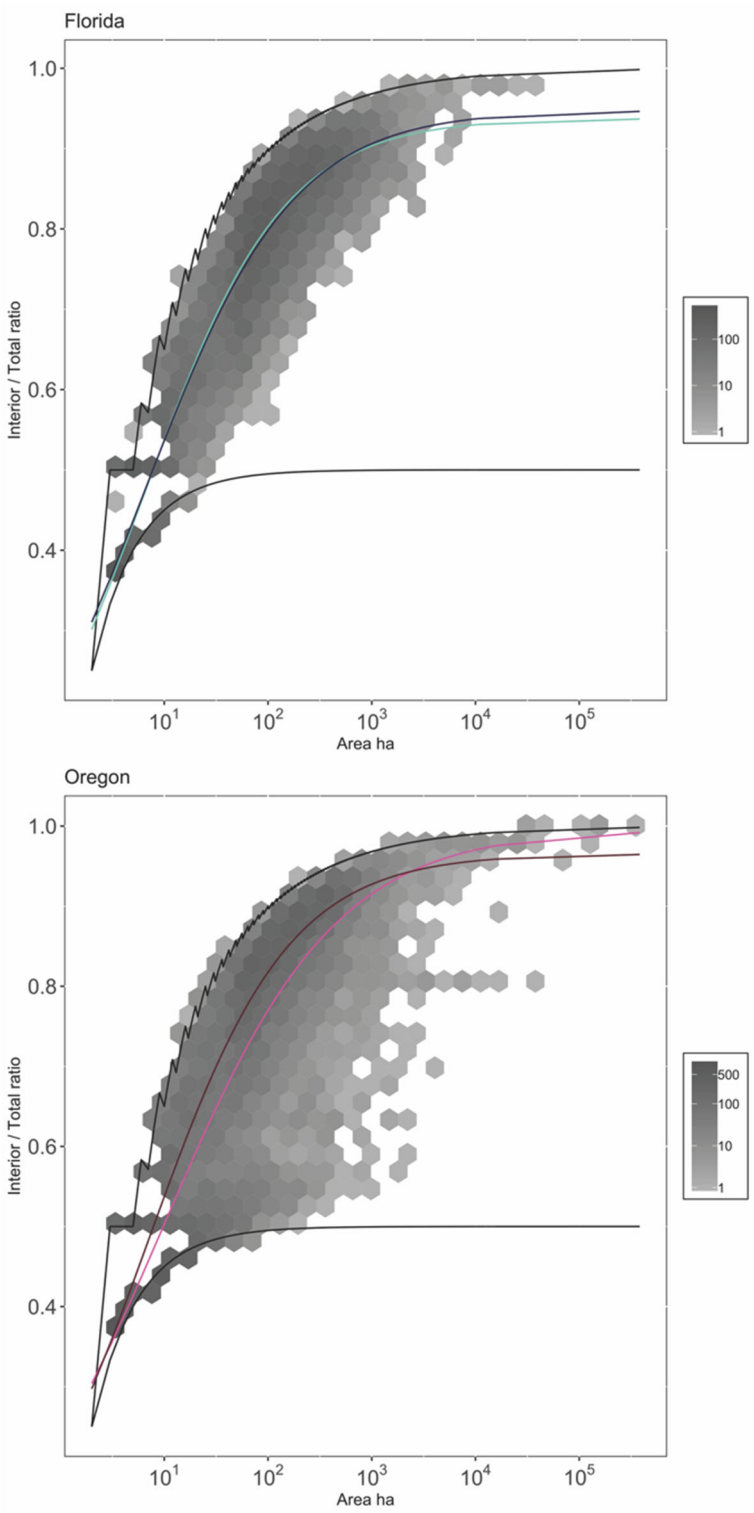

Figure 63. Mean trends of Ecoregion within State. Gray hexes correspond to binned-counts of number of disturbance events. Black lines correspond to core and linear bounding cases.

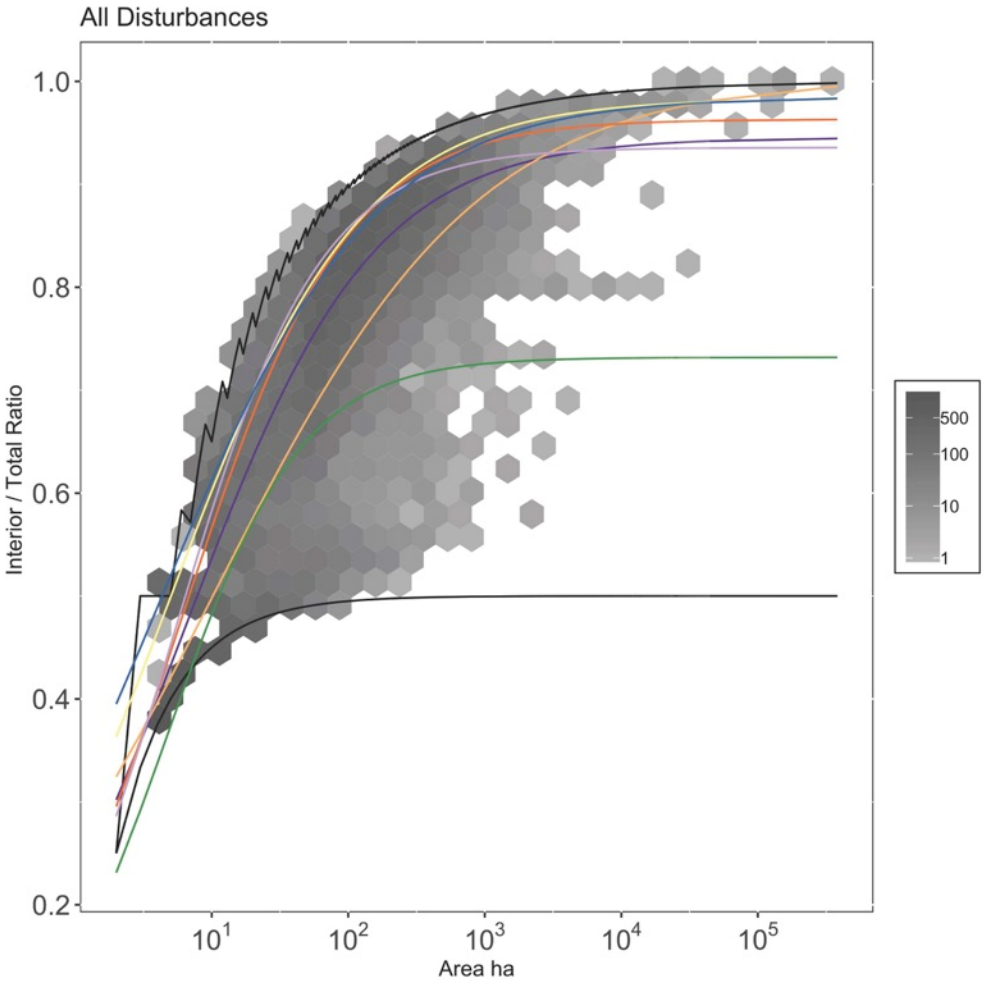

Figure 64. Mean trends of disturbance type. Gray hexes correspond to binned-counts of number of disturbance events. Black lines correspond to linear bounding cases.

PART 5: DECISION SUPPORT TOOL

TECHNICAL APPROACH

A final objective of our study is to synthesize our findings into a Decision Support Tool (DST) tailored to the needs of our partner installations (Figure 1, Table 1). A number of DSTs exist already pertaining to the implementation of prescribed fire, such as: FARSITE (Finney, 2004), SPITFIRE (Thonicke et al., 2010), First Order Fire Effects model (Hood & Lutes, 2017), FFI (Lutes et al., 2009), Interagency Fuels Treatment Decision Support System (Wells et al., 2009). However, these management decisions often are made in isolation from decisions concerning efforts to control plant invasions or mitigate tick-borne disease risk, for which there are no established DSTs at present to our knowledge. Therefore, we initiated development of a DST designed to integrate across multiple environmental management decisions in an effort to promote more holistic management practices better able to account for interacting environmental variables and multiple management objectives.

Structured Interviews with Installation Decisionmakers

To better understand installation needs for decision support surrounding tick-borne disease, invasive species, and fire, and how these fit into forest management goals more broadly, we designed interviews and reached out to contacts at DoD installations via email and phone. Within the nine participating DoD installations, we targeted six installations where we had established contacts from field sampling (therefore, Tyndall AFB, Moody AFB, and Camp Shelby were not included). We successfully completed 30-min structured interviews with a representative from five of the installations (Avon Park AFR, Camp Blanding, Eglin AFB, Fort Jackson, and Fort Benning), while the sixth was unavailable for an interview. Interviews were loosely organized around a script that included broad questions on the installation's decision-making process, and specific questions about how the installation could use data from our project (Appendix B1). Responses were recorded for reference. These responses highlighted what aspects of this project installation managers valued, how installation managers envisioned using a DST, and potential challenges and opportunities associated with DST implementations. Findings from these interviews allow us to tailor the design of our DST to shared priorities across installations.

This project was reviewed by the Boston University Institutional Review Board (IRB) and was determined to not meet the definition of human subject research and therefore did not require further IRB review and approval (Appendix B2).

R Shiny Web Application

We elected to build our DST as a R Shiny web application (Chang et al., 2019; R Core Team, 2019), because 1) most of the underlying analyses performed for this project were conducted in R making for straight-forward harmonization of data, and 2) R Shiny is user-friendly and yet can perform complex data visualizations. We chose a web application because they are more intuitive to use by non-experts, can be updated with new data and features, and are not tied to specific software requirements. PINEMAP, a research project that focused on the restoration of the same southeastern longleaf pine ecosystems in which we performed this research, had success implementing their decision support system as a web application (T. A. Martin, 2019).

RESULTS AND DISCUSSION

Structured Interviews with Installation Managers

Interviews with installation managers revealed that while most installations have similar goals, how those goals are prioritized varied by installation. Overall, common natural resource management goals were: accommodate military training, wildfire risk reduction, habitat and species conservation, and silviculture. All of the installations relied on prescribed fire as a primary management strategy, and managers structured burn schedules to maintain a frequent fire-return interval for priority areas. Most interviewees characterized conservation, silviculture, and reduction of wildfire risk as long-term goals, with evaluations happening at yearly, five-year, decadal and multidecadal timescales. Several spoke about multidecadal changes in Red Cockaded Woodpecker populations, pine populations (particularly longleaf pine), and anticipated changes to forest composition in the future. In general, when asked about investment in major themes of our project - ticks, invasive species, and climate projections - managers typically indicated they would value each theme based on how closely it mapped onto these central priorities (training, wildfire, conservation, silviculture).

However, there was quite a bit of variation among managers in how they weighed these priorities. For example, not all installations interacted with military training in the same way. At some installations military training and ground exercises dictated the day-to-day scheduling of prescribed burns. One interviewee suggested that a DST would only be useful if it incorporated military training activity. Some installation managers characterized military training as important but happening in parallel with natural resource management. One interviewee said that military training was largely independent from natural resource management. Of the installations that worked closely with military training personnel, interviewees said that military-motivated burns took priority unless there was a safety issue that needed to be addressed. One interviewee provided an example where conservation goals outweighed military goals: the military was considering clear-cutting a stand of longleaf pines to create a site to simulate desert conditions, and the natural resource team countered that the time it would take to regrow the longleaf population offset the gains of a new training site. However, this example was described as rare. On the whole, each installation shaped its long-term thinking around a varied military presence. Another source of contrast was how each installation handled management of invasive plant species. All of the installation managers considered invasive species a management problem, and that controlling them was essential to their conservation goals. Our questions focused on cogongrass, but it was by no means the only invasive species that installations were grappling with – or even the most difficult species to eliminate. Two other species mentioned as difficult to control were Japanese climbing fern (*Lygodium japonicum*) and kudzu (*Pueraria montana*). Some installation managers were optimistic about their successful control of cogongrass. As one interviewee stated, “Our longest running feud has been with cogongrass … and we are doing fairly well. We finally turned a corner”. However, others felt that it was a “losing battle” and that even if our project offered an insight into cogongrass control, they were “already at capacity” on cogongrass control, and would struggle to implement additional changes. Not all the installation managers we spoke to had cogongrass invasions, but all were monitoring for it. One interviewee said that our project could be a useful way to anticipate the effects of cogongrass when it reached their installation. Installations actively controlling cogongrass used for control methods some combination of burning and herbicides, and sometimes physical management techniques.

Installation managers agreed that data on tick populations and tick-borne pathogens were useful. 4 out of 5 of interviewees listed it as the most valuable topic our project covered. Most said that monitoring tick populations and pathogens would be helpful for the safety of their staff or the safety of installation personnel. As one interviewee stated, “To me, tick-borne disease is not a management goal but a health and safety goal”. One interviewee suggested that connecting invasive species to health outcomes like tick-borne diseases could better motivate invasive plant control. Most managers felt that prescribed burns were effective at controlling tick populations, but were still concerned about tick bites originating from infrequently burned areas, and about the illnesses associated with tick bites. Only one interviewee listed tick research as low-priority, citing the efficacy of permethrin-treated uniforms.

Climate projections were considered valuable when they were able to extend understanding of other important datasets into the future, but were considered lower-priority than other aspects of the project by 4 out of 5 interviewees. One interviewee listed it as most important, because they could inform demographic shifts in the forests over time. This interviewee was also interested in using climate projections to inform tree planting decisions, and ensuring that trees planted today would be able to tolerate future climates.

While many of our interview questions focused on the content of a DST from this project, we also asked about what forms of implementation would be effective. We learned that two installations already use a DST or ecosystem modeling in their planning. For example, Fort Benning uses a combination of monitoring plots and LANDIS-II modeling (K. L. Martin et al., 2015), and Eglin AFB uses a burn prioritization model that is maintained by a GIS specialist (Hiers et al., 2003). In general, GIS was the type of software most installations utilized. That said, two interviewees warned against designing a tool that required a specific operating system to run, or that needed to be run locally on a computer. This sentiment was echoed by others who explained that a variety of common software isn’t approved for use on installation computers, and that even approved software can be difficult to maintain locally because of access restrictions. One interviewee offered online tools, specifically QGIS, as a solution. One manager also cautioned that time-limited personnel may be slow to adopt a new tool, but suggested that an installation-specific demonstration could help.

Taken together, these conversations highlight that while the mechanics of management at each installation are different, all of the installations have similar objectives, challenges, and interests. We learned that installations differ enough in their on-the-ground operations that even with perfect information, it would be challenging to design a tool that met the everyday logistical needs of each installation. However, we also learned what information would be valuable for broad decision-making. Managers expressed interest in connecting management decisions to health of personnel, TBD risk monitoring, insights into cogongrass invasion prevention and quantifying cogongrass effects, and forest demographic changes. Existing DSTs used by installations offer concrete examples to draw from and complement. Finally, we were reassured that a web-based DST was the best method to host and share our findings. These insights will help us shape the features and dissemination of our DST.

Decision Support Tool

Our DST prototype contains an interactive map of tick-borne disease risk as estimated by tick population sampling (Part 1) and pathogen analysis (Part 3). It depicts three different estimates of TBD exposure risk based upon 1) tick abundance, 2) pathogen prevalence, and 3)

the product of tick abundance and pathogen prevalence, which is our best overall estimate of TBD exposure risk. Our site is live and available at: https://serdp2636.shinyapps.io/serdp2636/.

Decision Support Tool Documentation and Installation

Our DST may change as we receive feedback from partners. The most recent documentation for our DST is available at:
https://github.com/mccabete/SERDP_shiny/blob/main/README.md and examples for how to use the Decision Support Tool at the wiki page:
https://github.com/mccabete/SERDP_shiny/wiki.

Our tool requires an internet browser to access, and no other software to run. Graphics can appear differently depending on the browser. Data downloaded from our tool may require software to be opened or edited. We provide the options to download .csv files and .pdf files. The underlying code that generates the app is at:
https://github.com/mccabete/SERDP_shiny/tree/main/code

Decision Support Tool Feature Summary

Tick-Borne Disease

Disease Risk Map: Map of Tick-Borne Disease risk (Risk of pathogen exposure per 24 hours), Tick abundance, and Pathogen prevalence at each of the DoD installations. Data available for download.

Tick Pathogens: Searchable & downloadable database of pathogens that were detected at each base, and a key to diseases the pathogens cause.

Tick Hosts: Searchable & downloadable database of number of animal hosts detected at each installation.

Vegetation

Litter: Summary figures of litter depth and percent cover per installation. Data available for download.

Canopy cover: Summary of figures of percent canopy cover per installation. Data available for download.

Exploring Hypotheticals

Project Tick Populations: Project tick populations with new fire regimes, levels of vegetation biomass, canopy cover, and leaf litter. Figures available for download.

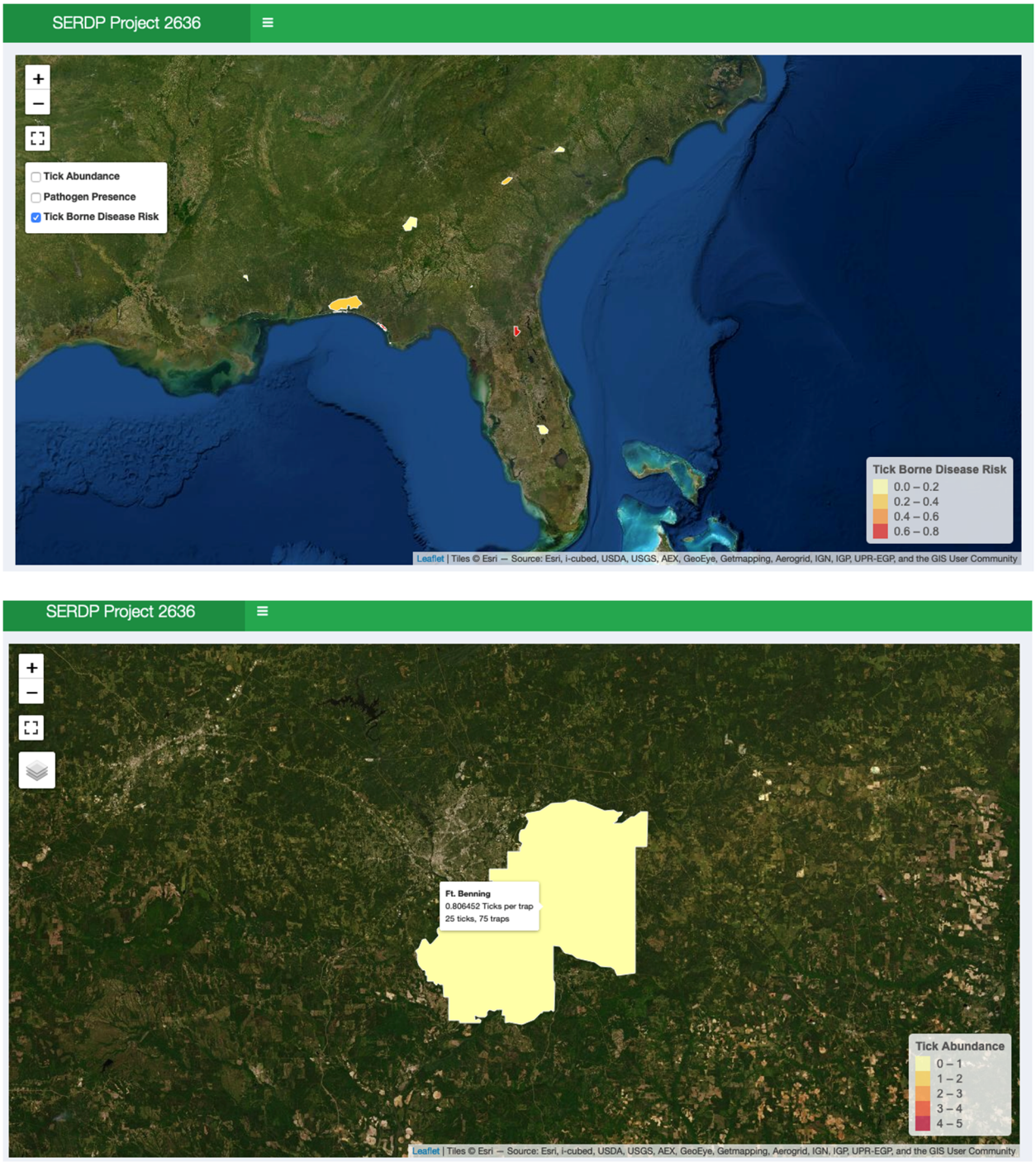

Figure 65. Two sample screenshots from decision support tool prototype. Data shown come from tick sampling and pathogen analyses from earlier sections. Prototype is hosted at https://serdp2636.shinyapps.io/serdp2636/

Literature Cited

(6400-09 Soil CO2 Flux Chamber Instruction Manual). 2003. 6400-09 Soil CO2 Flux Chamber Instruction Manual.

Abatzoglou, J. T., A. P. Williams, L. Boschetti, M. Zubkova, and C. A. Kolden. 2018. Global patterns of interannual climate-fire relationships. Global Change Biology.

Abramoff, R. Z., and A. C. Finzi. 2016. Seasonality and partitioning of Root allocation to rhizosphere soils in a midlatitude forest. Ecosphere. 7.

Adalsteinsson, S. A., V. D'Amico, W. G. Shriver, D. Brisson, and J. J. Buler. 2016. Scale-dependent effects of nonnative plant invasion on host-seeking tick abundance. Ecosphere. 7.

Ainsworth, E. A., and S. P. Long. 2004. What have we learned from 15 years of free-air CO2 enrichment (FACE)? A meta-analytic review of the responses of photosynthesis, canopy properties and plant production to rising CO2. New Phytologist. 165: 351–372.

Ainsworth, E. A., and A. Rogers. 2007. The response of photosynthesis and stomatal conductance to rising [CO2]: mechanisms and environmental interactions. Plant, Cell & Environment. 30: 258–270.

Alba, C., J. E. NeSmith, C. Fahey, C. Angelini, and S. L. Flory. 2017. Methods to test the interactive effects of drought and plant invasion on ecosystem structure and function using complementary common garden and field experiments. Ecology and Evolution. 7: 1442–1452.

Allan, S.A., L.A. Simmons and M.J. Burridge. 2001. Ixodid ticks on white-tailed deer and feral swine in Florida. Journal of Vector Ecology 26(1): 93-102.

Allan, B.F. 2009. Influence of prescribed burns on the abundance of Amblyomma americanum (Acari: Ixodidae) in the Missouri Ozarks. Journal of Medical Entomology 46:1030-1036.

Allan, B.F., H.P. Dutra, L.S. Goessling, K. Barnett, J.M. Chase, R.J. Marquis, G.C. Pang, G.A. Storch, R.E. Thach and J.L. Orrock. 2010a. Invasive honeysuckle eradication reduces tick-borne disease risk by altering host dynamics. Proceedings of the National Academy of Sciences 107:18523-18527.

Allan, B.F., L.S. Goessling, G.A. Storch and R.E. Thach. 2010b. Blood meal analysis to identify reservoir hosts for *Amblyomma americanum* ticks. Emerging Infectious Diseases 16: 433-440.

Anderson, H. E. 1982. Aids to determining fuel models for estimating fire behavior (No. INT-GTR-122). Ogden, UT: U.S. Department of Agriculture, Forest Service, Intermountain

Forest and Range Experiment Station. Retrieved from https://www.fs.usda.gov/treesearch/pubs/6447

Andrews, S. (2010). FastQC: a quality control tool for high throughput sequence data.

Berggoetz, M., M. Schmida, D. Stona, V. Wyssa, C. Chevillonb, A.-M. Pretoriusc, L. Gern. 2014. Tick-borne pathogens in the blood of wild and domestic ungulates in South Africa: interplay of game and livestock. Ticks & Tick-Borne Diseases 5: 166–175.

Bigelow, S.W., Whelan, A.W., 2019. Longleaf pine proximity effects on air temperatures and hardwood top-kill from prescribed fire. Fire Ecol. 15, 27.

Bloemer, S. R., E. L. Snoddy, J. C. Cooney, and K. Fairbanks. 1986. Influence of Deer Exclusion on Populations of Lone Star Ticks and American Dog Ticks (Acari: Ixodidae). Journal of Economic Entomology. 79: 679–683.

Bolger, A. M., Lohse, M., & Usadel, B. 2014. Trimmomatic: a flexible trimmer for Illumina sequence data. *Bioinformatics*, 30: 2114-2120.

Bova, A. S., and M. B. Dickinson. 2008. Beyond "fire temperatures": calibrating thermocouple probes and modeling their response to surface fires in hardwood fuels. Canadian Journal of Forest Research. 38: 1008–1020.

Bowman, D. M. J. S., C. Haverkamp, K. D. Rann, and L. D. Prior. 2017. Differential demographic filtering by surface fires: How fuel type and fuel load affect sapling mortality of an obligate seeder savanna tree. Journal of Ecology. 1–13.

Boyer, W. D. 1990. Pinus palustris Mill. Silvics of North America. 1: 405–412.

Bradley, B. A., D. S. Wilcove, and M. Oppenheimer. 2010. Climate change increases risk of plant invasion in the Eastern United States. Biol Invasions. 12: 1855–1872.

Brewer, S. 2008. Declines in plant species richness and endemic plant species in longleaf pine savannas invaded by Imperata cylindrica.

Brockway, D.G., Lewis, C.E., 1997. Long-term effects of dormant-season prescribed fire on plant community diversity, structure and productivity in a longleaf pine wiregrass ecosystem. For. Ecol. Manag. 96, 167–183.

Brodribb, T. J., D. Bienaimé, and P. Marmottant. 2016. Revealing catastrophic failure of leaf networks under stress. Proceedings of the National Academy of Sciences of the United States of America. 113: 4865–4869.

Brooks, M.L., D'Antonio, C.M., Richardson, D.M., Grace, J.B., Keeley, J.E., DiTomaso, J.M., Hobbs, R.J., Pellant, M., Pyke, D., 2004. Effects of invasive alien plants on fire regimes. Bioscience 54, 677–688.

Brose, P., Wade, D., 2002. Potential fire behavior in pine flatwood forests following three different fuel reduction techniques. For. Ecol. Manag. 163, 71–84.

Burger, N., & Bond, W. J. 2015. Flammability traits of Cape shrubland species with different post-fire recruitment strategies. *South African Journal of Botany*, 101: 40–48.

Bryson, C.T., Carter, R., 1993. Cogongrass, *Imperata cylindrica*, in the United States. Weed Technol. 7, 1005–1009.

Cabrera, S., D. Hiatt, W. W. Dillon, T. Clark, B. F. Allan, and S. L. Flory. 2021. Observations of Wild Turkey Nesting in Invasive Cogongrass. sena. 20: N42.

Chang, W., Cheng, J., Allair, J., Xie, Y., & McPherson, J. 2019. *shiny: Web Application Framework for R* (R package version 1.4.0) [Computer software]. https://CRAN.R-project.org/package=shiny

Chapman, H. H. 1932. Is the Longleaf Type a Climax? Ecology. 13: 328–334.

Childs, J.E., and C.D. Paddock. 2003. The ascendancy of *Amblyomma americanum* as a vector of pathogens affecting humans in the United States. Annual Review of Entomology 48: 307-37.

Christensen, N. L. 1981. Fire regimes in southeastern ecosystems, pp. 112–136. *In* Fire Regimes and Ecosystem Properties.

Civitello, D. J., S. L. Flory, and K. Clay. 2008. Exotic Grass Invasion Reduces Survival of Amblyomma americanum and Dermacentor variabilis Ticks (Acari: Ixodidae). JOURNAL OF MEDICAL ENTOMOLOGY. 45: 6.

Cottingham, K.L., Lennon, J.T., Brown, B.L., Frontiers, S., Apr, N., Cottingham, L., Lennon, J.T., Brown, L., 2015. Knowing When to Draw the Line: Designing More Informative Ecological Experiments Published by: Ecological Society of America 3, 145–152.

Cowdery, E., Meunier, F., Xu, X., Dietze, M. C. 2018. The Downside of Detail: Quantifying the Uncertainty Surrounding the Implementation of a Mechanistic Plant Hydraulic Module in a Dynamic Vegetation Model. Annual Meeting of American Geophysical Union. Poster Presentation. Washington, District of Columbia.

Cribari-Neto, F., and A. Zeileis. 2010. Beta Regression in R. Journal of Statistical Software. 34: 1–24.

Cronan, J.B., Wright, C.S., Petrova, M., 2015. Effects of dormant and growing season burning on surface fuels and potential fire behavior in northern Florida longleaf pine (*Pinus palustris*) flatwoods. For. Ecol. Manag. 354, 318–333.

Cruz, M. G., and P. M. Fernandes. 2008. Development of fuel models for fire behaviour prediction in maritime pine (Pinus pinaster Ait.) stands. Int. J. Wildland Fire. 17: 194–204.

Daneshgar, P., Jose, S., Collins, A., Ramsey, C., 2008. Cogongrass (*Imperata cylindrica*), an alien invasive grass, reduces survival and productivity of an establishing pine forest. For. Sci. 54, 579–587.

Davidson, W. R., D. A. Siefken, and L. H. Creekmore. 1994a. Seasonal and annual abundance of *Amblyomma americanum* (Acari: Ixodidae) in central Georgia. Journal of medical entomology. 31: 67–71.

Davidson, W. R., Siefken, D. A., & Creekmore, L. H. 1994b. Influence of annual and biennial prescribed burning during March on the abundance of Amblyomma americanum (Acari: Ixodidae) in central Georgia. *Journal of medical entomology*, 31: 72-81.

DeBano, L. F., DeBano, L. F., Neary, D. G., Ffolliott, P. F., 1998. *Fire effects on ecosystems*. John Wiley & Sons.

Dell, J.E., Richards, L.A., O'Brien, J.J., Loudermilk, E.L., Hudak, A.T., Pokswinski, S.M., Bright, B.C., Hiers, J.K., Williams, B.W., Dyer, L.A., 2017. Overstory-derived surface fuels mediate plant species diversity in frequently burned longleaf pine forests. Ecosphere 8, e01964.

Demma, L.J., R.C. Holman, J.H. McQuiston, J.W. Krebs and D.L. Swerdlow. 2005. Epidemiology of Human Ehrlichiosis and Anaplasmosis in the United States, 2001-2002. American Journal of Tropical Medicine and Hygiene 73:400-9.

Dickinson, M.B., Johnson, E.A., 2004. Temperature-dependent rate models of vascular cambium cell mortality. Can. J. For. Res. 34, 546–559.

Driscoll, D.A., Lindenmayer, D.B., Bennett, A.F., Bode, M., Bradstock, R.A., Cary, G.J., Clarke, M.F., Dexter, N., Fensham, R., Friend, G., Gill, M., James, S., Kay, G., Keith, D.A., MacGregor, C., Russell-Smith, J., Salt, D., Watson James, J.E.M., Williams Richard J., R.J., York, A., 2010. Fire management for biodiversity conservation: Key research questions and our capacity to answer them. Biol. Conserv. 143, 1928–1939.

Eisen, R. J., L. Eisen, and C. B. Beard. 2016. County-Scale Distribution of Ixodes scapularis and Ixodes pacificus (Acari: Ixodidae) in the Continental United States. Journal of Medical Entomology. 53: 349–386.

Elias, S. P., C. B. Lubelczyk, P. W. Rand, E. H. Lacombe, M. S. Holman, and R. P. Smith. 2006. Deer Browse Resistant Exotic-Invasive Understory: An Indicator of Elevated Human Risk of Exposure to Ixodes scapularis (Acari: Ixodidae) in Southern Coastal Maine Woodlands. JOURNAL OF MEDICAL ENTOMOLOGY. 43: 11.

Ellair, D.P., Platt, W.J., 2013. Fuel composition influences fire characteristics and understorey hardwoods in pine savanna. J. Ecol. 101, 192–201.

Ellsworth, D. S., R. Thomas, K. Y. Crous, S. Palmroth, E. Ward, C. Maier, E. Delucia, and R. Oren. 2012. Elevated CO 2 affects photosynthetic responses in canopy pine and

subcanopy deciduous trees over 10 years: A synthesis from Duke FACE. Global Change Biology. 18: 223–242.

Emery, S.M., Luke Flory, S., Clay, K., Robb, J.R., Winters, B., 2013. Demographic responses of the invasive annual grass *Microstegium vimineum* to prescribed fires and herbicide. For. Ecol. Manag. 308, 207–213.

Engstrom, J. D., Butler, J. K., Smith, S. G., Baxter, L. L., Fletcher, T. H., & Weise, D. R. 2004. Ignition behavior of live California chaparral leaves. *Combustion Science and Technology*, 176: 1577–1591.

Enloe, S. F., N. J. Loewenstein, D. W. Held, L. Eckhardt, and D. K. Lauer. 2013. Impacts of Prescribed Fire, Glyphosate, and Seeding on Cogongrass, Species Richness, and Species Diversity in Longleaf Pine. Invasive Plant Science and Management. 6: 536–544.

Estrada, J. A., C. H. Wilson, and S. L. Flory. 2020. Clonal integration enhances performance of an invasive grass. Oikos. 129: 1623–1631.

Etlinger, M. G., & Beall, F. C. 2004. Development of a laboratory protocol for fire performance of landscape plants. *International Journal of Wildland Fire*, 13: 479.

Fahey, C., C. Angelini, and S. L. Flory. 2018. Grass invasion and drought interact to alter the diversity and structure of native plant communities. Ecology. 99: 2692–2702.

Farquhar, G. D., S. von Caemmerer, and J. A. Berry. 1980. A biochemical model of photosynthetic CO2 assimilation in leaves of C3 species. Planta. 149: 78–90.

Feng, X., and M. Dietze. 2013. Scale dependence in the effects of leaf ecophysiological traits on photosynthesis: Bayesian parameterization of photosynthesis models. New Phytologist. 200: 1132–1144.

Fernandes, P. M., and M. G. Cruz. 2012. Plant flammability experiments offer limited insight into vegetation-fire dynamics interactions. New Phytologist. 194: 606–609.

Ferrari, S., and F. Cribari-Neto. 2004. Beta Regression for Modelling Rates and Proportions. Journal of Applied Statistics. 31: 799–815.

Finney, M.A., Martin, R.E., 1992. Calibration and field testing of passive flame height sensors. Int. J. Wildland Fire 2, 115–122.

Finney, M. A. 2004. FARSITE : Fire Area Simulator — Model Development and Evaluation, USDA Forest Service.

Fisher, R. A., C. D. Koven, W. R. L. Anderegg, B. O. Christoffersen, M. C. Dietze, C. E. Farrior, J. A. Holm, G. C. Hurtt, R. G. Knox, P. J. Lawrence, J. W. Lichstein, M. Longo, A. M. Matheny, D. Medvigy, H. C. Muller-Landau, T. L. Powell, S. P. Serbin, H. Sato, J. K. Shuman, B. Smith, A. T. Trugman, T. Viskari, H. Verbeeck, E. Weng, C. Xu, X. Xu, T.

Zhang, and P. R. Moorcroft. 2018. Vegetation demographics in Earth System Models: A review of progress and priorities. Global Change Biology.

Flory, S. L., K. Clay, S. M. Emery, J. R. Robb, and B. Winters. 2015. Fire and non-native grass invasion interact to suppress tree regeneration in temperate deciduous forests. Journal of Applied Ecology. 52: 992–1000.

Frost, C. 2007. History and Future of the Longleaf Pine Ecosystem, Springer series on environmental management. Springer, New York.

Ganteaume, A., 2018. Does plant flammability differ between leaf and litter bed scale? Role of fuel characteristics and consequences for flammability assessment. Int. J. Wildland Fire 27, 342.

Ganteaume, A., Jappiot, M., Curt, T., Lampin, C., & Borgniet, L. 2014. Flammability of litter sampled according to two different methods: comparison of results in laboratory experiments. *International Journal of Wildland Fire*, 23: 1061–1075.

Gill, A. M., & Zylstra, P. 2005. Flammability of Australian forests. *Australian Forestry*, 68: 87–93.

Gleim, E. R., L. M. Conner, R. D. Berghaus, M. L. Levin, G. E. Zemtsova, and M. J. Yabsley. 2014. The Phenology of Ticks and the Effects of Long-Term Prescribed Burning on Tick Population Dynamics in Southwestern Georgia and Northwestern Florida. PLoS ONE. 9: e112174.

Guiden, P. W., and J. L. Orrock. 2019. Invasive shrubs modify rodent activity timing, revealing a consistent behavioral rule governing diel activity. Behavioral Ecology. 30: 1069–1075.

Hair, J. A., J. R. Sauer, and K. A. Durham. 1975. Water Balance and Humidity Preference in Three Species of Ticks1. Journal of Medical Entomology. 12: 37–47.

Healy, R. W., R. G. Striegl, T. F. Russell, G. L. Hutchinson, and G. P. Livingston. 1996. Numerical Evaluation of Static-Chamber Measurements of Soil—Atmosphere Gas Exchange: Identification of Physical Processes. Soil Science Society of America Journal. 60: 740–747.

Hiatt, D., and S. L. Flory. 2020. Populations of a widespread invader and co-occurring native species vary in phenotypic plasticity. New Phytologist. 225: 584–594.

Hiatt, D., Serbesoff-King, K., Lieurance, D., Gordon, D.R., Flory, S.L., 2019. Allocation of invasive plant management expenditures for conservation: Lessons from Florida, USA. Conserv. Sci. Pract. 1, e51.

Hiers, J. K., Laine, S. C., Bachant, J. J., Furman, J. H., Greene, W. W., & Compton, V. 2003. Simple Spatial Modeling Tool for Prioritizing Prescribed Burning Activities at the Landscape Scale. *Conservation Biology*, *17*(6), 1571–1578.

Hijmans, R. J., 2019. raster: Geographic Data Analysis and Modeling. R package version 2.9-23. https://CRAN.R-project.org/package=raster

Holm, L. G., D. L. Plucknett, J. V. Pancho, and J. P. Herberger. 1977. The world's worst weeds. Distribution and biology. University press of Hawaii.

Hood, S., & Lutes, D. 2017. Predicting Post-Fire Tree Mortality for 12 Western US Conifers Using the First Order Fire Effects Model (FOFEM). *Fire Ecology*, *13*(2), 66–84.

Holzmueller, E. J., and S. Jose. 2012. Response of the invasive grass imperata cylindrica to disturbance in the southeastern forests, USA. Forests. 3: 853–863.

Jado, I., Escudero, R., Gil, H., Jiménez-Alonso, M. I., Sousa, R., García-Pérez, A. L., ... & Anda, P. 2006. Molecular method for identification of Rickettsia species in clinical and environmental samples. Journal of Clinical Microbiology, 44: 4572-4576.

Jaureguiberry, P., Bertone, G., & Díaz, S. 2011. Device for the standard measurement of shoot flammability in the field. *Austral Ecology*, 36: 821–829.

Jones, J.L., Webb, B.W., Butler, B.W., Dickinson, M.B., Jimenez, D., Reardon, J., Bova, A.S., 2006. Prediction and measurement of thermally induced cambial tissue necrosis in tree stems. Int. J. Wildland Fire 15, 3.

Jones, K. E., N. G. Patel, M. A. Levy, A. Storeygard, D. Balk, J. L. Gittleman, and P. Daszak. 2008. Global trends in emerging infectious diseases. Nature. 451: 990–993.

Kattge, J., S. Díaz, S. Lavorel, I. C. Prentice, P. Leadley, G. Bönisch, E. Garnier, M. Westoby, P. B. Reich, I. J. Wright, J. H. C. Cornelissen, C. Violle, S. P. Harrison, P. M. Van Bodegom, M. Reichstein, B. J. Enquist, N. A. Soudzilovskaia, D. D. Ackerly, M. Anand, O. Atkin, M. Bahn, T. R. Baker, D. Baldocchi, R. Bekker, C. C. Blanco, B. Blonder, W. J. Bond, R. Bradstock, D. E. Bunker, F. Casanoves, J. Cavender-Bares, J. Q. Chambers, F. S. Chapin Iii, J. Chave, D. Coomes, W. K. Cornwell, J. M. Craine, B. H. Dobrin, L. Duarte, W. Durka, J. Elser, G. Esser, M. Estiarte, W. F. Fagan, J. Fang, F. Fernández-Méndez, A. Fidelis, B. Finegan, O. Flores, H. Ford, D. Frank, G. T. Freschet, N. M. Fyllas, R. V. Gallagher, W. A. Green, A. G. Gutierrez, T. Hickler, S. I. Higgins, J. G. Hodgson, A. Jalili, S. Jansen, C. A. Joly, A. J. Kerkhoff, D. Kirkup, K. Kitajima, M. Kleyer, S. Klotz, J. M. H. Knops, K. Kramer, I. Kühn, H. Kurokawa, D. Laughlin, T. D. Lee, M. Leishman, F. Lens, T. Lenz, S. L. Lewis, J. Lloyd, J. Llusià, F. Louault, S. Ma, M. D. Mahecha, P. Manning, T. Massad, B. E. Medlyn, J. Messier, A. T. Moles, S. C. Müller, K. Nadrowski, S. Naeem, Ü. Niinemets, S. Nöllert, A. Nüske, R. Ogaya, J. Oleksyn, V. G. Onipchenko, Y. Onoda, J. Ordoñez, G. Overbeck, W. A. Ozinga, S. Patiño, S. Paula, J. G. Pausas, J. Peñuelas, O. L. Phillips, V. Pillar, H. Poorter, L. Poorter, P. Poschlod, A. Prinzing, R. Proulx, A. Rammig, S. Reinsch, B. Reu, L. Sack, B. Salgado-Negret, J. Sardans, S. Shiodera, B. Shipley, A. Siefert, E. Sosinski, J.-F. Soussana, E. Swaine, N. Swenson, K. Thompson, P. Thornton, M. Waldram, E. Weiher, M. White, S. White, S. J. Wright, B. Yguel, S. Zaehle, A. E. Zanne, and C. Wirth. 2011. TRY - a global database of plant traits. Global Change Biology. 17: 2905–2935.

De Kauwe, M. G., B. E. Medlyn, S. Zaehle, A. P. Walker, M. C. Dietze, T. Hickler, A. K. Jain, Y. Luo, W. J. Parton, I. C. Prentice, B. Smith, P. E. Thornton, S. Wang, Y. P. Wang, D. Wårlind, E. Weng, K. Y. Crous, D. S. Ellsworth, P. J. Hanson, H.- Seok Kim, J. M. Warren, R. Oren, and R. J. Norby. 2013. Forest water use and water use efficiency at elevated CO2: A model-data intercomparison at two contrasting temperate forest FACE sites. Global Change Biology. 19: 1759–1779.

Keenan, T. F., D. Y. Hollinger, G. Bohrer, D. Dragoni, J. W. Munger, H. P. Schmid, and A. D. Richardson. 2013. Increase in forest water-use efficiency as atmospheric carbon dioxide concentrations rise. Nature. 499: 324–327.

Keesing, F., R.S. Ostfeld, S. Okanga, S. Huckett, B.R. Bayles, R. Chaplin-Kramer, L.P. Fredericks, T. Hedlund, V. Kowal, H. Tallis, C.M. Warui, S.A. Wood and B.F. Allan. 2018. Consequences of integrating livestock and wildlife in an African savanna. Nature Sustainability 1: 566-573.

Keeley, J. E. 2009. Fire intensity, fire severity and burn severity: a brief review and suggested usage. *International Journal of Wildland Fire*, 18: 116-126.

Keirans, J. E., and T. R. Litwak. 1989. Pictorial Key to the Adults of Hard Ticks, Family Ixodidae (Ixodida: Ixodoidea), East of the Mississippi River. Journal of Medical Entomology. 26: 435–448.

Kelting, D. L., J. A. Burger, and G. S. Edwards. 1998. Estimating root respiration, microbial respiration in the rhizosphere, and root-free soil respiration in forest soils. Soil Biology and Biochemistry.

Kennard, D.K., Outcalt, K.W., Jones, D., O'Brien, J.J., 2005. Comparing Techniques for Estimating Flame Temperature of Prescribed Fires. Fire Ecol. 1, 75–84.

Kensinger, B.J. and B.F. Allan. 2011. Efficacy of dry-ice baited traps for sampling Amblyomma americanum (Acari: Ixodidae) varies with life-stage but not habitat. Journal of Medical Entomology 48: 708-711.

Kirkman, L. K., P. C. Goebel, B. J. Palik, and L. T. West. 2004. Predicting plant species diversity in a longleaf pine landscape. Ecoscience.

Kirkman, L. K., R. J. Mitchell, R. C. Helton, and M. B. Drew. 2001. Productivity and species richness across an environmental gradient in a fire-dependent ecosystem. American Journal of Botany. 88: 2119–2128.

Knülle, W., and D. Rudolph. 1982. CHAPTER 2 - Humidity Relationships and Water Balance of Ticks, Supported by Deutsche Forschungsgemeinschaft, Schwerpunktprogramm "Biochemische und physiologische Mechanismen ökologischer Anpassung von Tieren", pp. 43–70. *In* Obenchain, F.D., Galun, R. (eds.), Physiology of Ticks. Pergamon.

Koen Hufkens, David Basler, Tom Milliman, Eli K. Melaas, and Andrew D. Richardson. 2018. An integrated phenology modelling framework in R. Methods in Ecology & Evolution, 9(2), 1-10.

Kolaks, J. J., B. E. Cutter, E. F. Loewenstein, K. W. Grabner, G. Hartman, and J. M. Kabrick. 2004. Evaluation of passive flame height sensors for the central hardwoods region. In: Yaussy, Daniel A.; Hix, David M.; Long, Robert P.; Goebel, P. Charles, Eds. Proceedings, 14th Central Hardwood Forest Conference; 2004 March 16-19; Wooster, OH. Gen. Tech. Rep. NE-316. Newtown Square, PA: US Department of Agriculture, Forest Service, Northeastern Research Station: 520.

Kupfer, J. A., A. J. Terando, P. Gao, C. Teske, and J. K. Hiers. 2020. Climate change projected to reduce prescribed burning opportunities in the south-eastern United States. International Journal of Wildland Fire.

Kuzyakov, Y. 2006. Sources of CO2 efflux from soil and review of partitioning methods. Soil Biology and Biochemistry.

Landers, J.L., Van Lear, D.H., Boyer, W.D., 1995. The longleaf pine forests of the southeast: requiem or renaissance? J. For. 93, 39–44.

Leakey, A. D. B., C. J. Bernacchi, D. R. Ort, and S. P. Long. 2006. Long-term growth of soybean at elevated [CO2] does not cause acclimation of stomatal conductance under fully open-air conditions. Plant Cell Environ. 29: 1794–1800.

Lebauer, D. S., D. Wang, K. T. Richter, C. C. Davidson, and M. C. Dietze. 2013. Facilitating feedbacks between field measurements and ecosystem models Facilitating feedbacks between field measurem and ecosystem models. Source: Ecological Monographs Ecological Monographs. 83: 133–154.

Lefcheck, J. S. 2015. piecewiseSEM : Piecewise structural equation modeling in R for ecology, evolution, and systematics. Methods in Ecology and Evolution:1–7.

Leuning, R. 1995. A critical appraisal of a combined stomatal-photosynthesis model for C3 plants. Plant, Cell & Environment. 18: 339–355.

Lippincott, C. L. 2000. Effects of Imperata cylindrica(L.) Beauv.(Cogongrass) Invasion on Fire Regime in Florida Sandhill(USA). Natural Areas Journal. 20: 140–149.

Longo, M., R. G. Knox, N. M. Levine, A. L. S. Swann, D. M. Medvigy, M. C. Dietze, Y. Kim, K. Zhang, D. Bonal, B. Burban, P. B. Camargo, M. N. Hayek, S. R. Saleska, R. da Silva, R. L. Bras, S. C. Wofsy, and P. R. Moorcroft. 2019. The biophysics, ecology, and biogeochemistry of functionally diverse, vertically- and horizontally-heterogeneous ecosystems: the Ecosystem Demography Model, version 2.2 – Part 2: Model evaluation. Geoscientific Model Development Discussions. 1–34.

Loudermilk, E. L., Achtemeier, G. L., O'brien, J. J., Hiers, J. K., & Hornsby, B. S. 2014. High-resolution observations of combustion in heterogeneous surface fuels. *International Journal of Wildland Fire*, 23: 1016–1026.

Loudermilk, E. L., O'Brien, J. J., Mitchell, R. J., Cropper, W. P., Hiers, J. K., Grunwald, S., Fernandez-Diaz, J. C. 2012. Linking complex forest fuel structure and fire behaviour at fine scales. *International Journal of Wildland Fire*, 21: 882–893.

Lutes, D. C., Benson, N. C., Keifer, M., Caratti, J. F., & Streetman, S. A. 2009. FFI: A software tool for ecological monitoring. *International Journal of Wildland Fire*, *18*(3), 310.

MacDonald, G. E. 2004. Cogongrass (*Imperata cylindrica*)—Biology, Ecology, and Management. Critical Reviews in Plant Sciences. 23: 367–380.

Mack, R. N., and M. C. Smith. 2011. Invasive plants as catalysts for the spread of human parasites. NeoBiota. 13–29.

Mandli, J. T., X. Lee, G. M. Bron, and S. M. Paskewitz. 2021. Integrated Tick Management in South Central Wisconsin: Impact of Invasive Vegetation Removal and Host-Targeted Acaricides on the Density of Questing Ixodes scapularis (Acari: Ixodidae) Nymphs. Journal of Medical Entomology.

Makita, N., Y. Hirano, M. Dannoura, Y. Kominami, T. Mizoguchi, H. Ishii, and Y. Kanazawa. 2009. Fine root morphological traits determine variation in root respiration of Quercus serrata. Tree Physiology. 29: 579–585.

Marino, E., Dupuy, J.-L., Pimont, F., Guijarro, M., Hernando, C., Linn, R., 2012. Fuel bulk density and fuel moisture content effects on fire rate of spread: a comparison between FIRETEC model predictions and experimental results in shrub fuels. J. Fire Sci. 30, 277–299.

Martin, K. L., Hurteau, M. D., Hungate, B. A., Koch, G. W., & North, M. P. 2015. Carbon Tradeoffs of Restoration and Provision of Endangered Species Habitat in a Fire-Maintained Forest. *Ecosystems*, *18*(1), 76–88.

Martin, T. A. 2019. PINEMAP: Mapping the Future of Southern Pine Management in a Changing World. *Forest Resources and Conservation Speaker Series*.

Matlack, G. R. 2002. Exotic plant species in Mississippi, USA: Critical issues in management and research. Natural Areas Journal. 22: 241–247.

McCabe, T. D., & Dietze, M. C. 2019. Scaling Contagious Disturbance: A Spatially-Implicit Dynamic Model. Frontiers in Ecology and Evolution, 1–17.

Medvigy, D. M. 2006. The state of the regional carbon cycle: results from a constrained coupled ecosystem-atmosphere model.

Medvigy, D., S. C. Wofsy, J. W. Munger, D. Y. Hollinger, and P. R. Moorcroft. 2009. Mechanistic scaling of ecosystem function and dynamics in space and time: Ecosystem Demography model version 2. Journal of Geophysical Research. 114: G01002.

Michaletz, S.T., Johnson, E.A., Tyree, M.T., 2012. Moving beyond the cambium necrosis hypothesis of post-fire tree mortality: cavitation and deformation of xylem in forest fires. New Phytol. 194, 254–263.

Miller, A. D., M. C. Dietze, E. H. Delucia, and K. J. Anderson-Teixeira. 2016. Alteration of forest succession and carbon cycling under elevated CO2. Global Change Biology. 22: 351–363.

Mitchell, R. J., J. K. Hiers, J. J. O'Brien, S. B. Jack, and R. T. Engstrom. 2006. Silviculture that sustains: the nexus between silviculture, frequent prescribed fire, and conservation of biodiversity in longleaf pine forests of the southeastern United States. Canadian Journal of Forest Research.

Mixson, T.R., S.R. Campbell, J.S. Gill, H.S. Ginsberg, M.V. Reichard, T.L. Schulze, and G.A. Dasch. 2006. Prevalence of Ehrlichia, Borrelia, and Rickettsial agents in *Amblyomma americanum* (Acari: Ixodidae) collected from nine states. *Journal of medical entomology*, 43: 1261-1268.

Moorcroft, P. R., G. C. Hurtt, and S. W. Pacala. 2001. A method for scaling vegetation dynamics: The ecosystem demography model (ED). Ecological Monographs. 71: 557–586.

Morand, S., and C. Lajaunie. 2021. Outbreaks of Vector-Borne and Zoonotic Diseases Are Associated With Changes in Forest Cover and Oil Palm Expansion at Global Scale. Front. Vet. Sci. 8.

Morens, D. M., G. K. Folkers, and A. S. Fauci. 2004. The challenge of emerging and re-emerging infectious diseases. Nature. 430: 242–249.

Muturi, E. J., Kim, C. H., Bara, J., Bach, E. M., & Siddappaji, M. H. 2016. Culex pipiens and Culex restuans mosquitoes harbor distinct microbiota dominated by few bacterial taxa. *Parasites & vectors*, *9*(1), 1-11.

Needham, G. R., and P. D. Teel. 1991. Off-Host Physiological Ecology of Ixodid Ticks. Annual Review of Entomology. 36: 659–81.

Noss, R. F., E. T. LaRoe, and J. M. Scott. 1995. Endangered ecosystems of the United States: a preliminary assessment of loss and degradation. US Department of the Interior, National Biological Service Washington, DC, USA.

Ostfeld, R. S., T. Levi, F. Keesing, K. Oggenfuss, and C. D. Canham. 2018. Tick-borne disease risk in a forest food web. Ecology. 99: 1562–1573.

Oswald, B.P. and the Association for Fire Ecology. 2007. San Diego Declaration on climate change and fire management: ramifications for fuels management. In: Butler, B.W. and W. Cook, Comps. the fire environment innovations, management, and policy conference proceeding. 26-30 March 2007, Destin, FL.

Pausas, J. G., & Moreira, B. 2012. Flammability as a biological concept. *New Phytologist*, *194:* 610–613.

Platt, W. J., and R. M. Gottschalk. 2001. Effects of exotic grasses on potential fine fuel loads in the groundcover of south Florida slash pine savannas. International Journal of Wildland Fire. 10: 155–159.

Platt, W. J., S. L. Orzell, and M. G. Slocum. 2015. Seasonality of fire weather strongly influences fire regimes in south Florida savanna-grassland landscapes. PLoS ONE. 10: e0116952.

Pritt, B. S., Allerdice, M. E., Sloan, L. M., Paddock, C. D., Munderloh, U. G., Rikihisa, Y., ... & Schiffman, E. 2017. Proposal to reclassify Ehrlichia muris as Ehrlichia muris subsp. muris subsp. nov. and description of Ehrlichia muris subsp. eauclairensis subsp. nov., a newly recognized tick-borne pathogen of humans. International Journal of Systematic and Evolutionary Microbiology, 67: 2121.

Quinn Thomas, R., E. B. Brooks, A. L. Jersild, E. J. Ward, R. H. Wynne, T. J. Albaugh, H. Dinon-Aldridge, H. E. Burkhart, J. C. Domec, T. R. Fox, C. A. Gonzalez-Benecke, T. A. Martin, A. Noormets, D. A. Sampson, and R. O. Teskey. 2017. Leveraging 35 years of Pinus taeda research in the southeastern US to constrain forest carbon cycle predictions: Regional data assimilation using ecosystem experiments. Biogeosciences. 14: 3525–3547.

R Core Team. 2018. R: A Language and Environment for Statistical Computing. R Foundation for Statistical Computing, Vienna, Austria.

R Core Team. 2019. *R: A Language and Environment for Statistical Computing* [R]. R Foundation for Statistical Computing. https://www.R-project.org/

Racelis, A. E., R. B. Davey, J. A. Goolsby, A. A. P. de León, K. Varner, and R. Duhaime. 2012. Facilitative Ecological Interactions Between Invasive Species: Arundo donax Stands as Favorable Habitat for Cattle Ticks (Acari: Ixodidae) Along the U.S.-Mexico Border. Journal of Medical Entomology. 49: 410–417.

Rognes, T., Flouri, T., Nichols, B., Quince, C., & Mahé, F. 2016. VSEARCH: a versatile open source tool for metagenomics. *PeerJ*, *4*, e2584.

Rossa, C.G., Fernandes, P.M., 2017. Fuel-related fire-behaviour relationships for mixed live and dead fuels burned in the laboratory. Can. J. For. Res. 47, 883–889.

Ryan, K. C. 1981. Evaluation of a passive flame-height sensor to estimate forest fire intensity. United States Department of Agriculture, Portland, OR.

Sajise, P. E. 1973. Evaluation of cogon (Imperata cylindrica (L.) Beauv.) as a serial stage in Philippine vegetational succession: I. The cogonal serial stage and plant succession. II. Autecological studies on cogon.

Sauer, J. R., and J. A. Hair. 1971. Water Balance in the Lone Star Tick (Acarina: Ixodidae): the Effects of Relative Humidity and Temperature on Weight Changes and Total Water Content1. Journal of Medical Entomology. 8: 479–485.

Scholze, M., W. Knorr, N. Arnell and I.C. Prentice. 2006. A climate-change risk analysis for world ecosystems. Proceedings of the National Academy 103:13116-20.

Schulze, T. L., and R. A. Jordan. 2003. Meteorologically Mediated Diurnal Questing of *Ixodes scapularis* and *Amblyomma americanum* (Acari: Ixodidae) Nymphs. J Med Entomol. 40: 395–402.

Schulze, T. L., R. A. Jordan, and R. W. Hung. 1997. Biases Associated with Several Sampling Methods Used to Estimate Abundance of Ixodes scapularis and Amblyomma americanum (Acari: Ixodidae). Journal of Medical Entomology. 34: 615–623.

Schwartz, J. J., A. Gazumyan, and I. Schwartz. 1992. rRNA gene organization in the Lyme disease spirochete, Borrelia burgdorferi. J. Bacteriol. 174: 3757–3765.

Schwilk, D. W. 2003. Flammability Is a Niche Construction Trait: Canopy Architecture Affects Fire Intensity. *The American Naturalist*, 162*:* 725–733.

Schwilk, D.W., 2015. Dimensions of plant flammability. New Phytol. 206, 486–488.

Shappell, L.J., Koontz, S.M., 2015. Fire reintroduction increased longleaf pine (*Pinus palustris* L.) recruitment and shifted pine demographics in a long-unburned xeric sandhill assemblage. For. Ecol. Manag. 354, 344–352.

Shipley, B. 2000. A New Inferential Test for Path Models Based on Directed Acyclic Graphs. Structural Equation Modeling: A Multidisciplinary Journal 7:206–218.

Shipley, B. 2004. Cause and Correlation in Biology: A User's Guide to Path Analysis, Structural Equations and Causal Inference. Page Cambridge University Press.

Shipley, B. 2013. The AIC model selection method applied to path analytic models compared using a d-separation test. Ecology 94:560–564.

Shipley, B., and J. C. Douma. 2020. Generalized AIC and chi-squared statistics for path models consistent with directed acyclic graphs. Ecology 101:e02960.

Simard, A.J., Blank, R.W., Hobrla, S.L., 1989. Measuring and interpreting flame height in wildland fires. Fire Technol. 25, 114–133.

Simpson, K. J., Ripley, B. S., Christin, P. A., Belcher, C. M., Lehmann, C. E., Thomas, G. H., & Osborne, C. P. 2016. Determinants of flammability in savanna grass species. *Journal of Ecology*, 104: 138-148.

Starr, G., C. L. Staudhammer, H. W. Loescher, R. Mitchell, A. Whelan, J. K. Hiers, and J. J. O'Brien. 2015. Time series analysis of forest carbon dynamics: recovery of Pinus palustris physiology following a prescribed fire. New Forests. 46: 63–90.

Steere, A. C., J. Coburn, and L. Glickstein. 2004. The emergence of Lyme disease. J Clin Invest. 113: 1093–1101.

Stewart, P. S., R. A. Hill, P. A. Stephens, M. J. Whittingham, and W. Dawson. 2021. Impacts of invasive plants on animal behaviour. Ecology Letters. 24: 891–907.

Stromdahl, E. Y., J. Jiang, M. Vince and A. L. Richards. 2011. Infrequency of Rickettsia rickettsii in Dermacentor variabilis Removed from Humans, with Comments on the Role of Other Human-Biting Ticks Associated with Spotted Fever Group Rickettsiae in the United States. Vector-Borne and Zoonotic Diseases 11:969-977.

Swezy, D.M., Agee, J.K., 1991. Prescribed-fire effects on fine-root and tree mortality in old-growth ponderosa pine. Can. J. For. Res. 21, 626–634.

Thaxton, J. M., & Platt, W. J. 2006. Small-scale fuel variation alters fire intensity and shrub abundance in a pine savanna. *Ecology*, 87: 1331-1337.

Thonicke, K., Spessa, A., Prentice, I. C., Harrison, S. P., Dong, L., & Carmona-Moreno, C. 2010. The influence of vegetation, fire spread and fire behaviour on biomass burning and trace gas emissions: Results from a process-based model. *Biogeosciences*, *7*(6), 1991–2011.

Thornton, P.E., M.M. Thornton, B.W. Mayer, Y. Wei, R. Devarakonda, R.S. Vose, and R.B. Cook. 2016. Daymet: Daily Surface Weather Data on a 1-km Grid for North America, Version 3. ORNL DAAC, Oak Ridge, Tennessee, USA.

Tiribelli, F., Kitzberger, T., Morales, J.M., 2018. Changes in vegetation structure and fuel characteristics along post-fire succession promote alternative stable states and positive fire–vegetation feedbacks. J. Veg. Sci. 29, 147–156.

Trugman, A. T., D. Medvigy, W. A. Hoffmann, and F. A. Pellegrini. 2018. Sensitivity of woody carbon stocks to bark investment strategy in Neotropical savannas and forests. Biogeosciences.

Varner, J. M., J. K. Hiers, R. D. Ottmar, D. R. Gordon, F. E. Putz, and D. D. Wade. 2007. Overstory tree mortality resulting from reintroducing fire to long-unburned longleaf pine forests: the importance of duff moisture. Canadian Journal of Forest Research. 37: 1349–1358.

Varner, J. M., J. M. Kane, J. K. Kreye, and E. Engber. 2015. The Flammability of Forest and Woodland Litter: a Synthesis. Current Forestry Reports. 1: 91–99.

Wade, D. D., J. D. Lunsford, M. J. Dixon, and H. E. Mobley. 1989. A guide for prescribed fire in southern forests. Technical publication R8-TP-US Department of Agriculture, Forest Service, Southern Region (USA).

Walker, A., and P. Hanson. 2014. Comprehensive ecosystem model-data synthesis using multiple data sets at two temperate forest free-air CO2 enrichment experiments: Model performance at. Journal of Geophysical Research: Biogeosciences 119: 937–964.

Walker, J., and R. K. Peet. 1984. Composition and species diversity of pine-wiregrass savannas of the Green Swamp, North Carolina. Vegetation 55: 163–179.

Wei, C.-Y., J.-K. Wang, H.-C. Shih, H.-C. Wang, and C.-C. Kuo. 2020. Invasive plants facilitated by socioeconomic change harbor vectors of scrub typhus and spotted fever. PLOS Neglected Tropical Diseases. 14: e0007519.

Weise, D.R., Koo, E., Zhou, X., Mahalingam, S., Morandini, F., Balbi, J.-H., 2016. Fire spread in chaparral – a comparison of laboratory data and model predictions in burning live fuels. Int. J. Wildland Fire 25, 980.

Weise, D.R., Zhou, X., Sun, L., Mahalingam, S., 2005. Fire spread in chaparral—'go or no-go?'. Int. J. Wildland Fire 14, 99.

Wells, G., Rohling, K., Kapus, J., & Swedberg, T. 2009. A Powerful new Planning environment for Fuels Managers: The interagency Fuels treatment Decision Support System. *Fire Science Digest*, *7*.

Wenk, E.S., Wang, G.G., Walker, J.L., 2011. Within-stand variation in understorey vegetation affects fire behaviour in longleaf pine xeric sandhills. Int. J. Wildland Fire 20, 866–875.

Whelan, R. J. 1995. *The ecology of fire*. Cambridge university press.

Wickham, H. 2011. ggplot2. Wiley Interdisciplinary Reviews: Computational Statistics.

Williams, S. C., and J. S. Ward. 2010. Effects of Japanese Barberry (Ranunculales: Berberidaceae) Removal and Resulting Microclimatic Changes on Ixodes scapularis (Acari: Ixodidae) Abundances in Connecticut, USA. Environmental Entomology. 39: 1911–1921.

Williams, S. C., J. S. Ward, T. E. Worthley, and K. C. Stafford. 2009. Managing Japanese Barberry (Ranunculales: Berberidaceae) Infestations Reduces Blacklegged Tick (Acari: Ixodidae) Abundance and Infection Prevalence With Borrelia burgdorferi (Spirochaetales: Spirochaetaceae). Environ Entomol. 38: 977–984.

Wright, S. 1921. Correlation and causation. Journal of agricultural research 20:557–585.

Wolz, K. J., T. M. Wertin, M. Abordo, D. Wang, and A. D. B. Leakey. 2017. Diversity in stomatal function is integral to modelling plant carbon and water fluxes. Nature Ecology and Evolution. 1: 1292–1298.

Wyse, S. V., Perry, G. L. W., O'Connell, D. M., Holland, P. S., Wright, M. J., Hosted, C. L., Curran, T. J. 2016. A quantitative assessment of shoot flammability for 60 tree and shrub species supports rankings based on expert opinion. *International Journal of Wildland Fire*, 25: 466–477.

Yager, L.Y., Miller, D.L., Jones, J., 2010. Susceptibility of longleaf pine forest associations in south Mississippi to invasion by cogongrass [*Imperata cylindrica* (L.) Beauv.]. Nat. Areas J. 30, 226–232.

Xu, X., Medvigy, D., Powers, J. S., Becknell, J. M., & Guan, K. 2016. Hydrological niche separation explains seasonal and inter-annual variations of vegetation dynamics in seasonally dry tropical forests. In *AGU Fall Meeting*.

APPENDICES

Table A1. Weather during experimental fires. Date of fire, fuel structure, amount of biomass, air temperature averaged over the duration of the fire, relative humidity averaged over the duration of the fire, and wind speed averaged over the duration of the fire ± standard error.

Date	Structure	Biomass (g)	Air Temperature (ºC)	RH (%)	Wind speed (m s^{-1})	Fuel moisture (%)
2017-12-01	piled	250	27.9 ± 0.1	36.8 ± 0.1	0.9 ± 0.1	15.2
2017-12-01	standing	250	28.1 ± 0.1	36.3 ± 0.1	0.8 ± 0.1	19.6
2017-12-01	piled	500	27.8 ± 0.1	37.5 ± 0	0.4 ± 0.1	13.9
2017-12-01	standing	500	27.8 ± 0.1	37.2 ± 0.1	0.4 ± 0.1	9.2
2017-12-01	piled	1000	22.8 ± 0	64.4 ± 0.1	0 ± 0	9.6
2017-12-01	standing	1000	26.1 ± 0	44.8 ± 0.1	0.4 ± 0	15.0
2017-12-01	piled	1500	22.3 ± 0	67.7 ± 0.1	0 ± 0	9.7
2017-12-01	standing	1500	22.8 ± 0	66 ± 0.1	0 ± 0	12.4
2017-12-04	piled	2000	26.7 ± 0.1	55.9 ± 0.1	0.6 ± 0.1	14.6
2017-12-04	standing	2000	28.2 ± 0.1	54.3 ± 0.2	0.4 ± 0.1	13.1

2017-12-04	piled	250	25.8 ± 0	55.2 ± 0.1	0 ± 0	4.6
2017-12-04	standing	250	25.8 ± 0	55.2 ± 0.1	0 ± 0	8.0
2017-12-04	piled	500	25.3 ± 0.1	57.4 ± 0.1	0.3 ± 0.1	12.2
2017-12-04	standing	500	25.3 ± 0.1	57.4 ± 0.1	0.3 ± 0.1	13.0
2017-12-04	piled	1000	24.2 ± 0	60 ± 0.1	0.4 ± 0	9.8
2017-12-04	standing	1000	23.6 ± 0	61.6 ± 0.1	0.8 ± 0	15.2
2017-12-04	piled	1000	25.4 ± 0	59.7 ± 0.1	0.1 ± 0	15.2
2017-12-04	standing	1000	25.8 ± 0	58.3 ± 0.1	0 ± 0	14.3
2017-12-04	piled	2000	24.3 ± 0	63.5 ± 0.2	0 ± 0	10.3
2017-12-04	standing	2000	24.2 ± 0	62.5 ± 0	0 ± 0	15.5
2017-12-05	piled	250	26.9 ± 0.1	60.6 ± 0.1	1.1 ± 0.1	13.7
2017-12-05	standing	250	27.1 ± 0.1	60.5 ± 0.1	1.1 ± 0.1	10.3

2017-12-05	piled	500	28.7 ± 0.1	56.6 ± 0.1	0.7 ± 0.1	10.8
2017-12-05	standing	500	29.3 ± 0.1	55.9 ± 0.2	0.7 ± 0.1	9.5
2017-12-05	piled	1000	28.2 ± 0.1	56 ± 0.2	0.5 ± 0.1	11.1
2017-12-05	standing	1000	27.7 ± 0.1	57 ± 0.1	0.6 ± 0.1	10.7
2017-12-05	piled	1500	27.1 ± 0	59.6 ± 0.1	1 ± 0	9.0
2017-12-05	standing	1500	27.1 ± 0	59.6 ± 0.1	1 ± 0	7.4
2017-12-05	piled	2000	28.5 ± 0.1	52 ± 0.1	0.7 ± 0.1	11.1
2017-12-05	standing	2000	28.3 ± 0.2	52.2 ± 0.1	0.4 ± 0.2	6.8
2017-12-05	piled	1500	30.3 ± 0	47.6 ± 0	0 ± 0	8.8
2017-12-05	standing	1500	30.3 ± 0	47.6 ± 0	0 ± 0	8.0

Table A2. Time above 100 ºC model coefficients. Includes significant interaction term of biomass and fuel structure.

Probe height	Variable	Estimate	Std. Error	Crit. value	P value
50 cm	Intercept	13.83	12.23	1.13	0.27
	Biomass	0.06	0.01	6.27	$9e^{-7}$
	Structure: standing	1.51	17.30	0.09	0.93
	Biomass X Standing	-0.04	0.01	-2.71	0.01
25 cm	Intercept	33.01	9.69	3.41	$2e^{-3}$
	Biomass	0.08	0.01	9.77	$1.6e^{-10}$
	Structure: standing	-13.45	13.70	-0.98	0.33
	Biomass X Standing	-0.05	0.01	-4.60	$8.3e^{-5}$
0 cm	Intercept	-12.02	48.92	-0.25	0.81
	Biomass	0.28	0.04	6.88	$1.8e^{-7}$
	Structure: standing	52.91	69.18	0.76	0.45
	Biomass X Standing	-0.26	0.06	-4.60	$8.3e^{-5}$

Table A3. Maximum temperature model coefficients.

Probe height	Variable	Estimate	Std. Error	Crit. value	P value
50 cm	Intercept	658.85	47.82	0.17	0.02
	Biomass	0.34	0.04	9.96	$2.2e^{-11}$
	Structure: standing	66.0	43.43	1.33	0.11
	Air temperature	-24.44	9.52	-2.57	0.02
25 cm	Intercept	196.03	44.40	4.41	$1.3e^{-4}$
	Biomass	0.30	0.03	9.16	$4.7e^{-10}$
	Structure: standing	-92.67	40.32	-2.30	0.03
0 cm	Intercept	407.44	47.67	8.55	$2.0e^{-9}$
	Biomass	0.14	0.03	4.04	$3.6e^{-4}$
	Structure: standing	-194.49	43.29	-4.49	$1.0e^{-4}$

Table A4. Model coefficients for flame height, rate of spread, and proportion of mass consumed.

Response	Variable	Estimate	Std. Error	Crit. value	P value
Flame height	Intercept	9.91	15.70	0.63	0.01
	Biomass	0.054	0.01	4.36	$8.1e^{-5}$
	Structure: standing	-20.1	22.21	-0.97	0.33
	Air temperature	-6.52	2.46	-2.65	0.01
	Biomass X Standing	0.06	0.02	3.06	$2.0e^{-3}$
Rate of spread	Intercept	-0.61	0.29	-2.12	0.04
	Biomass	$9.5e^{-7}$	0.00	-0.02	0.99
	Structure: standing	-0.04	0.09	-0.44	0.66
	Air temperature	0.03	0.01	2.38	0.02
	Biomass X Standing	$2.0e^{-4}$	0.00	2.87	0.01
Percent consumed	Intercept	3.30	0.40	8.22	$2.1e^{-16}$
	Biomass	0.00	0.00	1.81	0.07
	Structure: standing	-4.64	0.46	-10.08	$7.7e^{-24}$
	Biomass X Standing	0.00	0.00	7.75	$9.4e^{-15}$

Figure A1. Experimental setup for simultaneous ignition of devices that have the same fuel loads but different fuel structures.

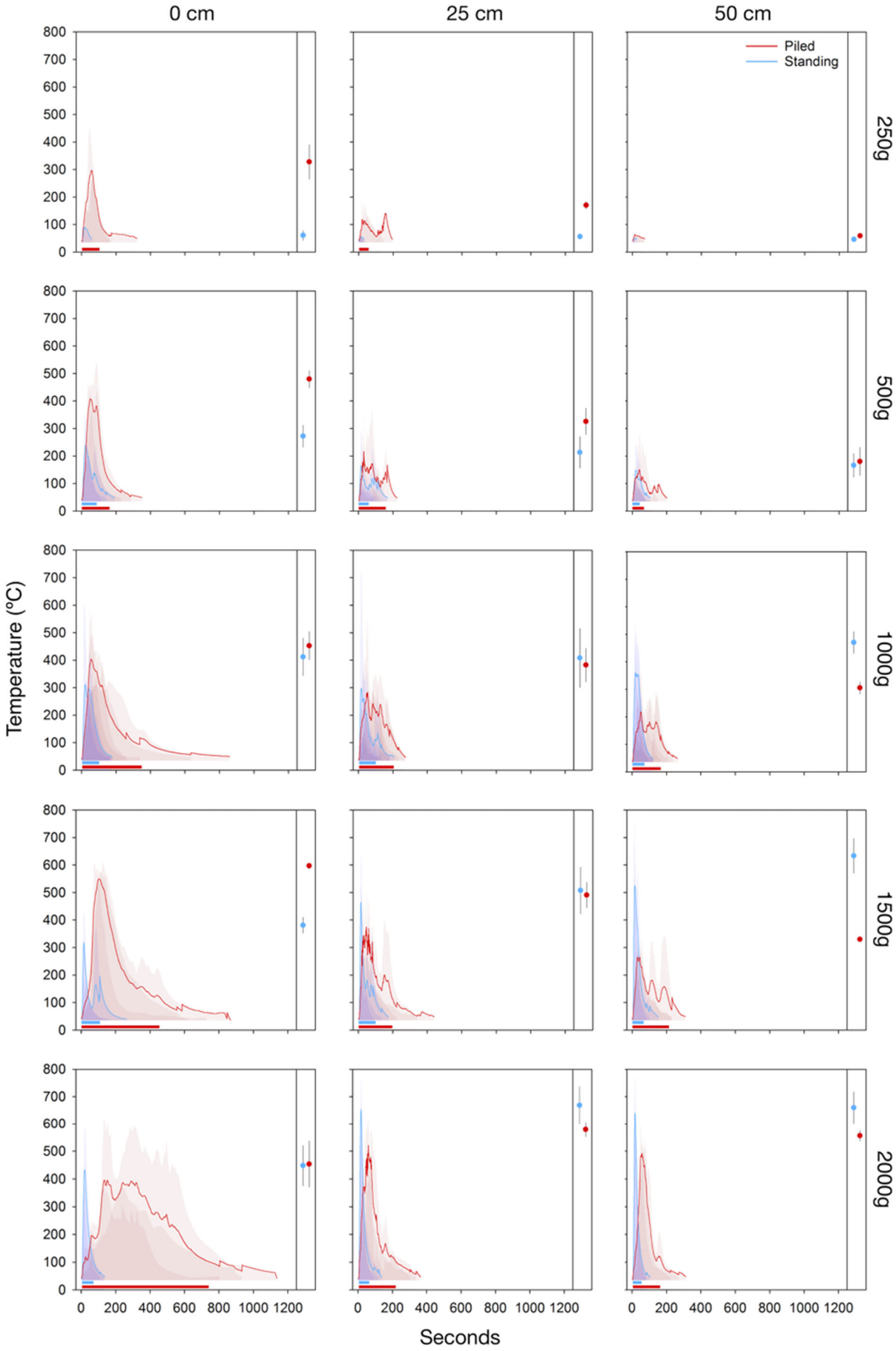
0 cm
25 cm
50 cm
Piled
Standing
250g
500g
1000g
1500g
2000g
Temperature (°C)
Seconds
0
100
200
300
400
500
600
700
800
0
200
400
600
800
1000
1200

Figure A2. Temperatures recorded each second during each experimental fire (shaded areas) with the average temperature profile across the fires at each fuel load and probe height (solid lines) for piled (red) and standing (blue) fuels at (0, 25, and 50 cm heights). The inset figure to the right in each panel shows the mean (+SE) of the maximum fire temperatures. The bottom inset figure in each panel shows the average time across the set of fires that temperature exceeded 100 °C.

APPENDIX B – STRUCTURED INTERVIEW SCRIPT

Hello and thank you for agreeing to meet with us!

My name is [Main interviewer], and this is [second interviewer], who will be taking notes.

We are both part of a research team that studied the effects of fire and invasive plant management on vegetation and tick populations on your installation [personal context- when did Whalen & Drew sample and who were they in contact with] .
One of the products of our contract is to design a "decision support tool". At this early design stage, by "decision support tool" we mean a tool that displays how land management decisions affect some aspect of your installation that we studied. For example, the effect of time since last burn on tick populations. We would like to know more about how you are making decisions and what you find valuable to make the final "decision support tool" as useful as possible.

Briefly, what is your role at the installation?

How does your installation make decisions around forested natural resources?

Do you use any decision support tools to make decisions now? Do you use any simulations or software to inform your decisions?

What goals does your installation have for its natural resources?

How do you prioritize goals?

How do you evaluate whether you've met your management goals?

What techniques do you use for management? Why?

How far into the future are you planning?

How often do troop training exercises conflict with natural resource management? Are areas that have been recently burned more likely to have troop training than areas that have a long history of no/minimal fires?

Our research has collected data on plant community composition, cogongrass invasion, climate projections, and tick populations and tick-borne pathogen prevalence at your installation. Are any of these topics relevant to your installation's management goals? If yes, what makes them relevant? If not, what research would be relevant to your goals?

If tick-borne disease risk could be incorporated into a decision support tool as an outcome of management, would that be useful and why?

If invasive species prevalence could be incorporated into a decision support tool as an outcome of management, would that be useful and why?

If climate projections could be incorporated into a decision support tool as an outcome of management, would that be useful and why?

What, if any, data do you collect for fire management, invasive species, or tick populations or tick-borne diseases?

What would be the most useful way of presenting our results? Have you had past collaborations we could emulate? What has worked well?

Hypothetically, if we had 10 or more years, and unlimited dedicated funding to build the decision support tool, and were building it just to cater to the needs of your installation, how would you advise us to design it?

Do you have any questions for us?

Would you be willing to give us feedback on an early version of the decision support tool?

Do you have colleagues that you think we should reach out to?

Thank you again!

APPENDIX C – PUBLICATIONS

Steven Cabrera, Drew Hiatt, Whalen W. Dillon, Taylor Clark, Brian F. Allan, and S. Luke Flory. 2021. Observations of Wild Turkey Nesting in Invasive Cogongrass. Southeastern Naturalist 20(1), N42-N49.

Whalen W. Dillon, Drew Hiatt, and S. Luke Flory. 2021. Experimental manipulation of fuel structure to evaluate the potential ecological effects of fire. Forest Ecology and Management, 482: 118884.

Tempest D. McCabe, and Michael C. Dietze. 2019. Scaling contagious disturbance: a spatially-implicit dynamic model. Frontiers in Ecology and Evolution 7, 64.